

NSTX Research Program Progress and Plans Toward 5 Year Plan Goals

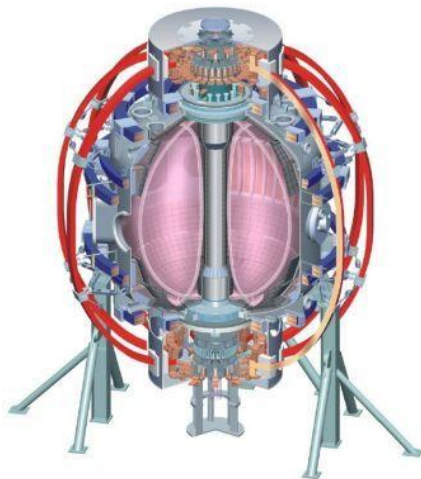
J. Menard

NSTX Program Director

For the NSTX Team

**Midterm Review of Major MFE Facilities
Germantown, MD
June 6, 2011**

*Columbia U
CompX
General Atomics
FIU
INL
Johns Hopkins U
LANL
LLNL
Lodestar
MIT
Nova Photonics
New York U
ORNL
PPPL
Princeton U
Purdue U
SNL
Think Tank, Inc.
UC Davis
UC Irvine
UCLA
UCSD
U Colorado
U Illinois
U Maryland
U Rochester
U Washington
U Wisconsin*



*Culham Sci Ctr
U St. Andrews
York U
Chubu U
Fukui U
Hiroshima U
Hyogo U
Kyoto U
Kyushu U
Kyushu Tokai U
NIFS
Niigata U
U Tokyo
JAEA
Hebrew U
Ioffe Inst
RRC Kurchatov Inst
TRINITI
NFRI
KAIST
POSTECH
ASIPP
ENEA, Frascati
CEA, Cadarache
IPP, Jülich
IPP, Garching
ASCR, Czech Rep*

Agenda

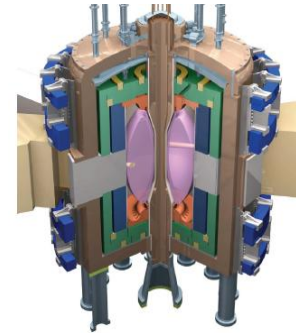
- J. Menard - Research Program Progress and Plans
 - 60-70 minutes
- M. Ono - Facility Status and Plans (+ NSTX Upgrade)
 - 30-40 minutes
- Discussion with panel
 - 40-60 minutes

Outline

- NSTX mission elements
- Changes in program since 5yr plan proposal
- Research goals, progress, and plans
- Summary
- Supplemental slides

NSTX Mission Elements

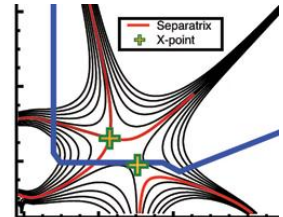
- Advance ST as candidate for Fusion Nuclear Science Facility (FNSF)
- Develop solutions for plasma-material interface
- Advance toroidal confinement physics for ITER and beyond
- Develop ST as fusion energy system



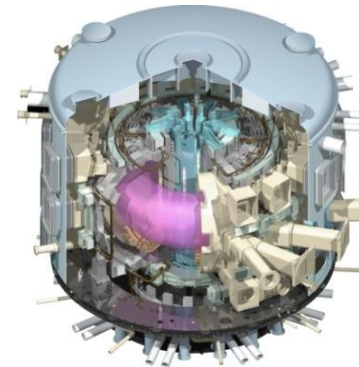
ST-FNSF



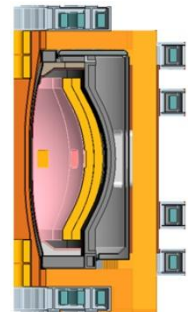
Lithium



“Snowflake”



ITER



ST Pilot Plant

Changes in program since 5 year plan proposal

2009 - ReNeW Thrust 16: Emphasizes developing physics basis of ST for FNSF

2010 - FES vision for next decade: Materials/PMI, FNSF, predictive capability

- 
- Stronger emphasis on FNSF + PMI + diagnostics and validation
 - Successful implementation of Upgrade Project highest NSTX priority

ReNeW Thrust 16: “Develop the ST to advance fusion nuclear science”
consists of 7 Thrust Elements:

1. Develop **MA-level plasma current formation and ramp-up**
2. Advance **innovative divertor magnetic geometries, first wall solutions**
3. Understand **ST confinement and stability** at fusion-relevant parameters
4. Develop **stability control techniques** for long-pulse, disruption-free ops
5. **Sustain current, control profiles** with beams, waves, pumping, fueling
6. Develop normally-conducting radiation-tolerant **magnets** for ST applications
7. **Extend ST performance** to near-burning-plasma conditions

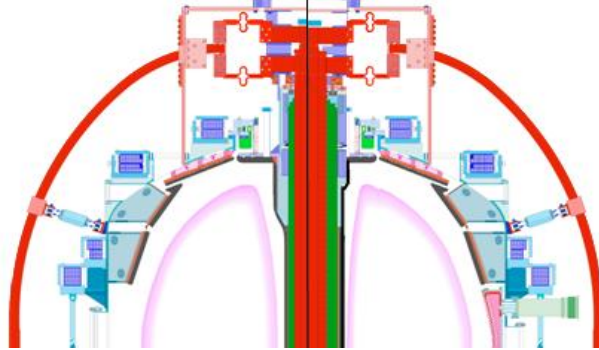
These elements provide outline for subsequent **FY09-13 results and plans**

NSTX Upgrade supports ReNeW ST physics thrust elements, bridges device and performance gaps toward ST-FNSF

New center stack for 1T, 2MA, 5s

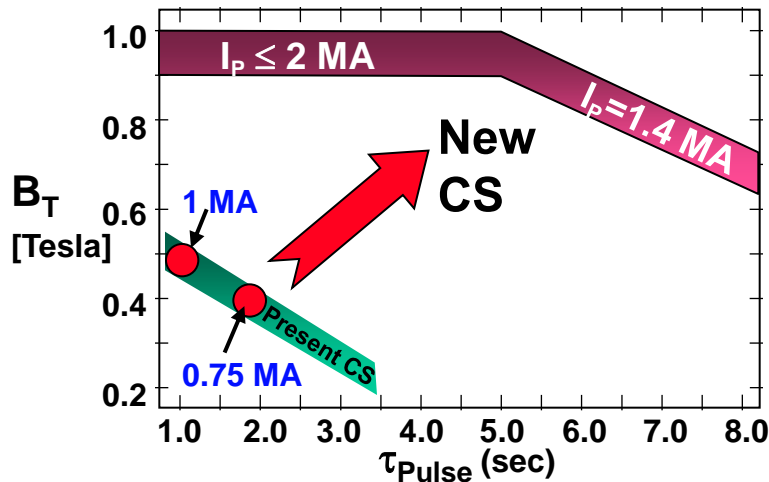
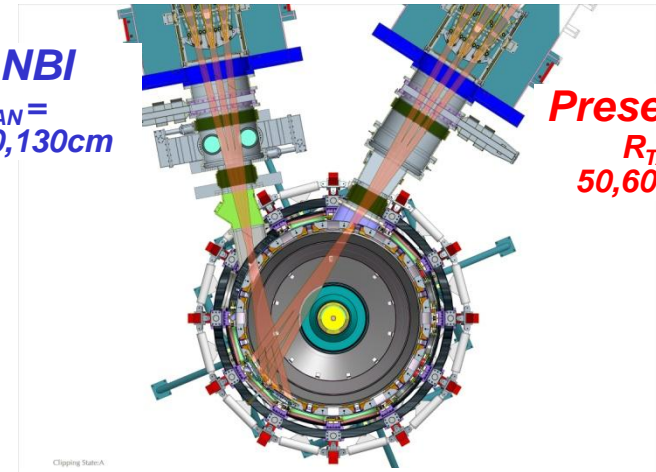
2nd NBI with 5 MW, 5s at larger $R_{Tangency}$

$R_0/a \leftarrow 1.25-1.3 \xrightarrow{\text{New CS}} 1.5-1.6$

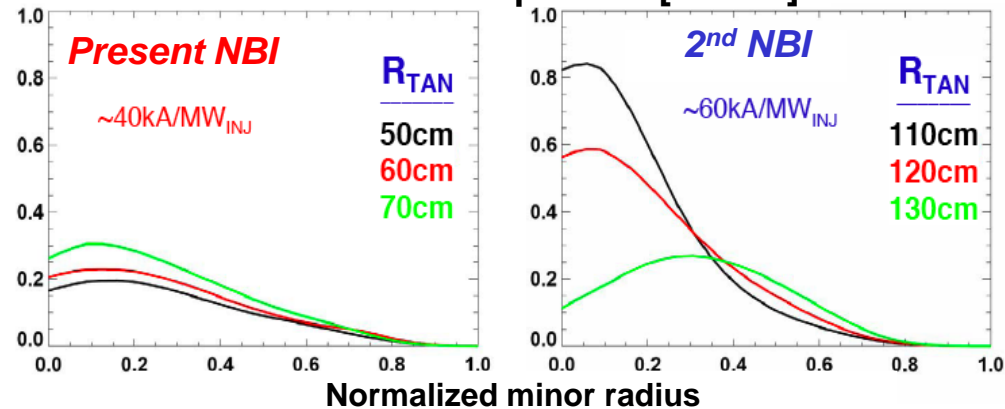


2nd NBI
 $R_{TAN} = 110, 120, 130\text{cm}$

Present NBI
 $R_{TAN} = 50, 60, 70\text{cm}$



NBI current drive profiles [MA/m²]



Magnet operation at $\sim 1\text{T}$ (vs. 0.55T):
 v^* reduced 3-6x, $nT\tau$ up to 10x higher

Up to 2x higher NBI current drive efficiency:
Non-inductive ramp-up, sustainment, $J(r)$ control

Schedule for NSTX Upgrade elements (new CS + 2nd NBI) has changed substantially since 5 year plan proposal

- Run-time and Upgrade schedule proposed in 5 year plan:



- Present run-time and Upgrade schedule:



- More cost effective, faster to implement new CS + 2nd NBI in single outage
- Upgrade project approved, approaching CD-3, highest NSTX priority
- Impact on original 5 year plan goals and schedule:
 - Higher $B_T = 1T$ not available in 2012 – impacts all research planned for 2012
 - ECH/EBW deferred due to funding limitations
 - Plasma guns deferred due to technical readiness / time constraints
 - Less run-time in 2012, no run-time in 2013 → ~3/4 of originally planned run-time

Outline of Topical Areas and Research Goals

(Aligned with NSTX Mission and ReNeW elements)

- **Solenoid-free Plasma Start-up and Ramp-up**
 - Develop helicity injection and fast-wave heating for plasma current formation and ramp-up
- **Lithium and Boundary Physics**
 - Assess lithium PFCs, develop high-flux-expansion divertors, understand edge transport/stability
- **Transport and Turbulence**
 - Measure, understand, predict instabilities responsible for ST transport, project to next-steps
- **Macroscopic Stability**
 - Develop predictive capability for accessing, controlling, sustaining very high plasma pressure
- **Energetic Particle Physics**
 - Establish predictive capability for fast-ion transport caused by *AE for ST, burning plasma
- **Wave Heating and Current Drive**
 - Demonstrate reliable wave heating and CD to enable advanced operating scenarios
- **Advanced Scenarios and Control**
 - Establish high-performance integrated scenarios and the necessary control capabilities
- **ITER Support**
 - Utilize unique ST/NSTX parameters and capabilities to extend tokamak understanding for ITER

Key for labels used
in this presentation:

• Publication or presentation

Collaborating institution

• Major award for NSTX researcher

NSTX Research Milestone: R-***

DOE 3 Facility Joint Research Target: FY JRT**

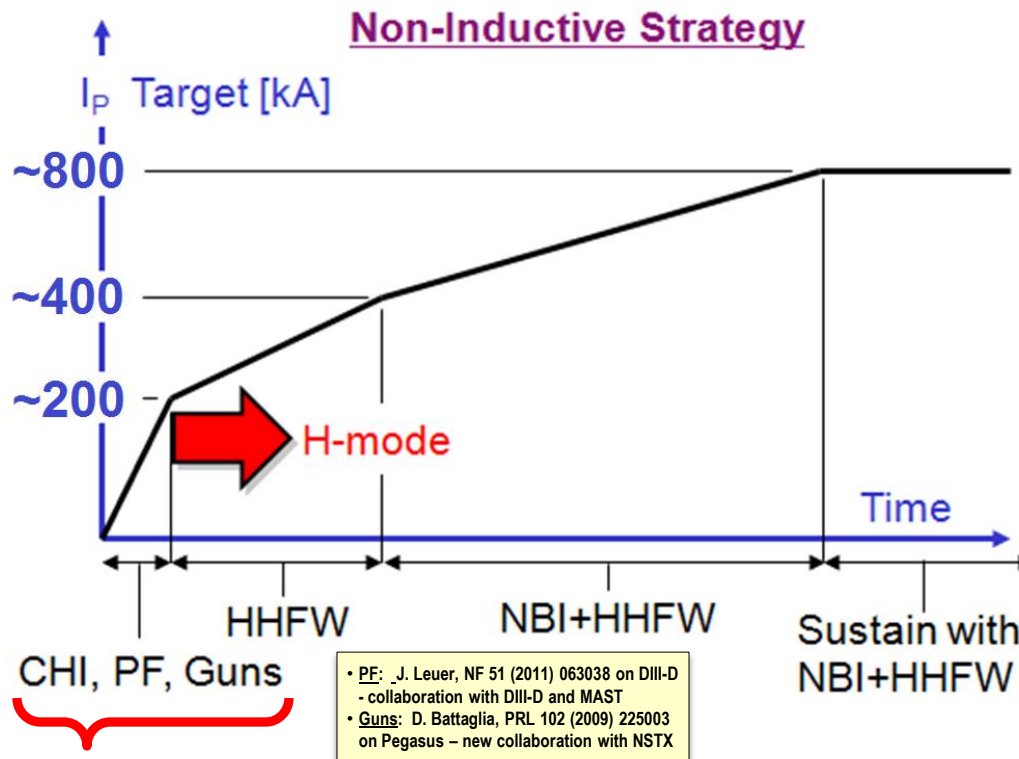
Plasma initiation with small or no transformer is unique challenge for ST-based Fusion Nuclear Science Facility

ST-FNSF has no/small central solenoid



Iron core and/or thin mineral insulated conductor transformer may be able to provide 1-2MA FNSF start-up current

- D. Gates, FED 86 (2011) 41-44
- Y-K.M. Peng, FST 56 (2009) 957



- Near-term Goal: ~0.3-0.4MA fully non-inductive start-up with CHI + fast wave
- Upgrade Goal: Use NBI current drive to ramp-up from 0.4MA to 0.8-1MA
 - More tangential 2nd NBI of upgrade has higher CD efficiency, better confinement at low I_p
- Upgrade goal is to provide physics basis for non-inductive ramp-up to high performance 100% non-inductive ST plasma → prototype FNSF

Solenoid-Free Plasma Start-up and Ramp-up

➤ Develop helicity injection and fast-wave heating for plasma current formation and ramp-up

5 year plan
timeline
and goals

	FY07	08	09	10	11	12	13
CHI		Test metal electrode operation Reduce absorber arcs, Use Liquid Li		Test Edge CD	Heat CHI target using ECH, then with HHFW. Test Relaxation CD	Increase current using 1T. Test synergism with Outer PF	Full integration with HHFW, NBI and outer PF startup
Plasma Guns		Supporting experiments on Pegasus. Design system for NSTX		Commission Plasma Guns	Test Plasma Gun Startup	Increase generated current using 1T TF. Test synergism with outer PF startup. Integrate with HHFW & NBI.	
Outer PF			Use CHI PI	Plasma Gun PI	Use ECH PI	Use 1T + ECH to adequately satisfy Lloyd parameter	
Ramp-up			Use Low Loop Voltage with Outer PF and Plasma Guns			Use 1T to achieve bootstrap overdrive	Use 2 nd NBI + 1T for Current Ramp-up demonstration
			Ramp from 250kA to 400-500kA with HHFW (FY10 milestone)		Sustain Ip at 500kA		

Progress and Plans

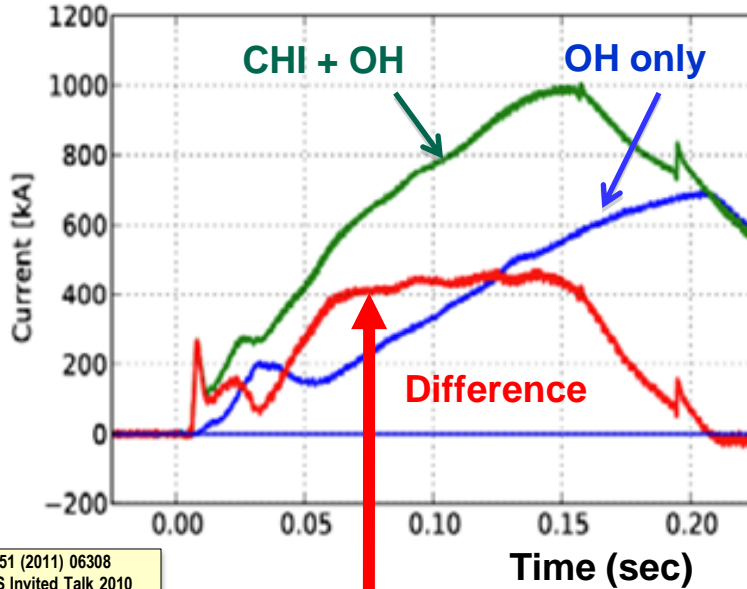
Gray italics indicates material provided in supplemental section

- **Coaxial Helicity Injection (CHI)**
 - Plasma current savings of up to 400kA using CHI start-up preceding inductive ramp-up
 - *Used CHI absorber coils to reduce/eliminate absorber arcs*
 - *Controlled density, reduced divertor impurities with evaporated lithium*
 - FY11-12: Test full metallic divertor: LLD Mo outboard + Mo tiles inboard (facility talk)
- **Plasma guns:** deferred – not technically ready
- **Outer PF:** deferred due to cost of ECH, collaborate on DIII-D
- **HHFW ramp-up:** antenna upgraded, utilized 2nd half of 2009 run
 - FY10: Heated 300kA ohmic target plasma to 3keV, 70% non-inductive fraction
 - FY11-12: Plan to increase power to 3-4MW level for 100% non-inductive, test ramp-up

Achieved substantial progress on Coaxial Helicity Injection (CHI) and fast wave heating of low-current plasmas in 2010

- Generated 1MA using 40% less flux than induction-only case
 - Low internal inductance ($I_i \approx 0.35$), and high elongation > 2
 - Suitable for advanced scenarios

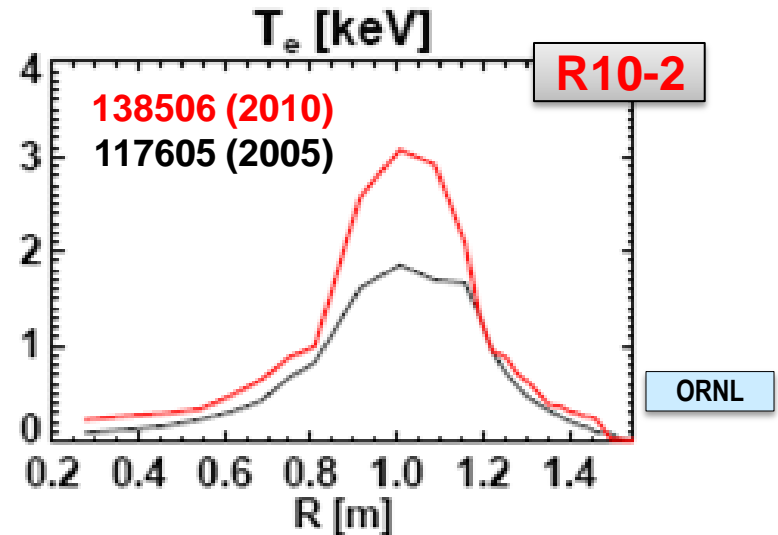
- Achieved high $T_e(0) \sim 3\text{keV}$ at $I_p=300\text{kA}$ w/ only 1.4MW HHFW
 - Previous best was $T_e(0) \sim 1.5\text{keV}$ at twice the RF power
 - Enabled by 2009 antenna upgrades



• B. Nelson, NF 51 (2011) 06308
 • R. Raman, APS Invited Talk 2010
 • R. Raman, PRL 104 (2010) 095003
 • D. Mueller, EPS Oral (2010)

Univ. Washington

$\Delta I_p = 400\text{kA}$ vs. 50kA in 2008



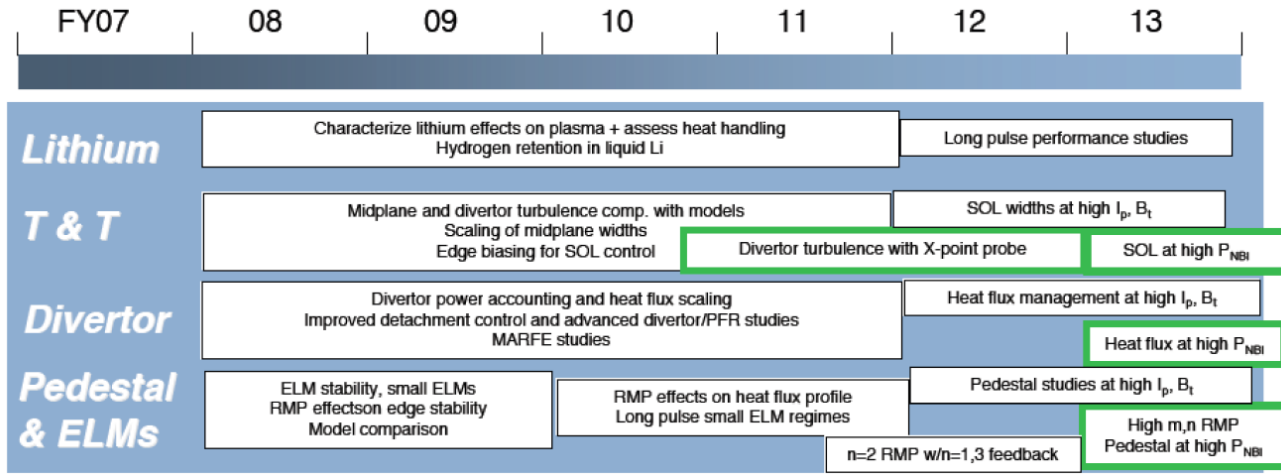
- Non-inductive fraction $\sim 60-70\%$ with 25-30% from RFCD from high $T_e(0)$
- Projects to $\sim 100\%$ NI at $P_{RF} = 3-4\text{MW}$

• **R12-2:** Test higher P_{RF} , HHFW heating of CHI-initiated plasmas

Lithium and Boundary Physics

➤ Assess lithium PFCs, develop high-flux-expansion divertors, understand edge transport/stability

5 year plan
timeline
and goals



Progress and Plans

Gray italics indicates material provided in supplemental section

- **Lithium Research:** Liquid Lithium Divertor (LLD) implemented in FY2010
 - LLD extensively tested: D pumping with LLD comparable to solid Li coatings
 - No evidence of Mo in plasma from LLD – preparing to test new Mo tiles on inboard divertor
- **Transport and Turbulence**
 - Heat flux width scalings determined - comparing to simulation, edge biasing has small effects
- **Divertor Physics**
 - Focusing on high-flux-expansion “snowflake” divertor to reduce heat-flux and impurities
 - *Partial detachment* and MARFE studies largely complete, power accounting studies planned
- **Pedestal and ELMs**
 - ELM stability modifications from lithium quantified, pedestal structure under study (FY11-12)
 - Assessed 3D field effects on pedestal, divertor (ITER section) - comparisons to theory ongoing

NSTX is a world leader in assessing lithium plasma facing components as a possible PMI solution for magnetic fusion

- **Solid Li surface coatings:** Pump D, increase confinement, stored energy, pulse length, eliminate ELMs, reduce core MHD instabilities

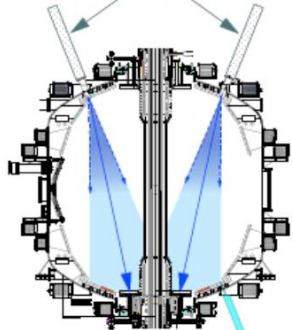
- H. Kugel, IAEA FEC 2010 Oral, FTP/3-6Ra
- H. Kugel, FED 85 (6) 865-873 (2010)
- M. Bell, PPCF 51 (12), (2009) 124054
- M. Bell, EPS Invited Talk 2009
- D. Mansfield, JNM 390-91, 764-767 (2009)
- H. Kugel, JNM 390-391, 1000-1004 (2009)

- **Liquid Lithium Divertor (LLD) motivation:** provide volume D pumping capacity (> solid Li coatings) to provide longer pumping duration + potential for handling high heat flux

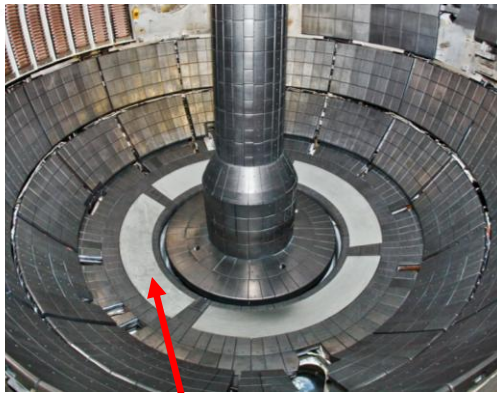
- JP Allain, NF 51 (2) 023002 (2011)
- V. Soukhanovskii, RSI 81 (10) 10D723 (2010)
- D. Stotler, Contrib. Plas. Phys. 50 (3-5) 368-373 (2010)
- H. Kugel, FED 84 (7-11), 1125-1129 (2009)
- R. Nygren, FED 84 (7-11), 1438-1441 (2009)

Sandia, ORNL, Purdue, LLNL

Dual Liquid Lithium Evaporator
For Li wall coatings
Now routinely used



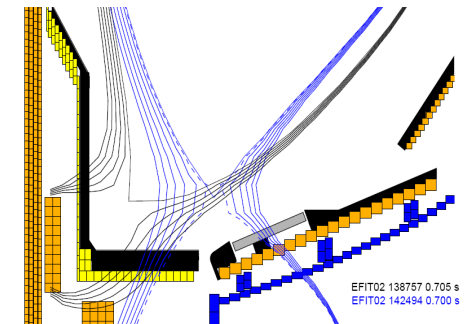
Li evaporators used to coat lower divertor, LLD



4 heatable LLD plates (Mo on Cu)
Surface temp: 160 – 350+ °C



LLD surface cross section:
plasma sprayed porous Mo

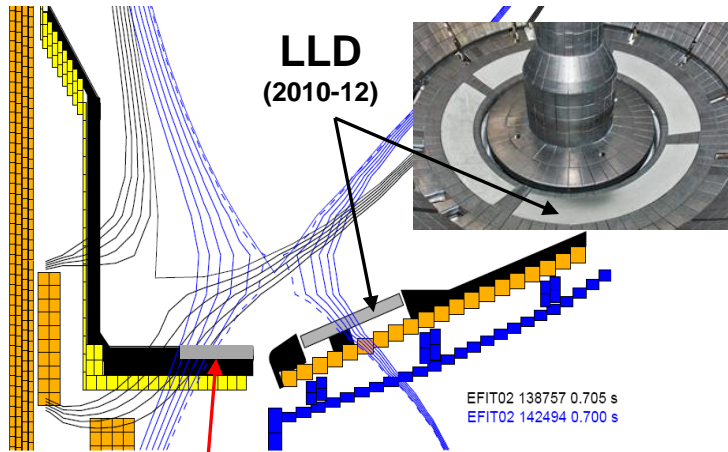


Controlled scans of strike-point location:
On inboard divertor
On LLD (outboard divertor)

EFIT02 138757 0.705 s
EFIT02 142494 0.700 s

- FY2010: First LLD tests - filled with 67g Li by evaporation (2x needed to fill porosity)
- **Brief results summary provided on next slide + more details in supplemental**

Operation with outer strike-point on Mo LLD (coated with Li) compatible with high plasma performance, low impurities

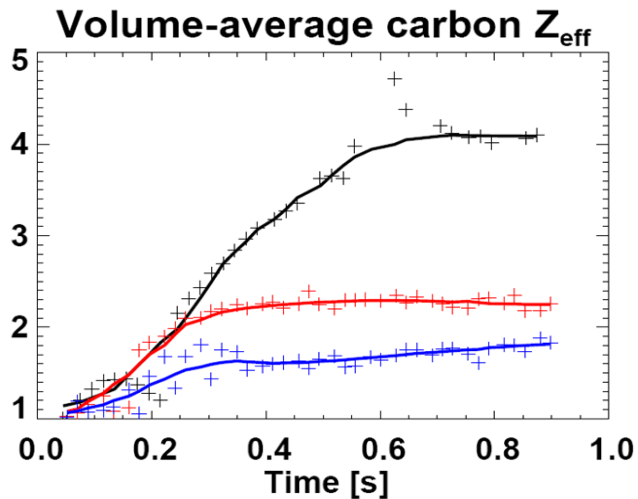


Mo tiles for upcoming run (2011-12)

LLD FY2010 results:

R10-2

- **LLD did not increase global D pumping beyond that achieved with LiTER**
 - Solid Li on C pumps D quite efficiently
 - Liquid Li reacts rapidly w/ background gases (LTX)
 - C on LLD may have impacted D pumping
- **Divertor T_e increases when $T_{LLD} > T_{Li-melt}$**
- **No evidence of Mo from LLD in plasma during normal operation**
- **Operation with strike-point (SP) on LLD reduced core impurities (due to ELMs?)**



◀ SP on inner carbon divertor (no ELMs)

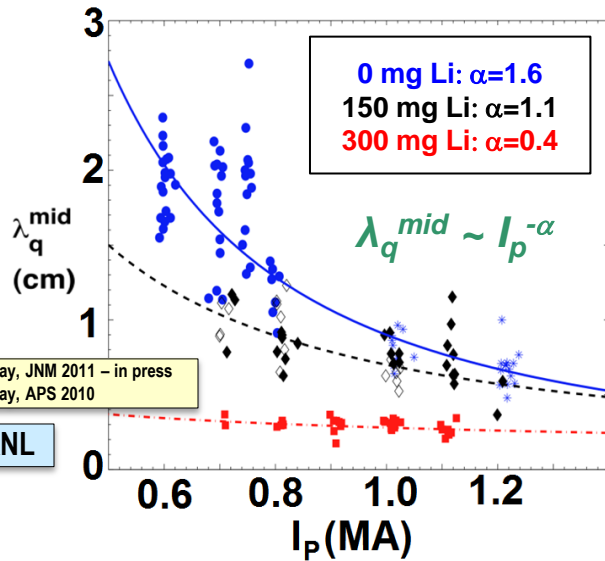
◀ SP on LLD, $T_{LLD} < T_{Li-melt}$

◀ SP on LLD, $T_{LLD} > T_{Li-melt}$ (+ fueling differences)

- **No ELMs, no \rightarrow small, small \rightarrow larger**
 \rightarrow High-Z impurities also reduced, $\beta_N > 4$ sustained

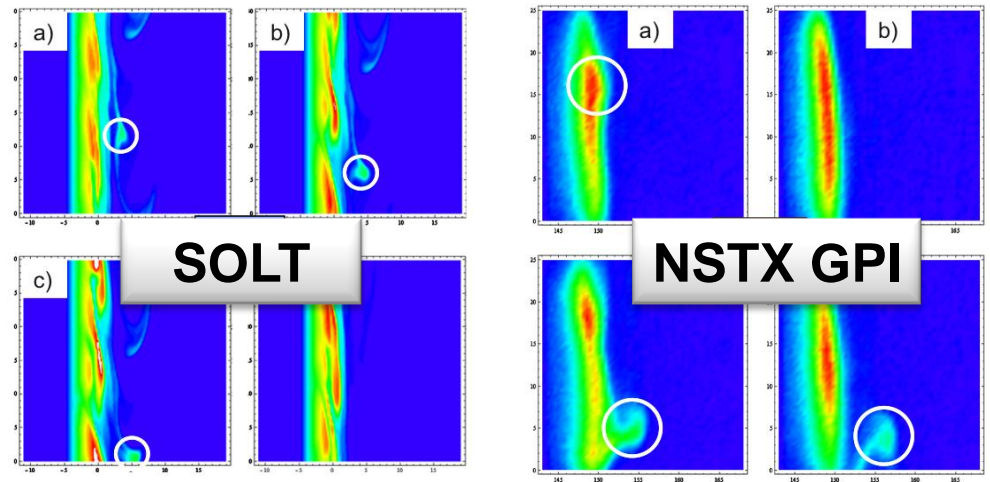
Need to separate effects of PFC material, ELMs - motivates Mo tiles on inboard divertor \rightarrow **facility talk**

NSTX has contributed strongly to **FY10 JRT** to characterize and understand divertor heat fluxes



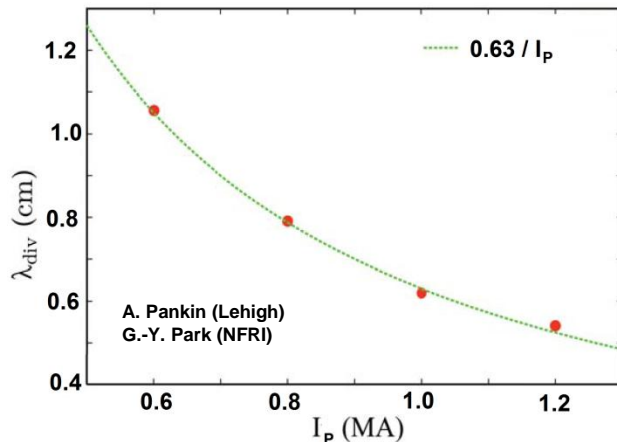
- Divertor heat flux width λ_q^{mid} decreases with increased plasma current I_p
 - Potentially major implications for ITER
 - NSTX: λ_q^{mid} further decreases with Li
 - Physics mechanisms not yet fully understood
- For NSTX-U parameters: $\lambda_q^{\text{mid}} = 3 \pm 0.5 \text{ mm}$

Blob formation in SOLT is similar to NSTX Gas Puff Imaging (GPI) diagnostic data

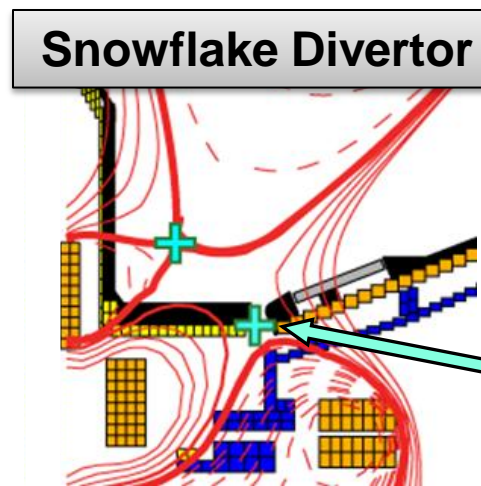
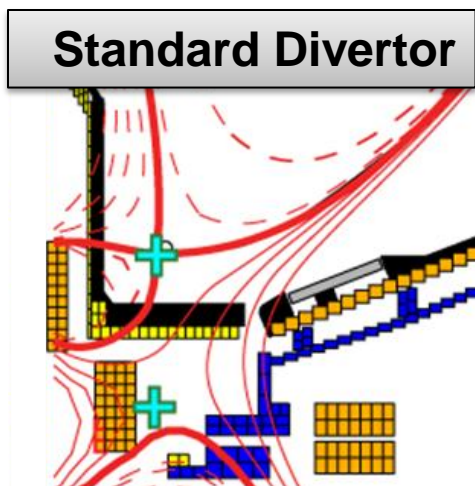


- SOLT scaling weaker than $1/I_p$

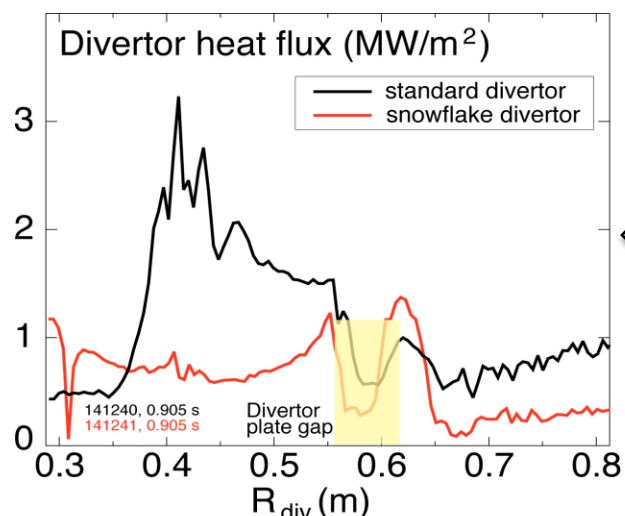
- XGC0 kinetic neoclassical consistent with $\sim 1/I_p$ scaling



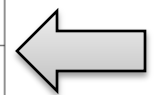
“Snowflake” divertor configuration provides significant divertor heat flux reduction and impurity screening



2nd X-point brought close to limiter boundary in divertor



Higher flux expansion (increased div wetted area)
Higher divertor volume (increased div. losses)



- **Peak heat flux reduced by 2-3×**
- Snowflake H-mode τ_E similar to standard divertor
- Core and pedestal carbon reduced by 50%
- Double-null snowflake is baseline divertor in Upgrade to maintain heat flux < 10MW/m² for 2MA, 15MW plasmas

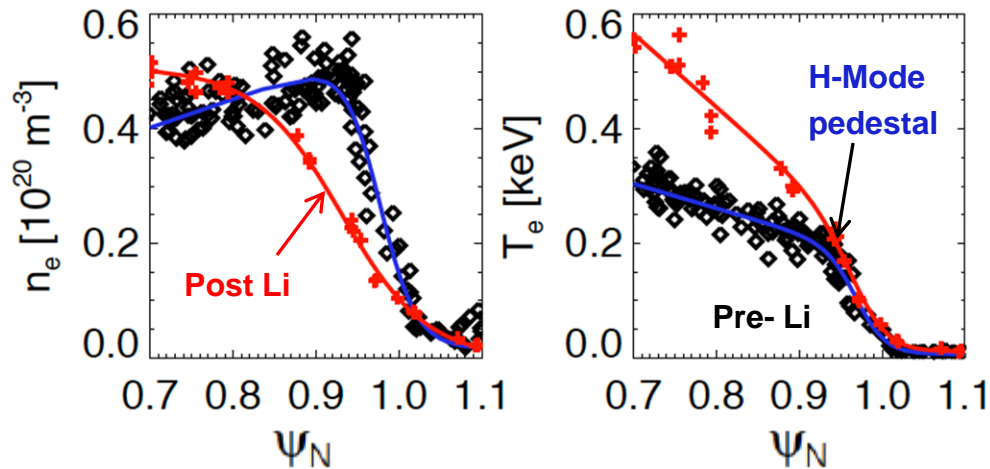
LLNL

• V. Soukhanovskii, NF 51 (1) 012001 (2011)
• V. Soukhanovskii, APS Invited 2010

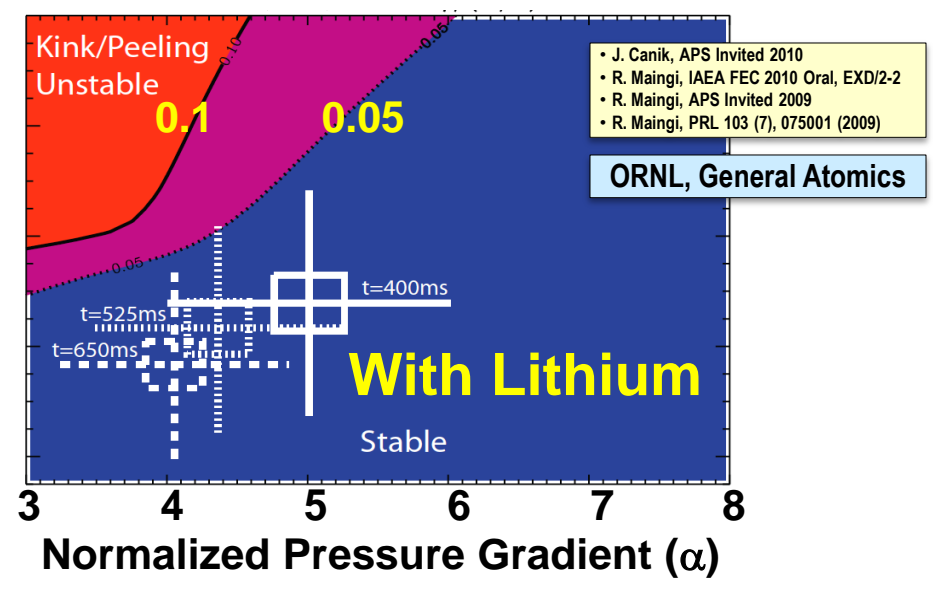
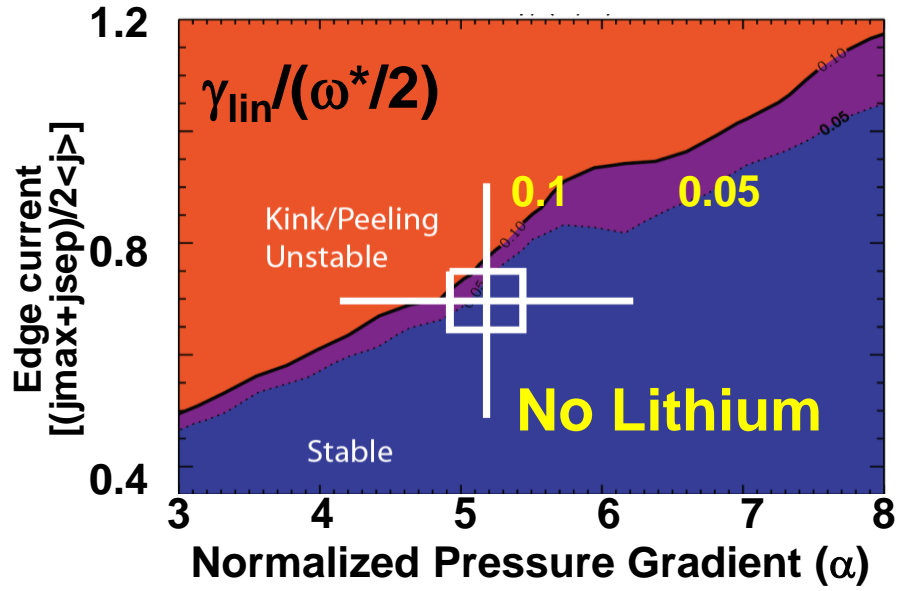
• V. Soukhanovskii: DOE Early Career Research Award - 2010

- **R11-3:** Assess control of U/D snowflake, possible synergies with Li, radiation

Li wall coatings broaden pedestal profiles, suppress ELMs – consistent with peeling-ballooning theory



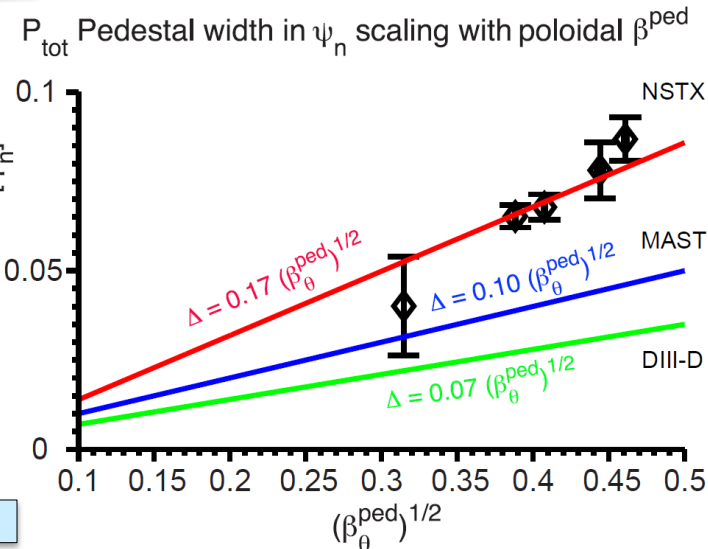
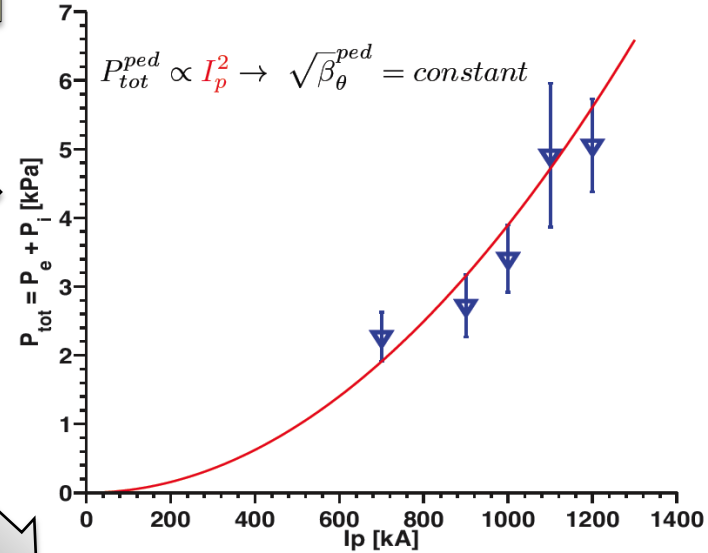
- Edge stability calculations (ELITE)
- Colors represent contours of ratio of linear mode growth rate to diamagnetic drift frequency
 - Pre-Li discharges close to kink/peeling stability boundary



Pedestal structure and underlying MHD/transport mechanisms being elucidated by **FY11 JRT** effort

• A. Diallo, submitted to NF (2011)

Peak total pedestal pressure scaling with I_p

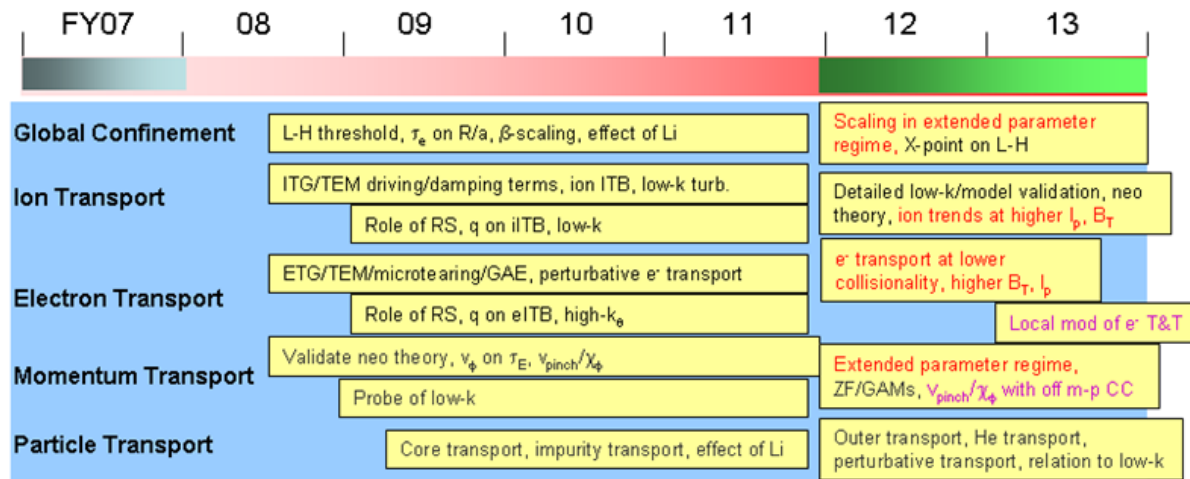


- Pedestal pressure scaling established
 - $P_{ped} \propto I_p^2$ and increases with triangularity
 - Builds up during ELM cycle, saturates at lower I_p late in ELM cycle
- Establishing pedestal width scaling
 - Analysis of pedestal data with peeling-ballooning theory (ELITE) ongoing
 - Initial calculations: ELM discharges are at kink/peeling boundary
- Planned research supporting **R11-4:**
 - Pedestal transport, turbulence, stability with 3D fields
 - Roles of particle and thermal heat transport

ORNL, General Atomics

Transport and Turbulence

➤ Measure, understand, predict instabilities responsible for ST transport, project to next-steps



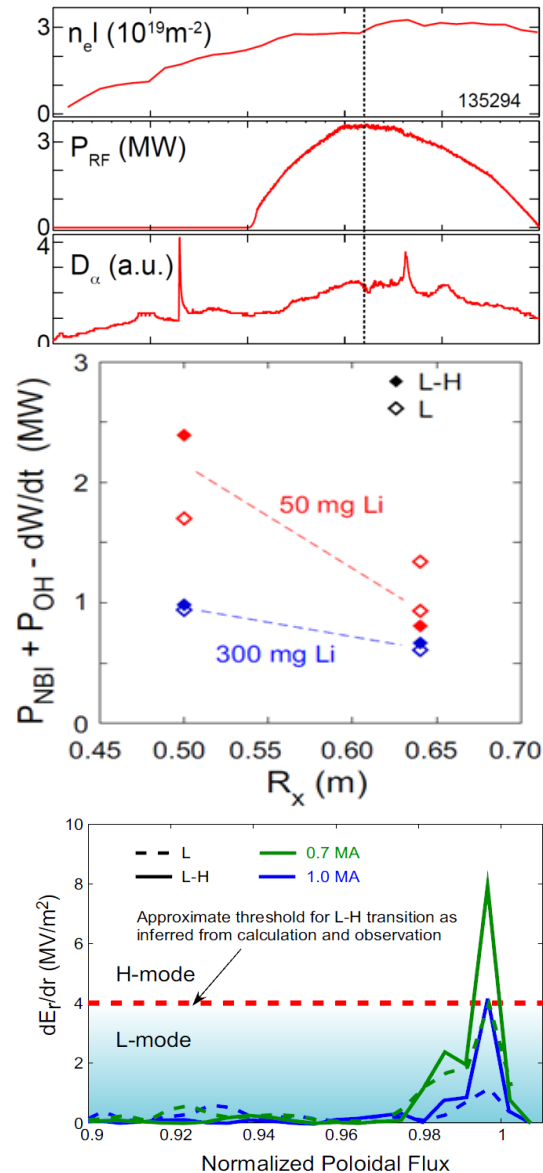
5 year plan
timeline
and goals

Progress and Plans

Gray italics indicates material provided in supplemental section

- **Global confinement**
 - Extensive L-H threshold studies performed, tests of effects of A, β , Li on confinement ongoing
- **Ion transport:** BES commissioned FY10 – will be used extensively in FY11-12
- **Electron transport**
 - ETG, micro-tearing, GAE, RS eITB experiments and gyro-kinetic modeling performed
- **Momentum transport**
 - Poloidal velocity measured, consistent w/ neoclassical - will improve edge resolution (FY11-12)
 - Initial momentum pinch studies completed/published – will revisit with low-k BES data (FY11-12)
- **Particle transport**
 - Impurity ion (Ne) transport consistent w/ neoclassical – large edge PS transport from high q
 - Beginning to explore D, C, Li transport with kinetic neoclassical transport with XGC-0

L-H threshold experiments in NSTX have explored a wide range of ITER and ST-relevant issues



- Species dependence

- $P_{LH}(\text{He}) \sim 1.2-1.4 P_{LH}(\text{D})$: RF-heated
- $H_{98y,2} \sim 1$ with no ELMs after L-H transition

- Non-axisymmetric field application

- P_{LH}/n_e increased $\sim 65\%$ with \sim few Gauss $n=3$ fields

- Plasma configuration

- Lower P_{LH} at increased major radius of X-point

- Lithium coatings **R10-3**

- P_{LH}/n_e decreased by $\sim 35\%$ with lithium coating
- Additive influence for R_x , USN vs. LSN

- Strong I_p dependence (ST effect)

- lower P_{LH} with lower I_p
- XGC0 calculations show larger E_r shear at lower I_p

- Role of ion-scale turbulence*

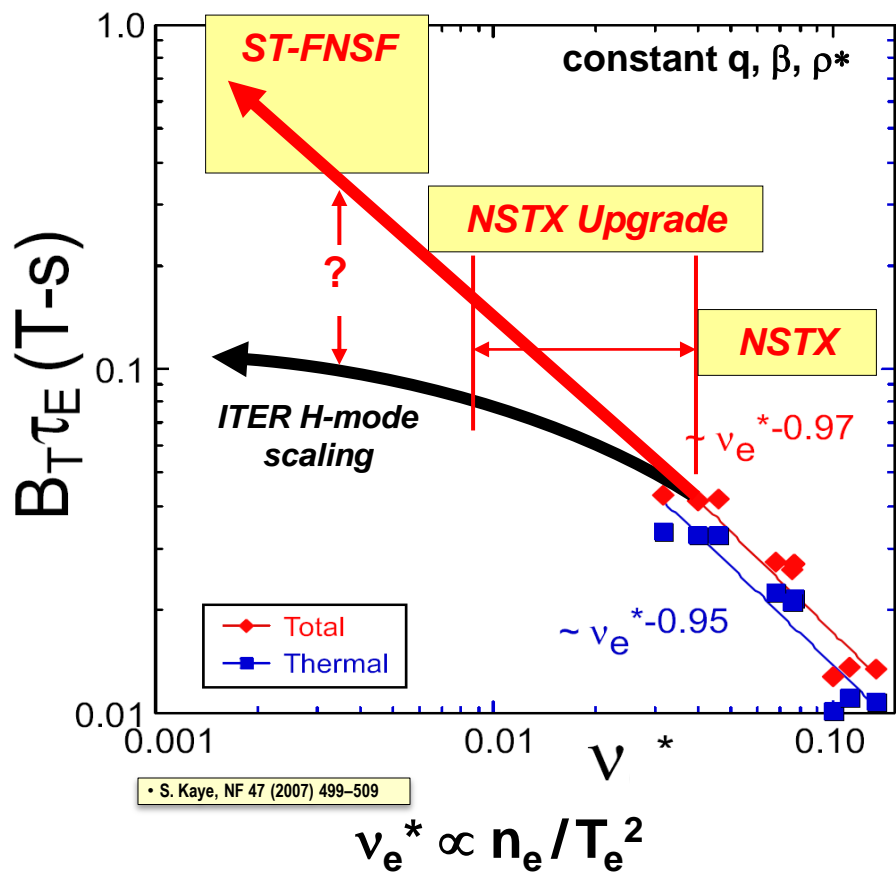
- Beam Emission Spectroscopy now being utilized

*More info on turbulence at L-H threshold in supplemental

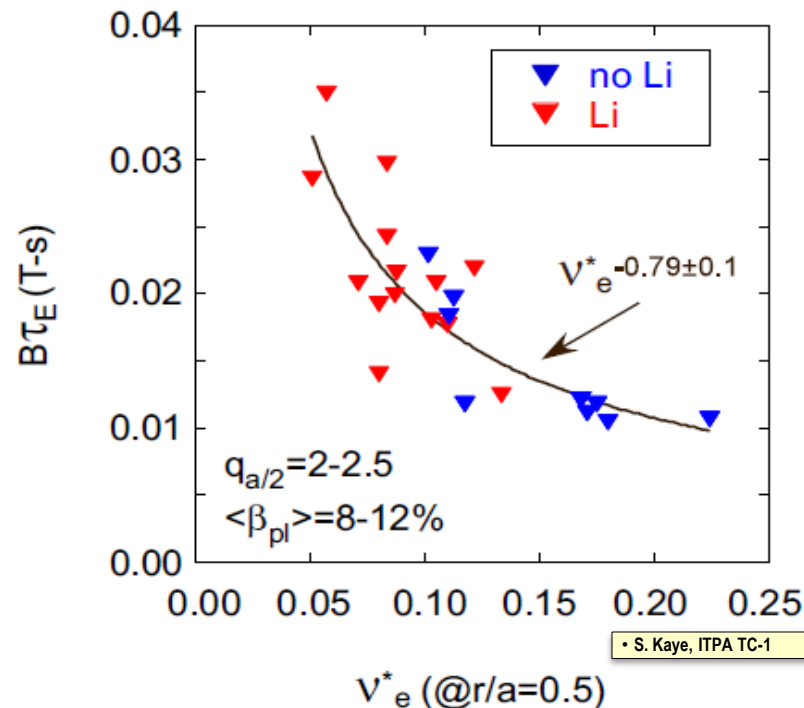
• S. Kaye, submitted to NF 2011
 • S. Kaye, IAEA FEC 2010 Oral, EXC/2-3Rb
 • R. Maingi, NF 50 (2010) 064010

ORNL, Univ. Wisconsin

NSTX is continuing to explore the favorable collisionality scaling ($\propto 1/v_{e^*}$) of ST energy confinement



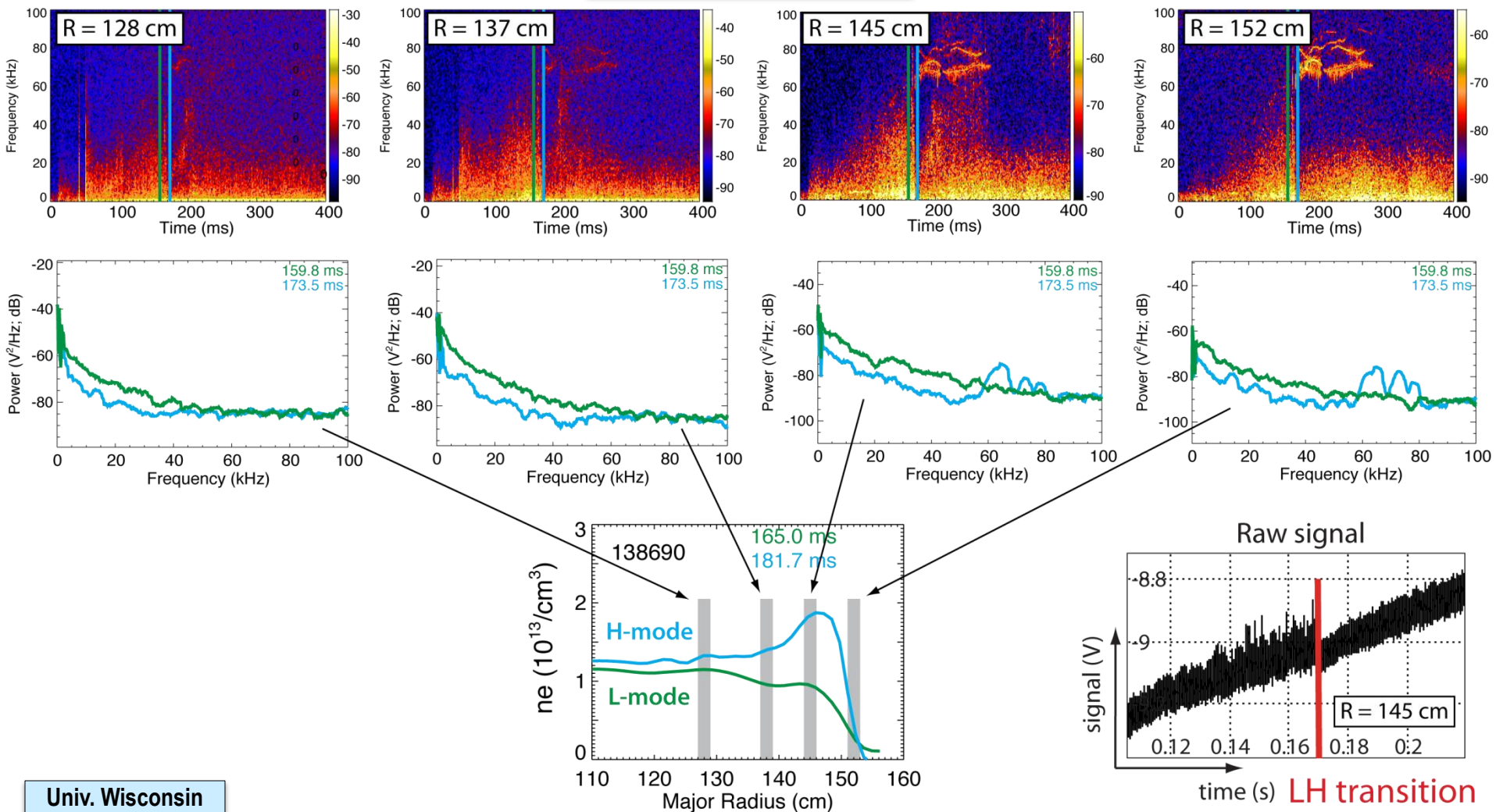
- Increased τ_E with lithium may be result of reduction in ν_e^*



- Expts also show weak β scaling: $\tau_{E-th} \sim \beta^{-0.12, -0.25}$ (no Li, with Li)
 - Important for high- β ST and AT scenarios
 - Beta scaling strong function of ELM character – Type III ELMs \rightarrow strong degradation

New BES commissioned in 2010: observed decrease in fluctuations at L-H transition from edge to core regions

R11-1, FY12 JRT

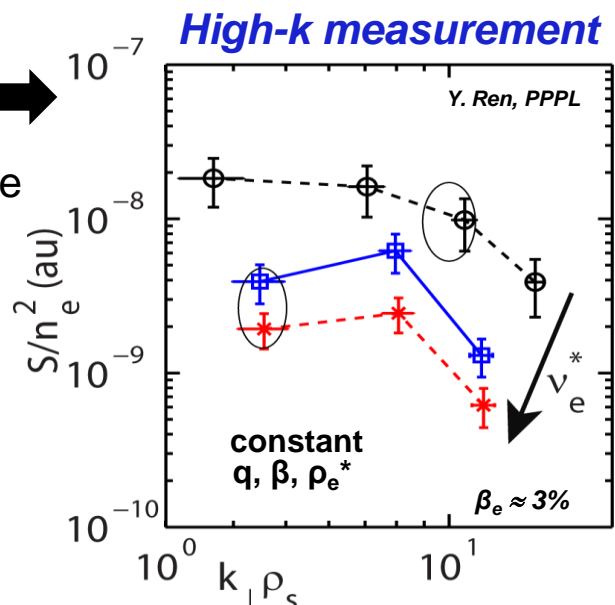


Univ. Wisconsin

R. Fonck, G. McKee, D. Smith, and I. Uzun-Kaymak (UW-Madison) and B. Stratton (PPPL)

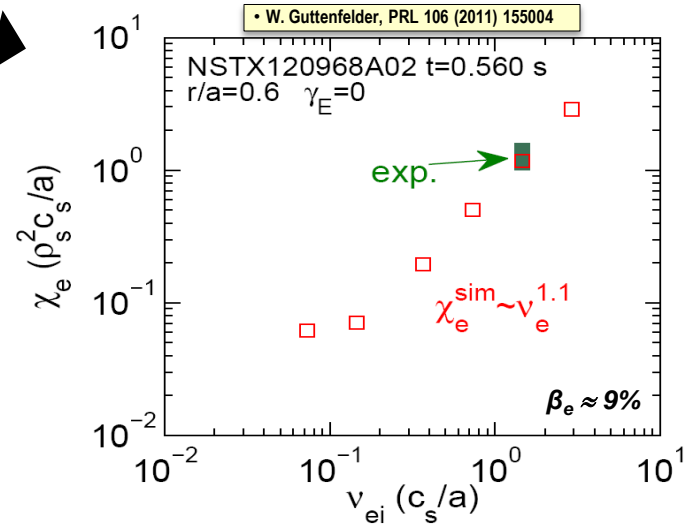
NSTX turbulence measurements and simulations are advancing the understanding of the collisionality scaling of τ_E

- High-k scattering measurements show increase at lower v_e^* , β_e
- Seemingly inconsistent with global confinement scaling from NSTX, MAST
 - Pursuing non-linear gyro-kinetic simulations with synthetic diagnostics to interpret results



General Atomics

- Non-linear GYRO simulations of lower-k μ -tearing predict $\chi_e \propto v_e^*$
 - Predominantly EM turbulence – result of high β
- What is role of μ -tearing in ST transport?

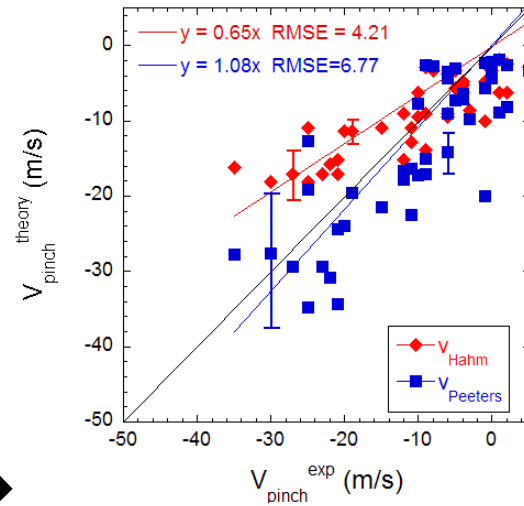
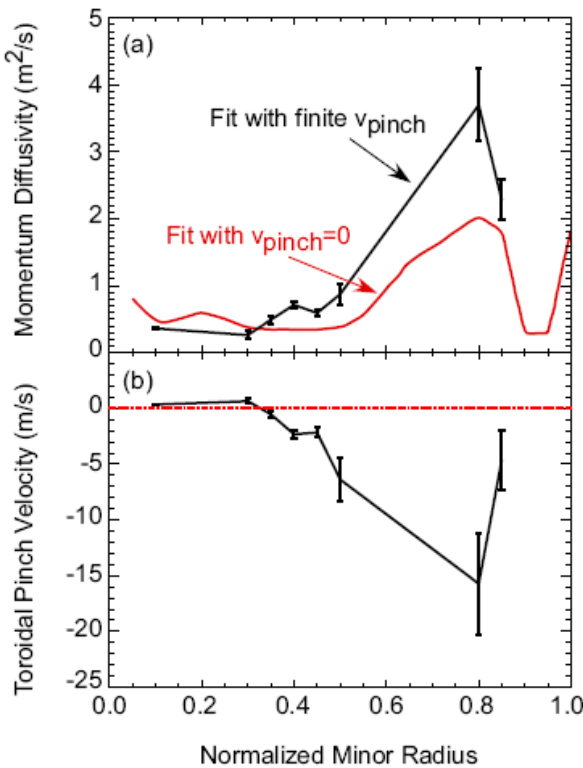


- **R11-1, FY12 JRT:** High-k scattering + 2D BES will measure full k-spectrum of fluctuations

Momentum transport may be best probe of low-k turbulence

- In NSTX, $\chi_\phi^{ss} < \chi_i, \ll \chi_e$
- Perturbative momentum transport studies using magnetic braking indicate significant inward pinch

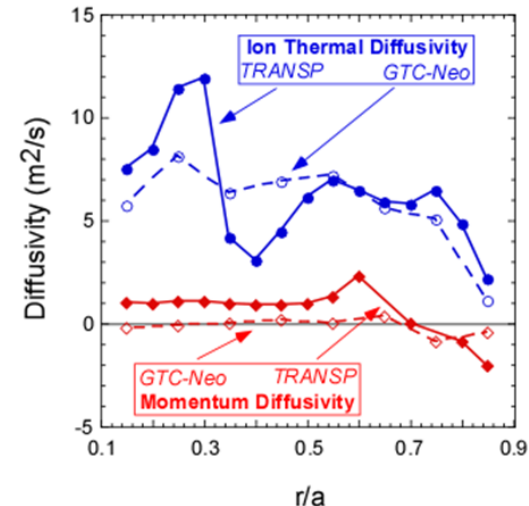
Theory predicts v_{pinch}/χ_ϕ ratio based on low-k turbulence – in agreement w/ expt



$$\Gamma_{i,turb} < \Gamma_{i,neo} \text{ while } \Gamma_{\phi,turb} > \Gamma_{\phi,neo}$$

Residual low-k fluctuations predicted to drive anomalous momentum transport

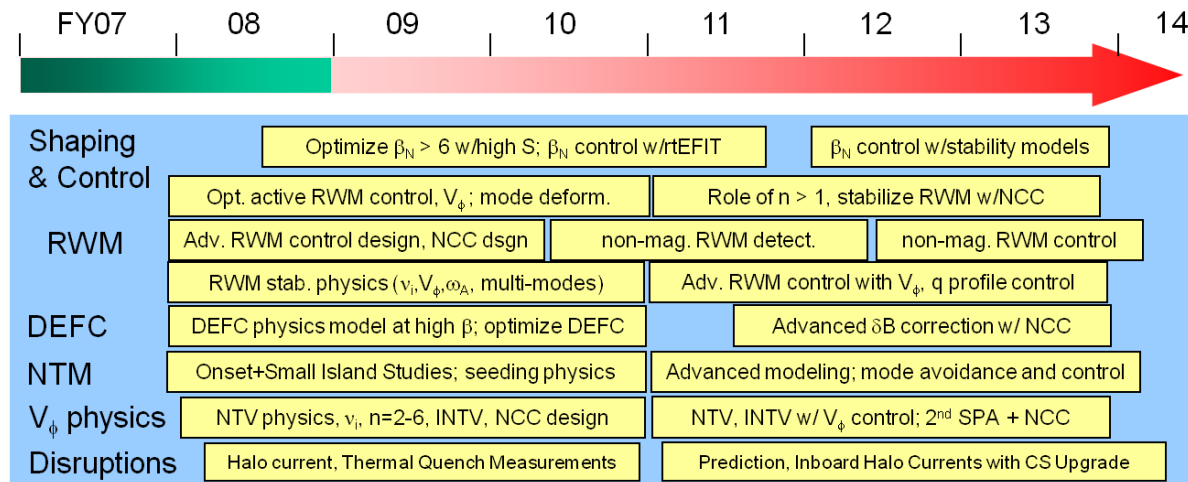
Test with non-linear gyro-kinetic codes + BES **R11-1**



- W. Solomon, APS Invited Talk 2010
- S. Kaye, NF 49, (2009) 045010
- W. Wang, PRL 102, (2009) 035005

Macroscopic Stability

➤ Develop predictive capability for accessing, controlling, sustaining very high plasma pressure



5 year plan timeline and goals

Progress and Plans

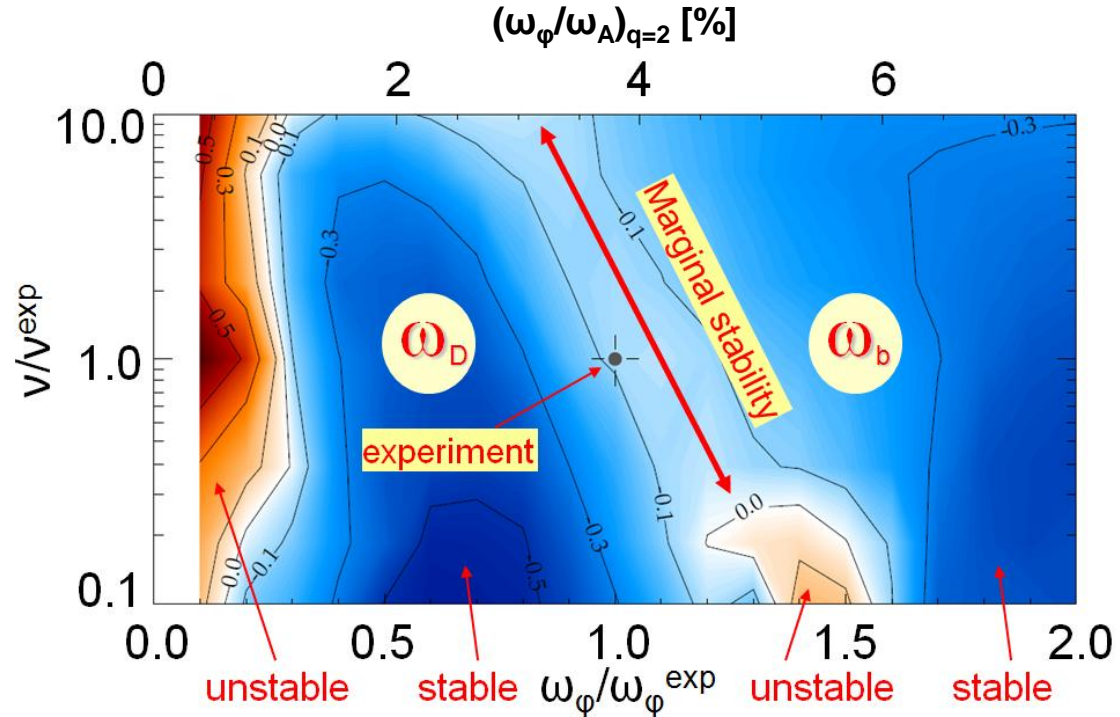
Gray italics indicates material provided in supplemental section

- **Shaping and β control:** (see Advanced Scenarios and Control section)
- **Resistive wall mode (RWM)**
 - Kinetic resonances found to play key role, advanced state-space controller successfully tested
- **Dynamic Error Field Correction (DEFC)**
 - *Improved sensor compensation \rightarrow feedback on B_R component of RFA/RWM (+ B_p sensors already used)*
- **Neoclassical Tearing Modes (NTM)**
 - Marginal island width scales with poloidal ion Larmor radius – joint studies with DIII-D
- **Toroidal rotation physics:** rotation control planned for FY2012
 - Incorporated plasma response via 3D perturbed equilibrium, studying (offset) rotation effects
- **Disruptions:**
 - Halo currents characterized, thermal quench studies started, *mitigation experiments planned*

Resistive Wall Mode (RWM) stability depends on thermal kinetic resonances and fast-ion content R09-1

Calculated growth rate γ_{τ_w} contours vs collisionality ν and rotation frequency ω_ϕ

- Observe that RWM can be unstable despite significant plasma rotation
- **MISK code** predicts stabilization of RWM from:
 - precession drift resonance ω_D at low rotation
 - bounce resonance ω_b at high rotation
- Plasma marginally unstable at intermediate rotation
- Stability to RWM improves with increased fast ion content
 - Developing kinetic damping models for arbitrary fast-ion distributions
 - Lower rotation speed required to stabilize RWM at higher FI density
 - Important for high-beta ST-FNSF and ITER advanced scenarios



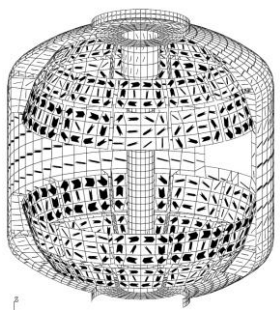
- J. Berkery, PRL 106 (2011) 075004
- S. Sabbagh, APS Invited Talk 2010
- J. Berkery, PRL 104 (2010) 035003
- J. Berkery, APS Invited Talk 2009
- S. Sabbagh, NF 50 (2010) 025020

Columbia Univ.

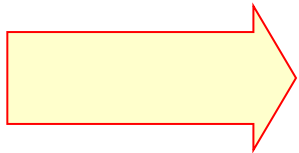
NSTX is first tokamak to implement advanced RWM state-space controller, and has utilized it to sustain high β_N

R10-1

Full 3-D model



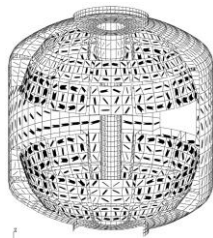
~3000+ states



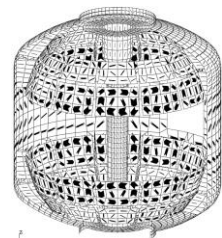
State reduction (< 20 states)

RWM eigenfunction (2 phases, 2 states)

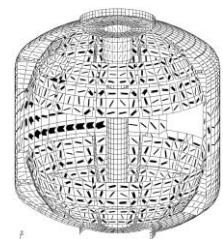
$$(\hat{x}_1, \hat{x}_2)$$



$$\hat{x}_3$$



$$\hat{x}_4$$



\hat{x}_N
truncate

- Device R, L, mutual inductances
- Instability B field / plasma response
- Modeled sensor response

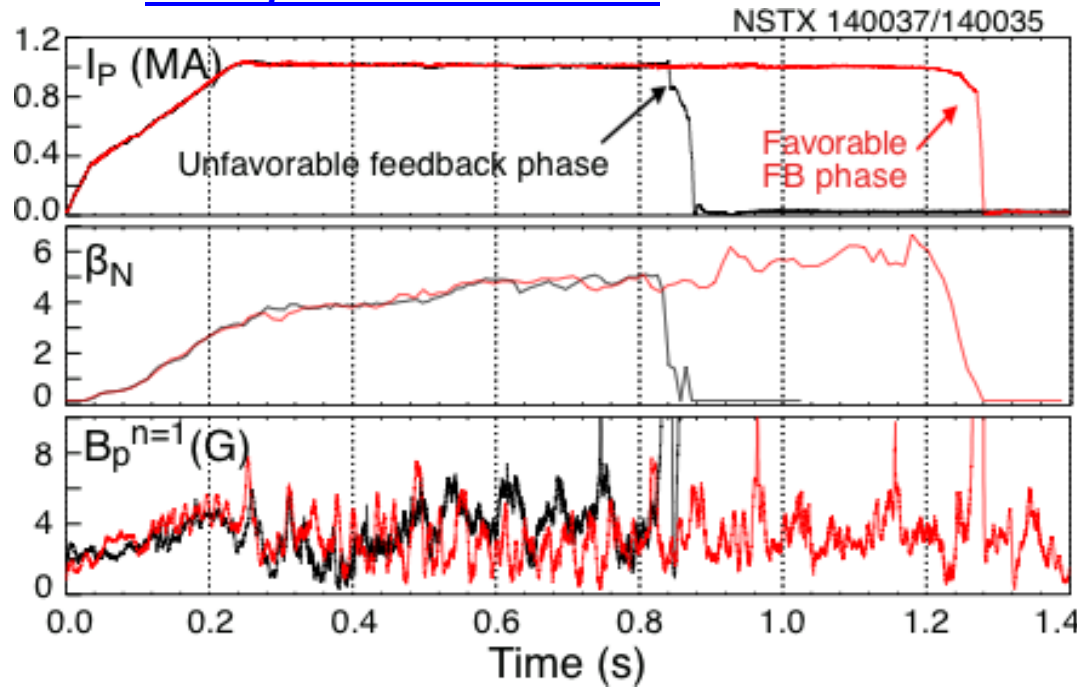
- **Controller can compensate for wall currents**
 - Including mode-induced current
 - Examined for ITER
- **Successful initial experiments**
 - Suppressed disruption due to n = 1 applied error field
 - Best feedback phase produced long pulse, $\beta_N = 6.4$, $\beta_N / I_i = 13$

• O. Katsuro-Hopkins, NF 47 (2007) 1157

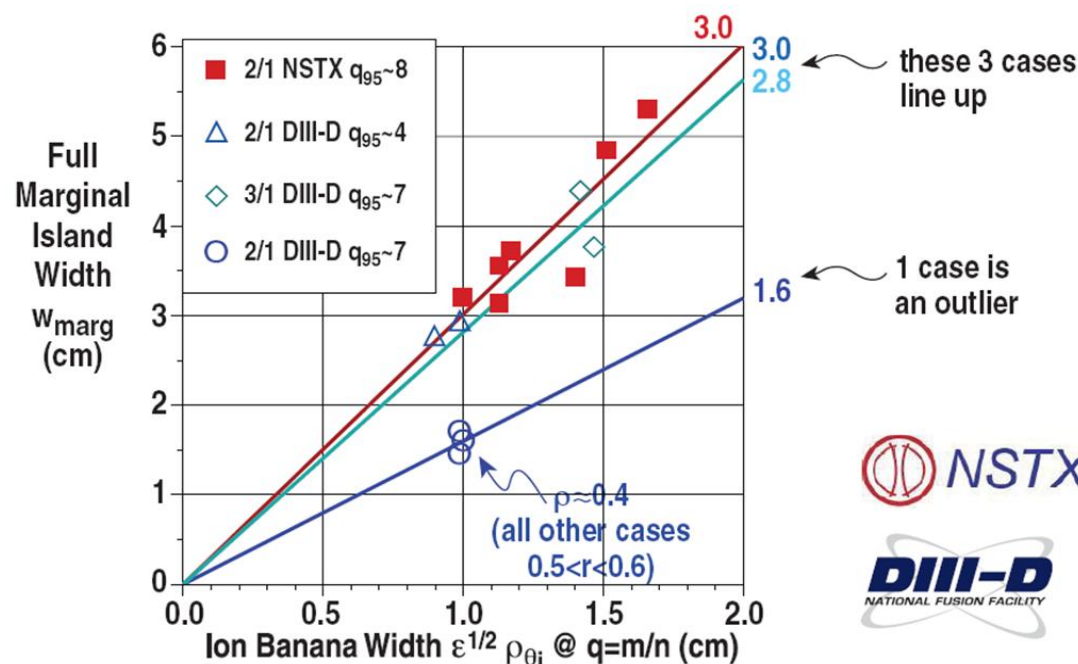
• S. Sabbagh, APS Invited Talk 2010
• S. Sabbagh, IAEA FEC 2010 Oral EXS/5-5

Columbia Univ.

State space feedback with 12



Measure of the marginal island width gives information on small island stabilizing physics

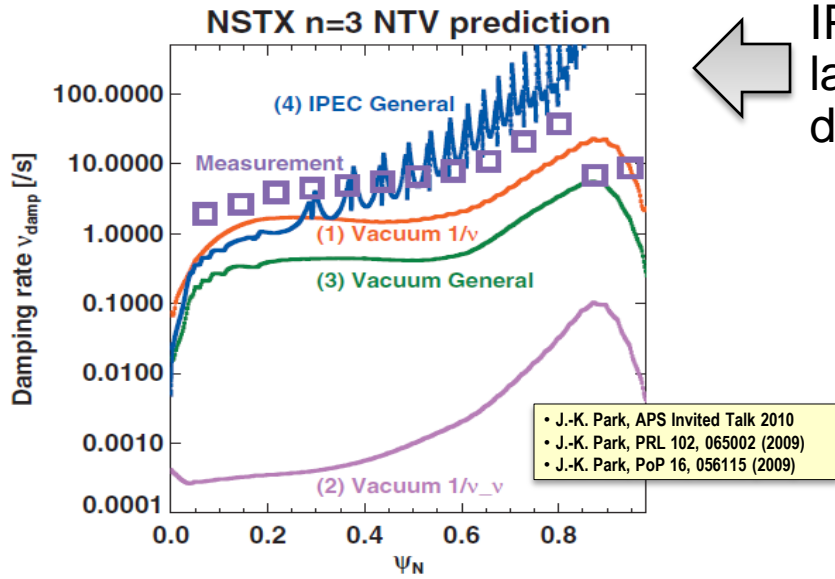


- R. La Haye, APS DPP 2010
- ITPA MHD 2010 MDC-4

- Empirically, marginal island width three times ion banana width
 - ★ except outlier is DIII-D 2/1 mode closer to axis at higher q_{95}

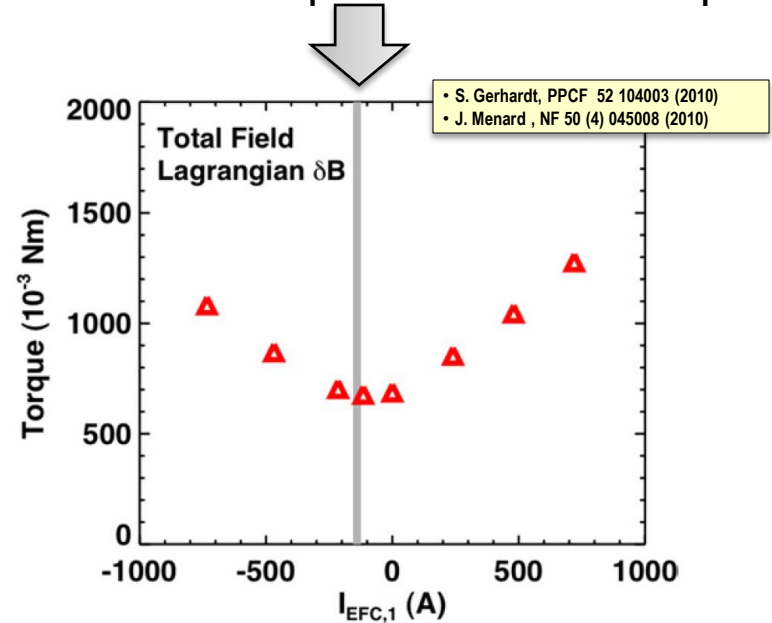
- Balance of terms in modified Rutherford equation shows that curvature term dominates over Δ' for NSTX plasmas; curvature term negligible for DIII-D plasmas
- Studying error field threshold scaling for mode locking in H-modes (Buttery; J-K Park)
- **2011-12 Plans:** Extend present mode locking density, and NTV offset rotation studies to low-torque (RF-heated) plasmas

Generalized theory of Neoclassical Toroidal Velocity (NTV) developed, linked to Ideal Perturbed Equilibrium Code (IPEC)



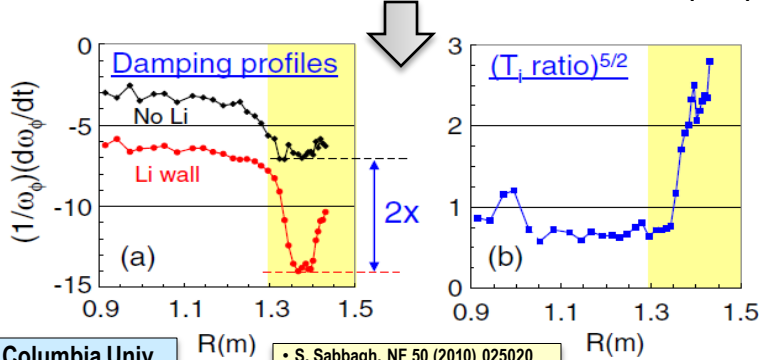
IPEC+NTV rotation damping predictions largely consistent with NSTX and DIII-D data (except for region near plasma edge)

Optimal n=3 error field correction consistent with minimization of predicted NTV torque



• J.-K. Park: Marshall N. Rosenbluth Outstanding Doctoral Thesis Award - 2010
 • J.-K. Park: DOE Early Career Research Award - 2010

Damping scales as expected $\propto p_i/v_i \sim T_i^{5/2}$

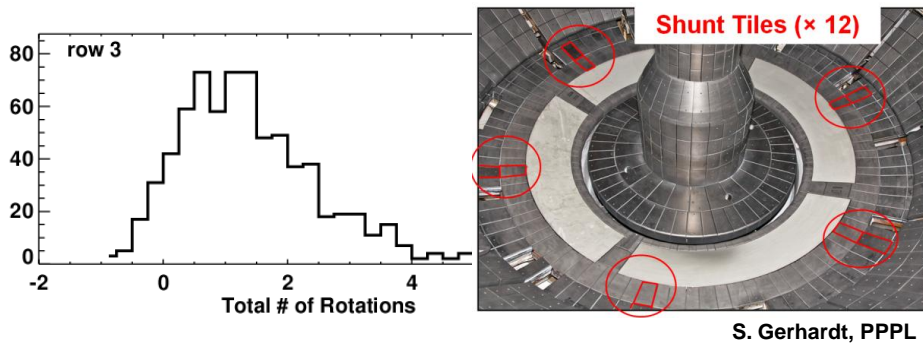


- Increased NTV damping at reduced collisionality, NTV dependence on $E \times B$ rotation important for ST-FNSF, ITER

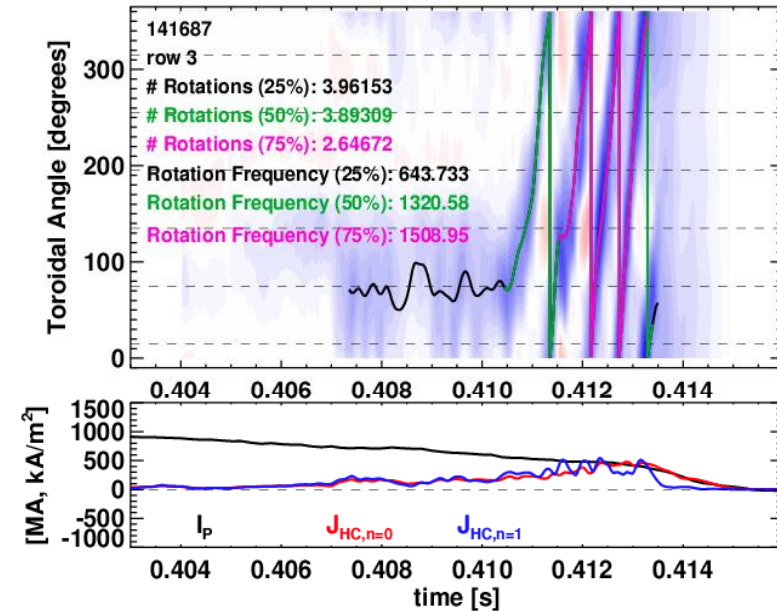
NSTX is addressing disruption physics for ITER and FNSF

• Example: halo current (HC) dynamics

- HC rotation is a key issue for ITER: mechanical resonances could cause significant damage
- NSTX studying parametric dependencies of the $n=1$ HC magnitude and rotation dynamics



Contours of halo current flowing into the lower divertor of NSTX



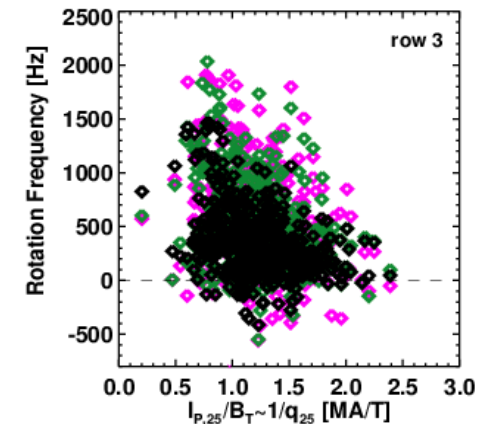
• Other key contributions:

- Current quench database physics
- Divertor heat loading with fast dual-band IR
- Fast and slow $n=1$ control, and rotation profile optimization, for avoidance of disruptive MHD
- 2011-12 – New disruption mitigation studies: Optimization of poloidal location of MGI

ORNL

Columbia University

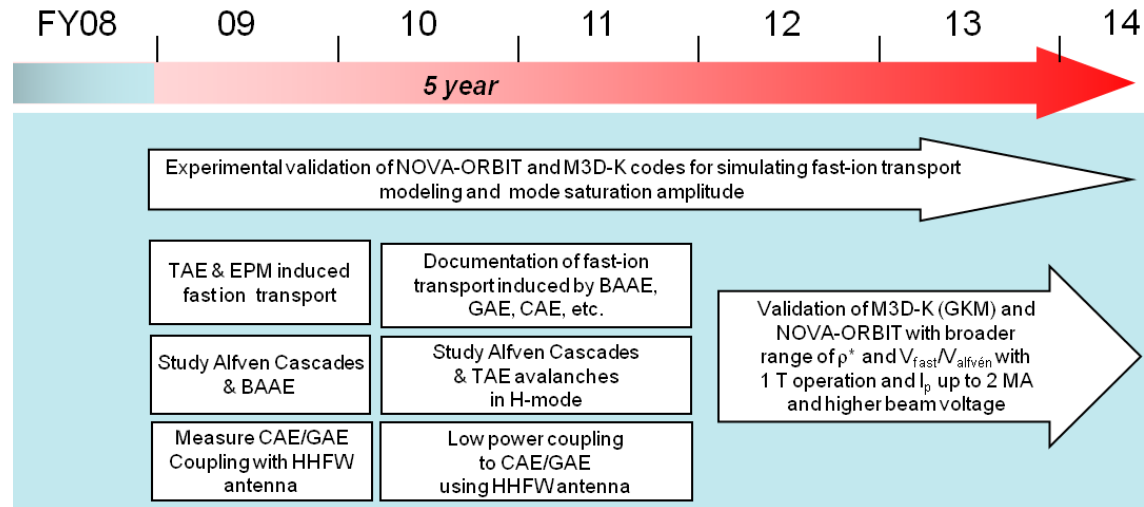
Univ. Washington



**More info on MGI experimental plans in supplemental*

Energetic Particle Physics

- Establish predictive capability for fast-ion transport caused by *AE for ST, burning plasma



**5 year plan
timeline
and goals**

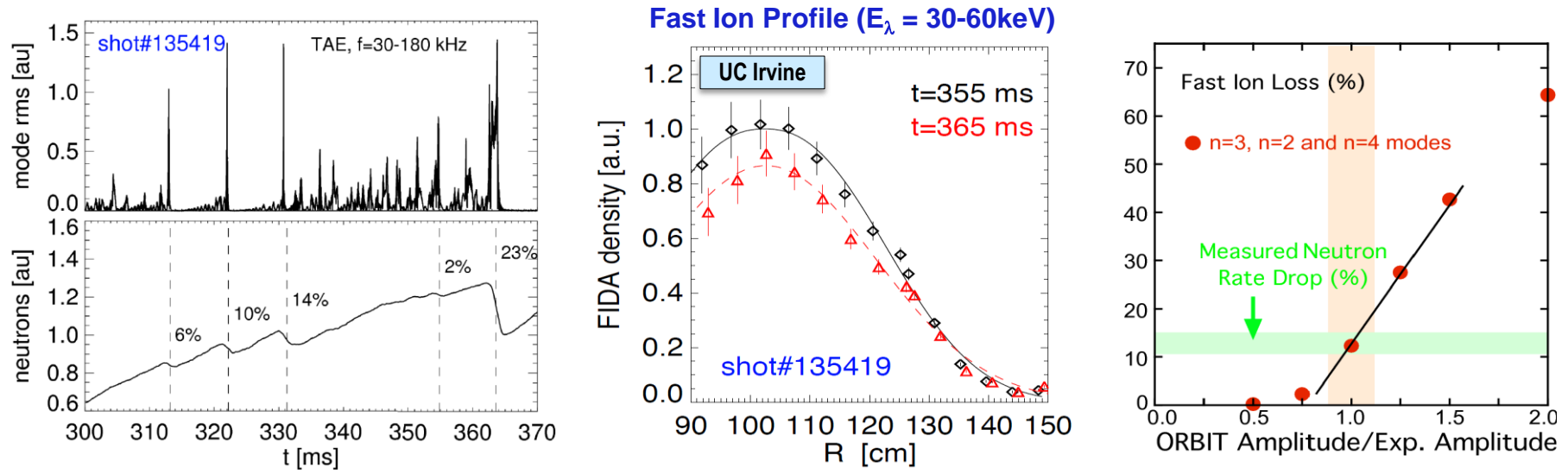
Progress and Plans

*Gray italics indicates
material provided in
supplemental section*

- **Model validation:**
 - TAE-avalanche induced neutron rate drop modeled successfully using NOVA+ORBIT
 - GAE-induced electron transport simulated with GAE model, high-k data, ORBIT calculations
 - *HYM code (fully kinetic ions) calculations of GAE eigenstructure consistent with experiment*
 - *Sub-cyclotron frequency modes are driven unstable via Doppler-shifted cyclotron resonance*
 - *Simulations show nonlinear saturation of GAEs due to particle trapping*
- **Upcoming experiments will utilize new diagnostics, tools**
 - BES: preliminary measurements of GAE eigenstructure in 2010 – extend in FY11-12
 - New tangential + existing perpendicular fast-ion D_α (FIDA) diagnostic for improved $f(v)$
- **Active coupling to *AE:** HHFW antenna usage deferred
 - Dedicated prototype TAE antenna to be commissioned and tested in FY11-12

TAE-avalanche induced neutron rate drop modeled successfully using NOVA and ORBIT codes R09-2

- Toroidal Alfvén Eigenmode (TAE) avalanches in NBI-heated plasmas associated with transient reductions in D-D (beam-target) neutron rate



- Change in beam-ion profile measured with Fast-ion D_α (FIDA)
- Modeled using NOVA-K + ORBIT codes
 - Mode structure obtained by comparing NOVA calculations w/ reflectometer data
 - Fast ion dynamics in the presence of TAEs calculated by guiding-center code ORBIT

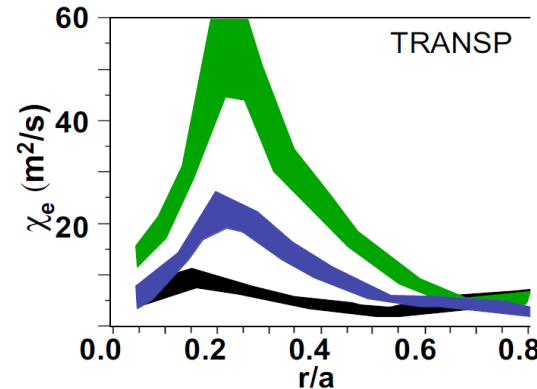
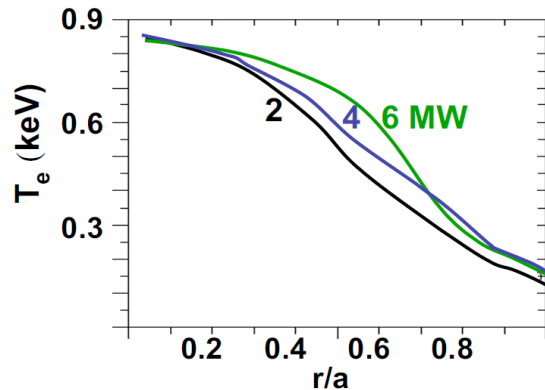
IR12-2: Improve predictive capability for TAE/GAE/CAE with self-consistent and advanced codes (M3D-K, HYM, SPIRAL)

- A. Bortolon, RSI 81 (2010) 10D728
- M. Podestà, PoP 16 (2009) 056104
- E. Fredrickson, PoP 16 (2009) 122505
- M. Podestà, PoP 17 (2010) 122501

UCLA

- G.-Y. Fu, IAEA-FEC 2010 THW/2-2Rb
- E. Fredrickson, IAEA-FEC 2010 EXW/P7-06
- N. Gorelenkov, PoP 16 (2009) 056107

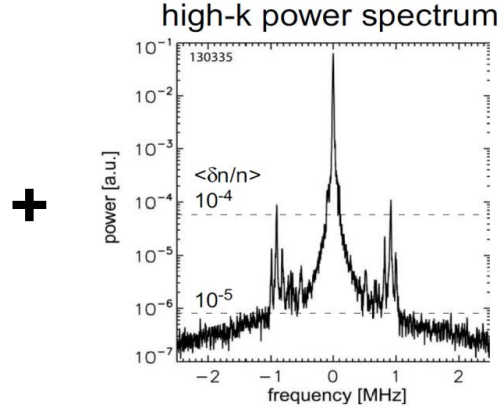
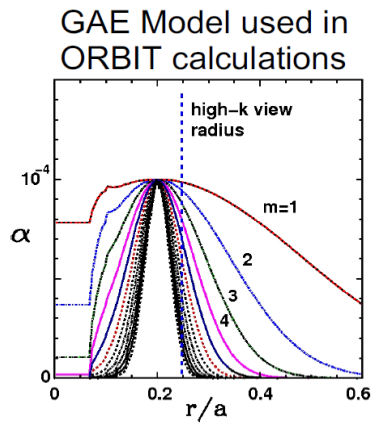
Global Alfvén Eigenmodes (GAE) candidate to explain high core electron thermal transport rates in NBI-heated H-modes



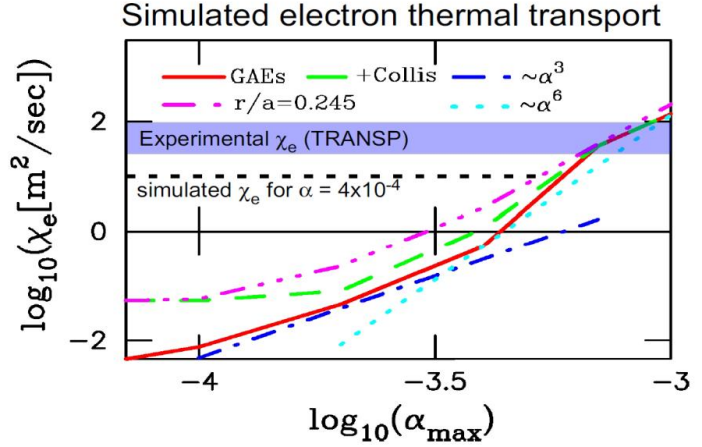
• K. Tritz, APS Invited Talk 2010
 • N. Gorelenkov, NF 50 (2010) 084012
 • D. Stutman, PRL 102 (2009) 115002

Johns Hopkins Univ.

- GAE model + high-k δn + ORBIT modeling roughly consistent w/ experiment:



$\langle \delta n_{rms} / n \rangle \sim 1.5 \times 10^{-4} \rightarrow \text{local } \delta n / n \sim 9 \times 10^{-4}$



- Also exploring coupling of *AE to other modes:
 - GAE/CAE can sometimes trigger TAE (via fast ion redistribution?)
 - TAE/EPM can interact with low-freq kink-like modes, impact rotation

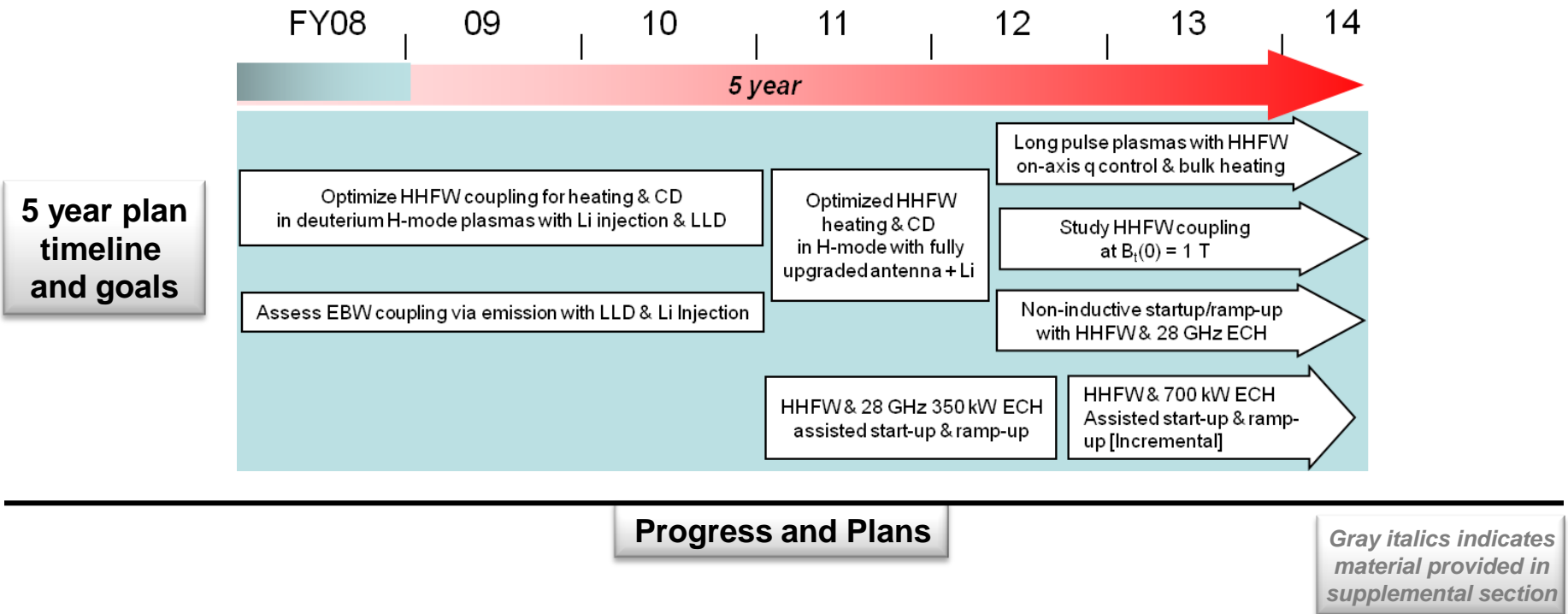
UCLA, UC Irvine

• E. Fredrickson, NF (in preparation)
 • E. Fredrickson, IAEA FEC 2010, EXW/P7-06

• M. Podestà, NF 51 (2011) 063035
 • M. Podestà, IAEA FEC 2010, EXW/P7-23
 • N. Crocker, PoP 16 (2009) 042513

Wave Heating and Current Drive

➤ Demonstrate reliable wave heating and CD to enable advanced operating scenarios



- **HHFW coupling optimization**

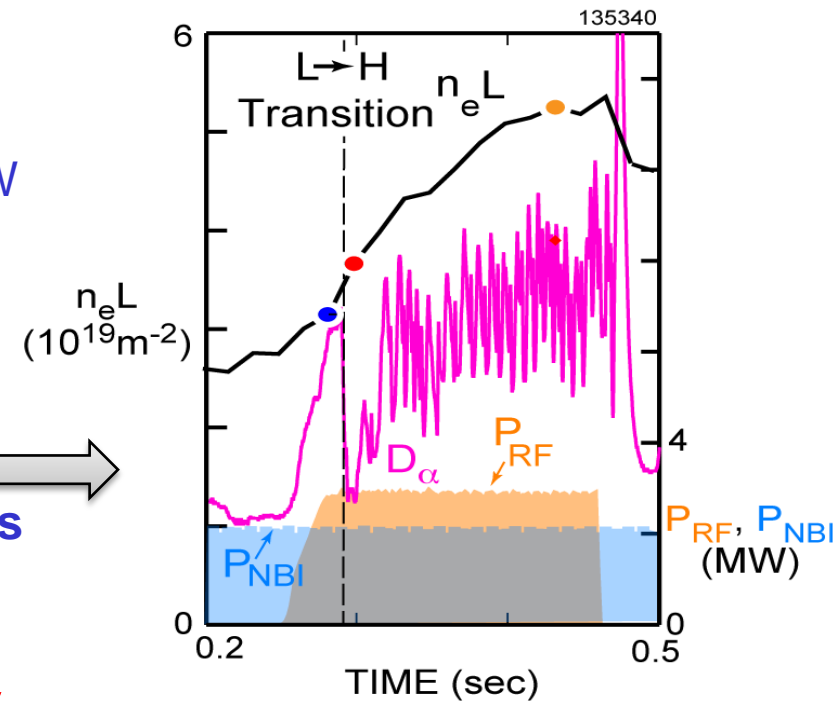
- HHFW performance summary on next slide
- Fast-ion interaction with HHFW successfully modeled by including finite orbit width effects
- Edge interaction modeling with fully 3D AORSA underway – initial results qualitatively similar to experiment

- **ECH/EBW coupling and heating studies:** deferred due to cost

Antenna upgrades performed in 2009 significantly improved HHFW heating performance

- Modifications to antenna described in M. Ono facility presentation
- Improvements in performance likely due to a combination of antenna upgrade and Li conditioning:

- Coupled > 4 MW into He L-mode
- Record $T_e(0) \sim 6.2$ keV with $P_{RF} \sim 2.7$ MW
- Allowed study of L-H and H-L transition in He & D with RF (not previously achievable)
- Maintained HHFW coupling through L-H transition and during relatively large repetitive ELMs during D plasmas (not previously achievable)

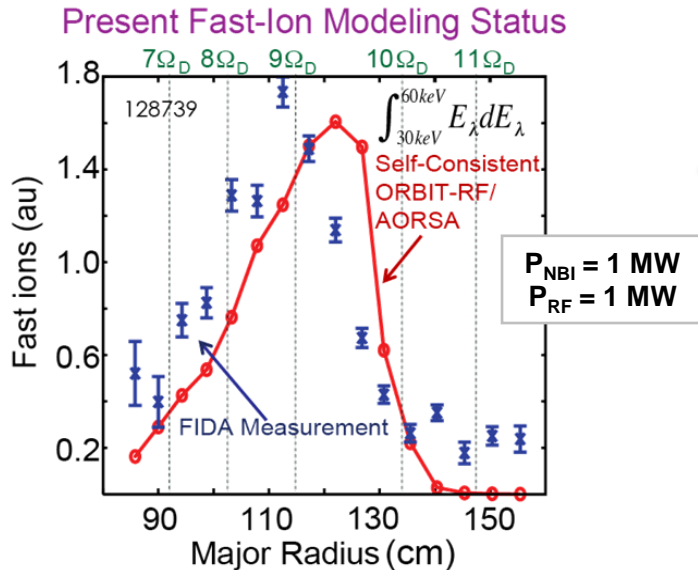
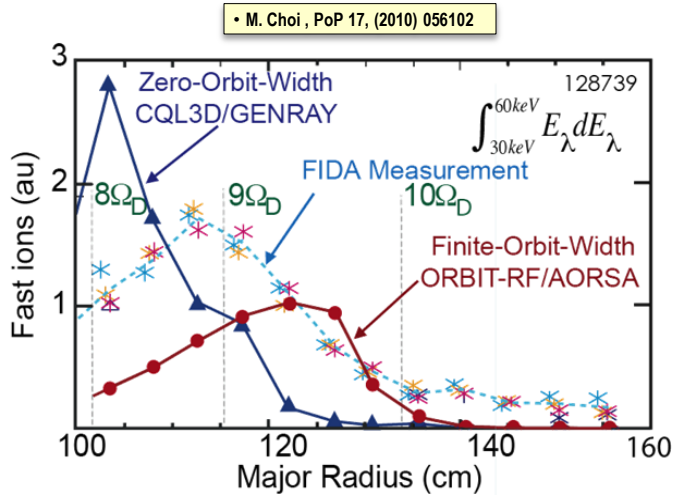


• G. Taylor, PoP 17, (2010) 056114
• G. Taylor, APS Invited Talk 2009

ORNL, MIT

- 2010: P_{RF} limited to 2MW, apparently from Li-oxide-dust-associated arcs
- Will re-establish 4MW operation in 2011 to support **R12-2** and other experiments

Self-consistent finite-orbit-width (FOW) ORBIT-RF/AORSA improves agreement with FIDA data for NBI+HHFW plasmas



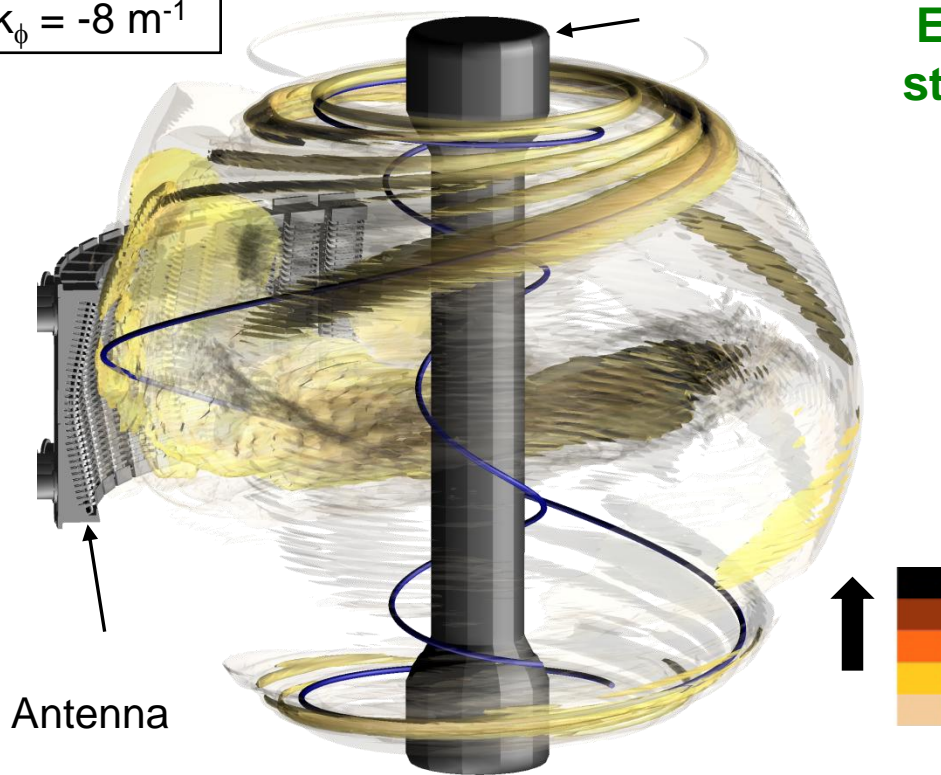
• M. Choi, US-Japan RF Workshop, Toba, Japan, February 2011

- HHFW interaction with NBI fast-ion can be significant
- There was previously significant disagreement between modeling & FIDA fast-ion profiles
- Good agreement between modeling & FIDA has now been achieved by including additional iterations between AORSA & FOW ORBIT-RF
- Work has also begun on a full FOW correction to CQL3D which is expected to be completed in late 2011

ORNL, General Atomics, CompX

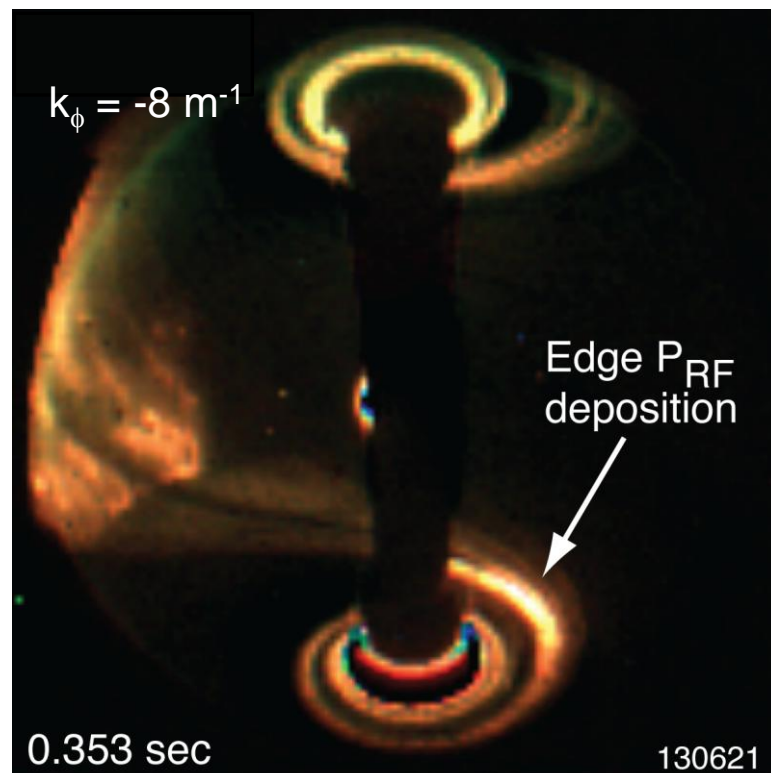
3-D AORSA full-wave model with 2-D wall boundary predicts large E_{RF} following magnetic field near top & bottom of NSTX

$$k_{\phi} = -8 \text{ m}^{-1}$$



*D. L. Green, ORNL
3D AORSA with boundary extended to wall*

Edge RF eigenmode similar to striated structures imaged by visible plasma TV

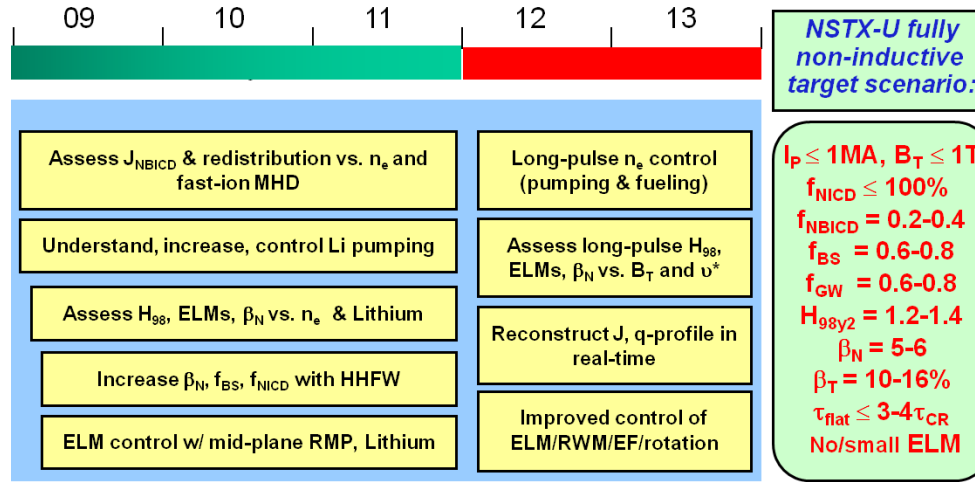


- In addition to RF power coupling to core, AORSA predicts some RF power propagates just inside LCFS as an edge localized RF eigenmode
- Initiated divertor tile current measurements to compare to theory

Advanced Scenarios and Control

- Establish high-performance integrated scenarios and the necessary control capabilities

5 year plan
timeline
and goals



Progress and Plans

Gray italics indicates material provided in supplemental section

- **Scenario development**
 - Developed range of scenarios with sustained high κ , β_N , and bootstrap fraction
 - Exploring scenarios for NSTX Upgrade: higher A and elongation, extend in FY11-12
 - Extended duration of H-mode scenarios with very high confinement (H_{98} up to 1.7)
- **NBI-driven current redistribution from *AE**
 - During large repeated TAE avalanches, substantial modification of $J(r)$ observed, simulated
- **Assess, optimize performance vs. n_e , lithium**
 - Need to develop and understand MHD-stable scenarios at low density – FY12 milestone
- **Increase NBI H-mode non-inductive fraction:** requires high P_{RF} - test in FY11-12
- **ELM control with mid-plane RMP, Li**
 - Utilized paced 3D fields and vertical jogs to trigger ELMs, reduce impurities, control density
- **Advanced control**
 - Implemented: β_N , multiple strike-points Planned: MIMO shape, improved $n=0$, snowflake, rotation

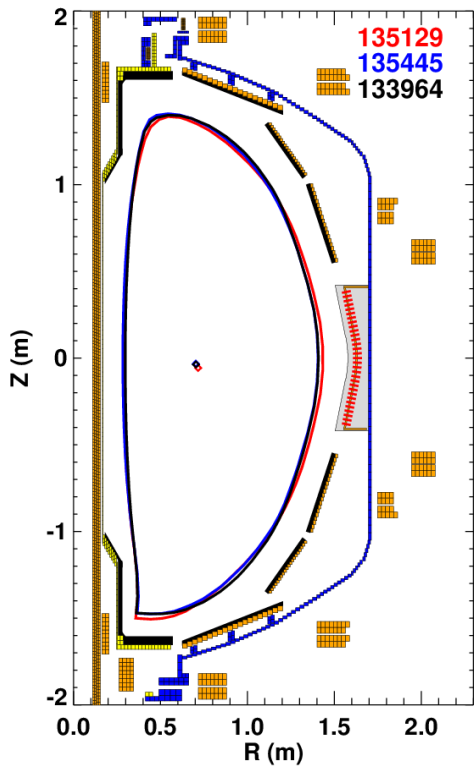
In 2009-10, NSTX demonstrated sustained high-elongation configurations over a range of currents and fields

R09-3

High- β_T
 $q^*=2.8$
 $B_T=0.44 T$
 $I_P=1100 kA$

Long Pulse
 $q^*=3.9$
 $B_T=0.38 T$
 $I_P=700 kA$

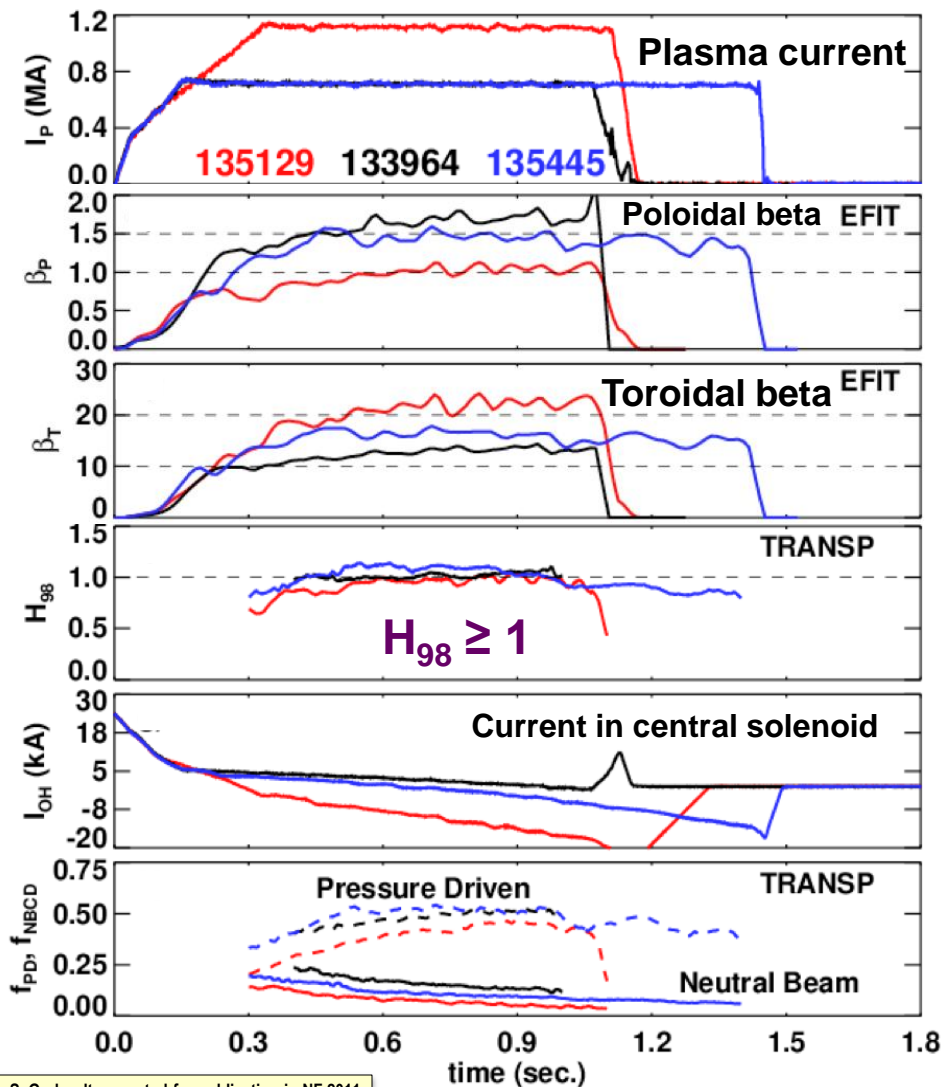
High- β_P
 $q^*=4.7$
 $B_T=0.48 T$
 $I_P=700 kA$



$$q^* = \frac{\epsilon(1 + \kappa^2)\pi a B_{T0}}{\mu_0 I_P}$$

$\kappa \sim 2.6-2.7$
 $\delta \sim 0.8$

Double Null

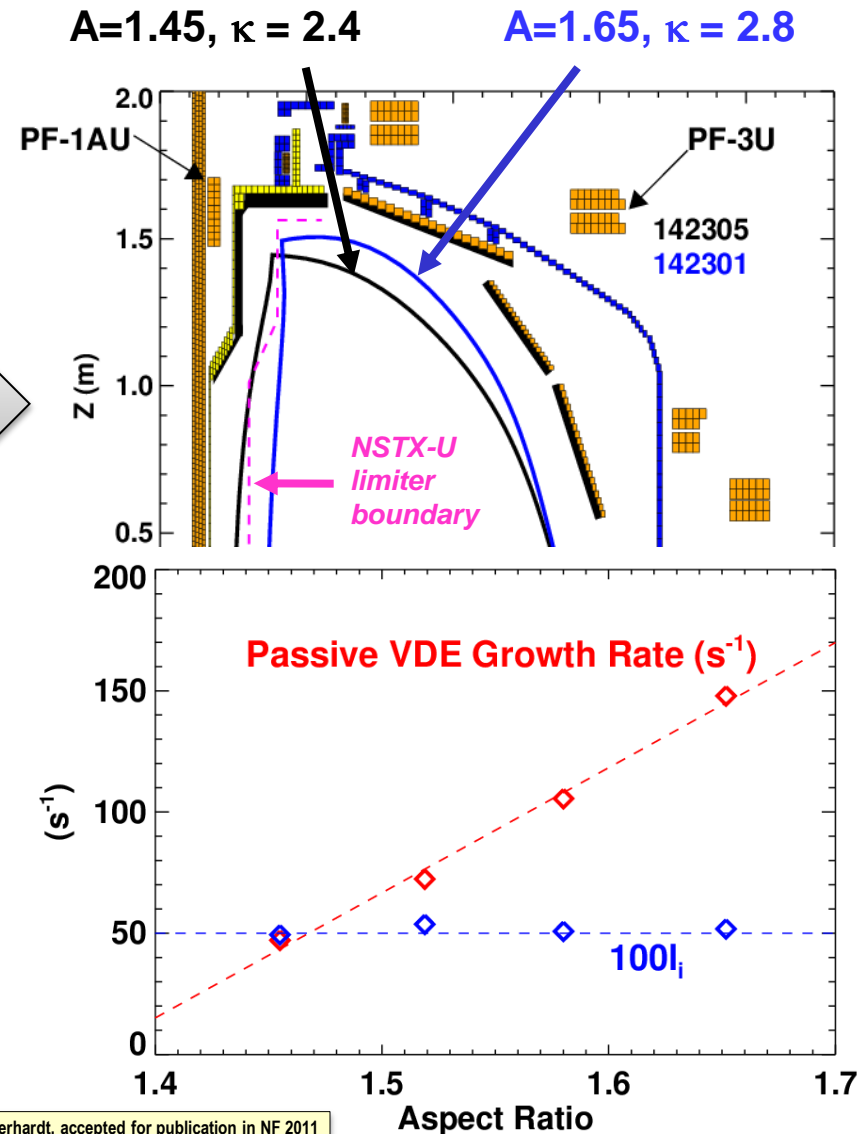
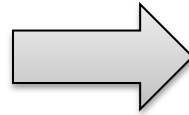


• S. Gerhardt, accepted for publication in NF 2011
 • S. Gerhardt, IAEA FEC 2010, EXS/P2-8

Pulse-lengths limited by OH, TF coil heating limits

NSTX is exploring stability impact of higher aspect ratio and elongation, and profiles in preparation for Upgrade, FNSF

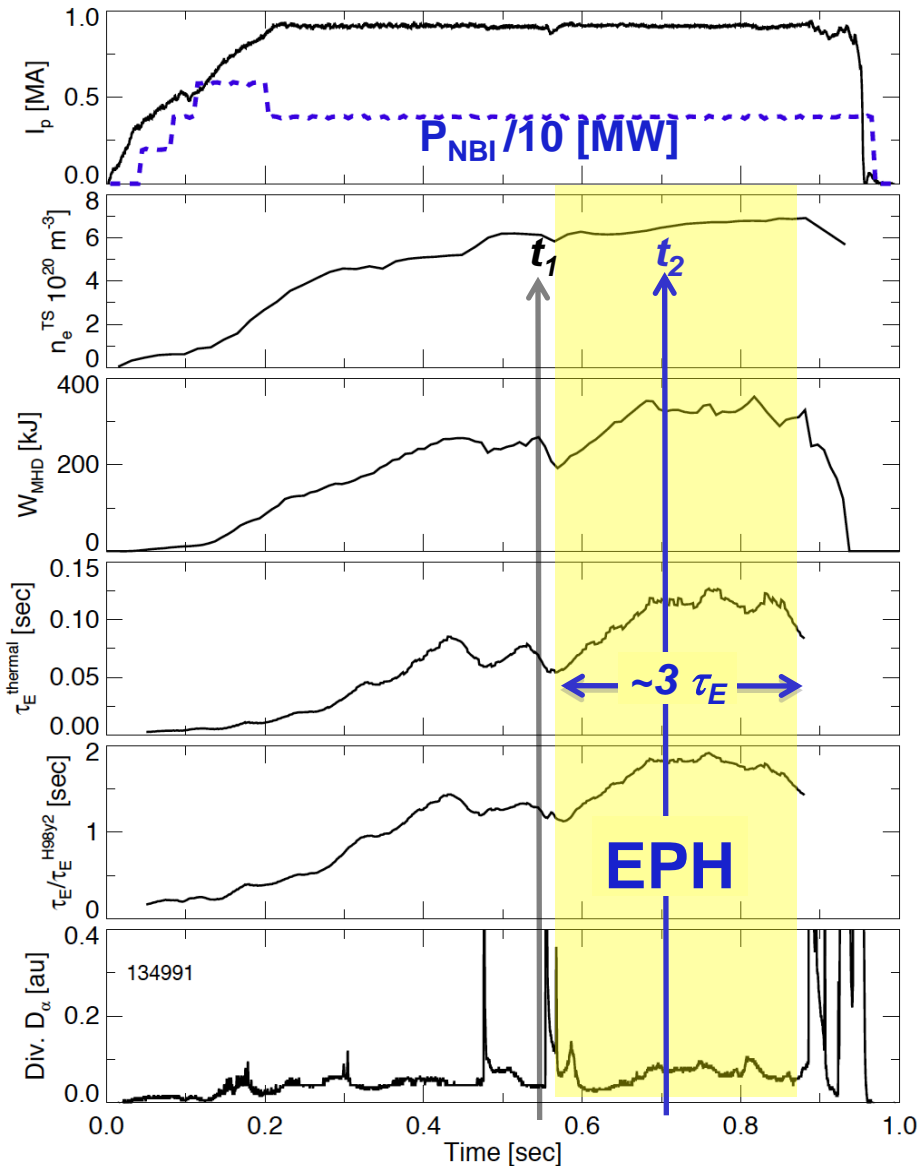
- Next-step ST designs assume increased $\kappa = 3-3.5$ and $A=1.6-1.7$
 - Maximizes fusion performance of low aspect ratio configurations
- NSTX has begun to explore the stability of higher κ and A
 - Also exploring how current profile (internal inductance I_i) varies with these geometric changes, since elongation depends strongly on I_i
- **R11-2** NSTX scenarios will be systematically extended toward shapes of Upgrade and next-steps
 - Assess maximum stable κ , I_i , β_N
 - Optimize RWM stability, control



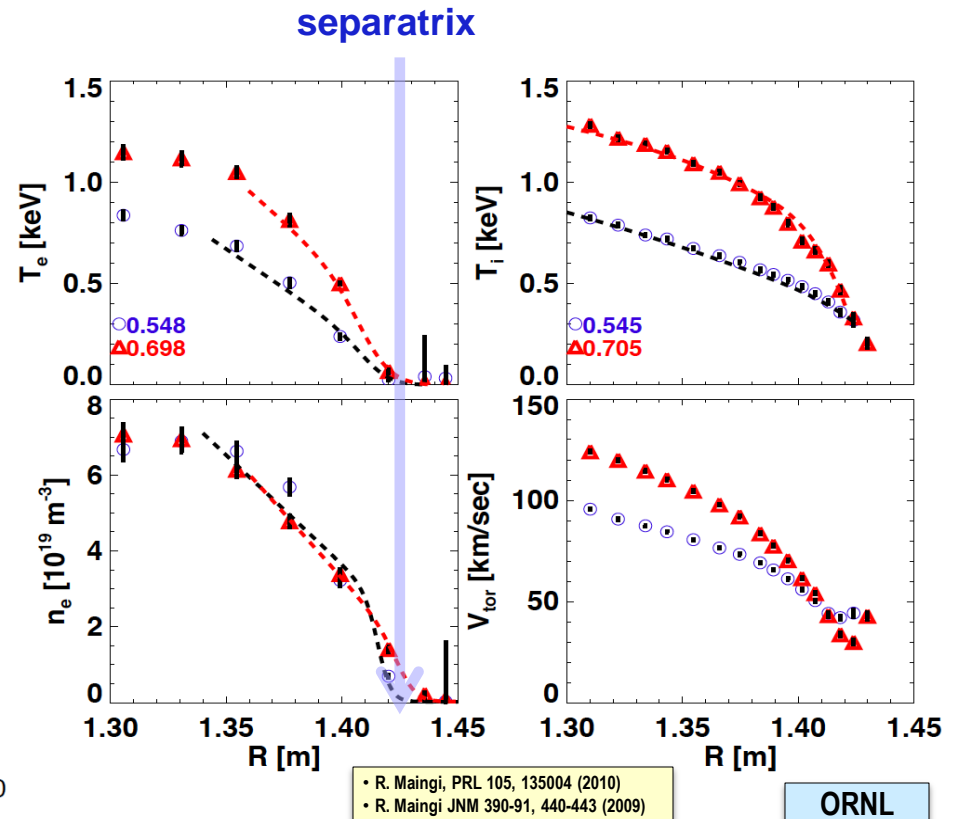
• S. Gerhardt, accepted for publication in NF 2011

High confinement H-Mode regime obtained with lithium

High Performance ST-FNSF/Pilot Plant level confinement: $H_{98y2} \leq 1.7$

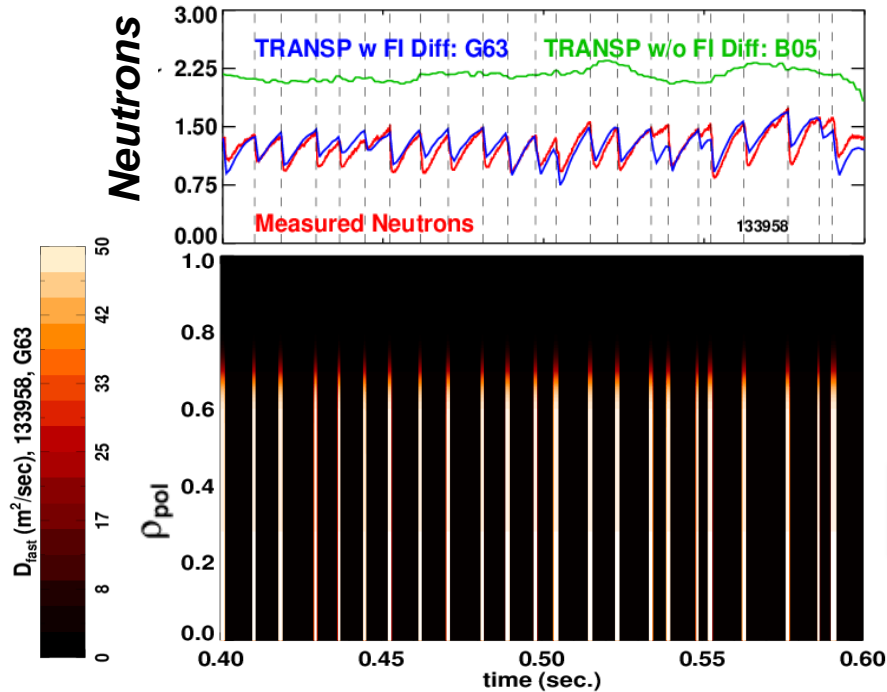


- Very high $H_{98y2} \leq 1.7$ is combination of Li confinement improvement and higher pedestal temperature and pressure
- ITER, FNSF fusion performance is highly dependent on pedestal pressure: $Q \sim p^2$

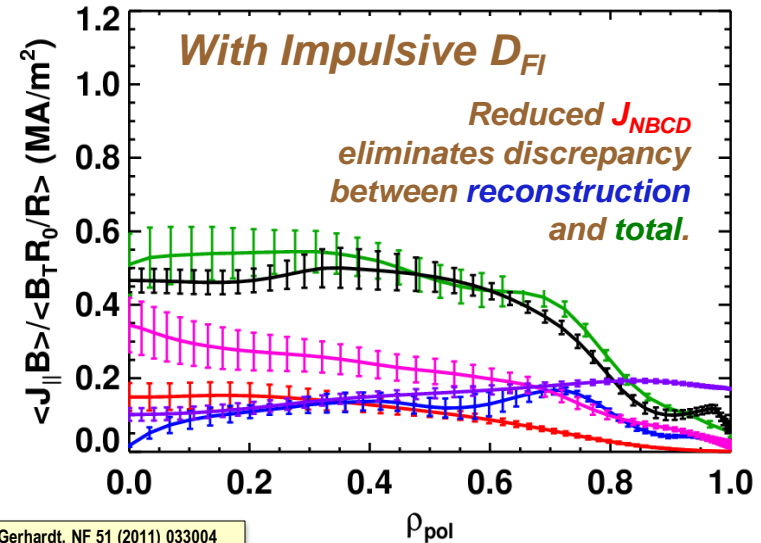
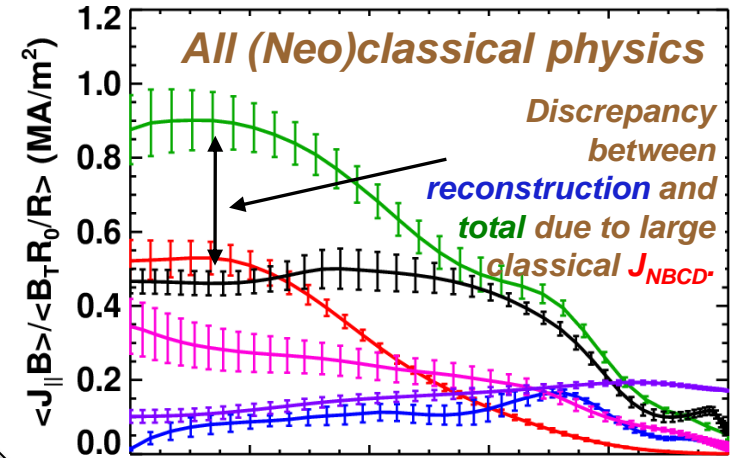


Toroidal Alfvén Eigenmodes (TAE) can strongly modify NBI current profile – important for FNSF, ITER-AT

R09-2



700 kA High- β_p with Rapid TAE Avalanches

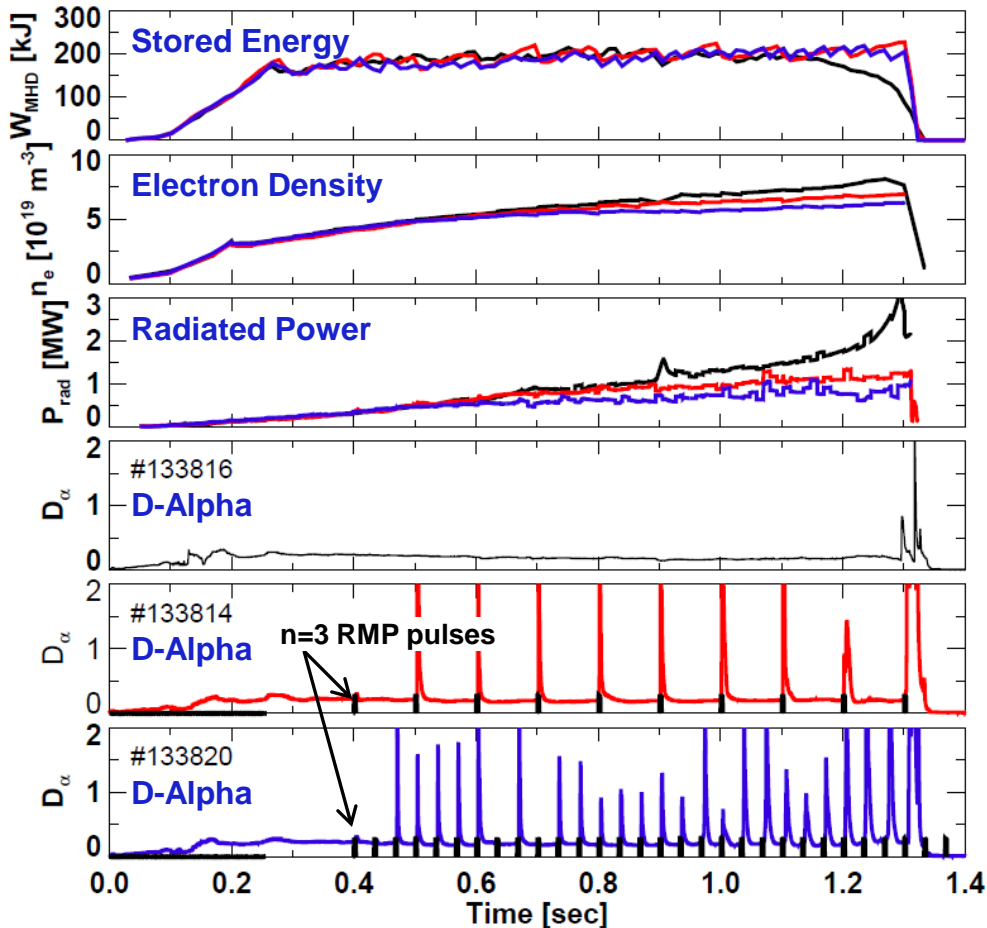


- Model TAE “avalanches” using spatially and temporally localized fast-ion diffusivity $D_{\text{FI}}(\psi, t)$
- **TAE avalanches could impact ST-FNSF scenarios with large fraction of NBI current**
- **IR12-2** Obtain new tangential FIDA data for M3D-K validation during Upgrade outage

• S. Gerhardt, NF 51 (2011) 033004

ELM pacing developed with pulsed non-resonant fields, vertical jogs – useful for controlling impurities

Rapid, Reliable Triggering with Pulsed 3-D Fields

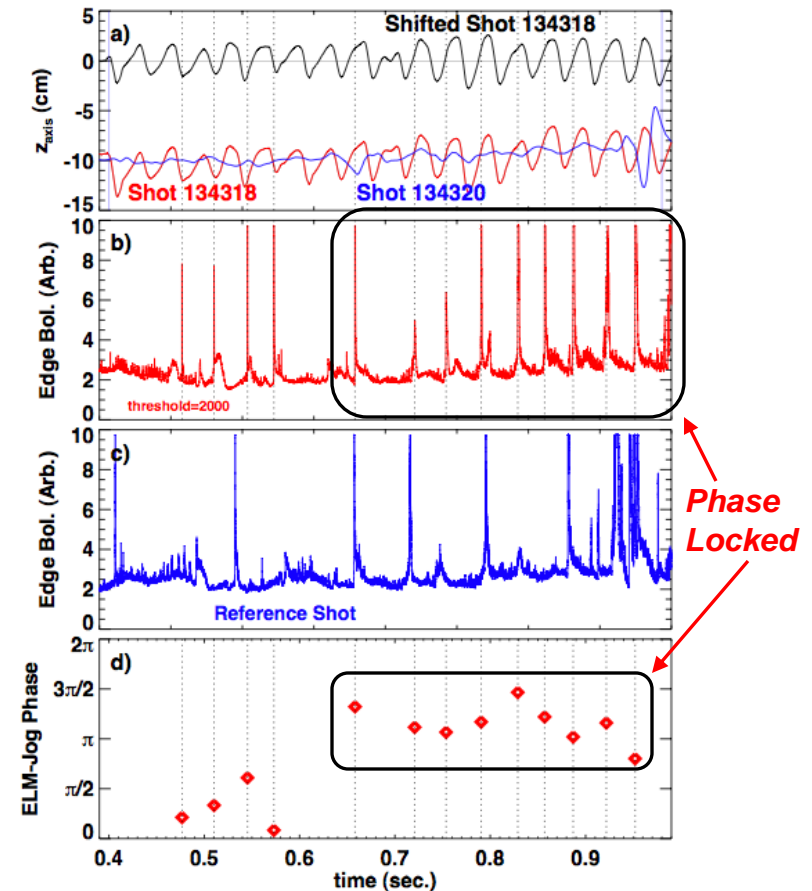


- Reduction in radiated power
- Rapid ELMs lead to smaller per-ELM energy loss

• J. Canik, IAEA FEC 2010 Oral, EXC/8-1
 • J. Canik, NF 50 (2010) 064016
 • J. Canik, PRL 104 (4), 045001 (2010)

ORNL

ELM Pacing Via Vertical Jogs



- Vertical joggng successful despite thick continuous vacuum vessel.
- ELMs become phase locked to upward motion

• S. Gerhardt, NF 50 (2010) 064015

Activities in support of ITER

➤ Utilize unique ST/NSTX parameters and capabilities to extend tokamak understanding for ITER

- Active ITPA participation

Gray italics indicates material provided in supplemental section

- ITER task agreements:

- *Study of error fields using the Ideal Perturbed Equilibrium Code*
- *Error field measurements in ITER without plasma*

- Divertor detachment thresholds with 3D fields + gas puffing
- Plasma transport and stability response to 3D fields

NSTX Participation in ITPA Joint Experiments and Activities

• Advanced Scenarios and Control (5)

- IOS-1.2 Study seeding effects on ITER baseline discharges
- IOS-4.1 Access conditions for advanced inductive scenario with ITER-relevant restrictions
- IOS-4.3 Collisionality scaling of confinement in advanced inductive plasmas
- IOS-5.2 Maintaining ICRH coupling in expected ITER regime
- IOS-6.2 li controller (Ip ramp) with primary voltage/additional heating

• Boundary Physics and Lithium Research (16)

- PEP-6 Pedestal structure and ELM stability in DN
- PEP-19 Basic mechanisms of edge transport with resonant magnetic perturbations in toroidal plasma confinement devices
- PEP-23 Quantification of the requirements for ELM suppression by magnetic perturbations from off-midplane coils
- PEP-24 Minimum pellet size for ELM pacing
- PEP-25 Inter-machine comparison of ELM control by magnetic field perturbations from midplane RMP coils
- PEP-26 Critical parameters for achieving L-H transitions
- PEP-27 Pedestal profile evolution following L-H/H-L transition
- PEP-28 Physics of H-mode access with different X-point height
- PEP-29 Vertical jolts/kicks for ELM triggering and control
- PEP-31 Pedestal structure and edge relaxation mechanisms in I-mode
- PEP-32 Access to and exit from H-mode with ELM mitigation at low input power above PLH
- PEP-33 Effects of current ramps on the L-H transition and on the stability and confinement of H-modes at low power above the threshold
- PEP-34 Non-resonant magnetic field driven QH-mode
- DSOL-20 Transient divertor reattachment
- DSOL-21 Introduction of pre-characterized dust for dust transport studies in divertor and SOL
- DSOL-24 Disruption heat loads

• Macroscopic Stability (7)

- MDC-1 Disruption mitigation by massive gas jets
- MDC-2 Joint experiments on resistive wall mode physics
- MDC-4 Neoclassical tearing mode physics – aspect ratio comparison
- MDC-12 Non-resonant magnetic braking
- MDC-14 Rotation effects on neoclassical tearing modes
- MDC-15 Disruption database development
- MDC-17 Active disruption avoidance

• Transport and Turbulence (11)

- TC-1 Confinement scaling in ELMy H-modes: beta degradation
- TC-2 Hysteresis and access to H-mode with H~1
- TC-4 H-mode transition and confinement dependence on ionic species
- TC-9 Scaling of intrinsic rotation with no external momentum input
- TC-10 Experimental identification of ITG, TEM and ETG turbulence and comparison with codes
- TC-11 He and impurity profiles and transport coefficients
- TC-12 H-mode transport and confinement at low aspect ratio
- TC-14 RF rotation drive
- TC-15 Dependence of momentum and particle pinch on collisionality
- TC-17 rho-star scaling of intrinsic torque
- TC-19 Characteristics of I-mode plasmas

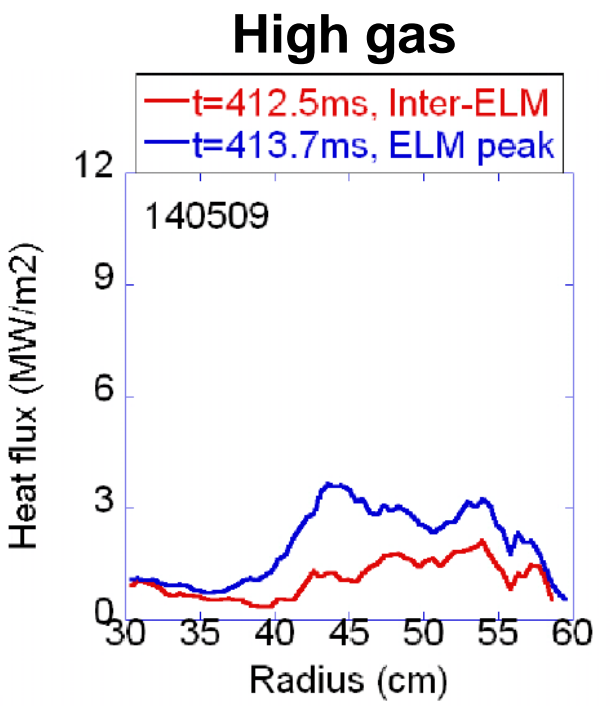
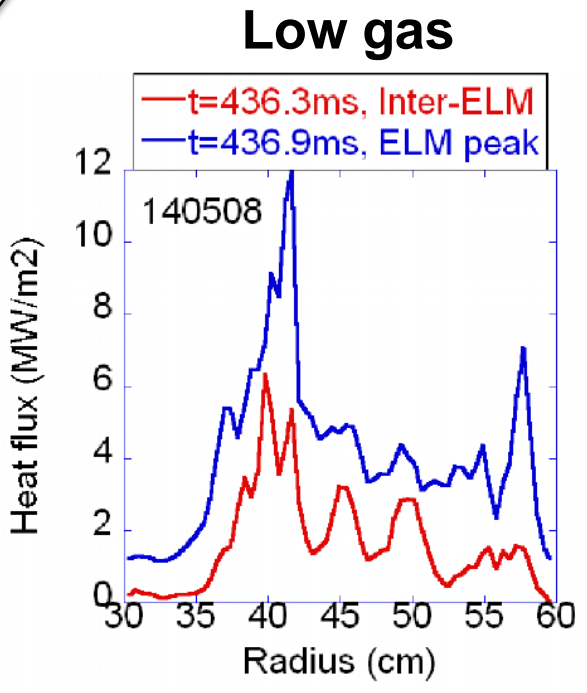
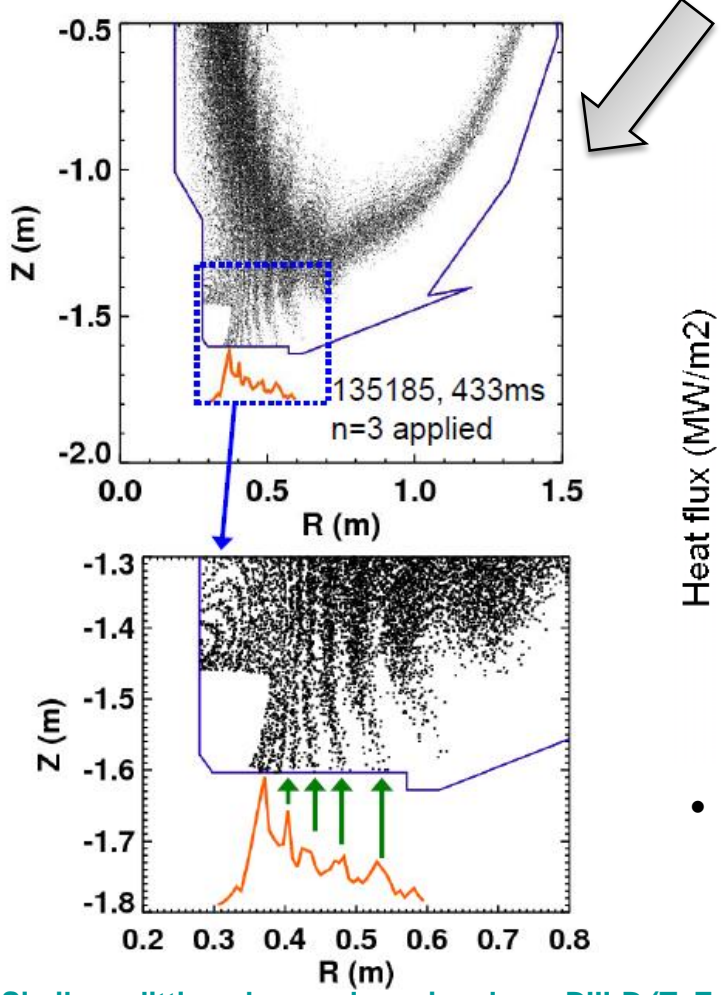
• Wave-Particle Interactions (5)

- EP-1 Measurements of damping rate of intermediate toroidal mode number Alfvén eigenmodes
- EP-2 Fast ion losses and redistribution from localized AEs
- EP-3 Fast ion transport by small scale turbulence
- EP-4 Effect of dynamical friction (drag) at resonance on nonlinear AE evolution
- EP-6 Fast ion losses and associated heat load from edge perturbations (ELMs and RMPs)

NSTX typically actively participates in ~25 Joint Experiments/Activities

3D fields used for RMP ELM control can cause toroidally asymmetric divertor heat & particle deposition, re-attachment

Distribution of splitting locations from measurement and vacuum field line tracing in good agreement



- Increased divertor gas puffing reduces heat-flux peaking and re-establishes divertor detachment

Similar splitting observed previously on DIII-D (T. Evans)

• J.-W. Ahn PoP 18 (5) 056108 (2011)
• J.-W. Ahn, APS Invited Talk 2010

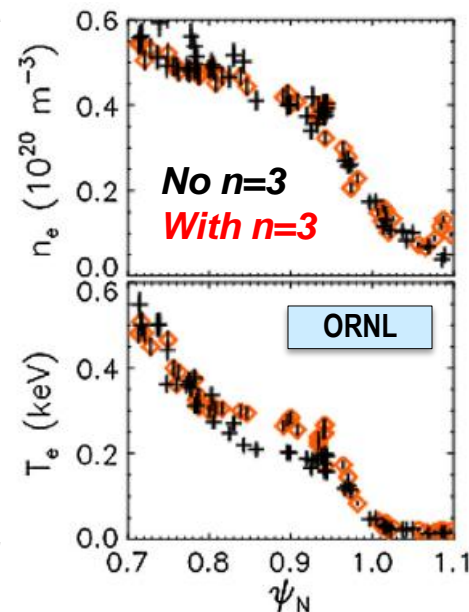
ORNL

NSTX investigating H-mode pedestal transport, turbulence, and stability response to 3D fields

R11-4

NSTX provides unique data to understand response to 3D fields for ELM control:

- ELMs stabilized by Li coatings
- ELMs triggered by 3D fields, not suppressed
 - Profile changes from 3D fields depend on Li, v^* , q_{95}



- Will study possible mechanisms for modifying transport
- Pedestal turbulence trends: BES, high-k scattering, gas-puff imaging
- Transport response: Improved Thomson, impurity injection, edge SXR
- Also supports **FY11 JRT** on H-mode pedestal structure

• J. Canik, IAEA FEC 2010 Oral, EXC/8-1
• J. Canik, NF 50 (2010) 064016
• J. Canik, NF 50 (2010) 034012
• J. Canik, PRL 104 (4), 045001 (2010)

NSTX successfully completed annual research milestones and is prepared to complete upcoming FY11-12 milestones

(blue = completed, red = ongoing/future, green = incremental)

	FY2009	FY2010	FY2011	FY2012
--	--------	--------	--------	--------

Run Weeks: 16 15 4 10 10 4

▪ Transport & Turbulence

R11-1

Measure fluctuations responsible for electron, ion, impurity transport

▪ Macroscopic Stability

R09-1

Understand physics of RWM stabilization & control vs. rotation

R10-1

Assess sustainable β & disruptivity near and above ideal no-wall limit

R11-2

Assess ST stability dependence on aspect ratio and boundary shaping

IR12-1

Investigate magnetic braking physics and toroidal rotation control at low v^*

▪ Boundary/Lithium Physics

R10-3

Assess H-mode characteristics vs. collisionality and Li conditioning

R11-3

Assess very high flux expansion divertor operation

R12-1

Assess relationship between lithium-conditioned surface composition and plasma behavior

▪ Waves and Energetic Particles

R09-2

Study how $j(r)$ is modified by super-Alfvénic ion-driven modes

R10-2

Characterize HHFW heating, CD, and ramp-up in deuterium H-mode

IR12-2

Assess predictive capability of mode-induced fast-ion transport

▪ Solenoid-free start-up, ramp-up

R12-2

Assess confinement, heating, and ramp-up of CHI start-up plasmas

▪ Advanced Scenarios & Control

R09-3

Perform high-elongation wall-stabilized operation at lower n_e

R12-3

Assess access to reduced n_e and v^* in high-performance scenarios

▪ ITER urgent needs, cross-cutting

R11-4

H-mode ped. transport, turbulence, stability response to 3D fields

▪ Joint Research Targets (3 US facilities):

FY09 JRT

Particle control and hydrogenic fuel retention

FY10 JRT

Understanding of divertor heat flux and transport in scrape-off layer

FY11 JRT

Characterize H-mode pedestal structure

FY12 JRT

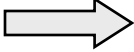
Understand core transport and enhance predictive capability

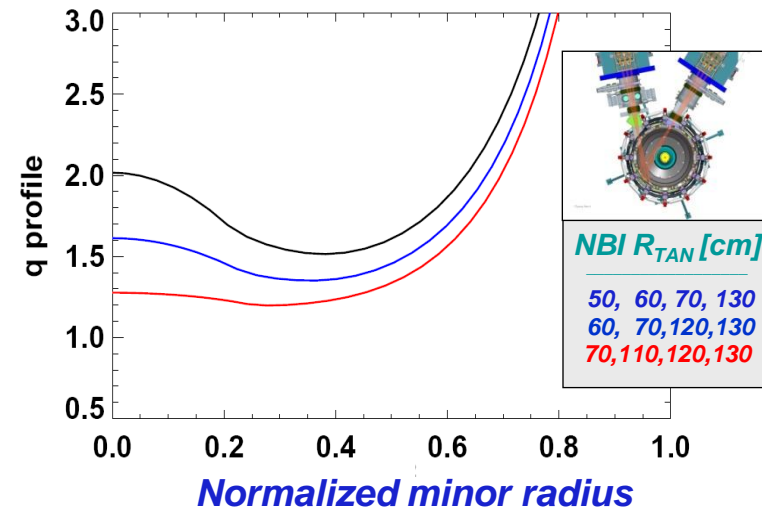
Plans for FY2012-13 analysis and research

- Complete analysis and publication of FY2011-12 data
- Planning and design studies supporting post-Upgrade ops:
 - Start-up: CHI upgrades, point helicity injection (plasma guns)
 - Boundary: Divertor cryo-pumps, divertor diagnostics
 - Lithium: Additional Mo tiles, next-generation LLD
 - Transport, EP: New high-k scattering, assess solid-state NPA
 - MHD: 3D-coil physics design for RWM/RMP/TM/EFC/NTV/TAE
 - Control: Real-time-MSE for NBI J-profile control, control of heat flux
- Develop, write NSTX Upgrade 5 year plan for 2014-18
- Update/extend physics design of ST-FNSF
 - LDRD to further develop design concepts, utilize NSTX team expertise
 - Predictive modeling of start-up, sustainment, transport, stability, divertor
- Will rely heavily on NSTX collaborators for 5 year plan preparation, post-Upgrade planning and design, FNSF physics design studies

Planning for FY2013 NSTX collaboration

- Solicited, received info on collaboration opportunities
 - Enthusiastic response: MAST, LTX, Pegasus, DIII-D, C-Mod, KSTAR, EAST, LHD
 - Also gathered info on PPPL NSTX researcher interests and skills
- ~1/3 time available for collaboration: ~10 FTE/yr for 2-3 yrs
- Presently aligning opportunities & skills with needs & goals
 - Experienced NSTX researchers can help advance off-site research
 - Can also bring back new experiences, ideas to NSTX Upgrade

- Example: NSTX-U goal of 100% NICD, high β , $q(r)$ control using 1st + new 2nd NBI 
 - Collaboration on advanced scenarios, profile control, energetic particles mutually beneficial:
 - DIII-D, EAST, KSTAR, MAST

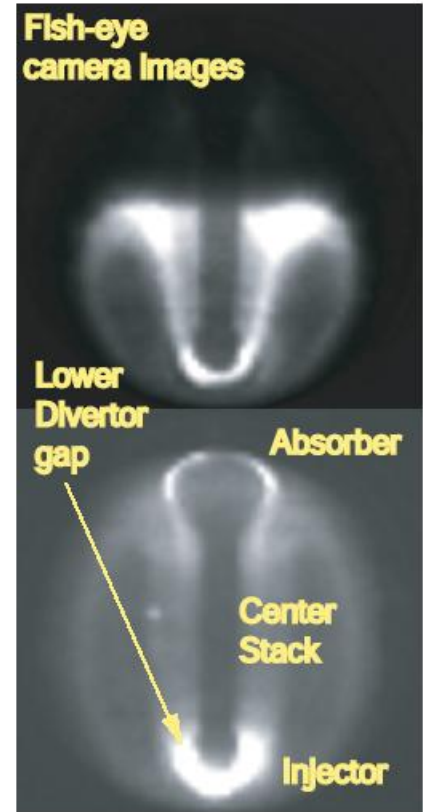
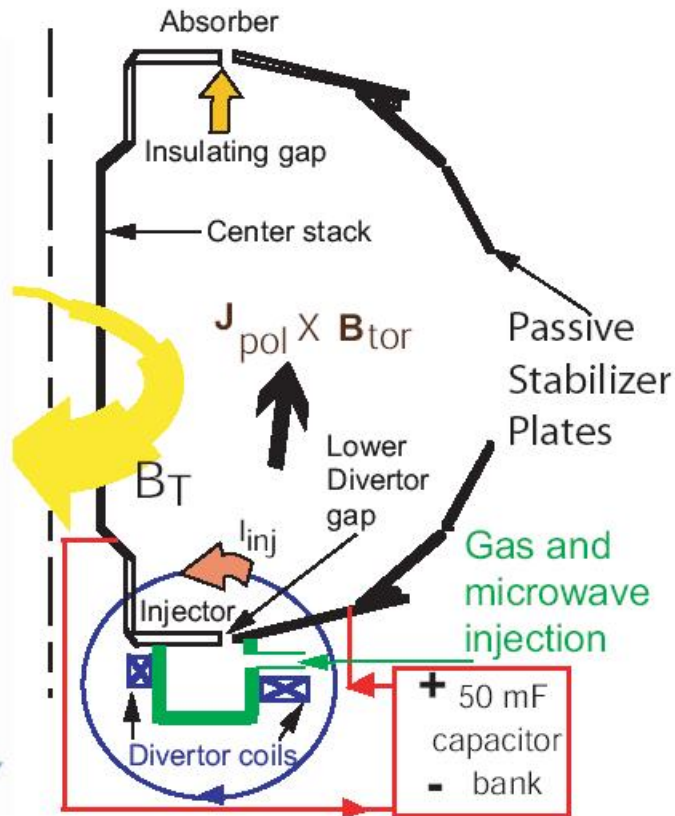
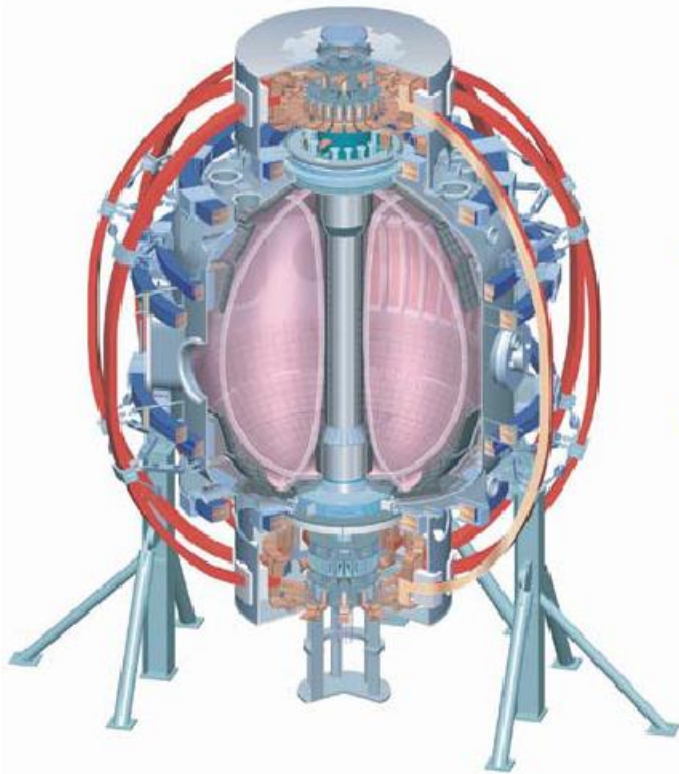


Summary: NSTX is contributing strongly to basis of ST-FNSF, advancing PMI solutions, supporting toroidal physics, ITER

- NSTX has completed all planned research milestones and produced many additional important results
- NSTX has had a very productive 2.5 years
 - See M. Ono talk for statistics on publications, invited talks, awards and recognition, facility utilization and diagnostic implementation
- Research program has adapted to, aligned with the ReNeW ST thrusts, FES vision: emphasis on FNSF, PMI, validation:
 - NSTX Upgrade highest priority, HHFW upgraded to support start-up research
 - Lithium/LLD, snowflake, high-Z PFCs contribute to potential PMI solutions
 - Drift-kinetic MHD, non-linear gyro-kinetic transport, non-linear *AE/fast-ions
- Developed comprehensive research plan for FY11-12 run
 - Emphasis on boundary, PMI, transport, MHD, prep for Upgrade
- Planning for Upgrade outage period is under way
 - Emphasis on post-upgrade operation prep, off-site collaboration

Start-up and Ramp-up Supplemental Slides

Transient CHI: Axisymmetric reconnection leads to formation of closed flux surfaces



Demonstration of closed flux current generation

- Aided by gas and EC-Pi injection from below divertor plate region

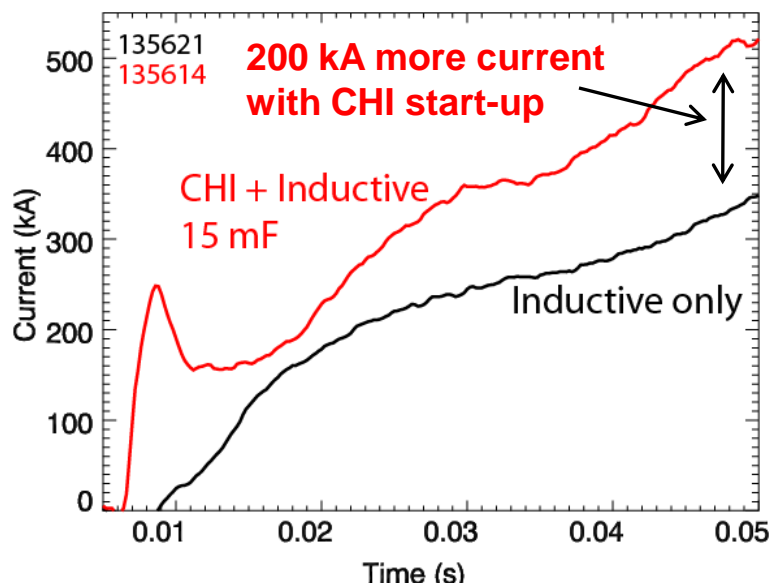
Demonstration of coupling to induction (2008)

- Aided by staged capacitor bank capability

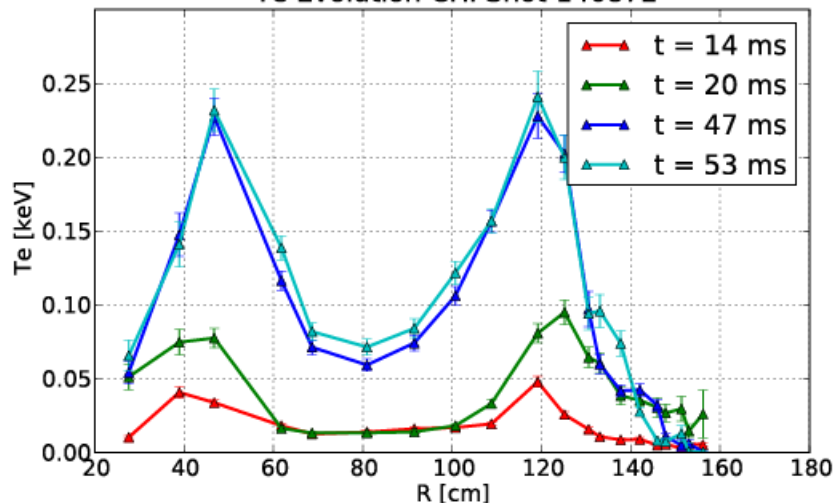
CHI for an ST: T.R. Jarboe, Fusion Technology, 15 (1989) 7

Transient CHI: R. Raman, T.R. Jarboe, B.A. Nelson, et al., PRL 90, (2003) 075005-1

Coaxial Helicity Injection (CHI) has Produced Substantial Flux Savings and Scales Favorably with Size and B_T



Te Evolution CHI Shot 140872



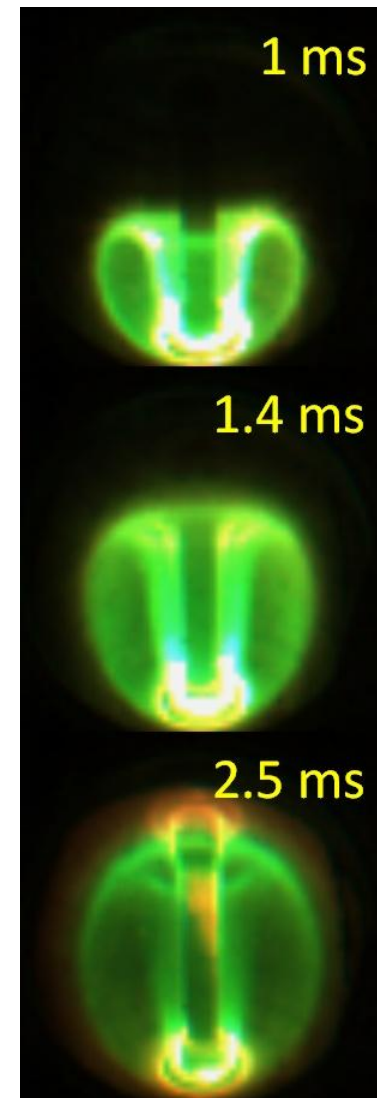
Enabling capabilities

- Elimination of arcs in absorber region
- Conditioning of lower divertor

Generated 1MA using 40% less flux than induction-only case

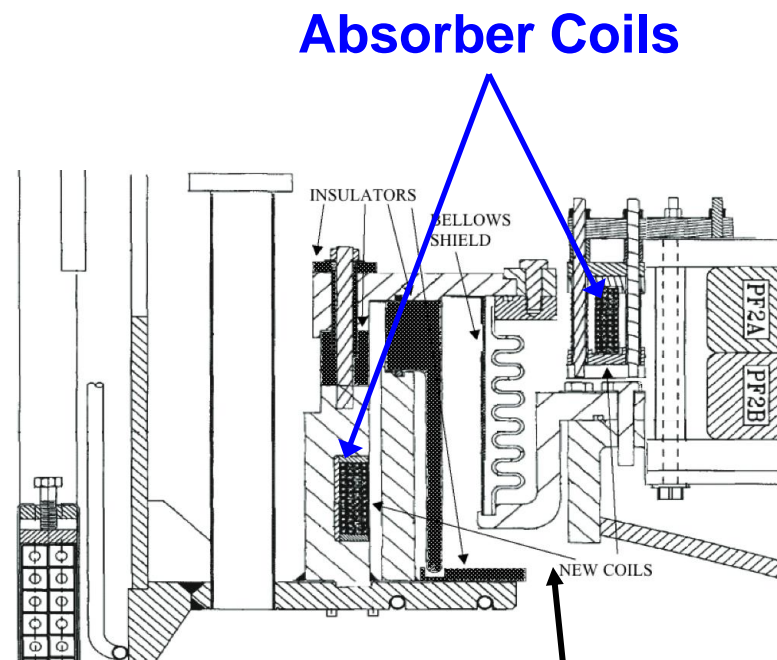
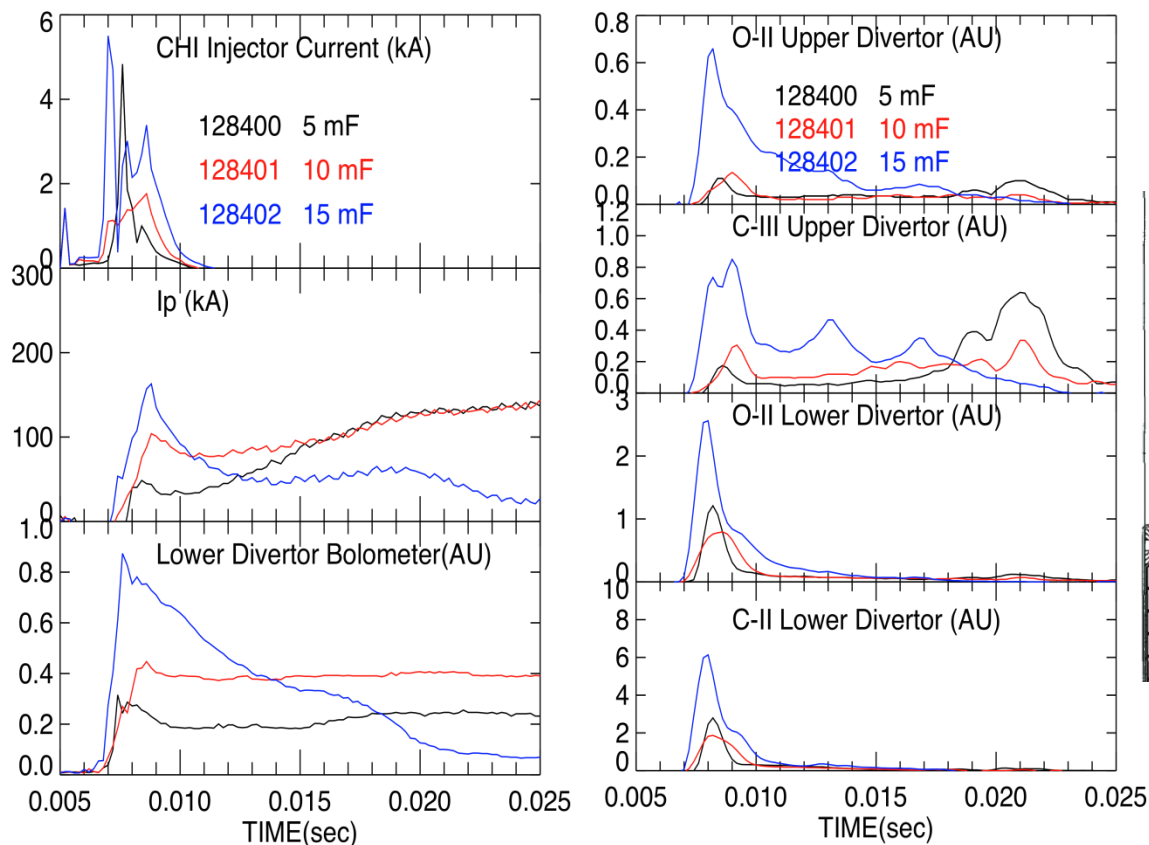
- Hollow T_e maintained during ramp
- Low internal inductance ($I_i \approx 0.35$)
- High elongation
- Suitable startup for advanced scenarios

Time after CHI starts



B.A. Nelson EXW/P2-8

In 2008, low Z impurities limited the ability to ramp-up a CHI discharge with central solenoid



Absorber Coils

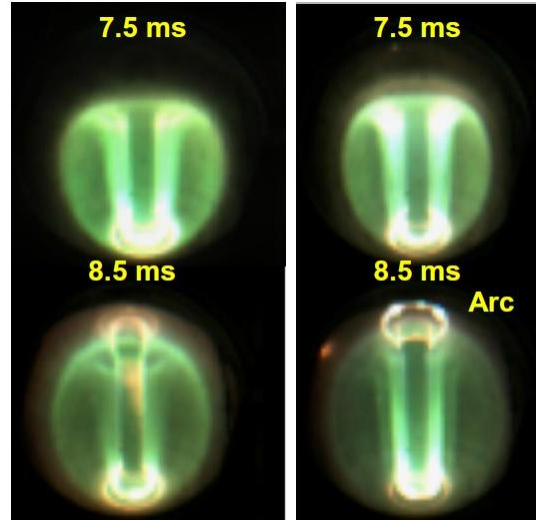
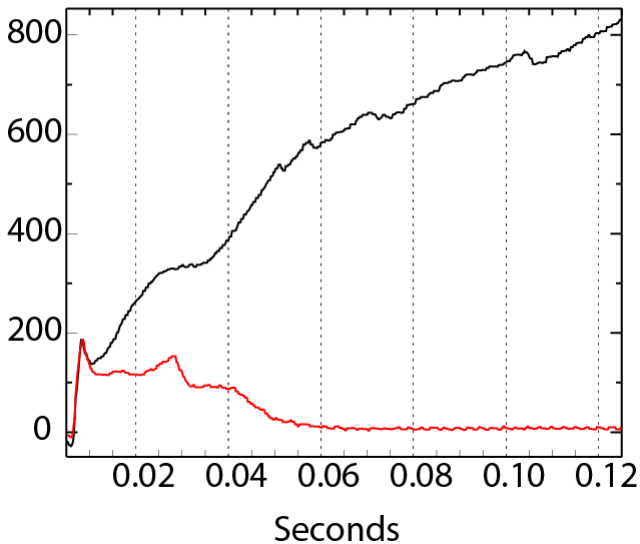


CHI exhibits low Z impurities that increase with increasing capacitor energy. As the discharges grow upwards to fill the vessel absorber arcs occur

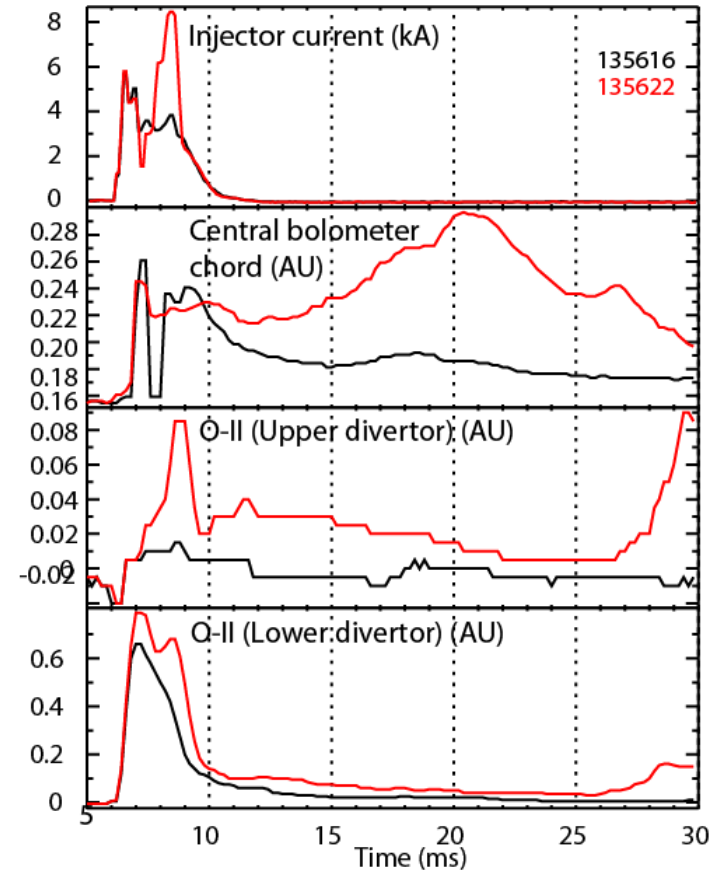
FY2009: Used absorber coils to provide buffer flux and prevent arcs

Absorber Coils Suppressed Arcs in Upper Divertor and Reduced Influx of Oxygen Impurities

135616 (With Absorber coils) **FY 2009**
 135622 (Without coils)



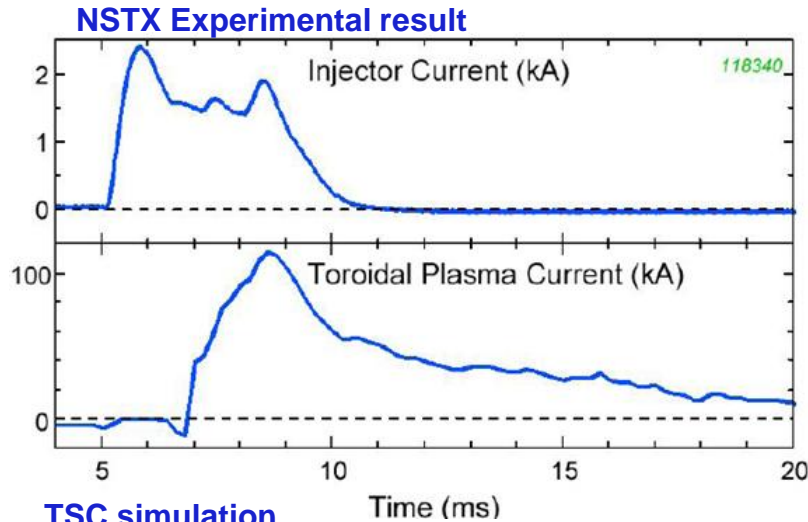
With Absorber coils **Without coil**



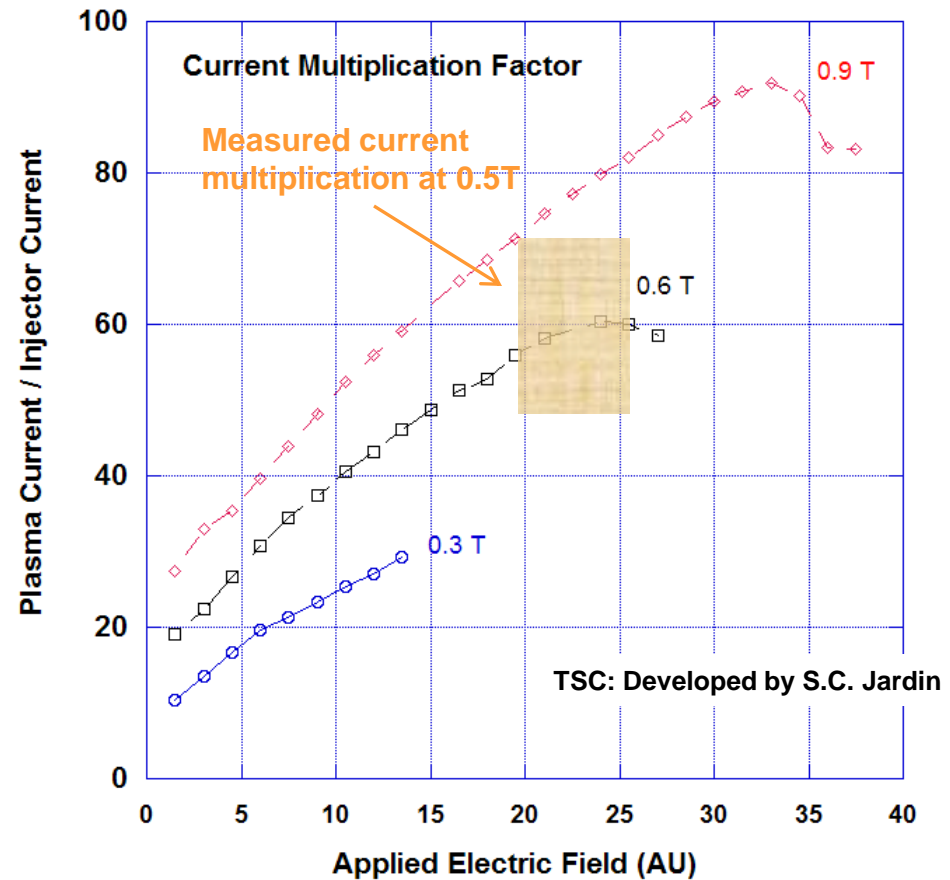
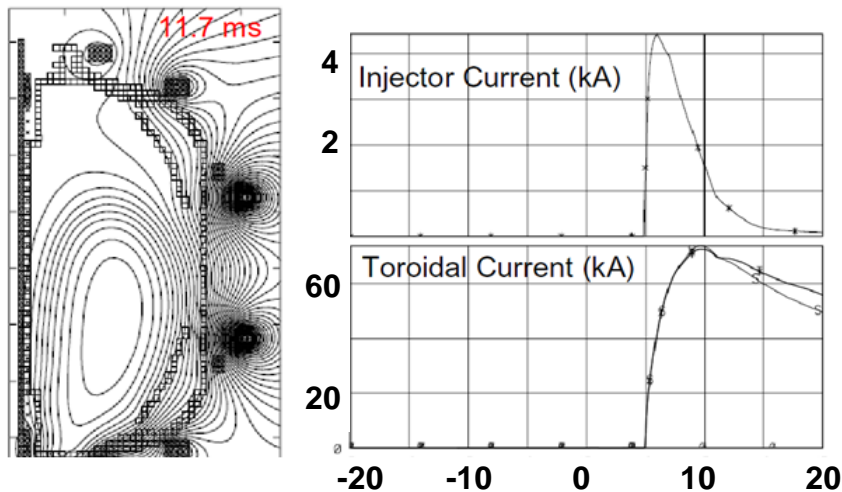
- Divertor cleaning and lithium used to produce reference discharge
- Buffer field from PF absorber coils prevented contact of plasma with upper divertor

R. Raman, D. Mueller, B.A. Nelson, T.R. Jarboe, et al., PRL 104, (2010) 095003

TSC Simulations Show Increasing Current Multiplication as TF is Increased (NSTX geometry)



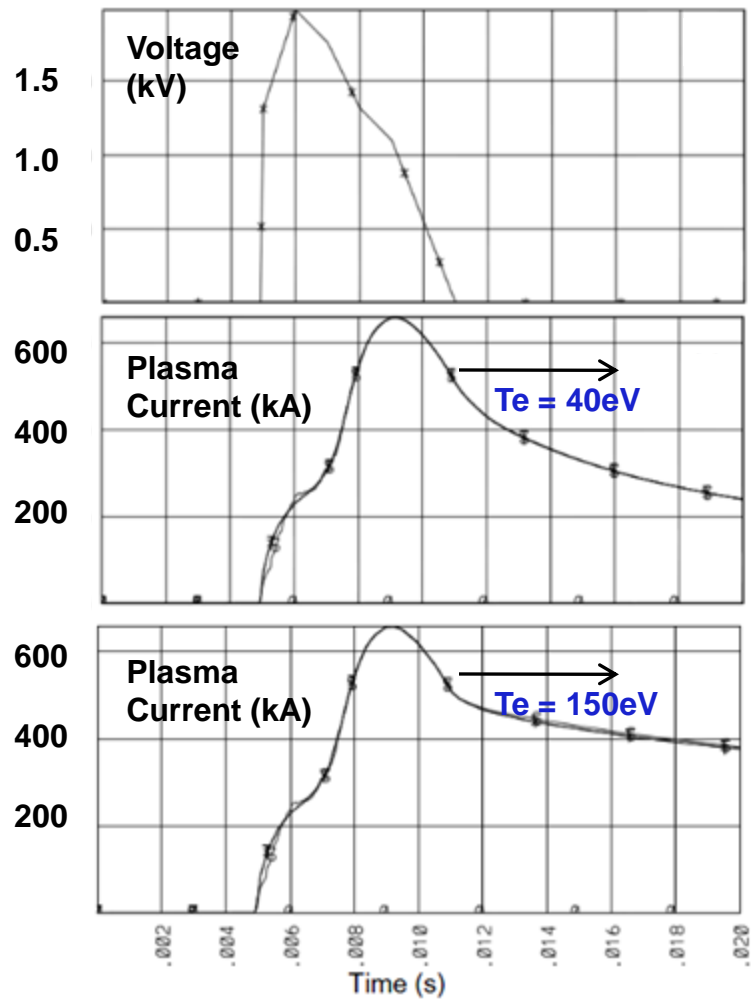
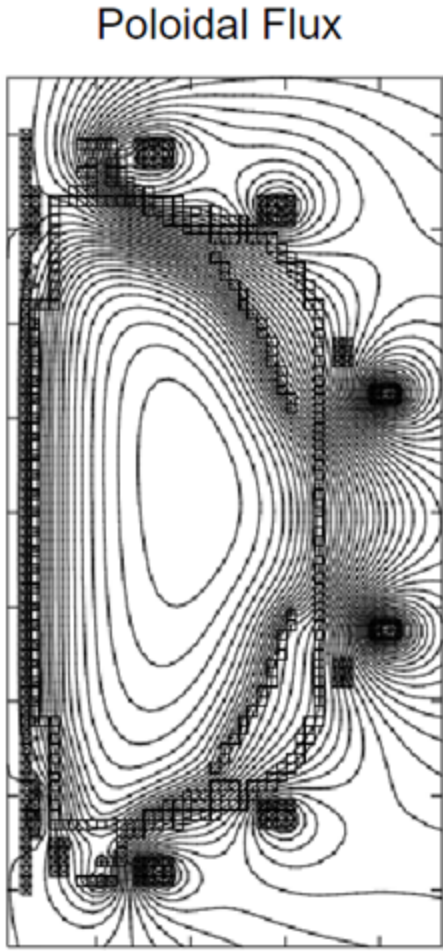
TSC simulation



- Current multiplication factors similar to observations in NSTX
- Higher toroidal field important as it reduces injector current requirement

Now starting to use NIMROD code (in collaboration with Bick Hooper, LLNL)

TSC Simulations Show 600kA CHI Start-up Capability in NSTX as TF is Increased to 1T



Projected closed flux plasma current for NSTX-U is $>450 \text{ kA}$ $[I_p = I_{inj}(\psi_{Tor}/\psi_{Pol})]^*$

- Based on 11 kA injector current
- Current multiplication of 55 (achieved in NSTX)
- Applied voltage $\sim 2x$ that at 0.5T, further optimization may reduce voltage requirement

Consistent with present experimental observations in NSTX that attain $>300\text{kA}$ at 0.5T

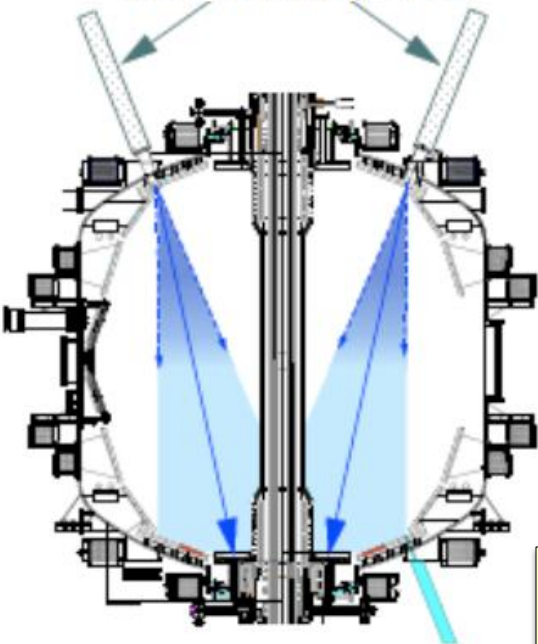
* T.R. Jarboe, FT (1998)

Lithium Research Supplemental Slides

Solid lithium surface coatings pump D, increase confinement, stored energy, and pulse length, and eliminate ELMs

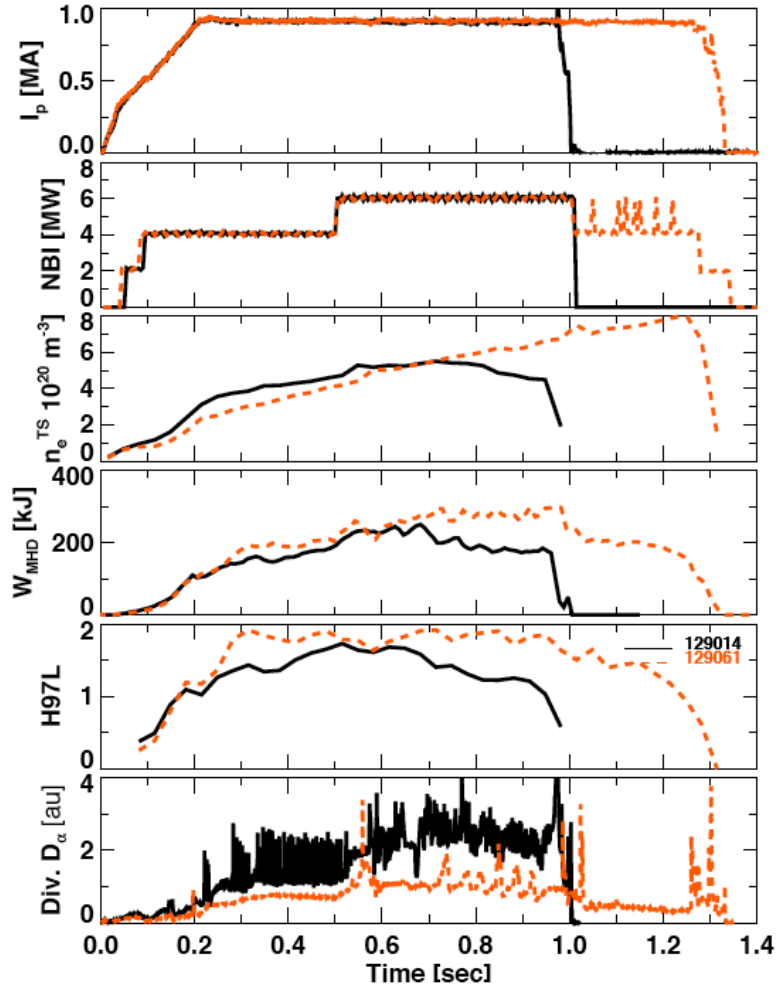
• 2009: Lithium evaporation became baseline wall-conditioning tool

Dual Liquid Lithium Evaporator
For Li wall coatings
Now routinely used

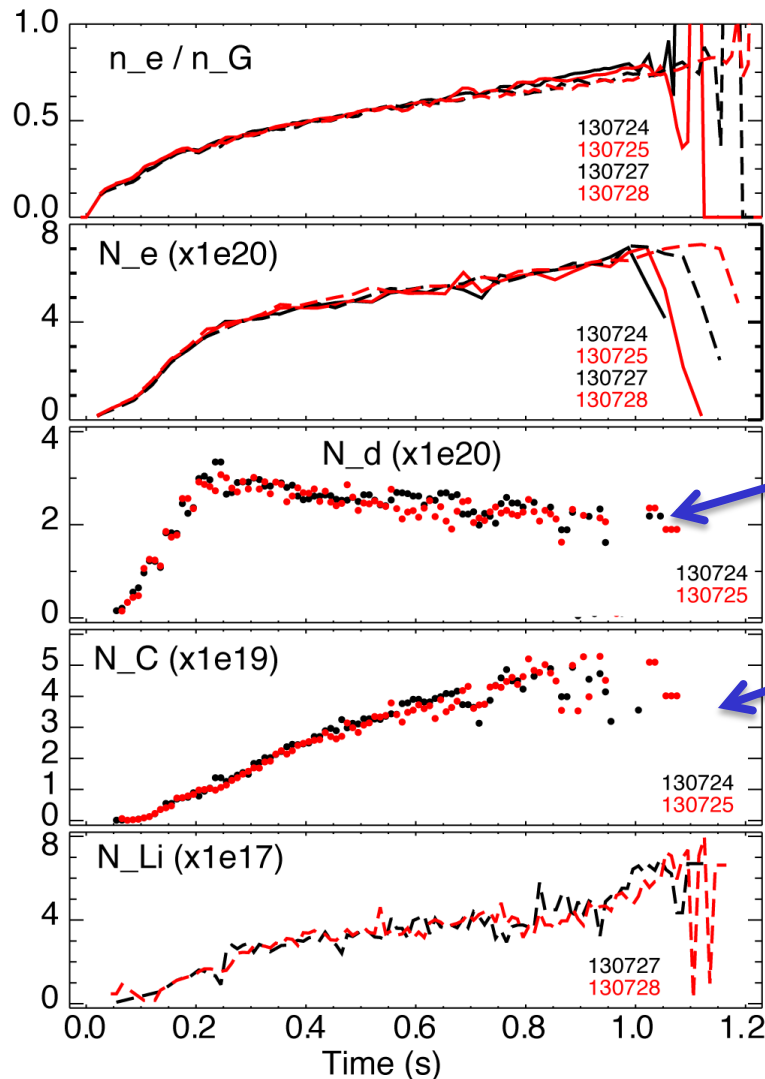


- H. Kugel, IAEA FEC 2010 Oral, FTP/3-6Ra
- H. Kugel, FED 85 (6) 865-873 (2010)
- M. Bell, PPCF 51 (12), (2009) 124054
- M. Bell, EPS Invited Talk 2009
- D. Mansfield, JNM 390-91, 764-767 (2009)
- H. Kugel, JNM 390-391, 1000-1004 (2009)

- No longer perform between-shot He glow
- Typically deposit 50 to 300mg Li between shots



With lithium coating pumping, deuteron inventory is constant or even decreasing, C accumulates, Li saturates



Electron density rises monotonically in lithium induced ELM-free H-mode

Strongly Li-pumped discharges exhibit D inventory pump-out

but C inventory increases

Li inventory increases slowly, remains at very low value

➤ Lithium screening efficiency is high, penetration factor is low: $N_{Li} / \Gamma_{Li} \sim 0.0001$

As a result, NSTX is shifting emphasis from D inventory control to C impurity reduction

R. Bell, M. Podestà (PPPL) V. Soukhanovskii (LLNL)

NSTX contributed unique Li data to FY09 joint research milestone on "...particle control and hydrogenic fuel retention in tokamaks"

Edge pressure and wall inventory changes with Li

FY09 JRT

With Li:

- lower edge neutral pressure
- higher wall particle inventory.
- Additional D wall inventory is released after discharge.

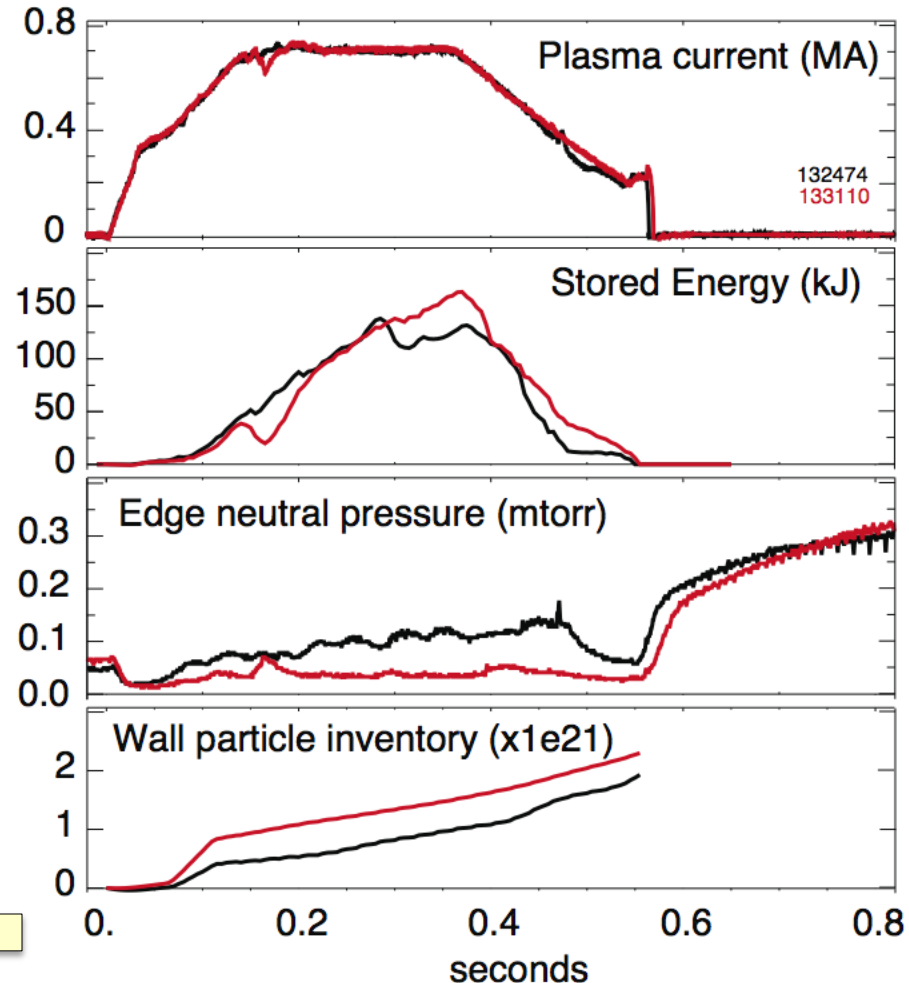
Retention Summary	Before Li	With Li
Ohmic	92%	94% (48 mg Li)
NB heated	87%	93% (137 mg Li)

Wall inventory calculated by dynamic particle balance model.

V. Soukhanovskii

• C. Skinner, JNM (2011) – in press

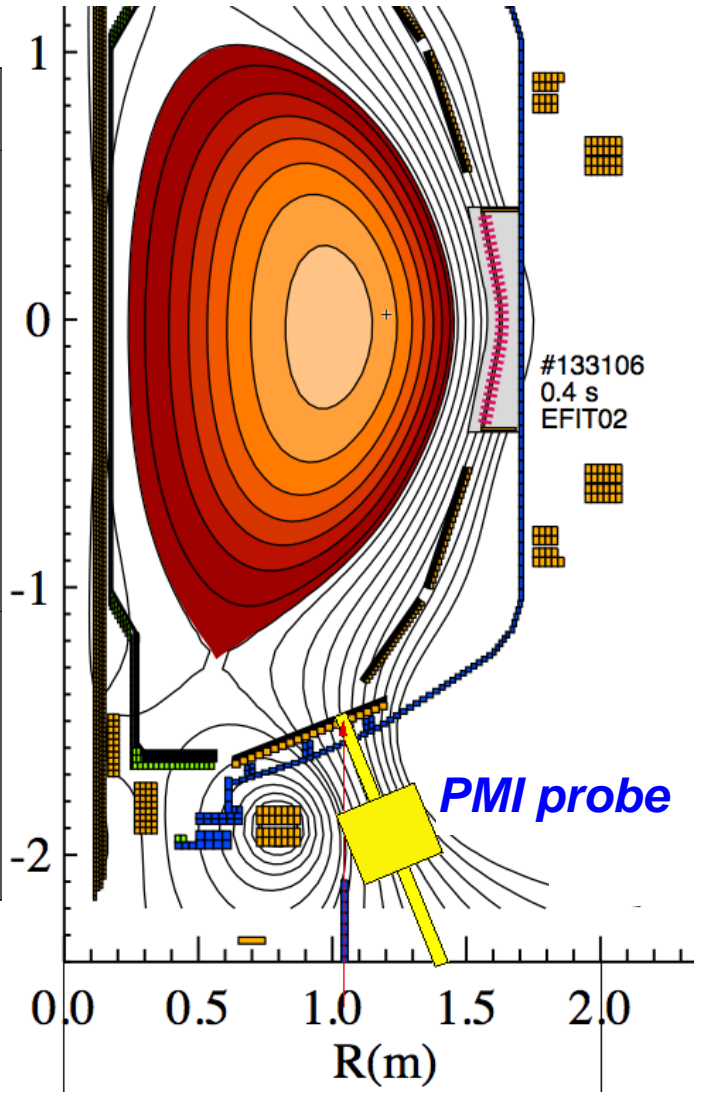
Pre-Li and **with Li** NB heated discharge



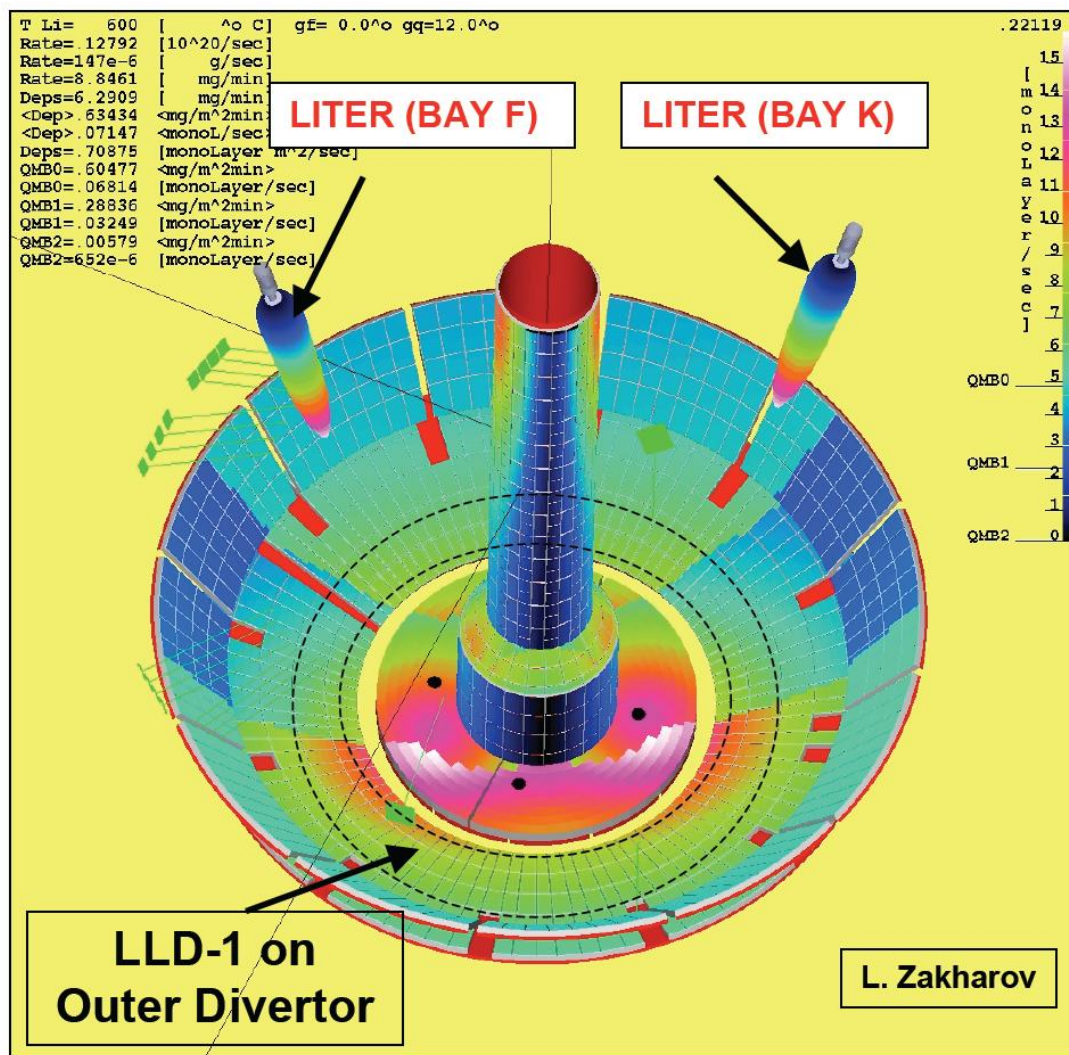
Gas balance retention measurements correlate with in-situ PMI surface science measurements

GAS BALANCE:	SURFACE ANALYSIS
Retention higher with Li, difference increases with Li concentration	X-ray Photo-electron Spectroscopy shows D atoms are weakly bound in regions near lithium atoms bound to either oxygen or the carbon matrix. Chemical bonding changes with Li concentration.
Additional D retained with Li is released promptly after discharge	Weak D bonding with Li conditioning observed in Thermal Desorption Spectroscopy.

DOE FY09 JRT



2010: LLD Loaded With Lithium Using LITER



- **LITER Deposition Capability**
 - for LLD-1 to pump NSTX plasma from $7 \times 10^{13} \text{ cm}^{-3} \rightarrow 5 \times 10^{13} \text{ cm}^{-3}$ will require the absorption of 2.4×10^{20} D particles, every particle confinement time ($\sim 50 \text{ ms}$), for 1000 ms, for a total of 4.8×10^{21} D particles absorbed.
 - for a 1:1 D/Li ratio requires at least $5.5 \times 10^{-2} \text{ g}$ of lithium ($2 \mu\text{m}$).
 - present LITER deposition efficiency on to LLD $\sim 7\%$ of its total output, then the total lithium need is 0.79 g.
 - using two evaporators at 30 mg/min (FY07 typ) will require about 13 min to coat the LLD-1.
 - if lower concentration ratio 0.1D/Li is required, then need 7.9 g of lithium ($20 \mu\text{m}$), or 4 g per LITER, operating at 100 mg/min for 40 min.

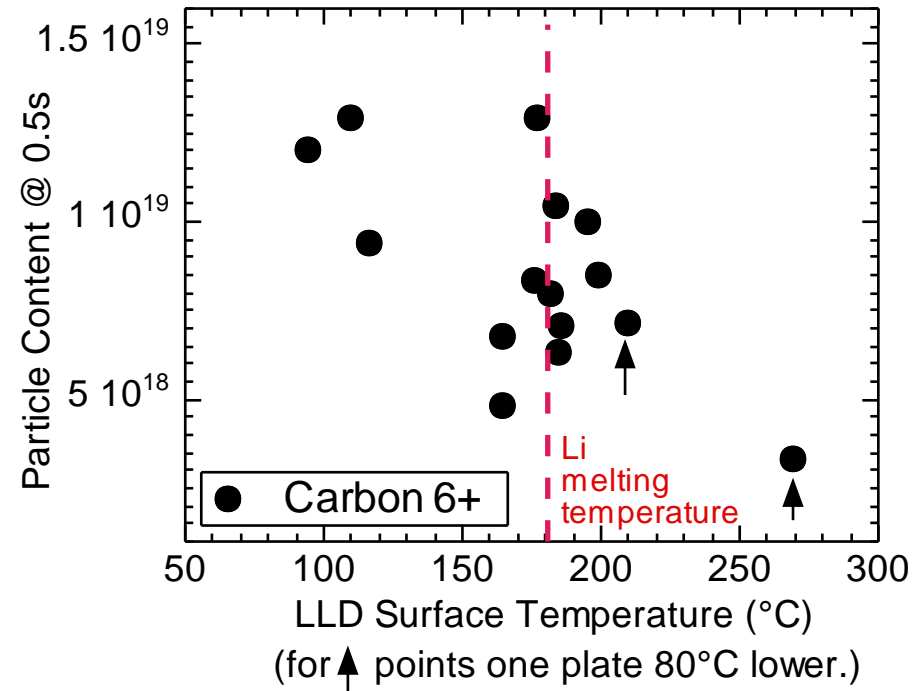
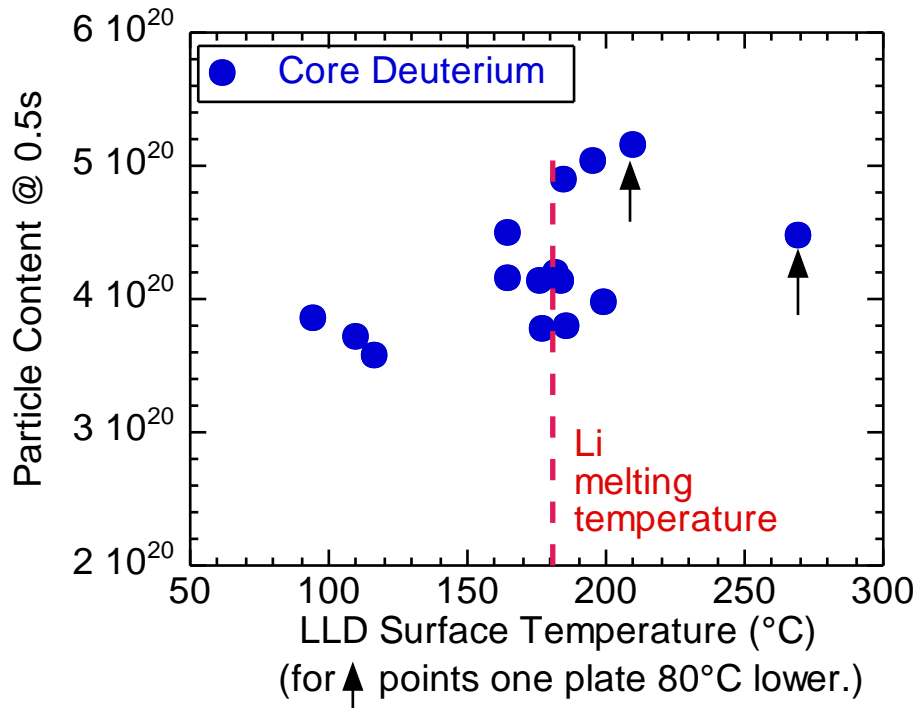
Overview and chronology of LLD results and plans

- 2007-10: LLD designed, implemented with goal of providing 30-50% reductions in n_e to enable variations in collisionality and NBI CD fraction
- During this time, routine Li evaporator operation successfully implemented
 - Deuterium inventory control demonstrated for 1-1.5s, $n_e / n_{\text{Greenwald}}$ from $D^+ = 0.2-0.4$
 - Substantial fraction of n_e can come from accumulation of C^{6+} and high-Z due to lack of ELMs
- Decision made to use LiTER to fill/replenish LLD during first year of ops
 - Completing and installing LLD + implementing LLD diagnostics consumed available resources
 - 2010 plan: Develop liquid lithium fill system for LLD during 2010 to utilize in 2011-12
- 2010 results: **LLD did not exhibit D pumping beyond that achieved w/ LiTER**
 - No Mo observed with strike-point on LLD, core impurities reduced (may be due to low- δ /ELMs)
 - Plasma heat can melt Li during shot (re-solidifies after) – minimizes Li reactivity between shots
 - Some evidence of divertor T_e increase when $T_{\text{LLD-surface}} > T_{\text{Li-melt}}$ – enhanced local pumping?
- LLD technical problems during 2010 run
 - Insufficient plate grounding + disruptions → arcing to surrounding tiles and heating and cooling tubes, mechanical damage to plate supports, eventual failure of most electrical heaters
 - Insufficient time/resources to restore LLD heating capability → rely on plasma heat to melt Li
- 2011-12: Improved LLD grounding/supports, added Mo inboard divertor tiles
 - Assess pumping/impurities w/ Li + inboard + outboard Mo PFCs → use Mo PFCs in Upgrade?

FY10 Li /LLD operational summary

- Rapid startup with Li conditioning and without boronization.
- Total of 1.3 kg Li evaporated (2x 2009 level), extensive lithium coverage of PFCs.
- Devoted 11 run days, 6 XPs, 452 discharges to LLD commissioning and characterization.
- Performed 0.6 run day for increased Li delivery via Li powder injection.
- Explored plasma D content and gas balance vs.
 - LLD Li fill,
 - LLD temperature,
 - strike point location,
 - fueling,
 - divertor gas injection etc...
- Porous Mo (LLD) and ATJ samples exposed by PMI probe, retrieved and analyzed.
- 2-color thermography and high density Langmuir probe array commissioned.

LLD pumping similar above or below Li melting temperature

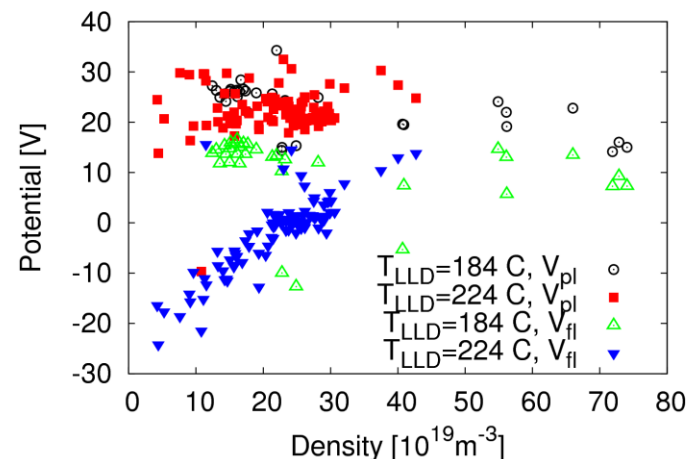


- Constant deuterium fueling for LLD 100% Li fill conditions, 4 plates air heated.
- As LLD surface temperature transitioned from solid temperatures to the liquid regime, the plasma electron and deuterium content remain relatively constant.
- Core carbon C6+ content decreased - may be due in part to increased ELMing and edge turbulence.
- No systematic trend in D-alpha, wall inventory, or ion pumping with a transition above the Li melting temperature.

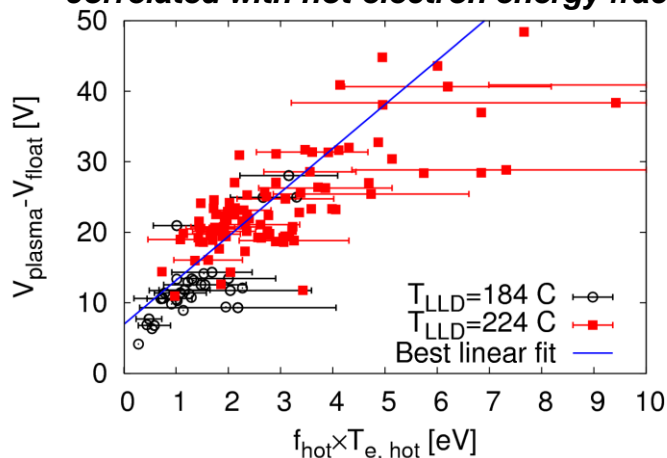
Higher local electron temperature during LLD melting sequence despite increased fueling

- Langmuir probes indicate increase in near-surface electron temperature during LLD experiments
 - Discharge sequence indicated decreased fueling efficiency during LLD heating (gas increased, N_e constant)
 - Non-local and classical probe interpretations applied, increase in T_e consistent with increase in $V_p - V_f$ difference
 - Temperature rise occurs in hot-electron population of the distribution function
 - Observations consistent with plasma-absorbing PFC

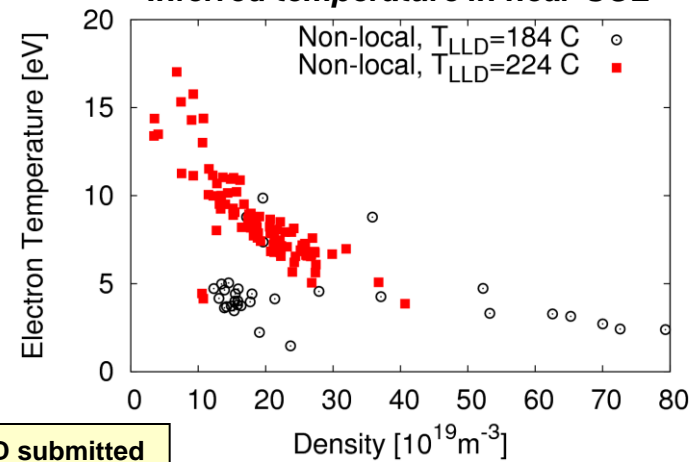
Floating and Plasma Potentials



Difference in potentials most strongly correlated with hot-electron energy fraction

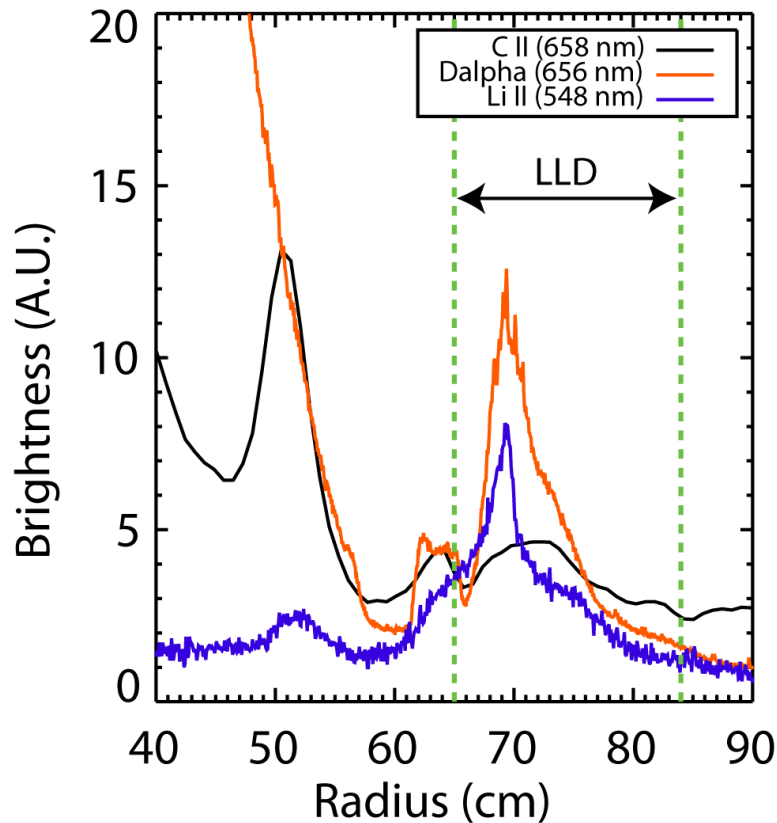


Inferred temperature in near-SOL



M.A. Jaworski, ISLA oral, FED submitted

LLD surface was not pure Li



- Carbon, lithium, and deuterium emission extends across LLD surface after overnight Li evaporation.
- No marked change at LLD location

LLD after vent at end of run



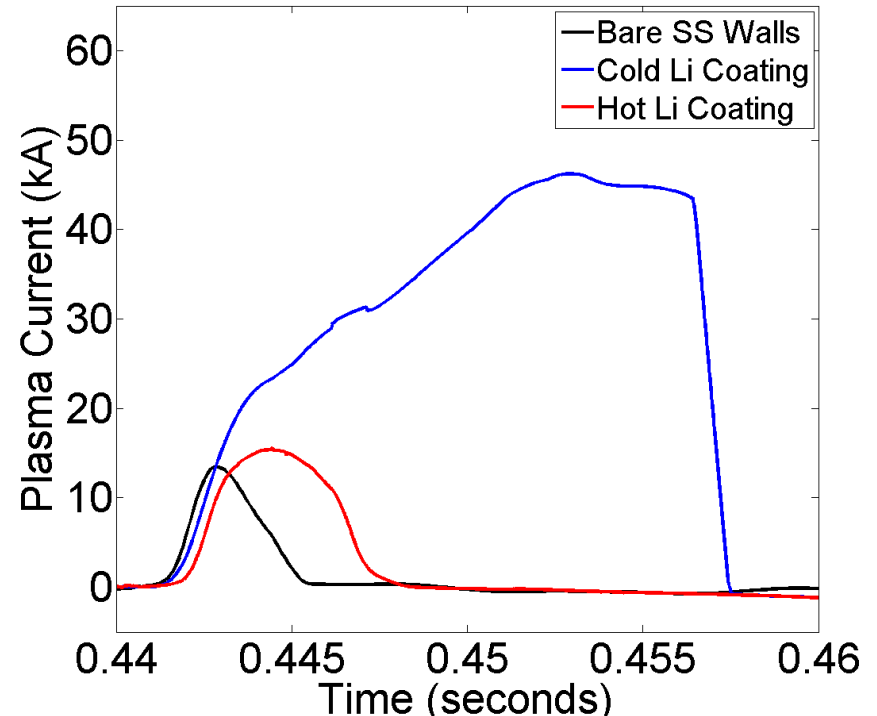
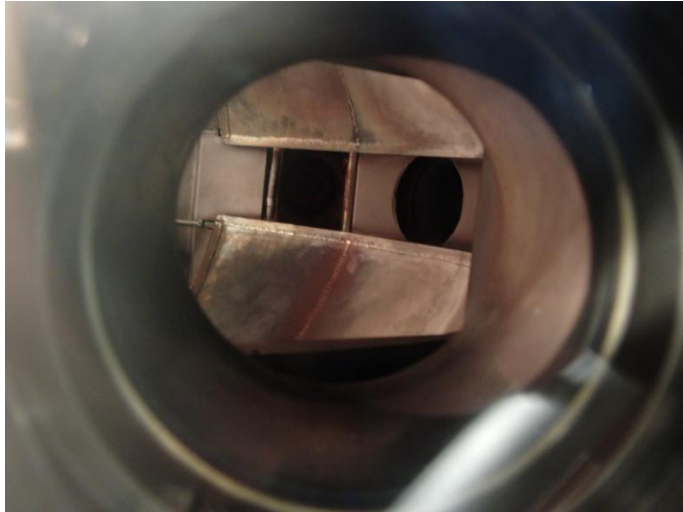
60 Radius (cm) 80

- LLD surface converted to Li_2CO_3 following vent
- LLD edges exhibit evidence of sputtered graphite from plate to graphite tile (vessel-ground) arcing.
- Acetic acid tests on the LLD after run suggests that Li does wick into Mo pores and is depleted from the surface at blackened region.
- Reactions with residual gasses also likely

Full metal wall data from LTX shows thin liquid film reacts rapidly with residual/background gasses



- ◆ LTX is a full high temperature, high Z wall operation of a tokamak
 - lithium evaporated into 5 mTorr helium fill to disperse coating.

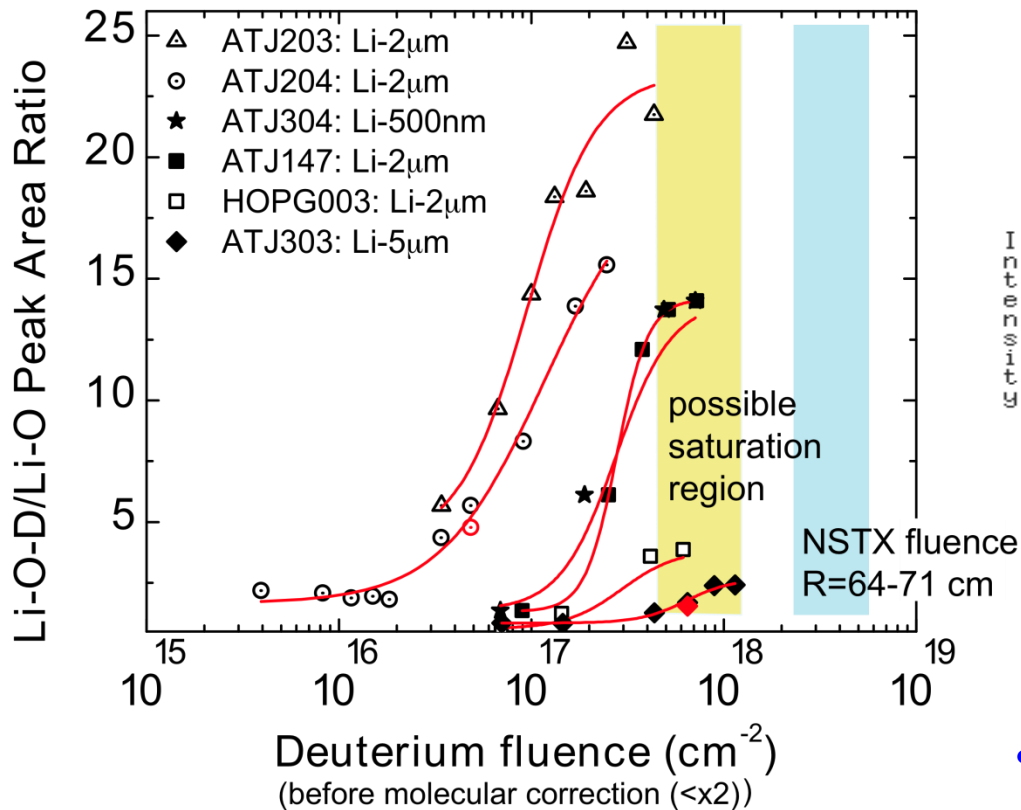


- ◆ Deposition rate ~0.75 g/hour/evaporator
 - 3 hour duration
 - est. 1.6 micron average thickness.
- ◆ Thin liquid lithium coating darkened rapidly
 - indicative of reactions with background gases or oxidized substrate
 - no visual evidence of metallic surface.

- Hot (300 °C) shell with thin lithium coatings does *not* exhibit reduced recycling
 - but strong lithium emission observed
 - relevant to NSTX LLD operation.

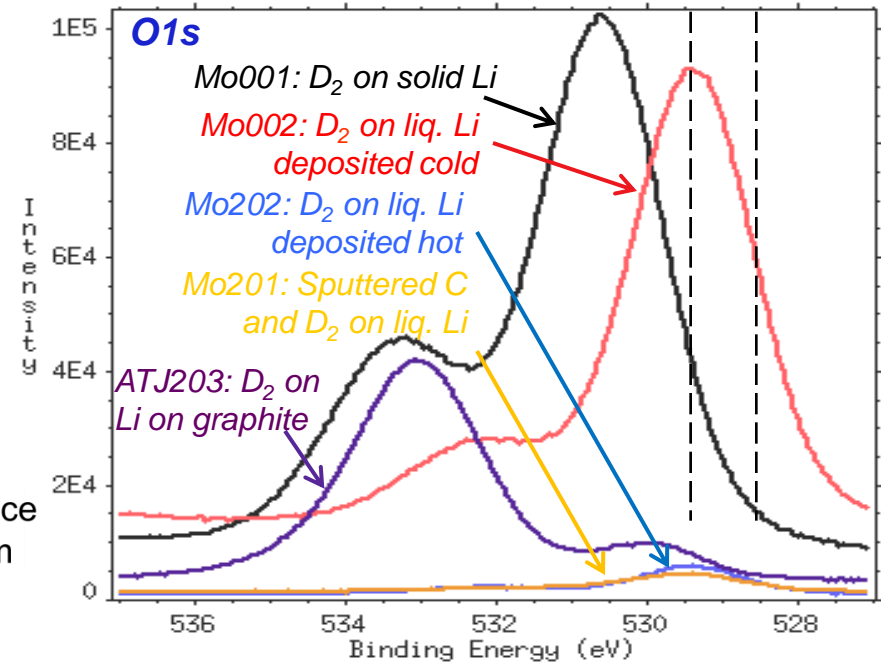
Lab analysis of NSTX exposed samples (Purdue U.)

Deuterium saturation of Li



- Modeling by the TBDFT code showed the probability for D to bond to a Li-C complex is 3 x larger than to C

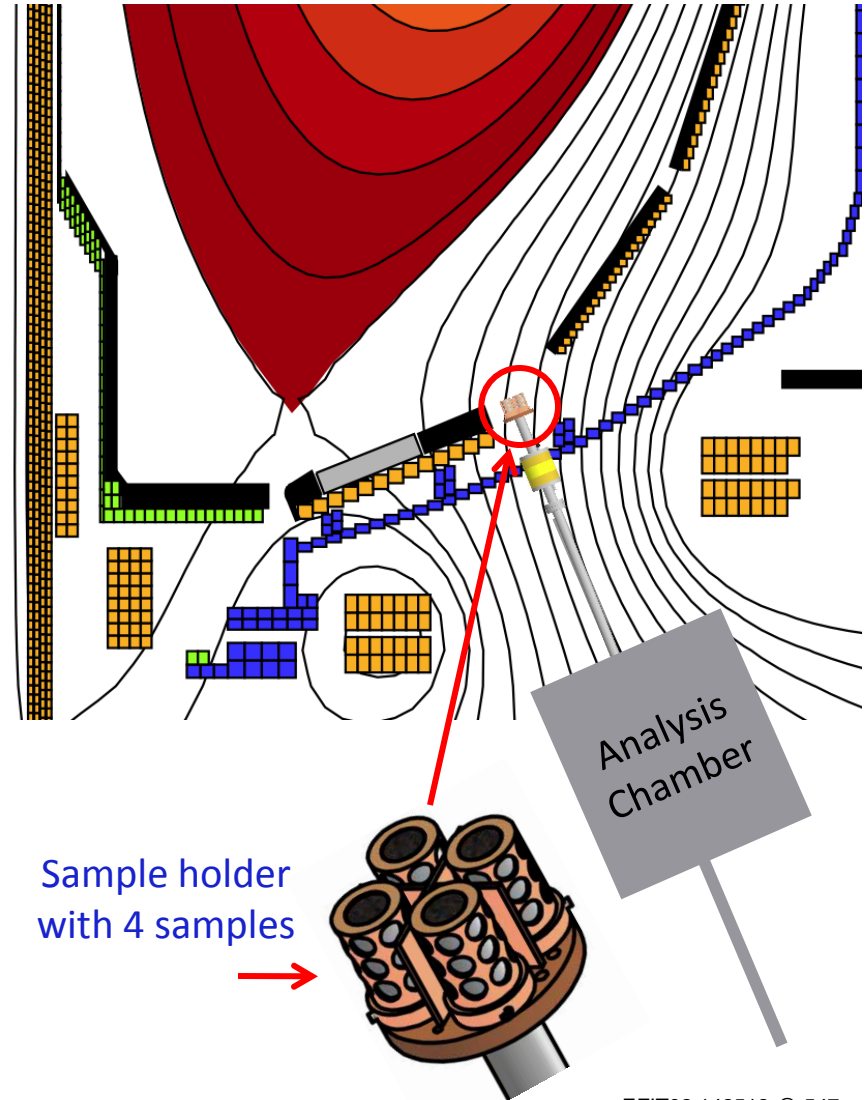
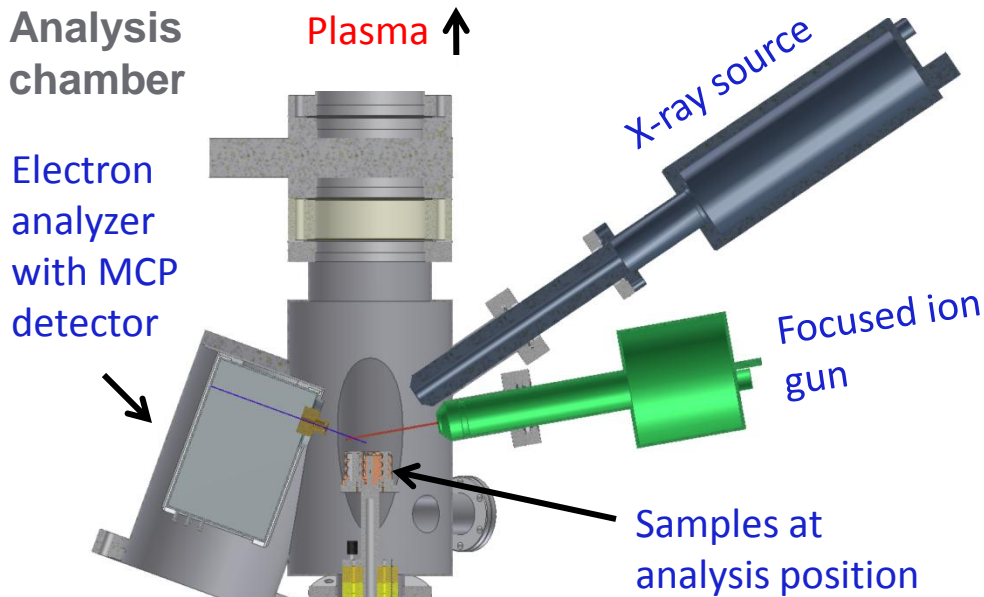
XPS O1s spectra for the LLD samples 30 mins D_2 irradiation of Li on:



- XPS O1s spectra show changes in surface chemistry with D irradiation of Li deposited on cold / hot / C contaminated Mo and graphite.
- Suggests Li on Mo is interacting with D and diffusing into Li.

MAPP probe will be installed for FY11-12

- MAPP is the first in-vacuo surface analysis diagnostic directly attached to a tokamak, capable of shot-to-shot chemical surface analysis of material samples (solid Li, liquid Li, Mo etc).
- MAPP will enable the correlation of PFC surface chemistry with plasma conditions and point the way to improved plasma performance. (R12-1)

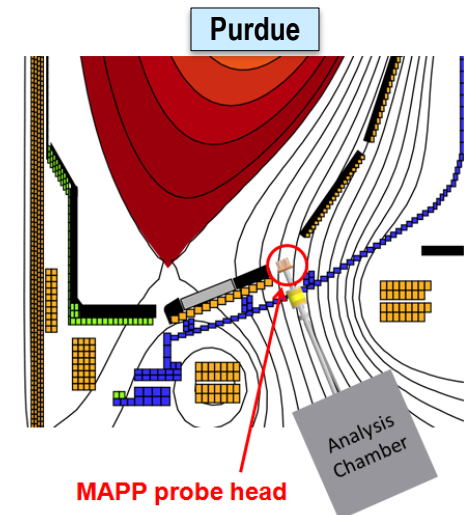


EFIT02 142512 @ 547 ms

New diagnostics will be used to investigate relationship between Li-conditioned surface composition & plasma behavior R12-1

• JP Allain, JNM 390-391 (2009) 942-946

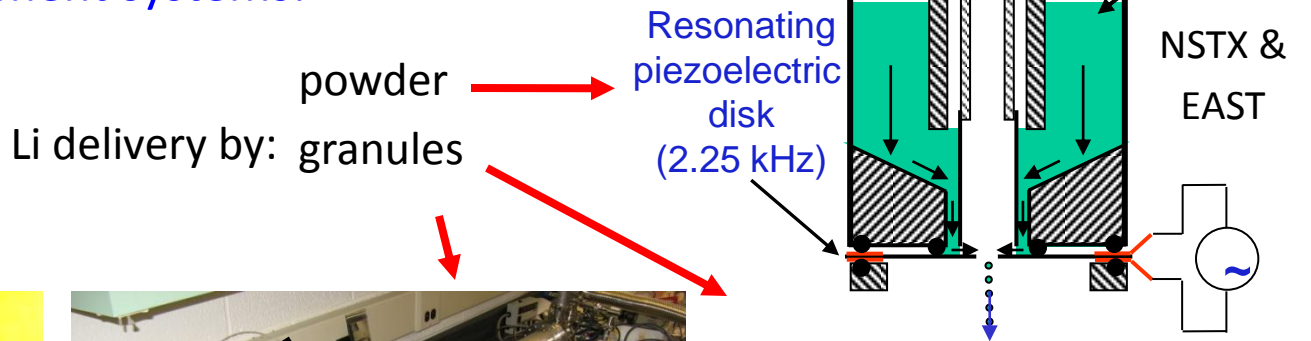
- Chemistry of Li on C/Mo critical, complex, **under-diagnosed**
- Li very chemically active → *prompt* surface analysis required to characterize the lithiated surface conditions during a shot
- An in-situ materials analysis particle probe (MAPP) being installed on NSTX to provide prompt surface analysis
 - Ex-vessel but in-vacuo surface analysis **within minutes** of plasma exposure using state of the art tools
- Li experiments will utilize MAPP to study:
 - Reactions between evaporated Li and PFCs, gases
 - Correlation surface composition and plasma behavior, comparisons to lab experiments, modeling
 - Characterizations of fueling efficiency, recycling



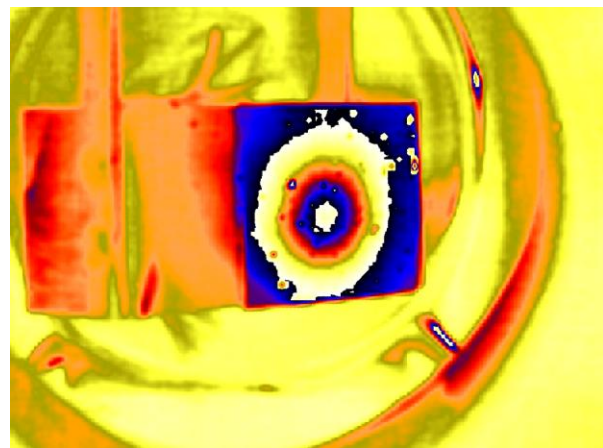
• J.-P. Allain: DOE Early Career Research Award - 2010

Lithium Technology developed for NSTX needs

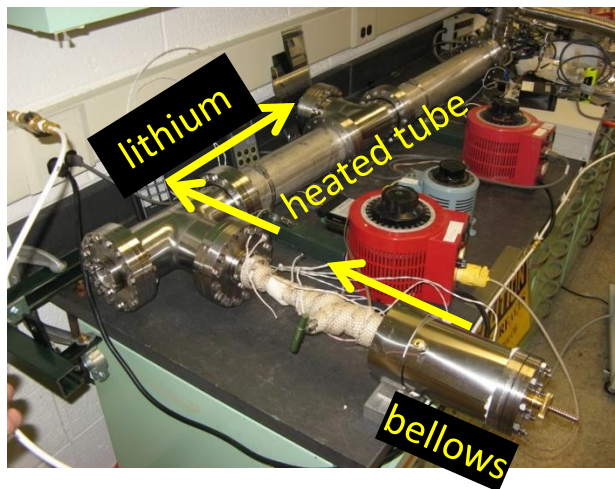
- R&D continuing for LLD performance at high heat flux.
- Continuous Li replenishment systems:



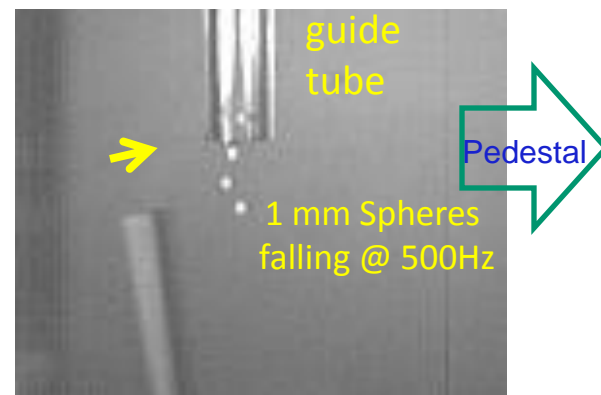
High heat flux test



False color image of LLD sample during NB exposure
 $T \leq 225 \text{ }^\circ\text{C}$ @ 1.5 MW/m^2 - 3s.
 Potential PFC for upgrade



10 g of molten Li moved
 1.1m in vacuum and
 ejected 7.6 cm from nozzle



500 Hz Impeller Rotating @ 95 m/s
 Midplane injection for
 ELM pacing

Boundary Physics Supplemental Slides

Partial divertor detachment (PDD) and associated heat flux reduction achieved with D₂ divertor gas puffing

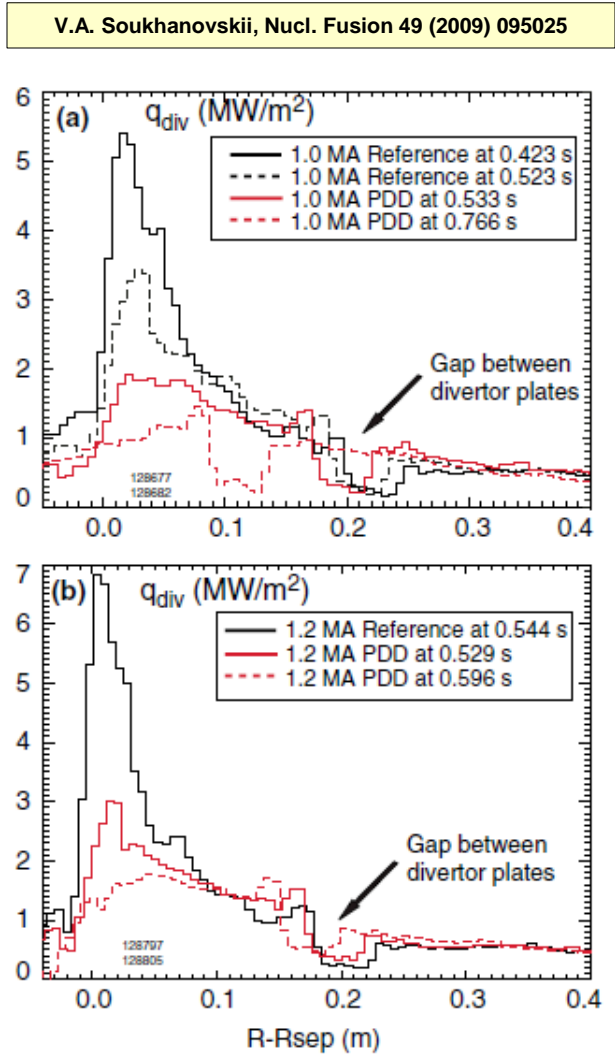
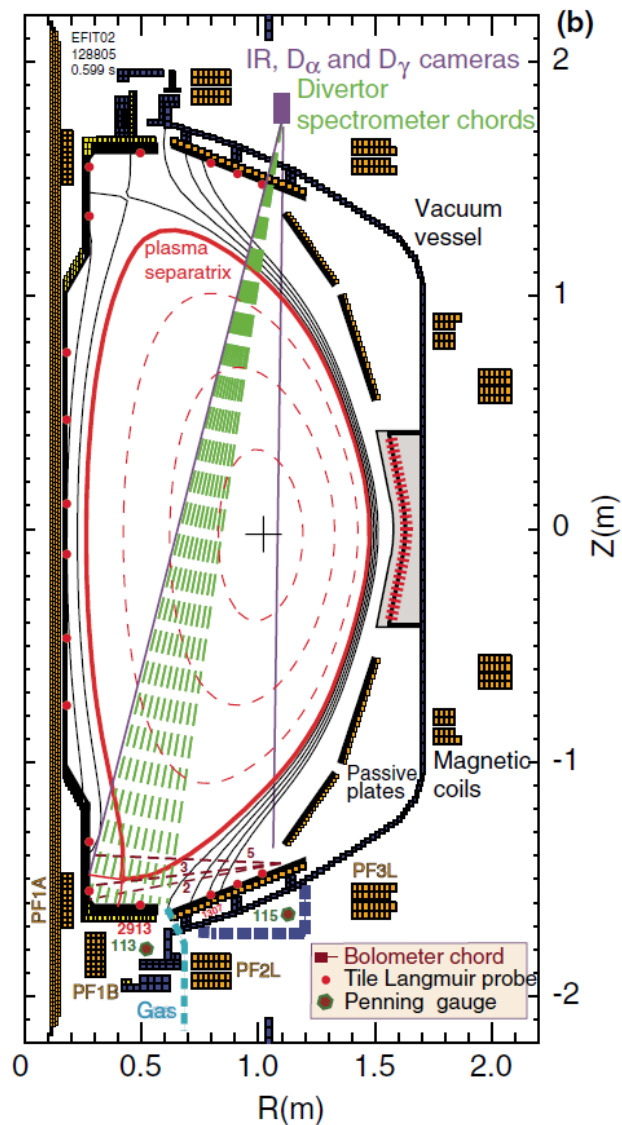
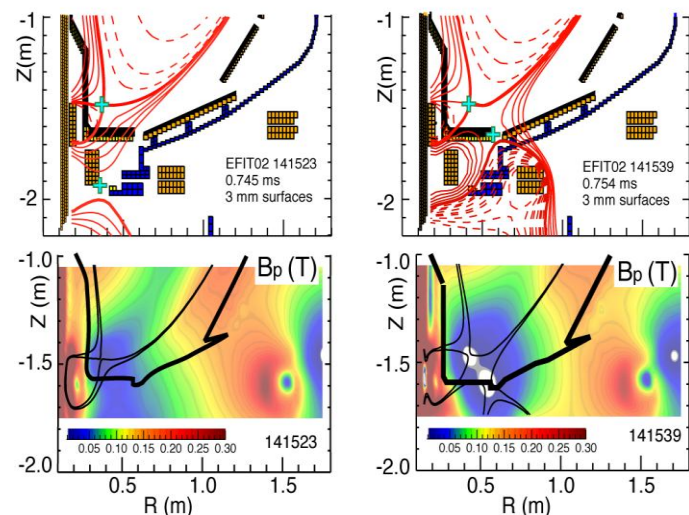
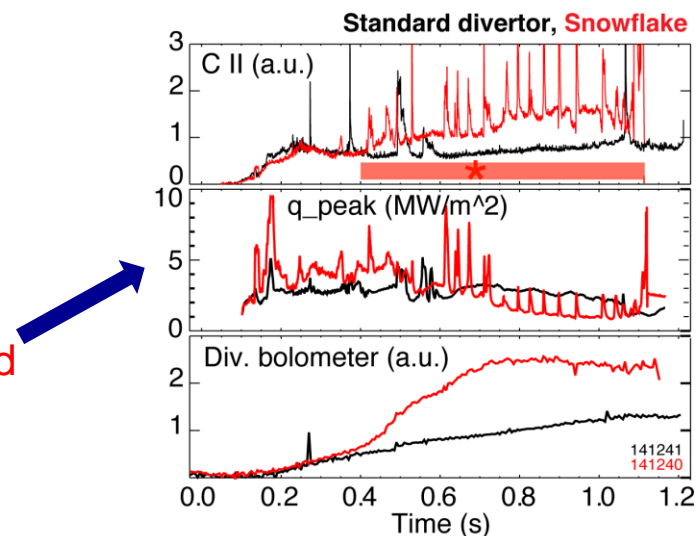


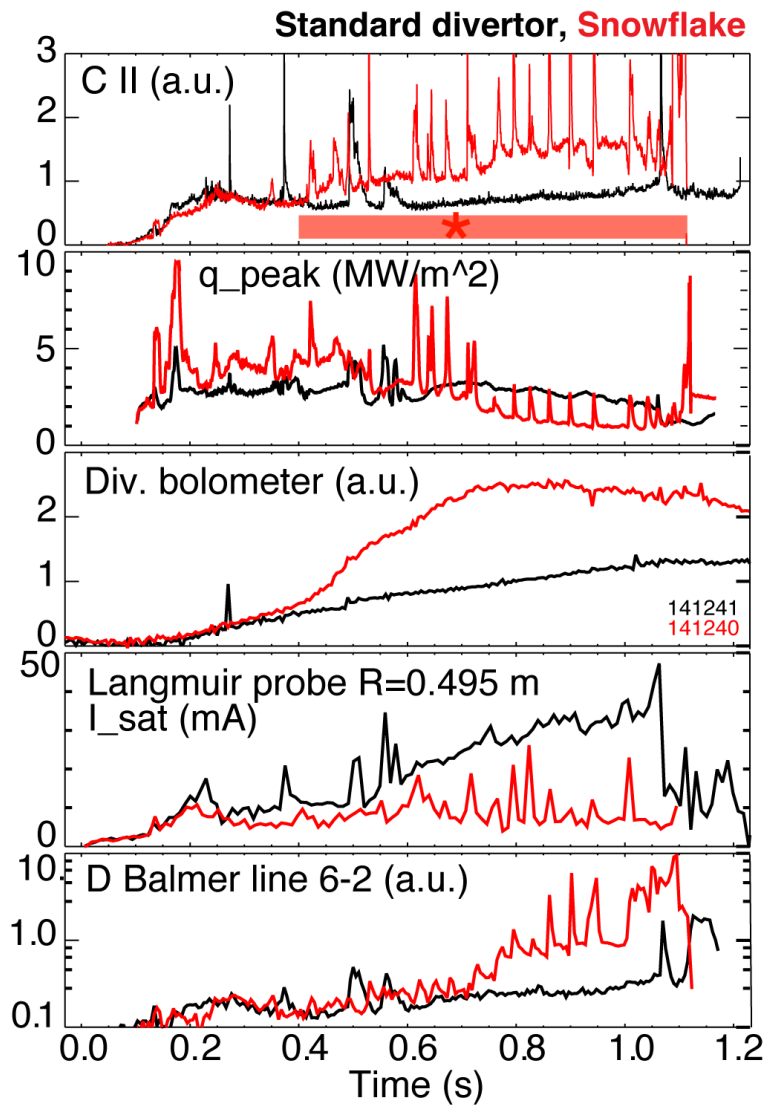
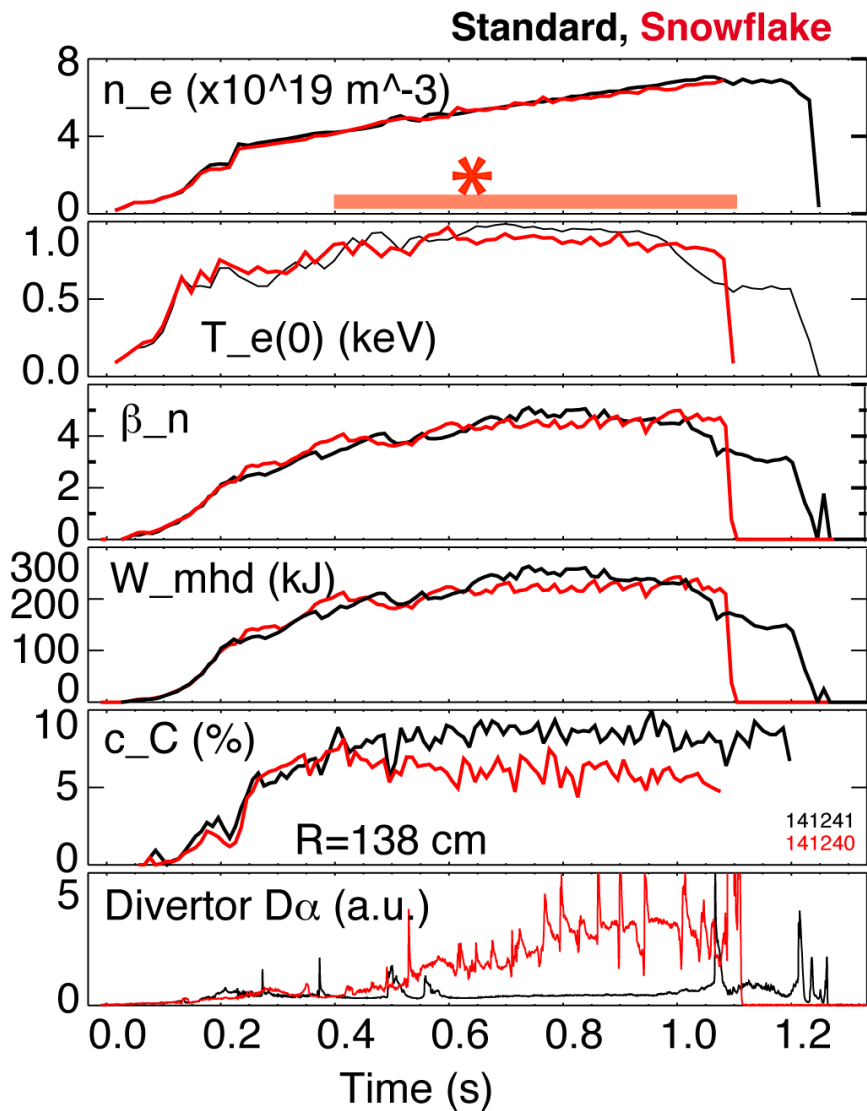
Figure 4. Divertor heat flux profiles in the reference and PDD discharges: (a) 1.0 MA and (b) 1.2 MA.

Snowflake divertor studies inform divertor solutions for NSTX-U, future high power density tokamaks

- Progress in snowflake divertor studies
 - Magnetic control: snowflake-minus w/ three divertor coils up to 600 ms
 - Partial detachment of outer strike point
 - q_{pk} reduced from 3-7 to 0.5-1 MW/m² at $P_{SOL} \sim 3$ MW due to increased divertor P_{rad} (up to 50 %) and high flux expansion (increased up to 90 %)
 - Core and pedestal carbon concentration reduced by up to x 50 %
 - ELM regime modification (no ELMs -> Type I)
 - UEDGE modeling commencing
- Planned research (R11-3, R12-3)
 - Divertor power balance, radiation and turbulence characteristics, pumping with lithium, impurity seeding
 - Pedestal structure, P.-B. stability, ELM control
 - NSTX-U divertor scenarios
 - NSTX-U shaping, upper+lower snowflake



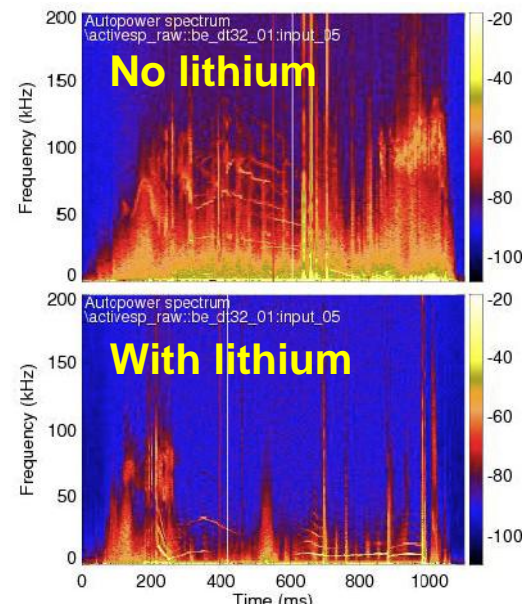
Good H-mode confinement with reduced impurities and outer strike point detachment with snowflake divertor



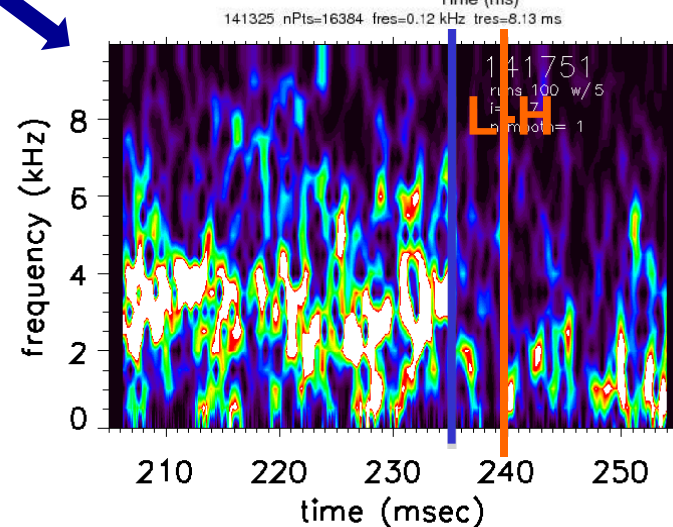
Pedestal / SOL turbulence measurements and modeling contributing to edge transport and L-H transition studies

- Transport and turbulence with lithium
 - Turbulence reduction with lithium
 - Low-k $\delta n/n$ in pedestal measured by BES
 - $\delta n/n$ from $\sim 10\%$ to 1% from edge reflectometer
 - $\delta n/n$ in pedestal measured by high-k scattering
 - UEDGE and SOLPS transport modeling
- L-H transition physics
 - Edge zonal flow/GAM and turbulence modulation at ~ 3 kHz preceding L-H transition (from velocimetry of edge turbulence flow speed)
 - No systematic changes in poloidal flow shear during ~ 1 msec just before L-H transition at ± 3 cm around separatrix – no clear L-H trigger
- FY2011-12 planned research:
 - Spatial localization of L-H transition
 - Validation of SOLT, GAMs, XGC-1, BOUT simulations using NSTX data
 - Effect of 3D fields, SOL currents, X-points on edge transport and ELMs

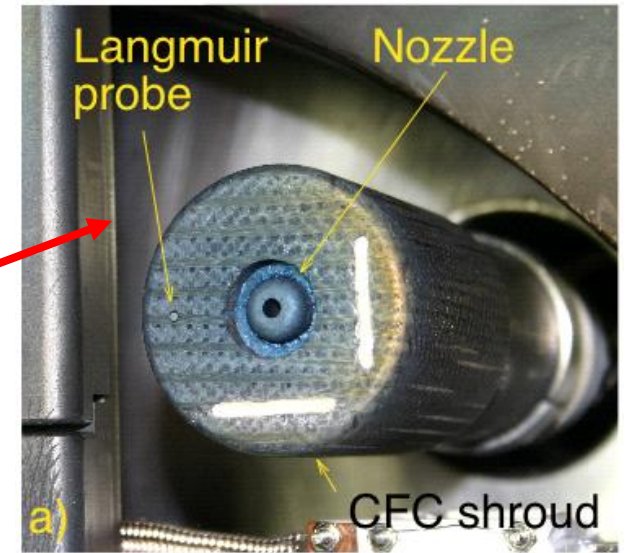
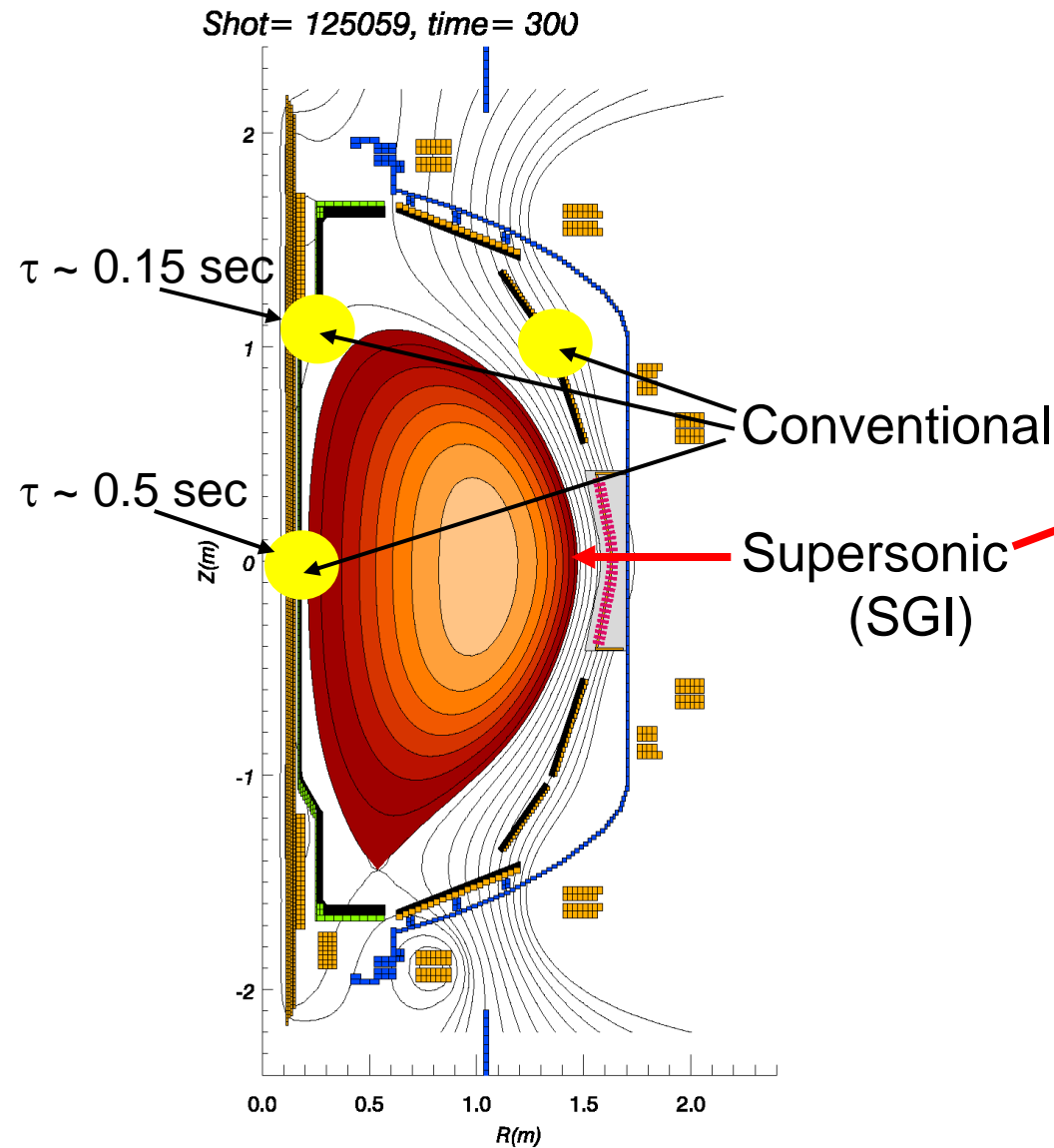
U. Wisconsin
UCLA



U. Colorado



NSTX gas fueling locations and turn-off time-scales

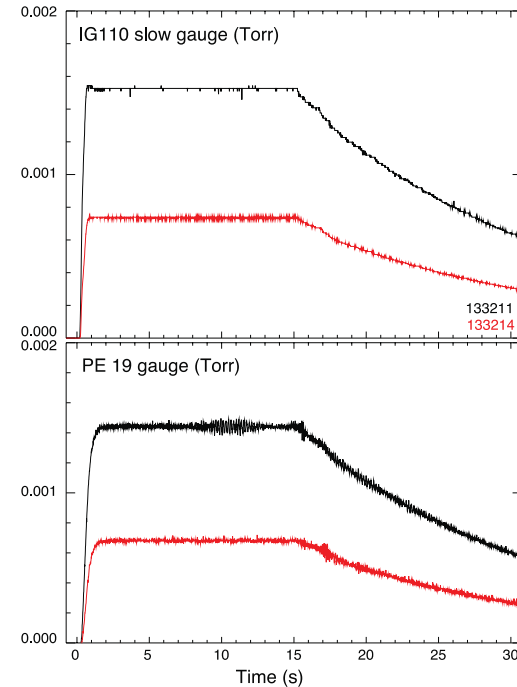
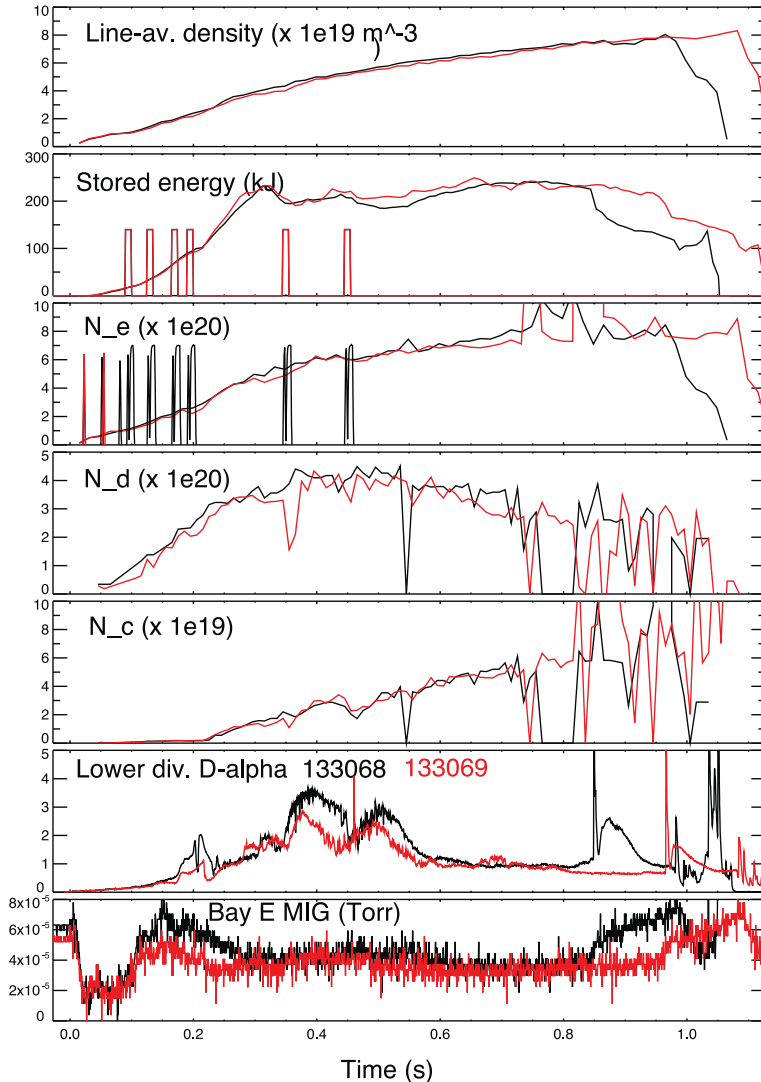


- SGI provides efficient, controllable fueling

V. Soukhanovskii, LLNL

SGI fueling results in higher fueling efficiency, lower edge neutral pressure

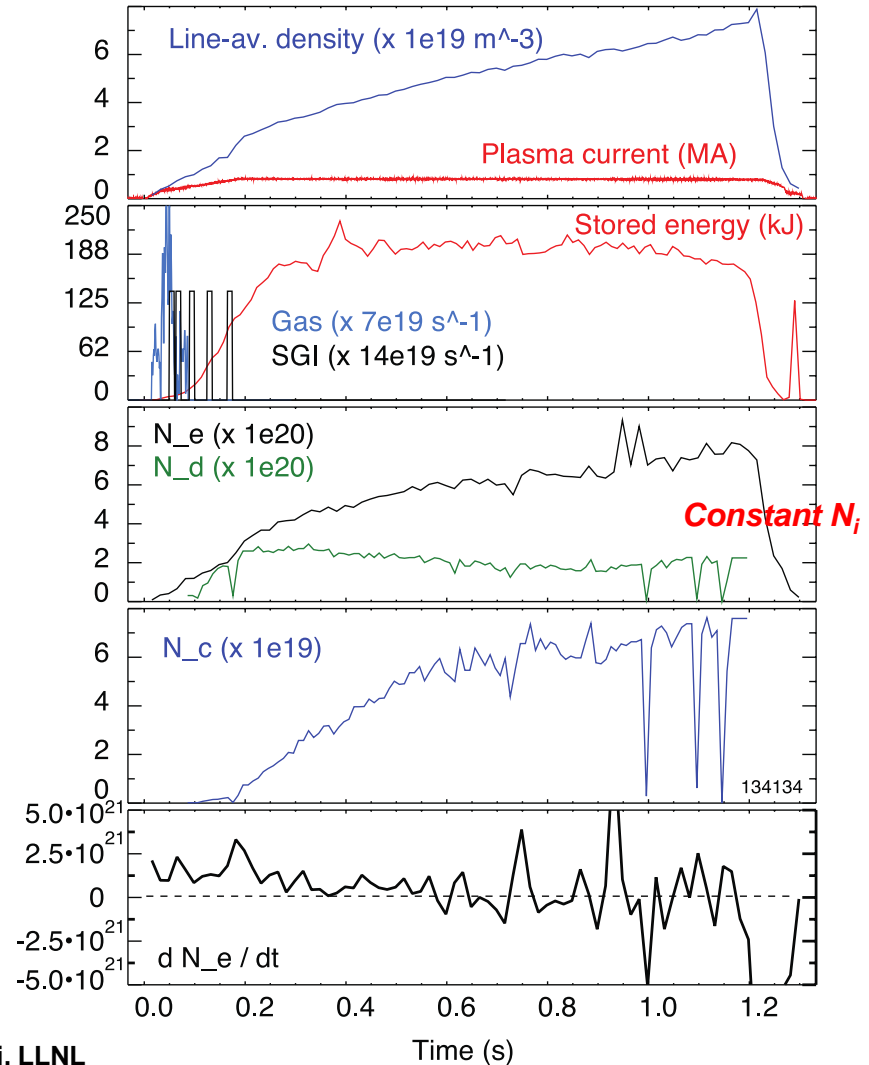
- Comparison between **SGI** and **conv. gas injection** was only possible by 1) matching density in 1 MA, 6-4 MW discharges; 2) comparing gas injection rate and total gas inventory



V. Soukhanovskii, LLNL

SGI-only fueling scenario with steady-state ion inventory developed

- Obtained good n_e and T_e profiles (at outer gap ~ 10 cm) to compare SGI and LFS fueling
 - Will analyze pedestal height and width in collaboration with ORNL
- Developed shoulder and SGI long pulse fueling scenarios
- Developed SGI-only fueling scenario with ion density control
 - N_i constant, while N_e is rising due to carbon; LITER at 9 mg/min

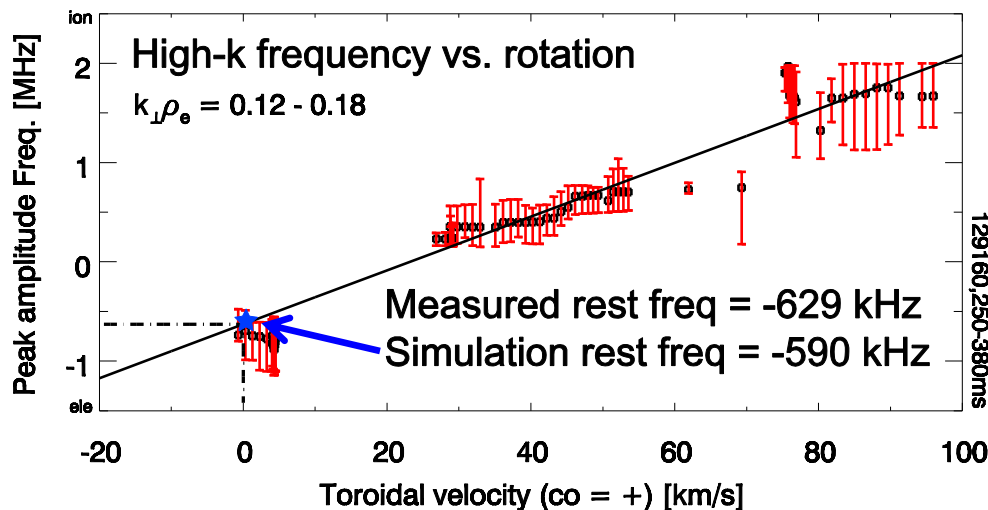


V. Soukhanovskii, LLNL

Transport and Turbulence Supplemental Slides

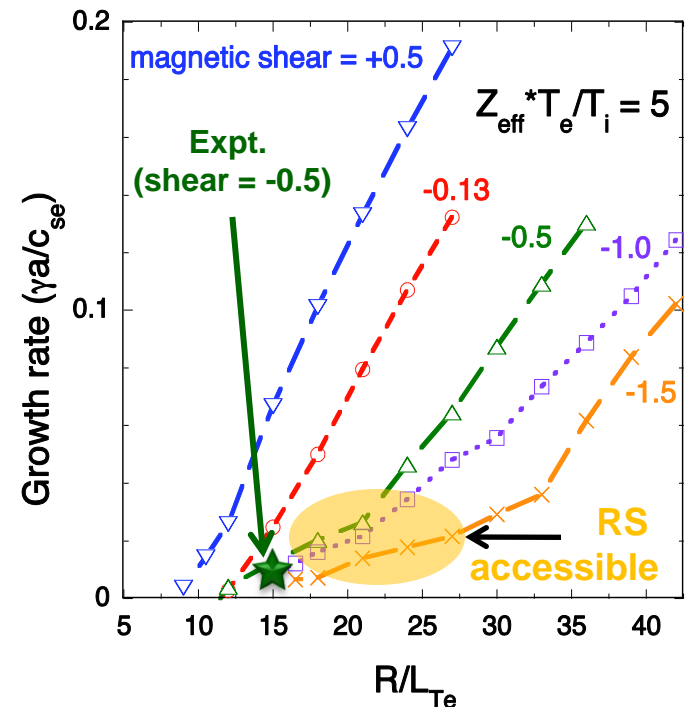
ETG turbulence proposed as possible cause of anomalous electron transport

- ETG mode has been identified by comparing linear growth rate and rest frequency of measured fluctuations to linear GS2/GYRO calculations
- ETG in e-ITB found to be suppressed by reversed magnetic shear, allows access to supercritical electron temperature gradients



Rest frequency of peak amplitude mode measured by subtraction of Doppler shift due to plasma rotation

H. Yuh, PRL 106, 055003 (2011)

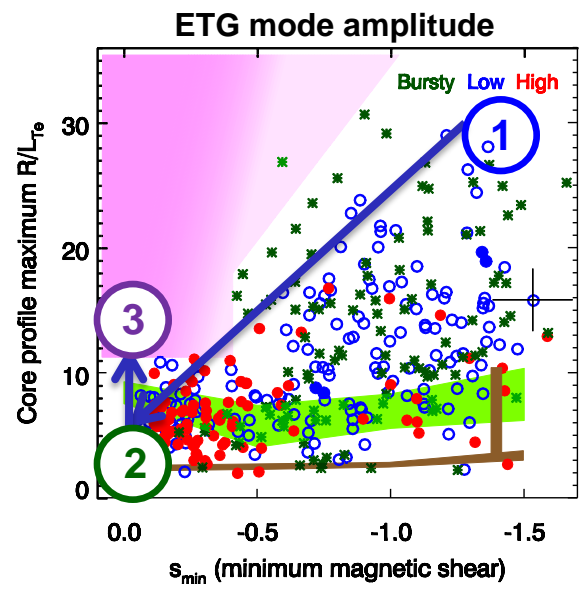
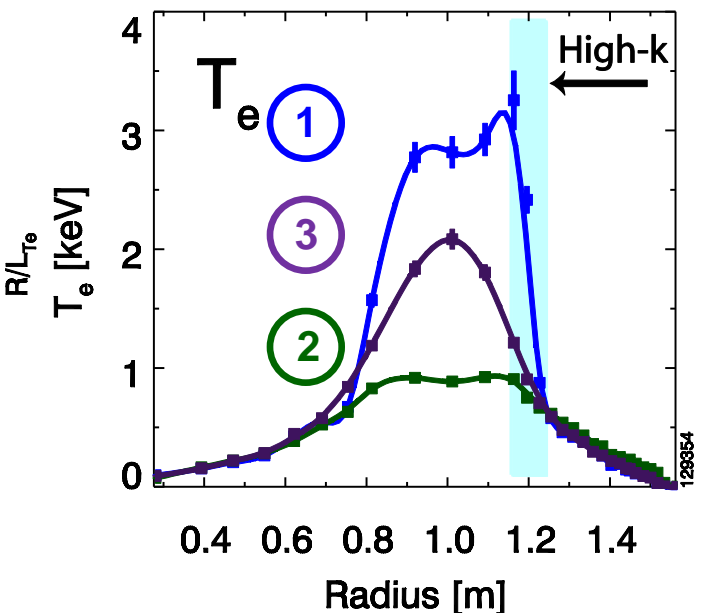
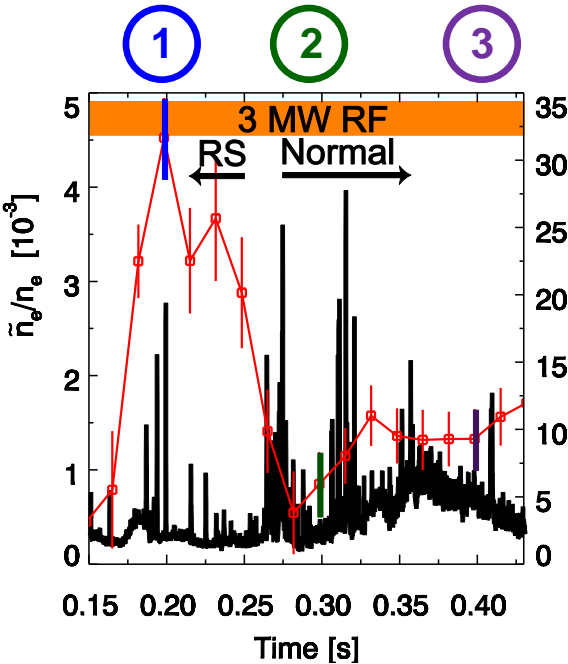


Linear GS2 / GYRO simulations of ETG mode growth rates are consistent with high-k measurements

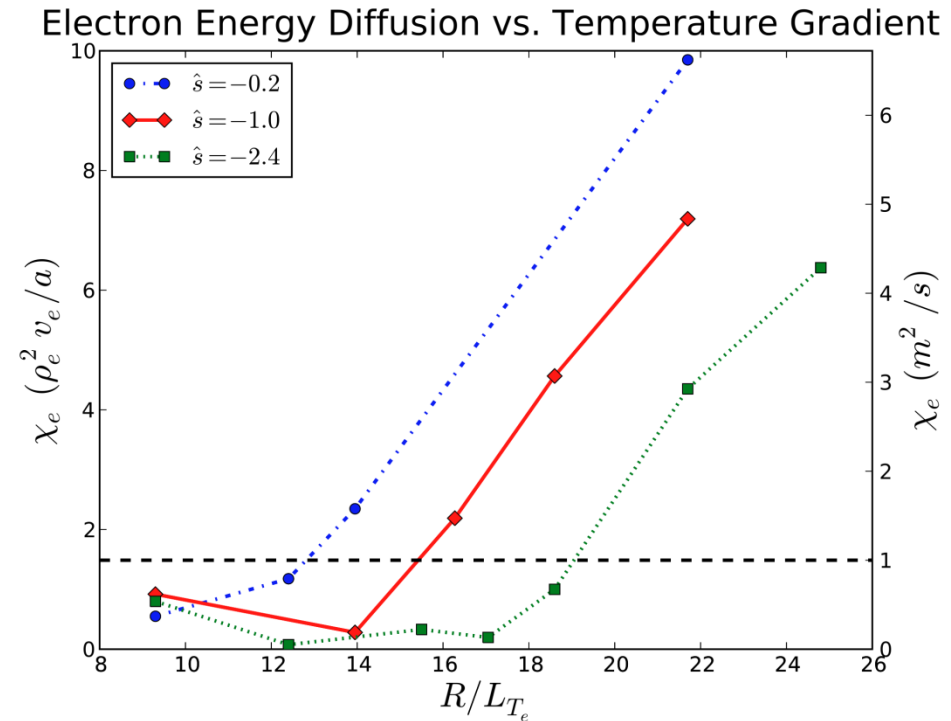
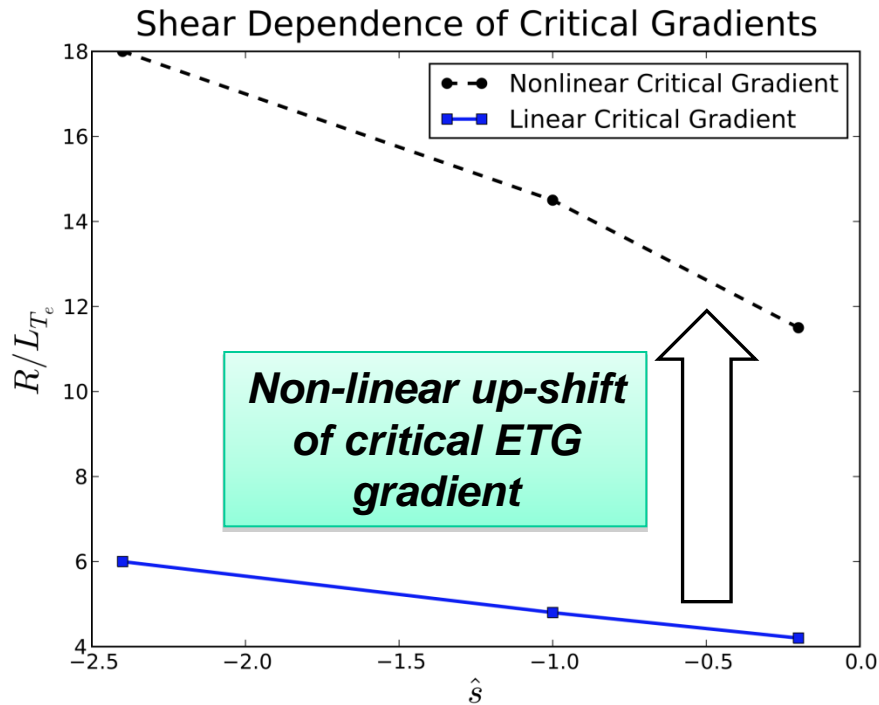
Reversed shear suppresses mode growth even at supercritical ETG gradients during e-ITBs

- ① Intermittent, short duration bursts of ETG observed during RS phase
 - Average ETG mode amplitude low, T_e gradient well above ETG critical
 - GYRO simulations indicate **non-linear up-shift** of critical ETG gradient
- ② A series of large amplitude, closely spaced in time ETG bursts collapse T_e profile
 - Magnetic shear becomes zero/positive due to anomalous current redistribution
- ③ T_e profile can only be reheated to ETG critical gradient at zero shear
 - ETG mode amplitude grows to a moderate continuous level

H. Yuh, PRL 106, 055003 (2011)



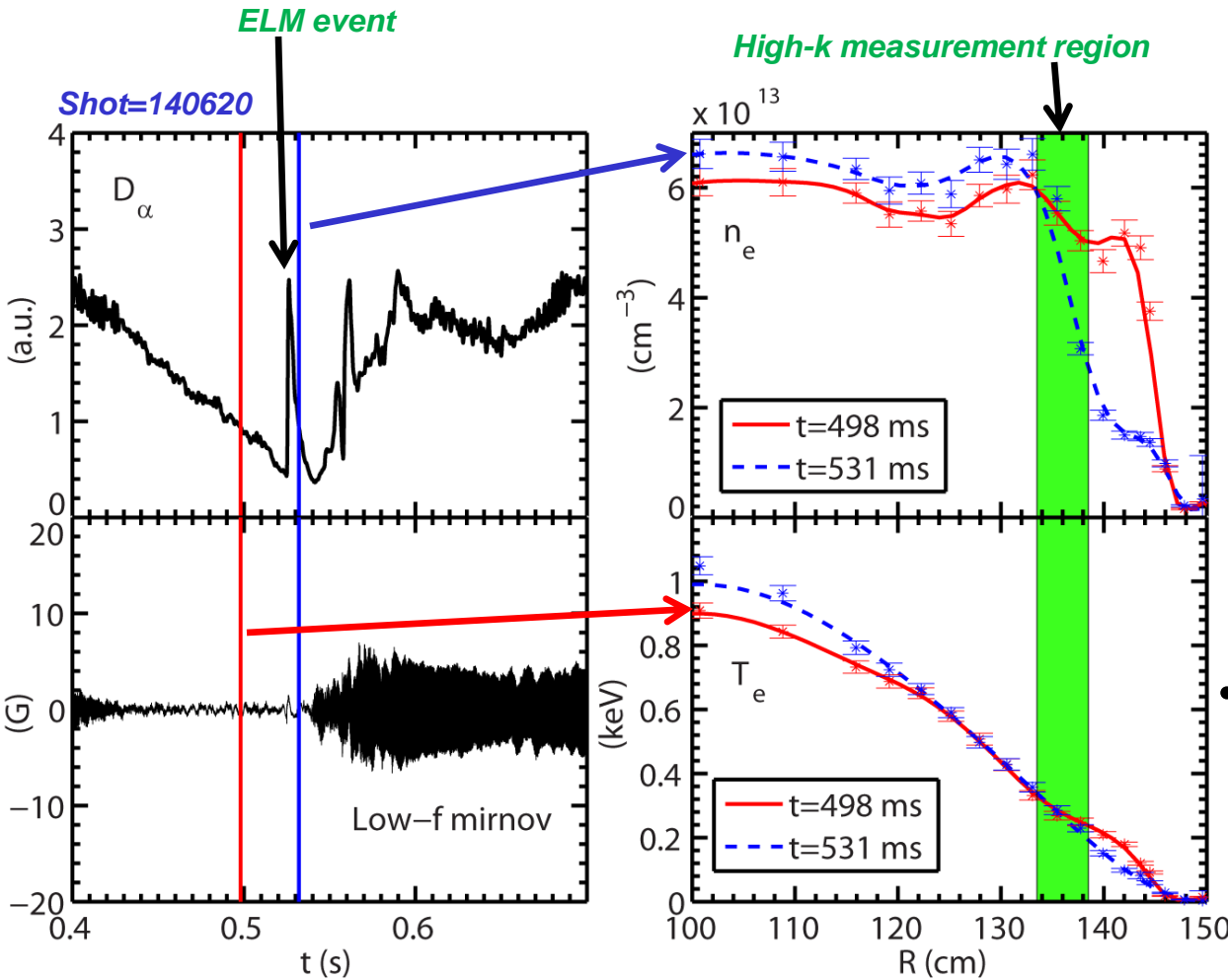
Nonlinear GYRO Simulations of NSTX Reversed Shear Show Strong Up-Shift of Critical Gradient for ETG Turbulence



Scan in shear and electron temperature gradient for NSTX e-ITB baseline parameters
Nonlinear critical gradient for transport has large up-shift during reversed shear

H. Yuh, PRL 106, 055003 (2011)

Large Density Gradient Induced by an ELM Event



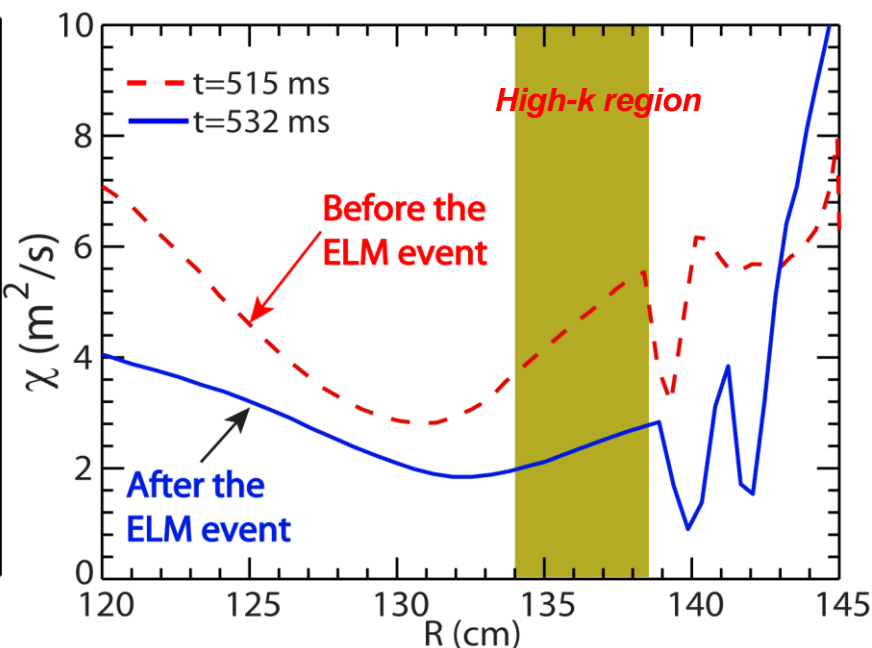
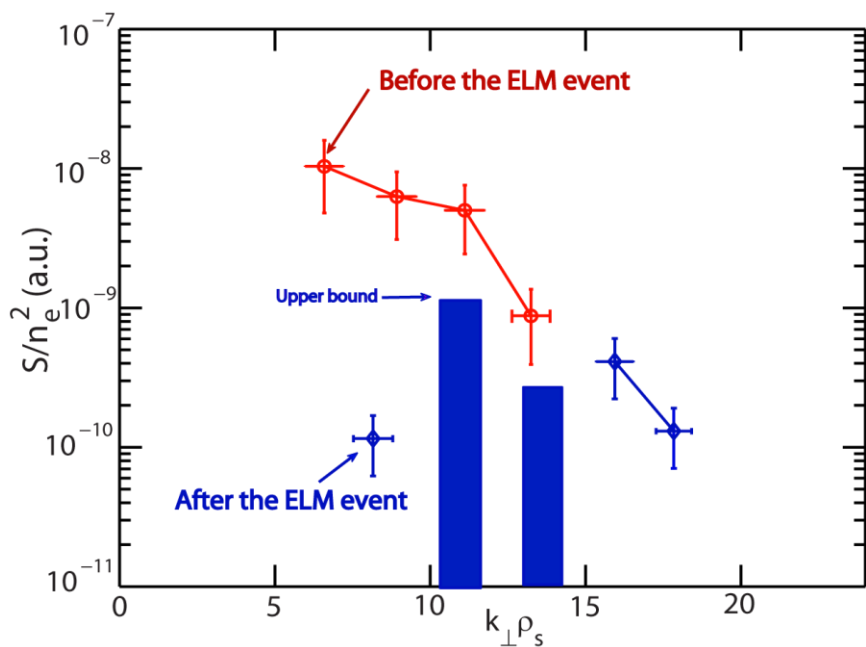
Ren et al., PRL, 106, (2011) 165005

- After the ELM event:
 - A factor of 4 increase in density gradient
 - 60% increase in electron temperature gradient
 - 60% decrease in ion temperature gradient
 - 40% increase in T_i
 - Less than 25% variation in all other equilibrium quantities
- No large global MHD mode appears before and right after the ELM event

Correlation Found between Reduction of Turbulence Spectral Density and Improvement of Plasma Thermal Confinement

- Significant decrease in wavenumber spectral power is observed for modes with longer wavelength, $k_{\perp}\rho_s \lesssim 10$
- The spectral power of the large wavenumbers, $k_{\perp}\rho_s \gtrsim 15$, is unaffected

- Plasma thermal diffusivity is decreased by about a factor of 2 after the ELM event
- This increase correlates well with the decrease of the spectral power of the longer wavelength mode



Ren et al., PRL, 106, (2011) 165005

Poloidal CHERs detection planes and viewing sightlines

- R. Bell, Phys. Plasmas 17, 082507 (2010)
- R. Bell, APS Invited Talk 2009

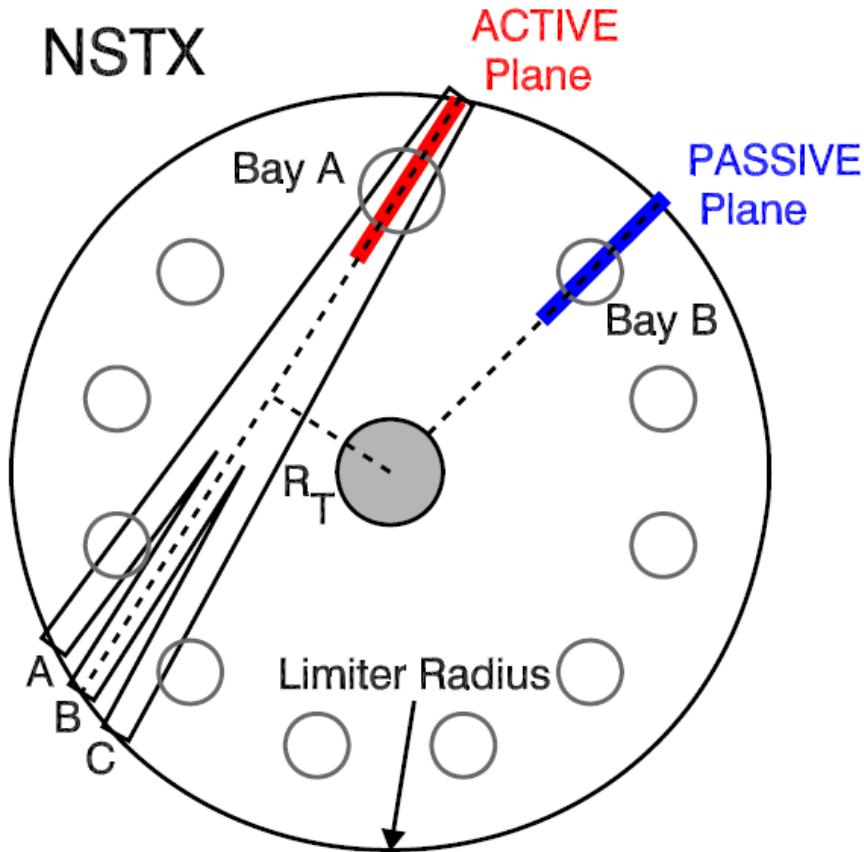


FIG. 1. (Color online) Plan view of NSTX midplane showing the locations of the active and passive detection planes. The active plane has the same tangency radius R_T as the central of three neutral beam sources labeled A, B, and C.

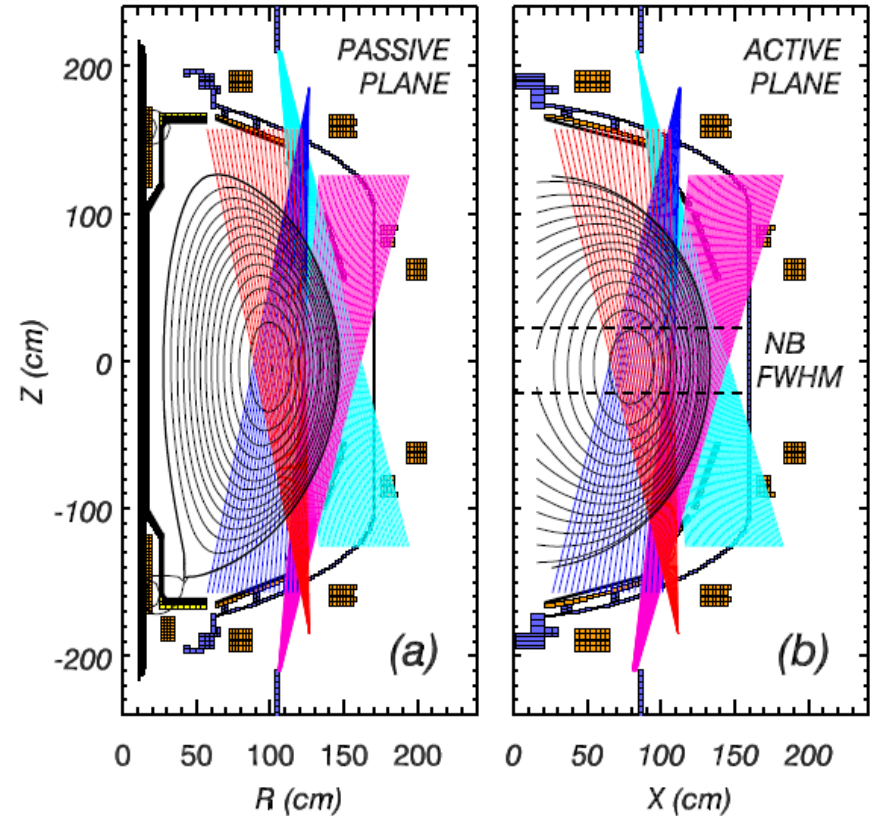
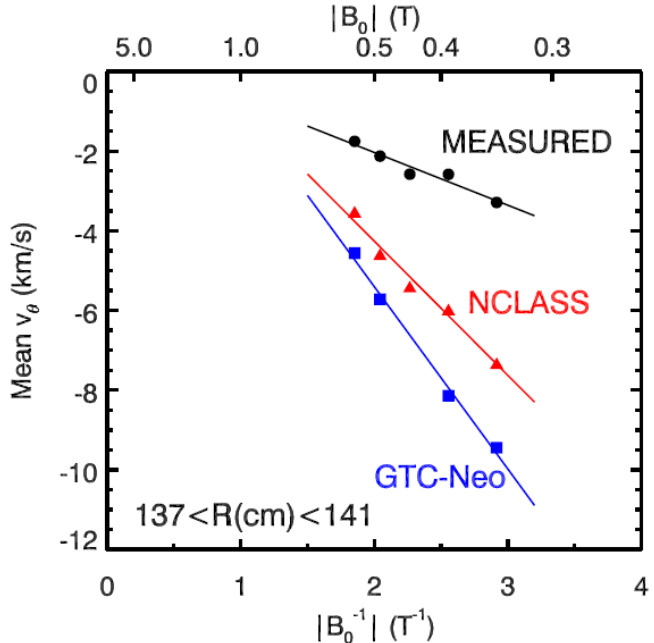
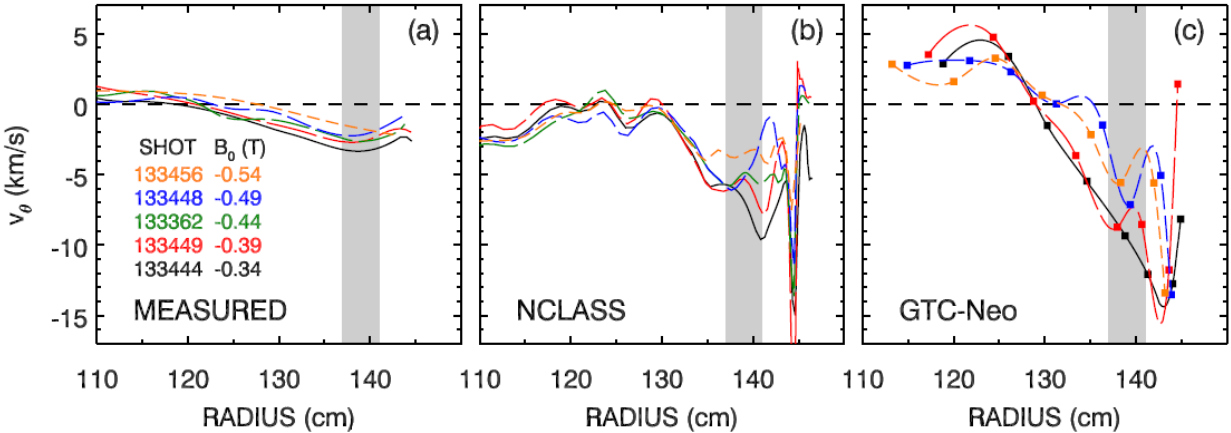
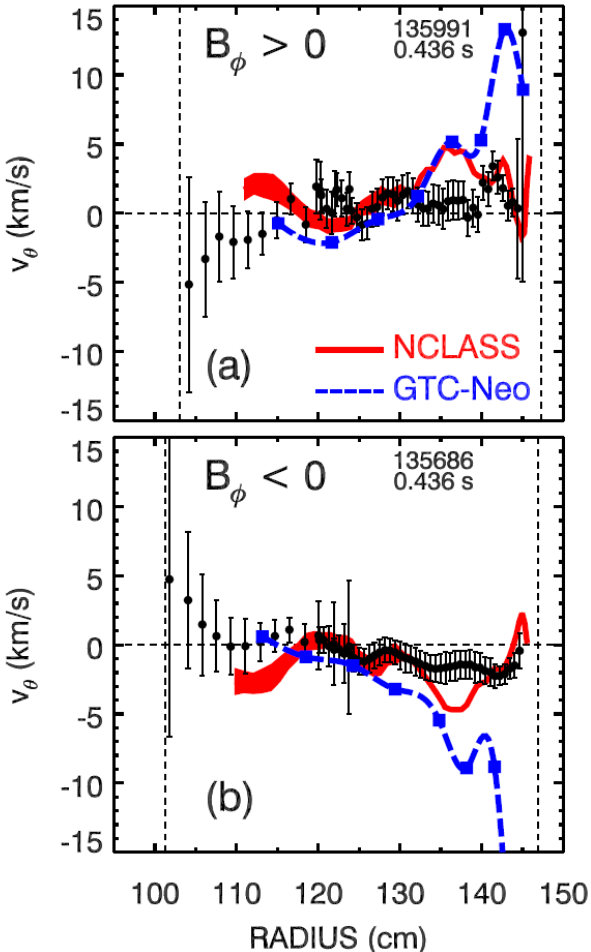
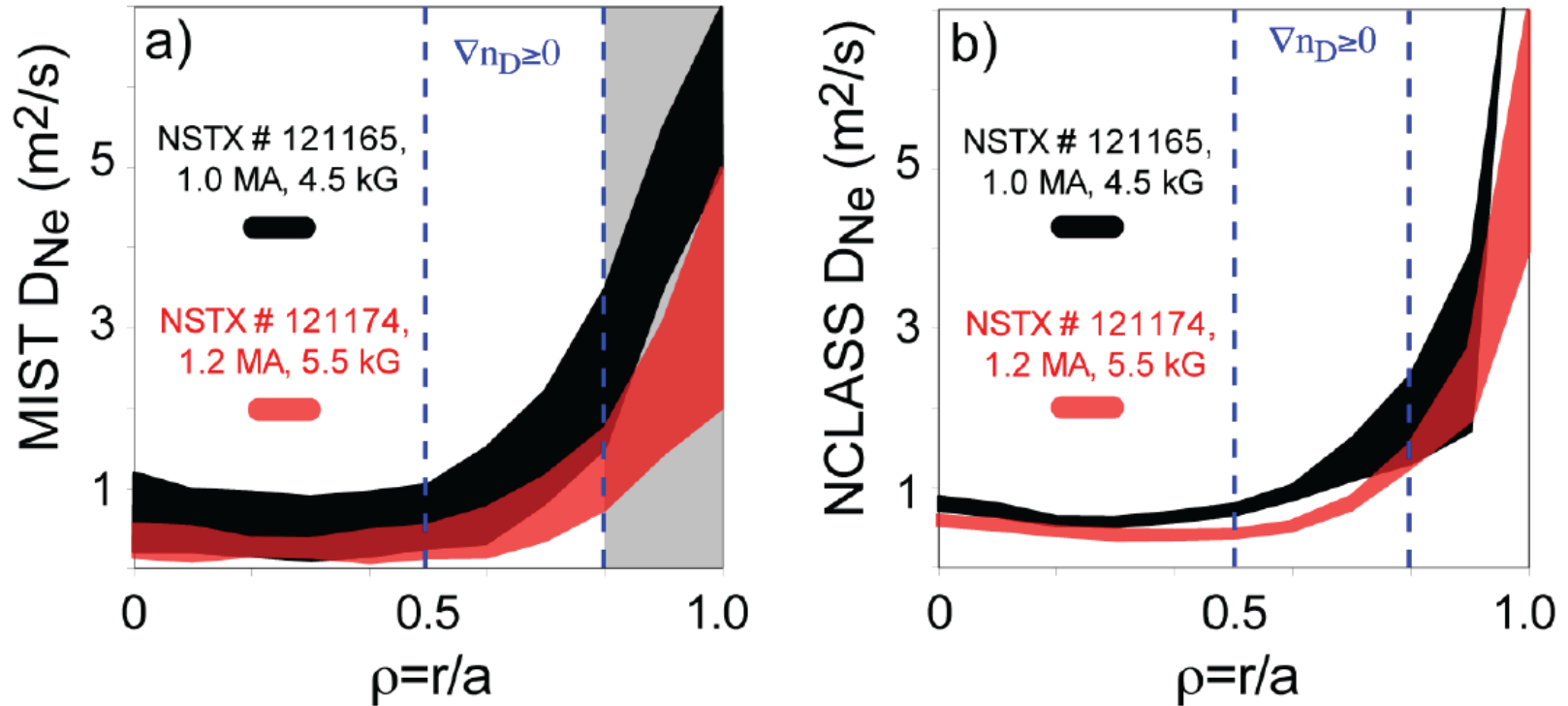


FIG. 2. (Color online) Cross section of NSTX showing poloidal viewing sightlines in (a) passive plane and (b) active plane. Each upward and downward viewing pair of sightlines is precisely aligned at the midplane. There are 63 pairs of sightlines in the passive view and 75 pairs of sightlines in the active view.

Poloidal velocity dependence on field consistent w/ predicted neoclassical trends, magnitudes differ by ~ factor of 2



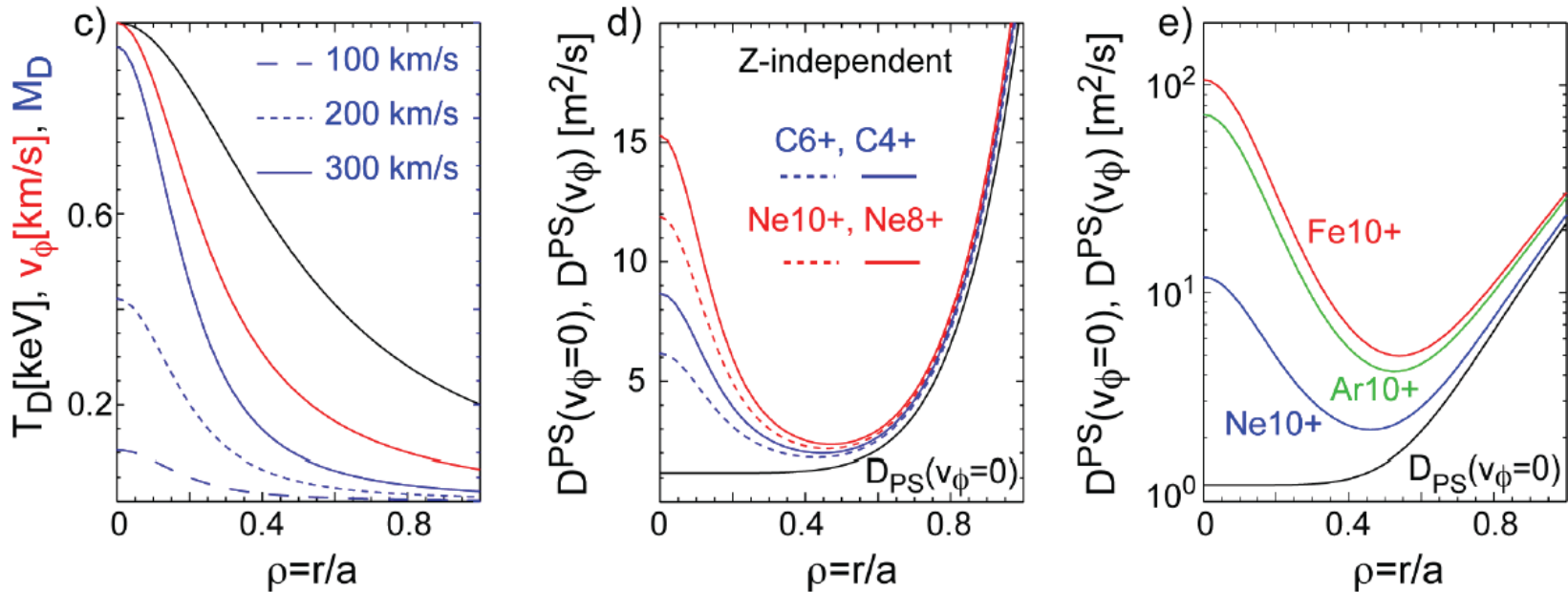
Experimental neon diffusivity in agreement with neoclassical models



- Note large increase in D_{neo} and D_{exp} at $r/a > 0.8$
- Neoclassical ordering in the core is $\sim 1 m^2/s$

L. Delgado-Aparicio, et al., Nucl. Fusion, 49, 085028, (2009).

Core impurity diffusivity can be affected by rotation in NSTX ($\times 10\text{-}100$ static D_{Neo})

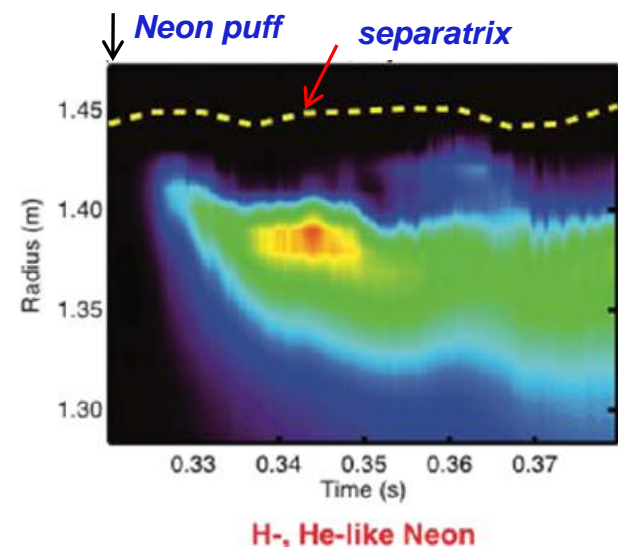
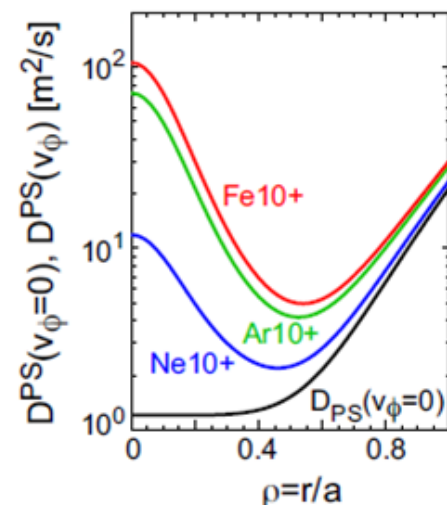


- ① Charge-states from heavy impurities can have different $D^{PS}(v_\phi)$ that can be several times larger than that of the conventional neoclassical transport.
- ② This mechanism explains enhanced core diffusivities without the need of invoking the presence of long wavelength electrostatic turbulence.

L. Delgado-Aparicio, et al., Nucl. Fusion, 49, 085028, (2009).

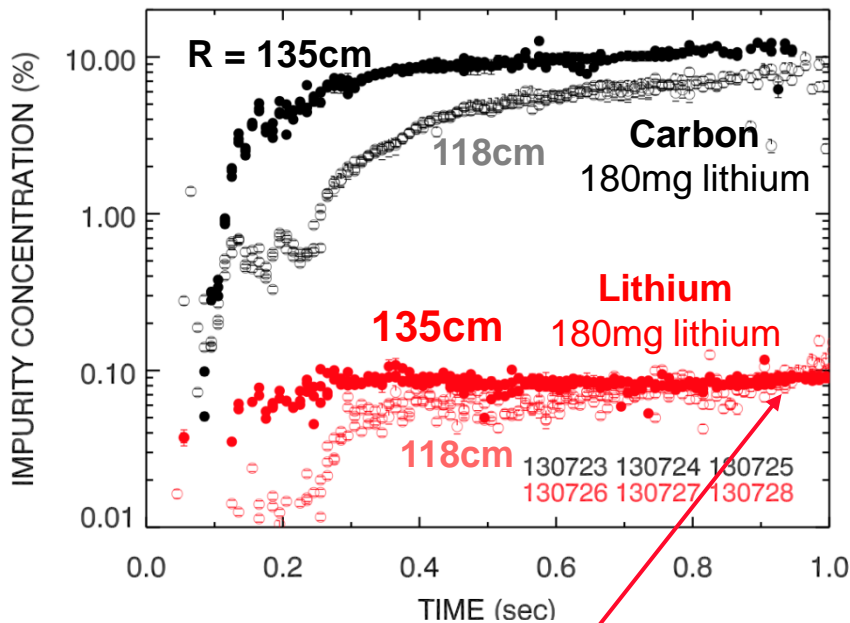
Impurity Transport Studies will Exploit New Diagnostics and Modeling Capabilities (R11-1, 2012 JRT)

- Neon diffusivity neoclassical in the core accompanied by some anomalous convection
 - Under-resolved at the edge and suffered from low signal
- Plasma rotation enhancing core impurity transport without invoking low-k turbulence
- New Multi-Energy Soft X-Ray diagnostic in 2010
 - ~1 cm resolution; <100 μ s response; high SNR; $r/a > 0.65$
- STRAHL transport code being used
 - Neoclassical calculation embedded
 - Up-to-date atomic data
- Impurity transport study at plasma edge
 - Carbon build up in ELM-free discharges
 - Z dependence of impurity transport
 - Measure edge turbulence and its relation to impurity transport (BES, High-k, reflectometer etc.)



Lithium concentration in plasma core remains very low compared to higher-Z carbon

- Quantitative measurements of C^{6+} , Li^{3+} with charge-exchange recombination spectroscopy
- $n_C/n_{Li} \sim 100$
- Hollow profiles early for both C and Li fill in as time progresses



No sign of Li accumulation in core

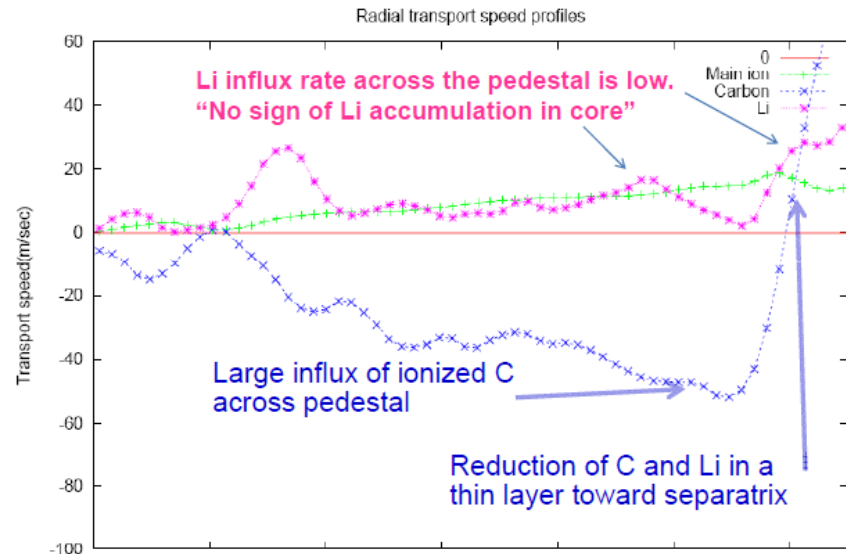
R. E. Bell (PPPL)

Status:

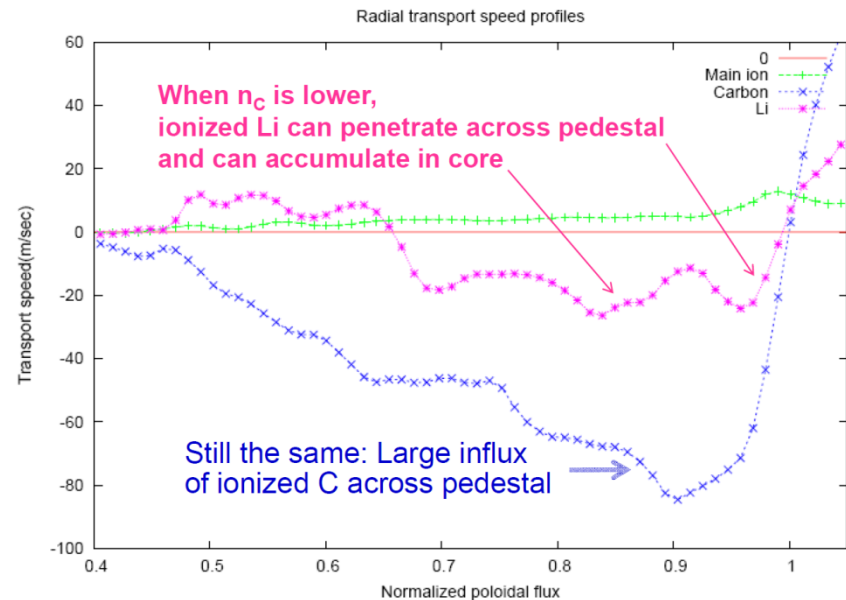
- Low lithium core contamination continues to hold true for LLD operation
- Favorable result for lithium based divertor concepts
- Low level of lithium accumulation consistent with neo-classical theory (C.S. Chang *et al.*)
- A quantitative model still lacking

Preliminary: XGC0 Kinetic neoclassical transport calculations being used to model, interpret lithium transport

- For $n_C/n_e=10\%$, Li moves outward while C^{6+} moves in at $\psi_N < 1$



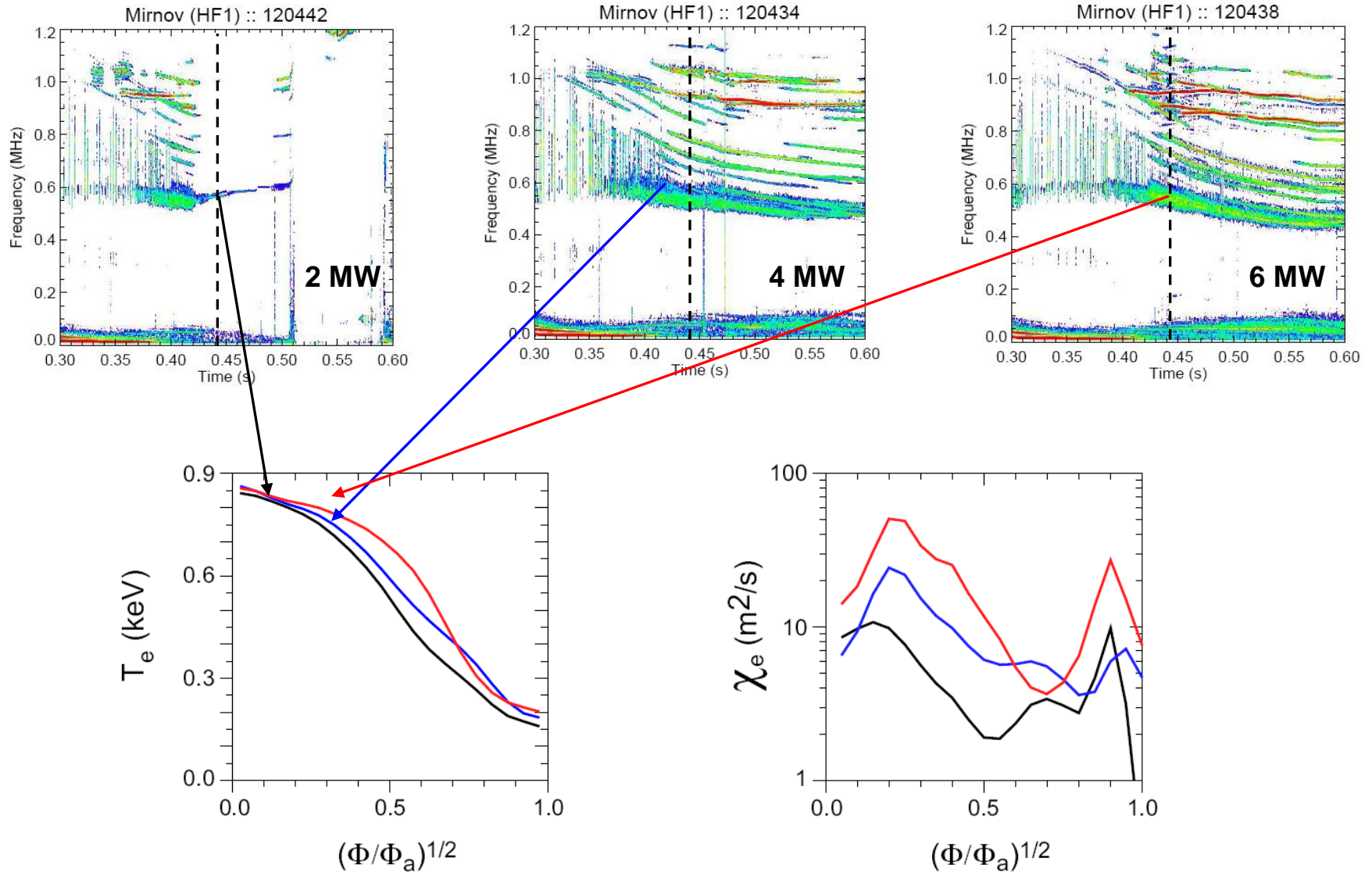
- For $n_C/n_e=5\%$, Li moves inward at much slower speed than C^{6+}



C.S. Chang (PPPL) - in collaboration with Kyuho Kim (KAIST) and GY Park (KSTAR now) and the CPES Team

Presented at 2nd International Symposium on Lithium Applications for Fusion Devices - April 27-29, 2011 - PPPL

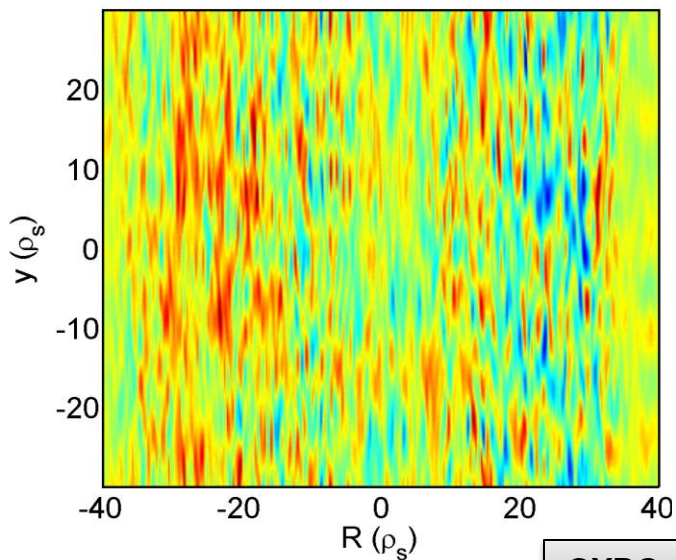
High-frequency core GAE electromagnetic fluctuations can apparently cause large core electron transport



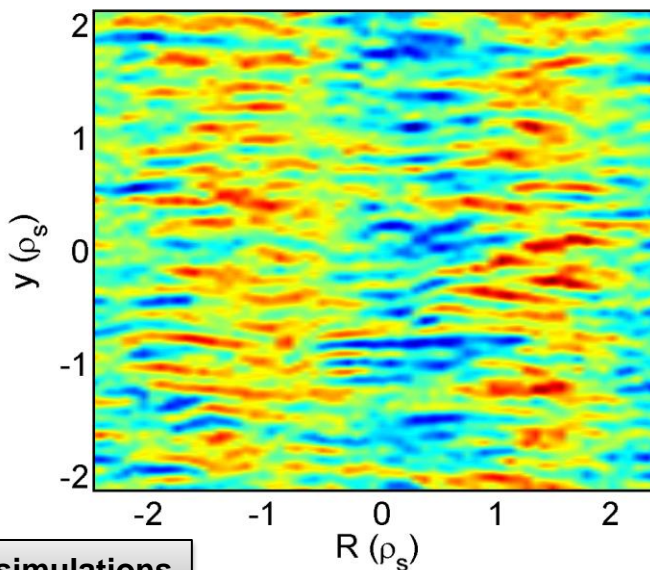
Measuring micro-tearing turbulence with high-k scattering system

- Micro-tearing turbulence has significant density fluctuations
 - Very Different 2D k spectrum anisotropy than ETG
 - Significant spectral power in large k_r (electron-scale) is expected for micro-tearing turbulence
- The present high-k system measures mostly k_r spectrum and is able to distinguish the different anisotropies

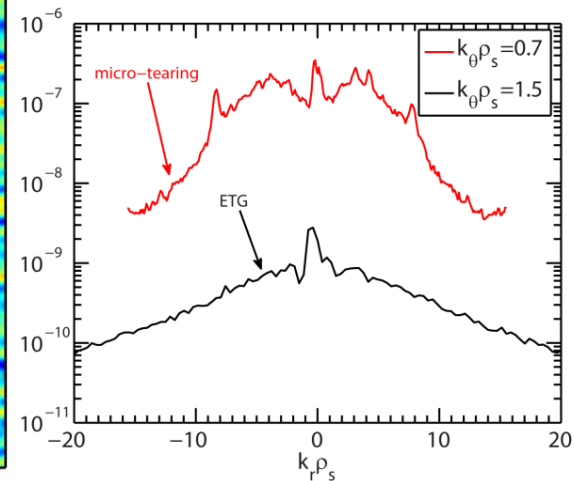
Micro-tearing density fluctuation
NSTX H-mode



ETG density fluctuations
NSTX L-mode

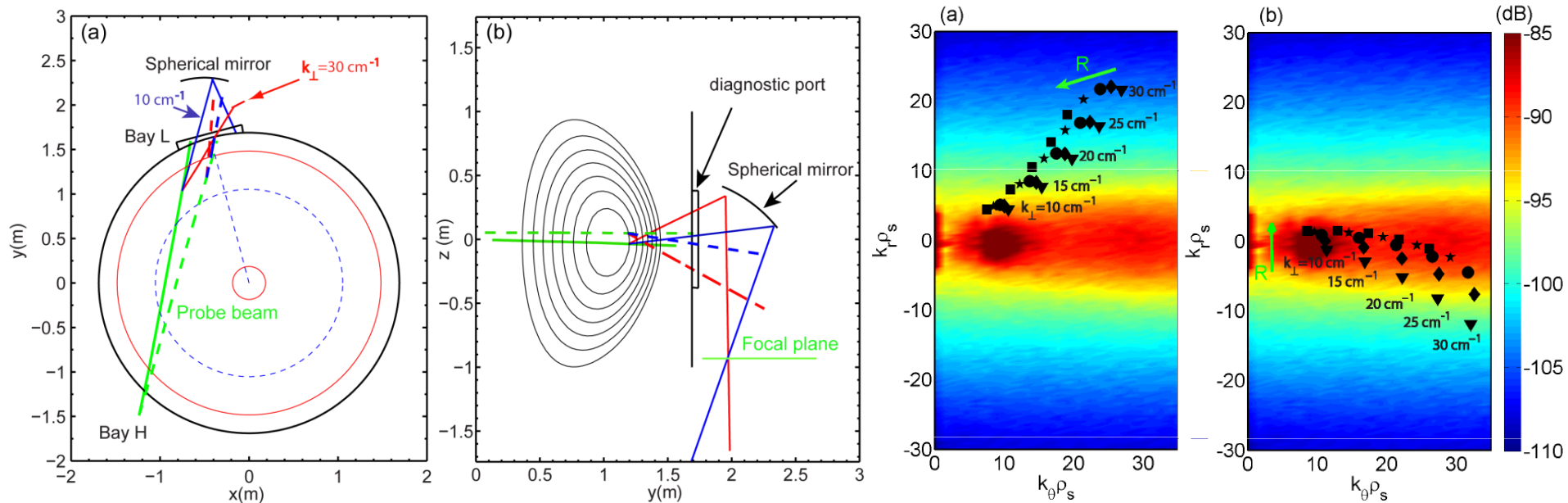


GYRO simulations



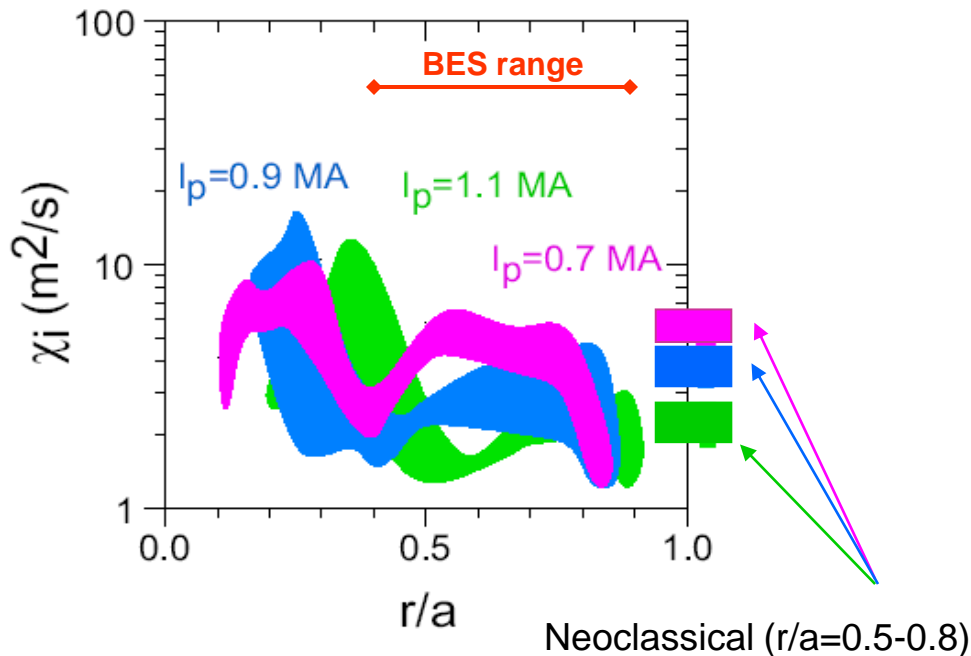
Preliminary Design of the New High-k Scattering System for NSTX-Upgrade

- The design utilizes the launching port of the present high- k_r system and its microwave hardware
- Two scattering configurations of the system allow it to measure 2D k spectrum



Ion Transport Typically Found to be Near Neoclassical in H-mode Plasmas

Controls τ_E scaling with I_p



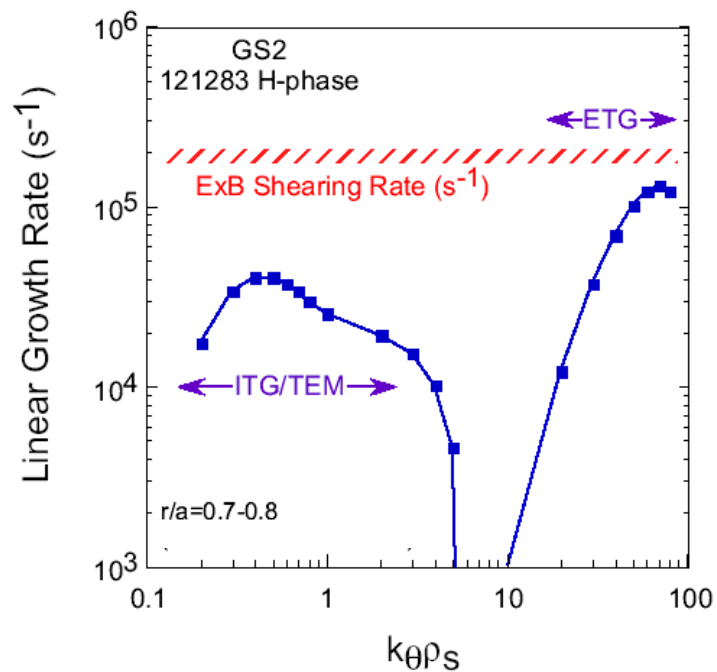
Neoclassical levels determined from GTC-Neo: includes finite banana width effects (non-local)

Need BES to confirm conclusions

S. Kaye, Nucl. Fusion 47 (2007) 499–509

Linear GS2 calculations indicate possible suppression of low-k turbulence by ExB shear during H-phase

- Supported by non-linear GTC results



χ_i routinely anomalous in high density L-modes
 $(\gamma_{lin, ITB} > \gamma_{ExB})$

Macroscopic Stability Supplemental Slides

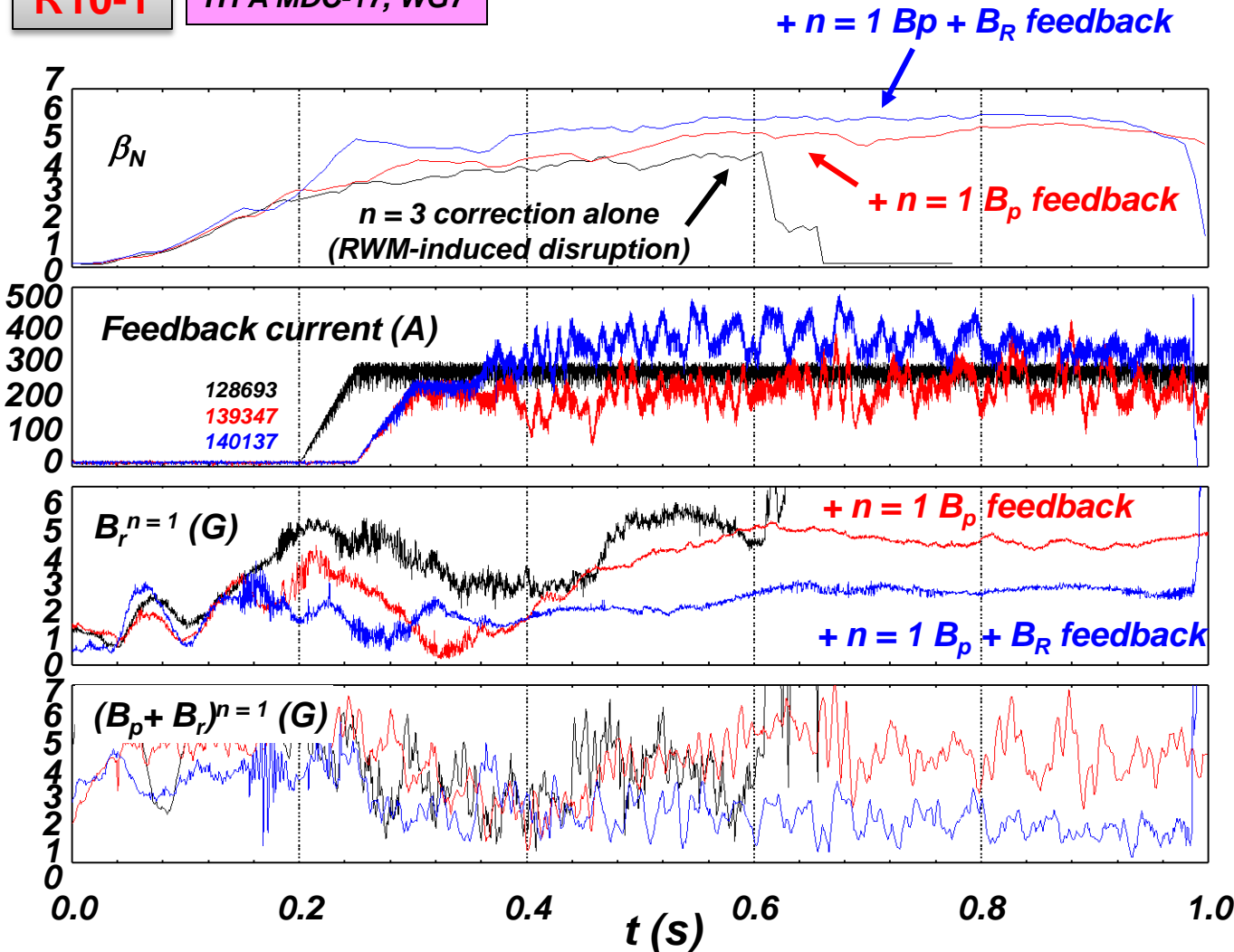
Use of combined $B_r + B_p$ RWM sensor $n=1$ feedback yields best reduction of $n=1$ field amplitude / improved stability

R10-1

ITPA MDC-17, WG7

- Combination of DC error field correction, $n=1$ feedback

- Dedicated scans to optimize B_r , B_p sensor feedback phase and gain
- $n=3$ DC error field correction alone subject to RWM instability
- $n=1$ B_p sensor fast RWM feedback sustains plasma
- Addition of $n=1$ B_r sensors in feedback reduce the combined $B_p + B_r$ $n=1$ field to low level (1–2 G)

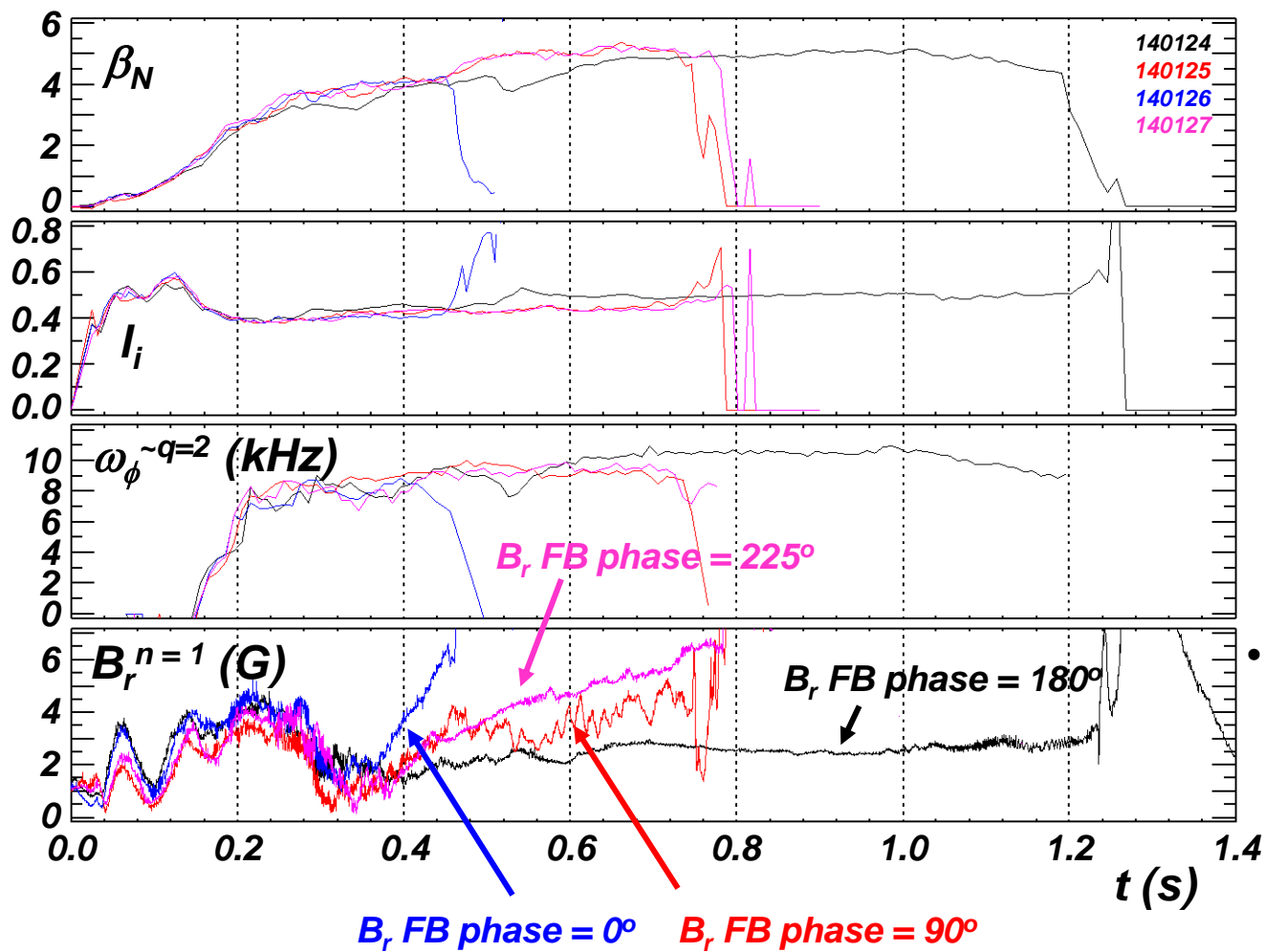


RWM B_r sensor $n = 1$ feedback phase variation shows clear settings for improved feedback when combined with B_p sensors

$n = 1 B_R + B_p$ feedback
(B_p gain = 1, B_R gain = 1.5)

R10-1

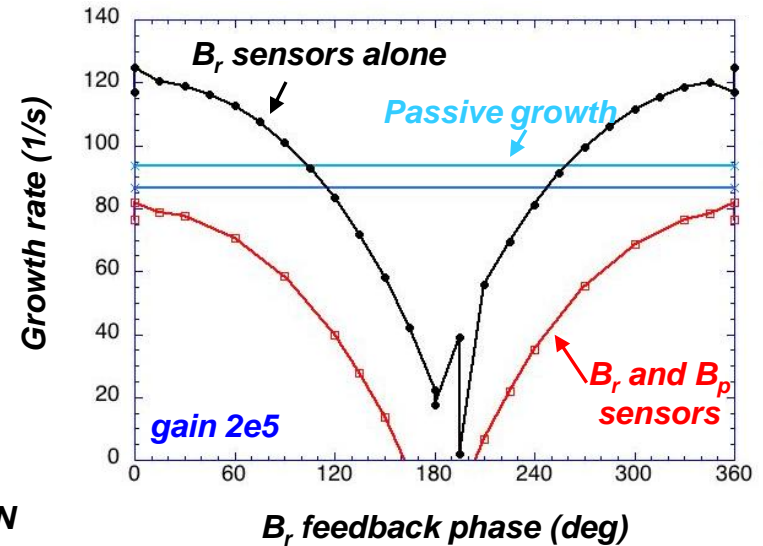
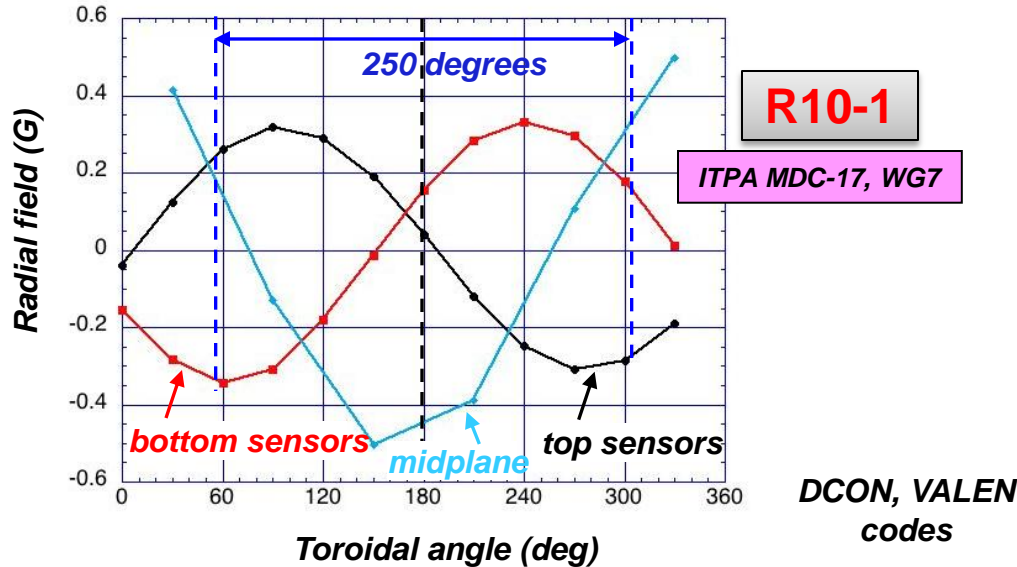
ITPA MDC-17, WG7



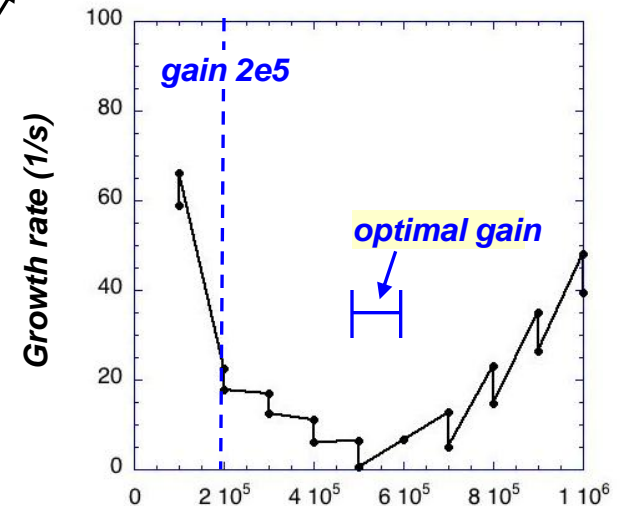
- Recent corrections to B_r sensors improve measurement of plasma response
 - Removed significant direct pickup of time-dependent TF intrinsic error field
 - Positive/negative feedback produced at theoretically expected phase values
- Adjustment of B_p sensor feedback phase from past value further improved control performance

RWM feedback using upper/lower B_p and B_r sensors modeled and compared to experiment

Modeled B_r field at sensors and midplane

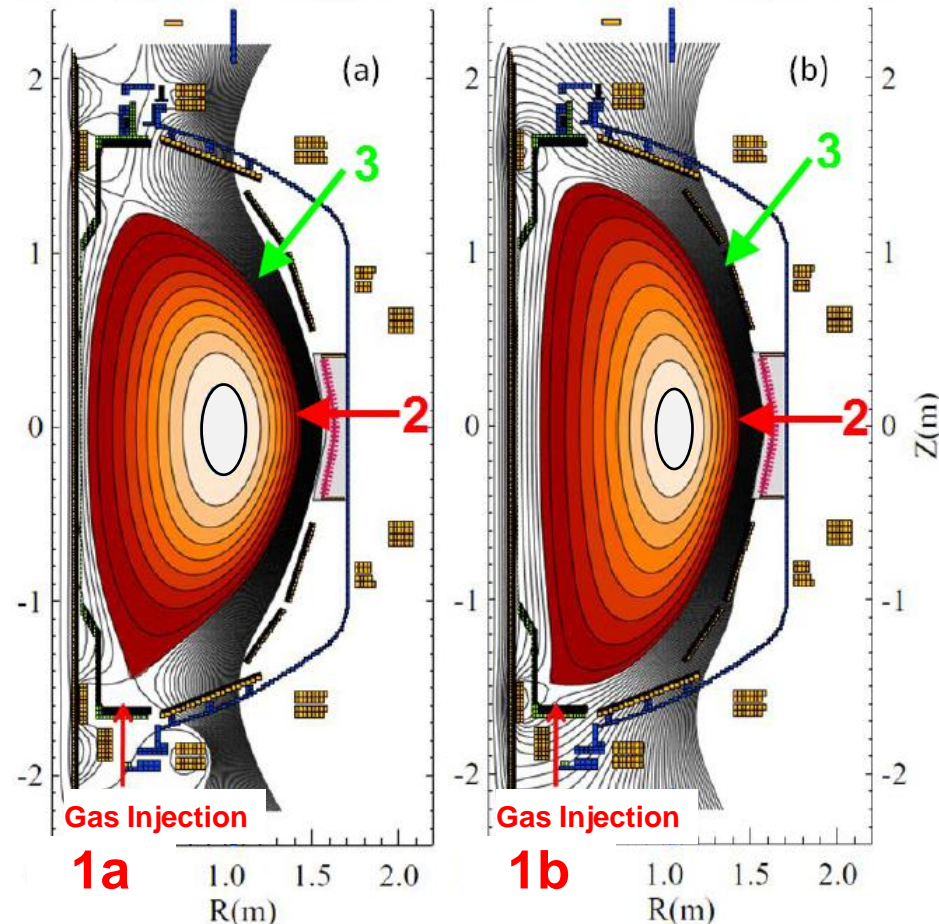


- Both B_r , B_p feedback contribute to active control
 - B_r mode structure and optimal feedback phase agrees with parameters used in experiment
 - B_r feedback alone provides stabilization for growth times down to ~ 10 ms with optimal gain
 - Physics of best feedback phase for B_p sensors in low I_i plasmas under investigation
 - Present analysis mismatches experiment – 3D conducting structure model, plasma response model being investigated



FY11-12: NSTX will contribute to disruption mitigation research → optimum Massive Gas Injection (MGI) locations for ITER

\EFIT02, Shot 134986, time=583 \EFIT02, Shot 129986, time=395ms



- 1a:** Private flux region **1b:** lower SOL
2: Conventional mid-plane injection
3: Variation in poloidal location

Unique capability of NSTX:
Assess benefits of injection into the private flux region & the high-field side region vs. LFS mid-plane

- **Initial Experiments (FY11):**
 - Compare MGI into private flux region to mid-plane and to SOL
 - 100cc plenum at 5000Torr
 - He, Neon & D2
- **More Detailed Experiments (FY12):**
 - Modify plenum size and valve throughput rates
 - Consider other poloidal locations
 - Simultaneous injection from multiple locations to maintain cold edge mantle and reduce poloidal asymmetries

Plan for Integration of Diagnostics and Resulting Data for MGI Experiments

Thomson scattering, EFIT, neutral pressure gauges

Physics of gas penetration (fraction that penetrates separatrix)

H-alpha array, neutral pressure gauges

System response time (gas trigger time to first detection of injected gas interacting with the plasma edge)

Multi-color Soft X-ray, H-alpha, I_p , EFIT, Thomson scattering, Mirnov coils

Delay in current quench after the gas contacts plasma edge

Rate of current quench and vertical dynamics of the plasma

3-D MHD response to the whole equilibrium and MHD activity

Thermal quench evolution & pedestal collapse

Bolometer array- Core radiated power dynamics

Halo current sensors- Dependence on halo current amplitude on gas assimilation (Mitigated vs. beta limit and a VDE disruption)

Two color divertor fast infrared camera and Eroding thermocouples

Spatial distribution of Thermal loads & fast heat flux measurements

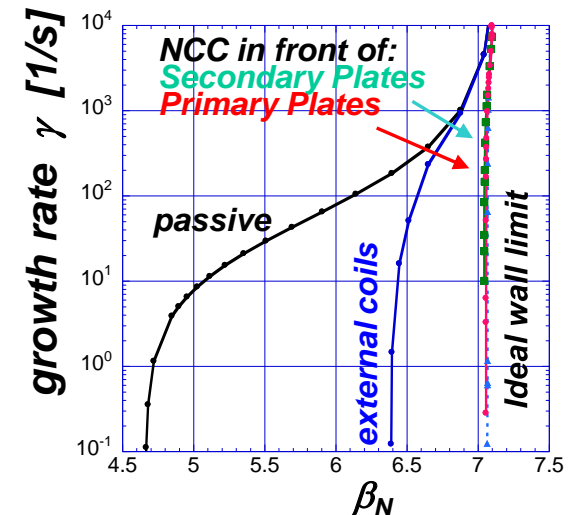
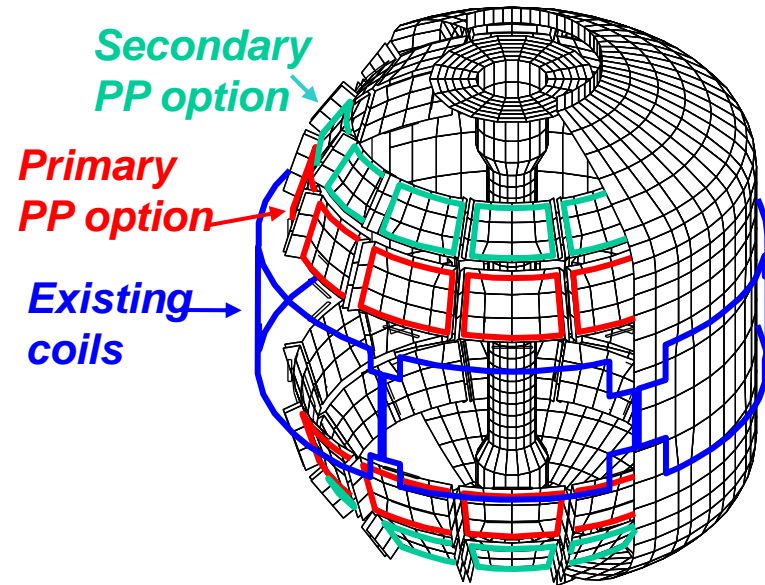
Locked mode, RWM mode - $n=0$ mode detectors - Precursors to disruption

Provide data to groups involved in NIMROD, KPRAD, EIRENE-SOLTPS

Proposed Nonaxisymmetric Control Coil (NCC)

Expand Control Capabilities, Understanding of 3D Effects

- Non-axisymmetric control coil (NCC) – at least four applications:
 - RWM stabilization ($n > 1$, up to 99% of $n=1$ with-wall β_N)
 - DEFC with greater poloidal spectrum capability
 - ELM control via RMP ($n = 6$).
 - $n > 1$ propagation, increased V_ϕ control).
 - Similar to proposed ITER coil design.
- Addition of 2nd SPA power supply unit:
 - Feedback on $n > 1$ RWMs
 - Independent upper/lower $n=1$ feedback, for non-rigid modes.
- Design activities continue:
 - GA collaboration (T. Evans) computed favorable coil combinations/variations for RMP ELM suppression of NSTX plasmas (2009)
 - CU group assessing design for RWM stabilization capabilities compatible with ELM control

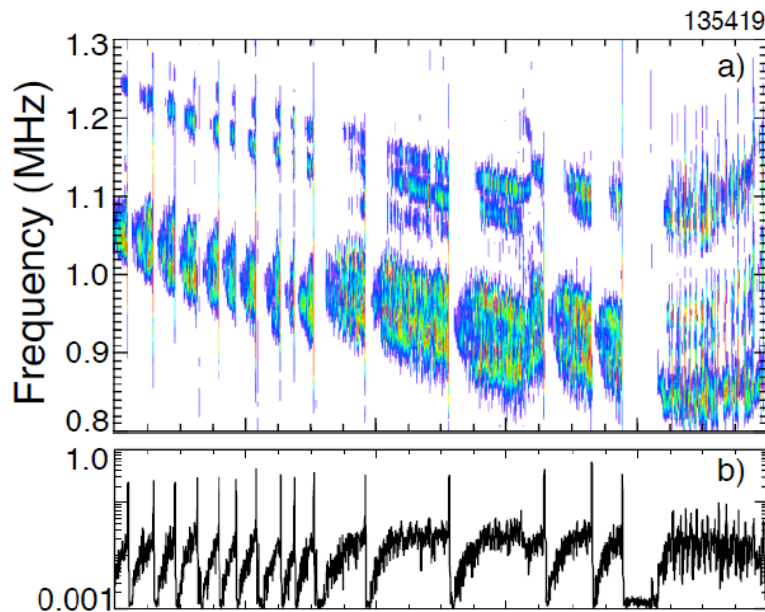


J. Bialek (Columbia U.)

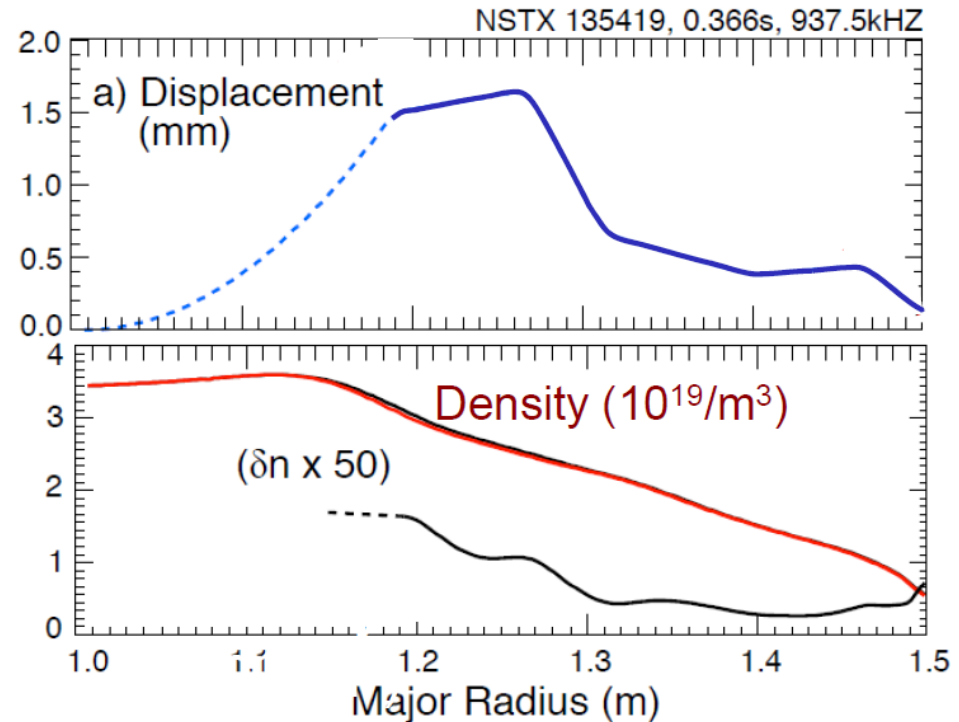
Energetic Particle Physics Supplemental Slides

Observation of Global Alfvén Eigenmodes in NSTX

[E. Fredrickson et al, IAEA 2010]



(a) Spectrogram showing GAE modes,
 (b) magnetic fluctuations $0.8\text{MHz} < \text{freq} < 1.3\text{MHz}$

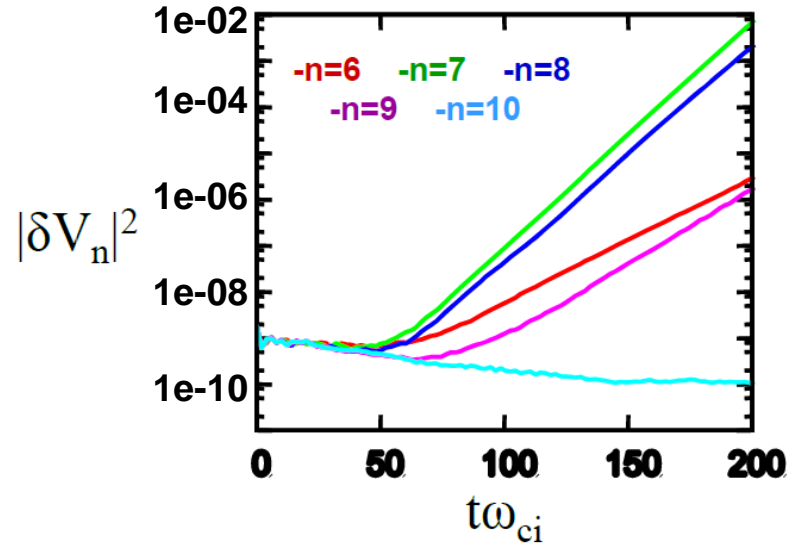


a) Mode amplitude profile.
 b) Density profile and perturbed density.

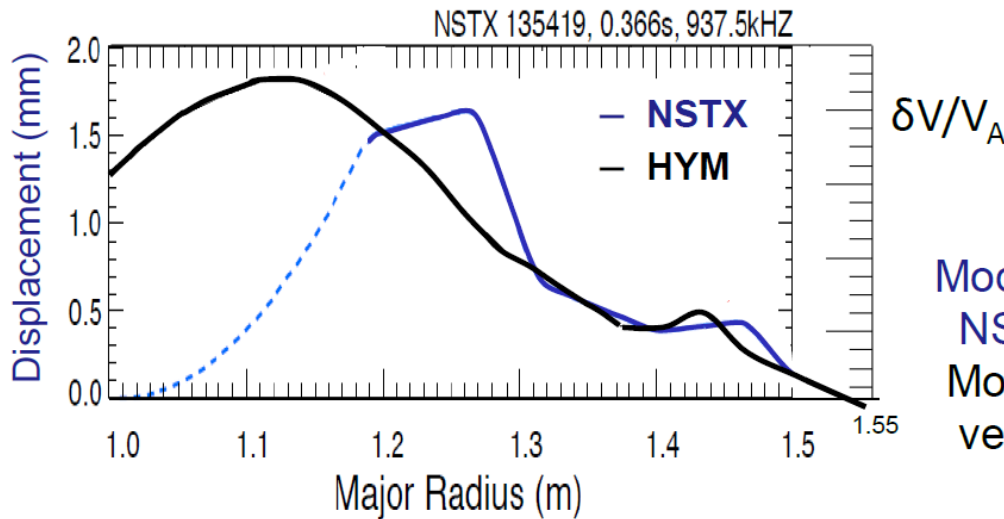
At the edge the compressional component dominates $\delta B_{\parallel} > \delta B_{\perp}$, $\delta n \sim 10^{-2} n_0$.

HYM simulations of GAE mode structure compare favorably with NSTX experimental measurements

- Several modes are unstable with toroidal mode numbers $n=6 - 9$ and frequencies $f=0.4-0.8\text{MHz}$ (plasma frame) compared to experimental results of $n=7 - 11$, and $f=0.8-1\text{MHz}$.
- GAE modes.
- Similar mode structure.



Time evolution of kinetic energy from linearized simulations with $n=6-10$.



Mode amplitude profile - displacement NSTX#135419 [E. Fredrickson, IAEA 2010].
Mode structure from HYM simulations – velocity profile for $n=9$.

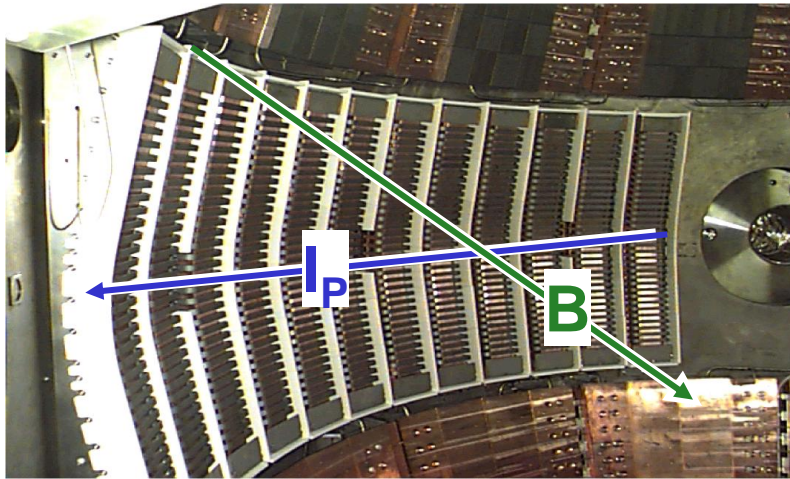
Summary of “Numerical Modeling of NBI-Driven Sub-Cyclotron Frequency Modes in NSTX”

E. Belova, APS Invited Talk 2010

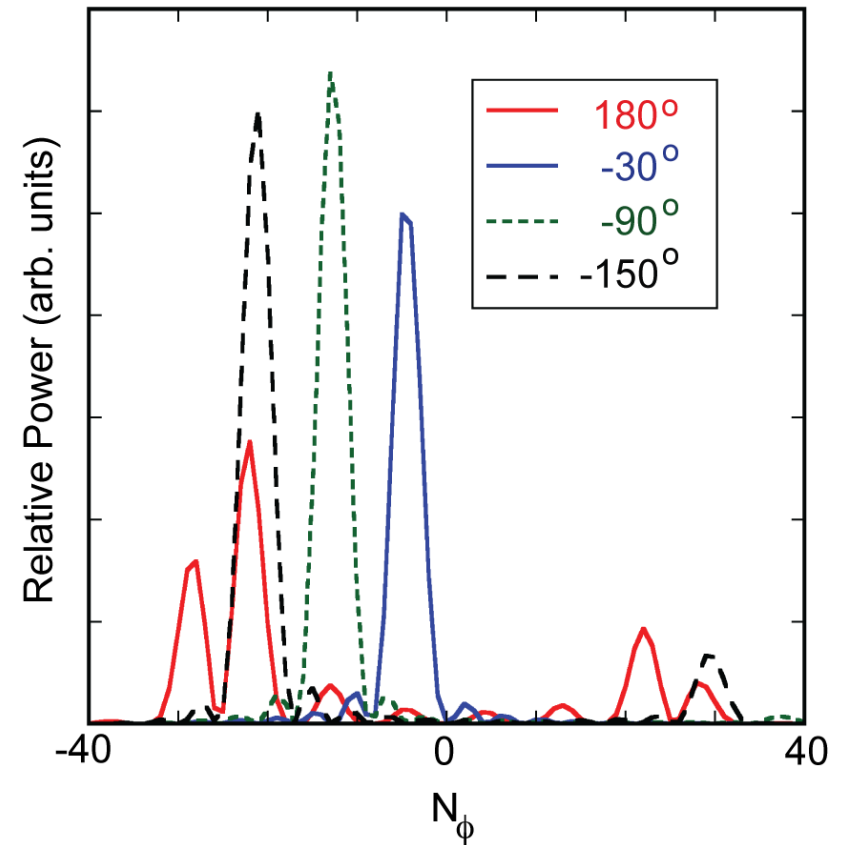
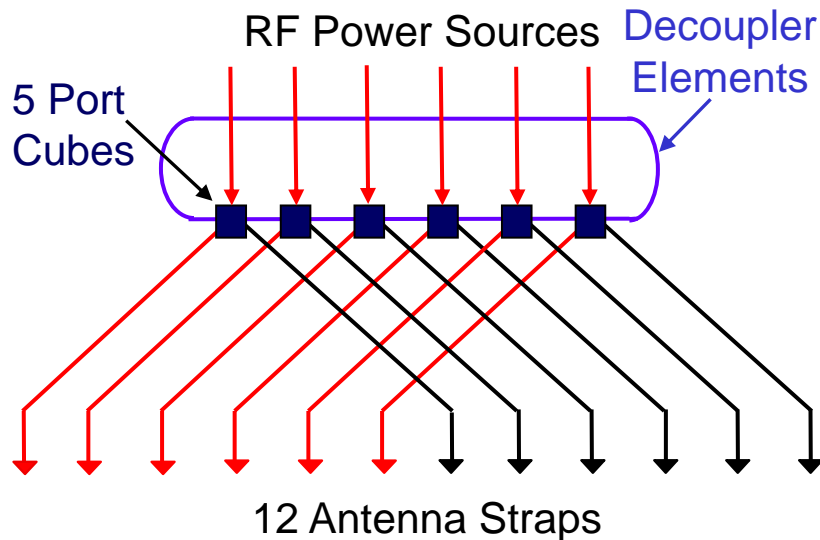
- Self-consistent simulations using the HYM code show that for large injection velocities, and strong anisotropy in the pitch-angle distribution, many Alfvén modes can be excited by NBI ions.
- Sub-cyclotron frequency modes are driven unstable via Doppler-shifted cyclotron resonance.
- Multiple fast ion resonances are seen for each mode (poloidal mode number).
- Magnetic mode structure for GAE in NSTX shows significant compressional component at the edge.
- Simulations show nonlinear saturation of GAEs due to particle trapping.
- Saturation amplitudes and mode structure are comparable with the experimental measurements.
- Drift-kinetic electron model has been implemented in the HYM code, and it will be used to study the effects of GAE modes on the electron transport.

Wave Heating and Current Drive Supplemental Slides

NSTX HHFW antenna has well defined spectrum, ideal for studying phase dependence of heating

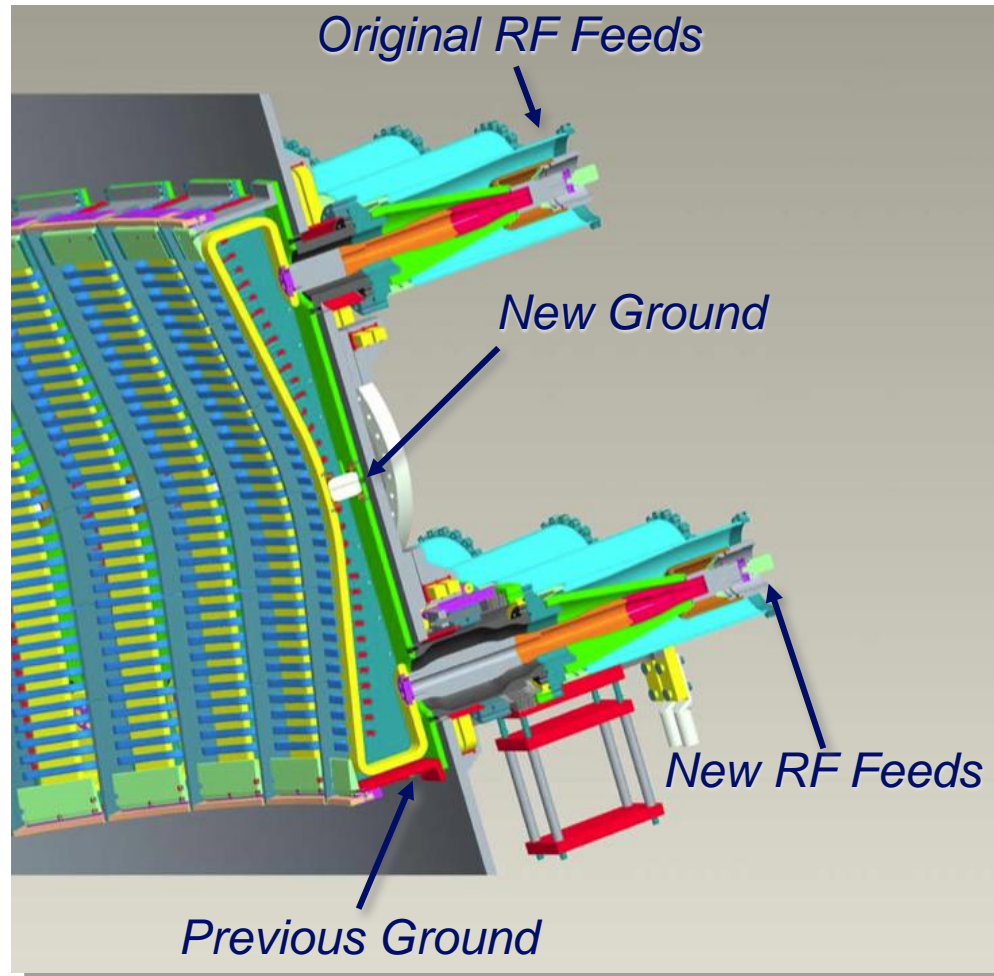


HHFW antenna extends toroidally 90°



Phase between adjacent straps easily adjusted between $\Delta\phi = 0^\circ$ to $\Delta\phi = 180^\circ$

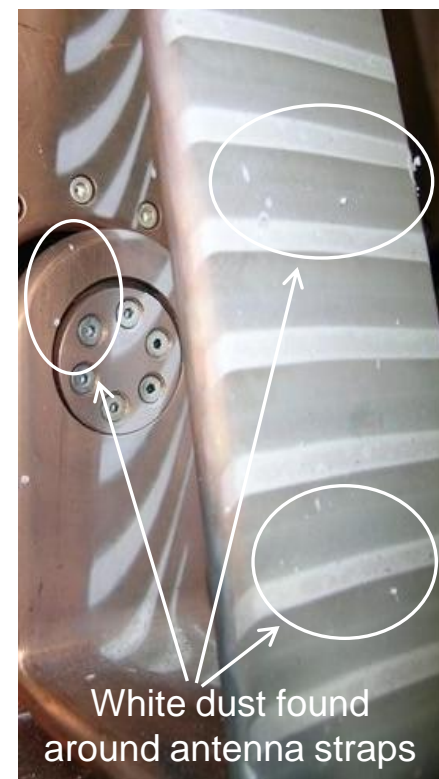
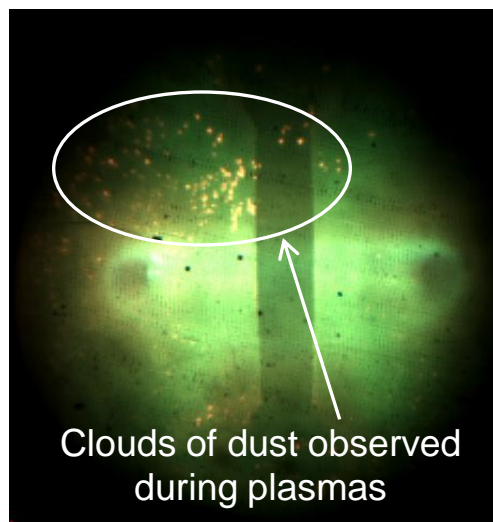
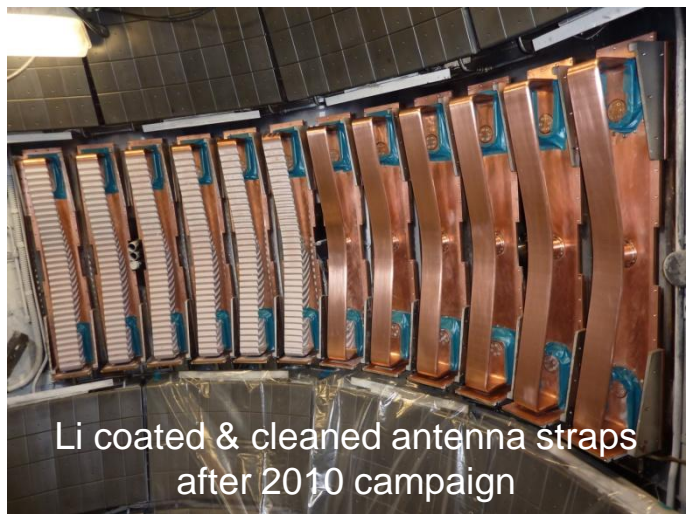
HHFW double end-fed upgrade was installed in 2009, shifted ground from end to strap center to increase maximum P_{RF}



- Designed to bring system voltage limit with plasma (~ 15 kV) to limit in vacuum (~ 25 kV):
 - Increasing $P_{RF} \sim 2.8$ times
- Antenna upgrade was beneficial:
 - Reached arc-free $P_{RF} \sim 4$ MW after a few weeks of operation at the end of 2009 campaign
- In 2008-9, Li wall conditioning was observed to enhance HHFW coupling by decreasing edge density

Increased lithium usage in 2010 significantly degraded performance of the upgraded antenna compared to 2009

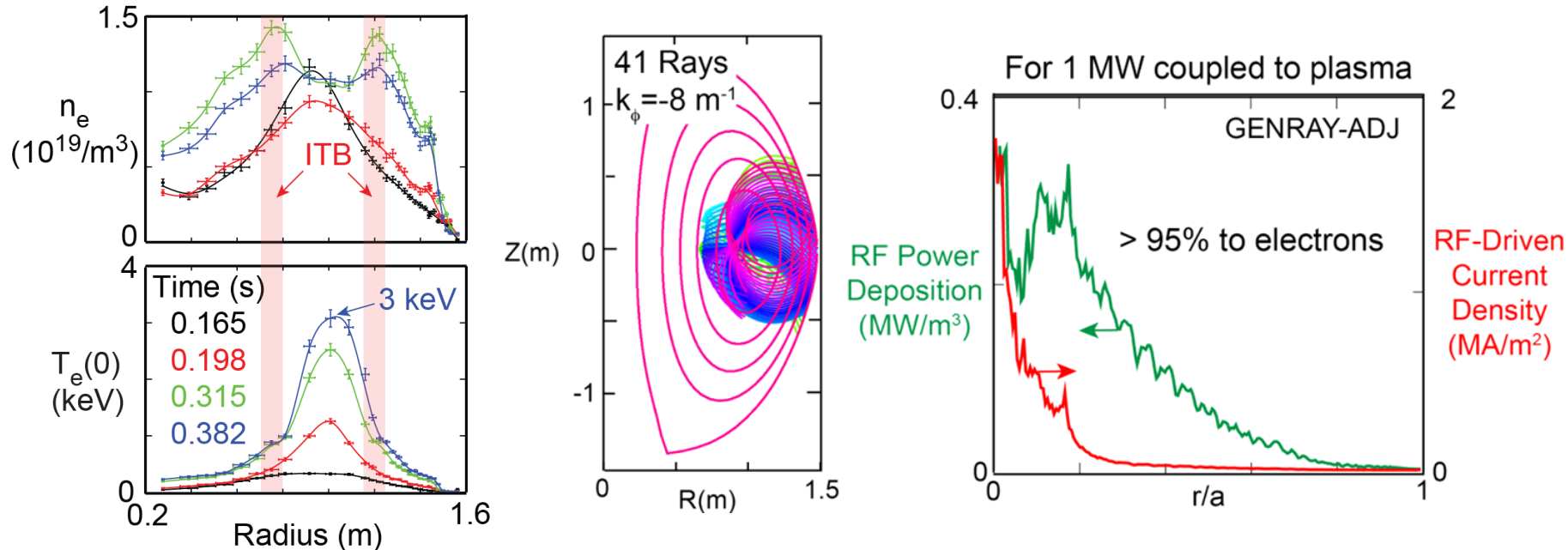
- In 2010 RF plasma operations started after extensive Li injection, only reached arc-free $P_{RF} \sim 1.4$ MW; observed copious Li ejections during arcs
 - Before run quickly reached stand-off voltage ~ 25 kV during vacuum conditioning
 - After extensive Li injection difficult to reach ~ 15 kV in vacuum
 - Dust seen during plasmas & inside antenna



- For FY11-12 will return to FY09 Li levels:
 - should be okay for HHFW operations
- Tested prototype ELM/arc discrimination system in 2010:
 - Worked well on bench using recorded data, but tripped undesirably 20-30 times during real shot

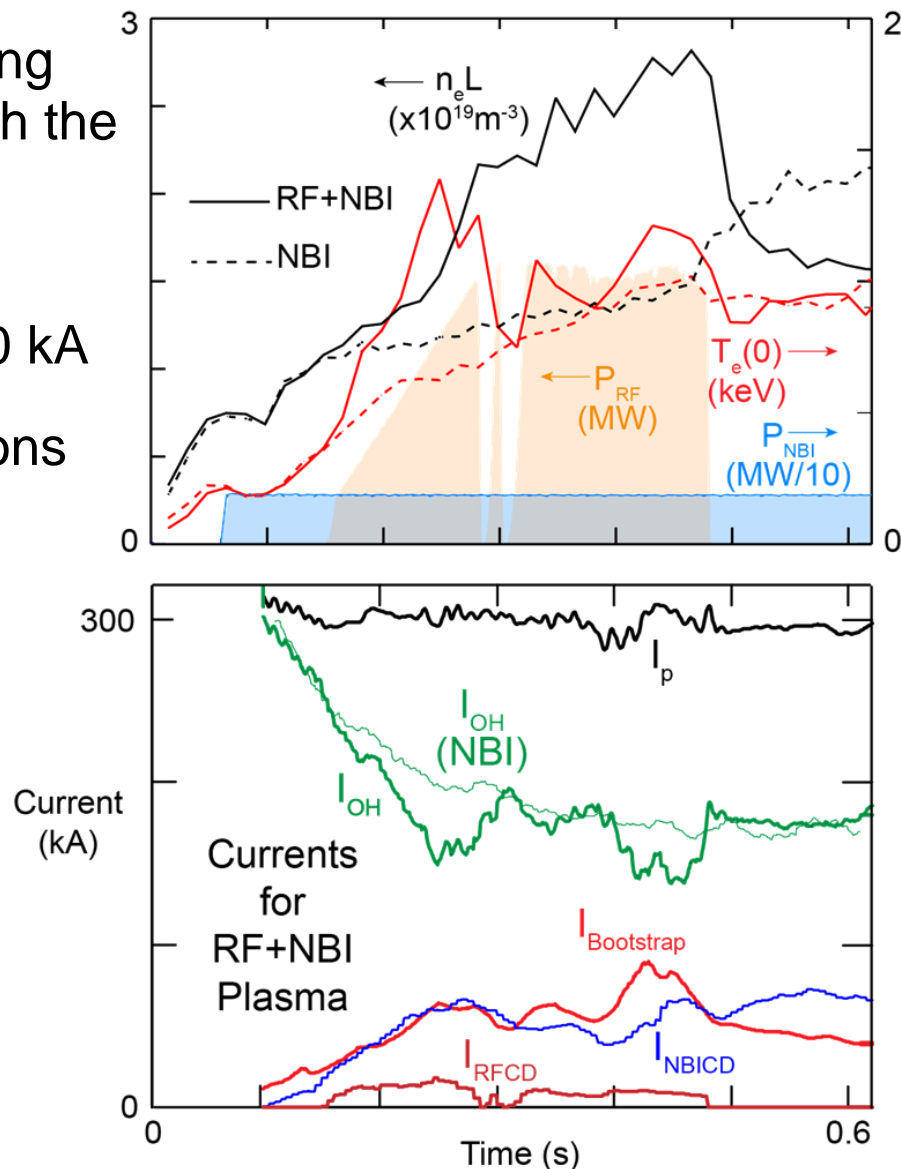
Progress made in sustaining HHFW heating during $I_p=300$ kA RF-only H-mode plasma; $T_e(0) = 3\text{keV}$ with only 1.4 MW

- Low I_p HHFW experiments in 2005 could not maintain P_{RF} during H-mode
- Produced sustained RF-only H-mode in 2010:
 - Better plasma-antenna gap control than in 2005, due to reduced PCS latency
 - Modeling predicts $I_{RFCD} \sim 85$ kA, $I_{Bootstrap} \sim 100$ kA $\rightarrow f_{NI} \sim 60\%$
 - High f_{NI} enabled by positive feedback between ITB, high $T_e(0)$ and RF CD
 - $f_{NI} \sim 100\%$ requires $P_{RF} \sim 3$ MW, well below arc-free P_{RF} available in 2009
 - No q-profiles for these RF-only plasmas – MSE-LIF will enable this in FY11-12

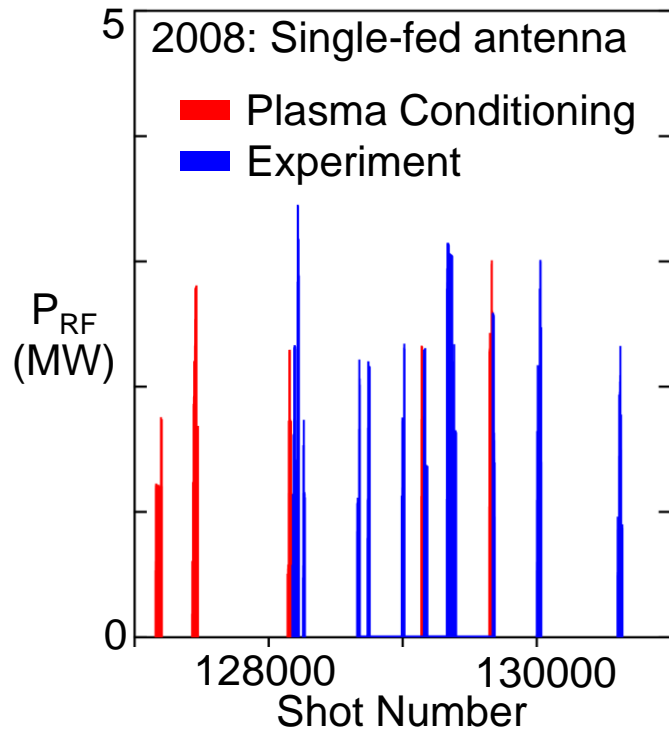


Adding NBI to $P_{RF} = 1.4 \text{ MW}$, $I_p = 300 \text{ kA}$ plasma resulted in lower f_{NI} due to RF absorption on fast-ions & higher n_e

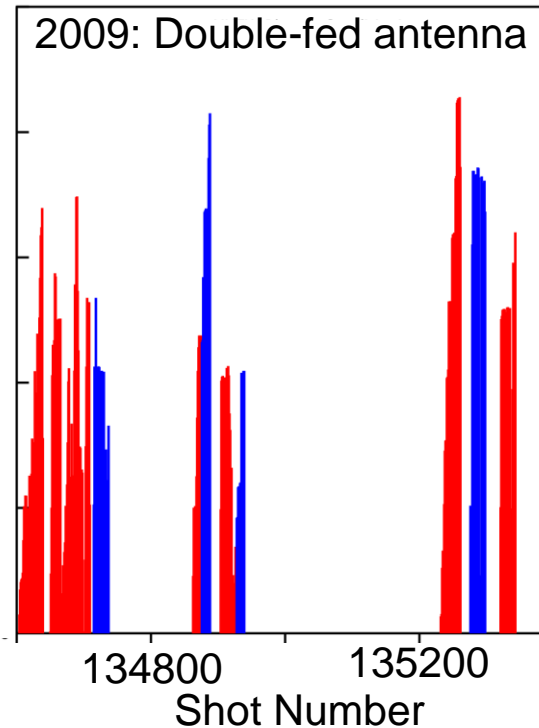
- Density increased during HHFW heating probably due to fast-ion interaction with the antenna
- Much lower $T_e(0)$ & higher $n_e(0)$ than RF-only H-mode, resulted in $I_{RFCD} \sim 20 \text{ kA}$
- 60% of P_{RF} to electrons, 40% to fast-ions
- $\sim 50\%$ of injected NBI fast-ions are promptly lost at this low current:
 - Predict $\sim 80\%$ will be confined using more tangential 2nd NBI in NSTX-U
- $I_{\text{Bootstrap}} = 60\text{-}90 \text{ kA}$, $I_{\text{NBICD}} = 50\text{-}70 \text{ kA}$
- $f_{NI} \sim 50\%$



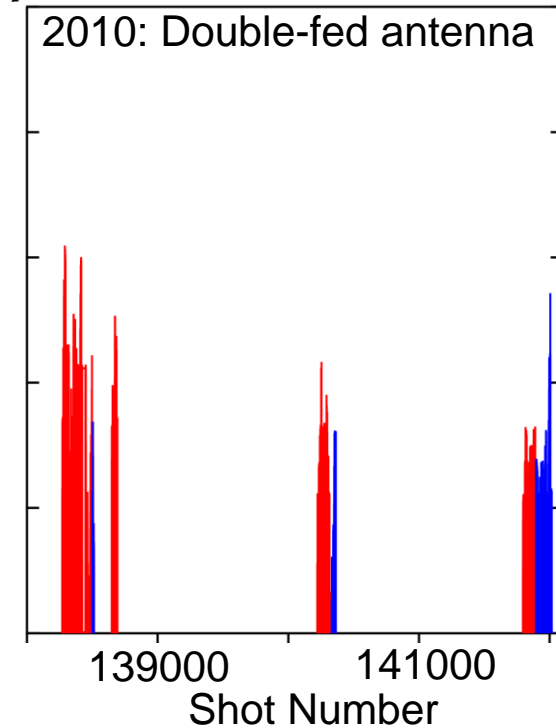
Double-fed HHFW antenna operation improved with time in 2009, but degraded over time in 2010



Operation spread out evenly over ~ 5 months
Initial plasma conditioning, then majority of time on experiments
Most operation in 2-3 MW range throughout campaign

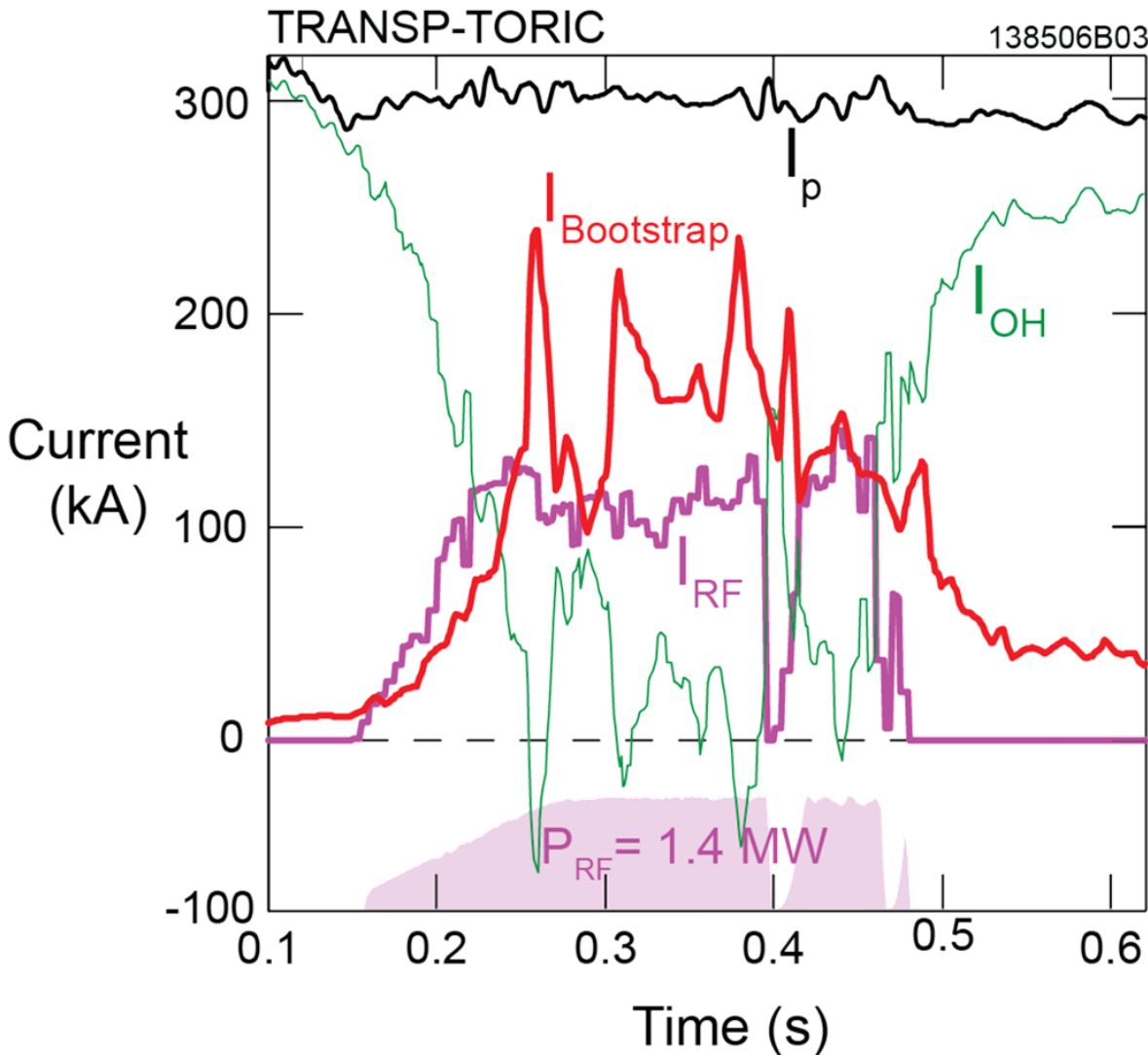


2009 operation concentrated in last 4 weeks
Majority of time spent on plasma conditioning
Operation in 2.5-4 MW range, improved with time



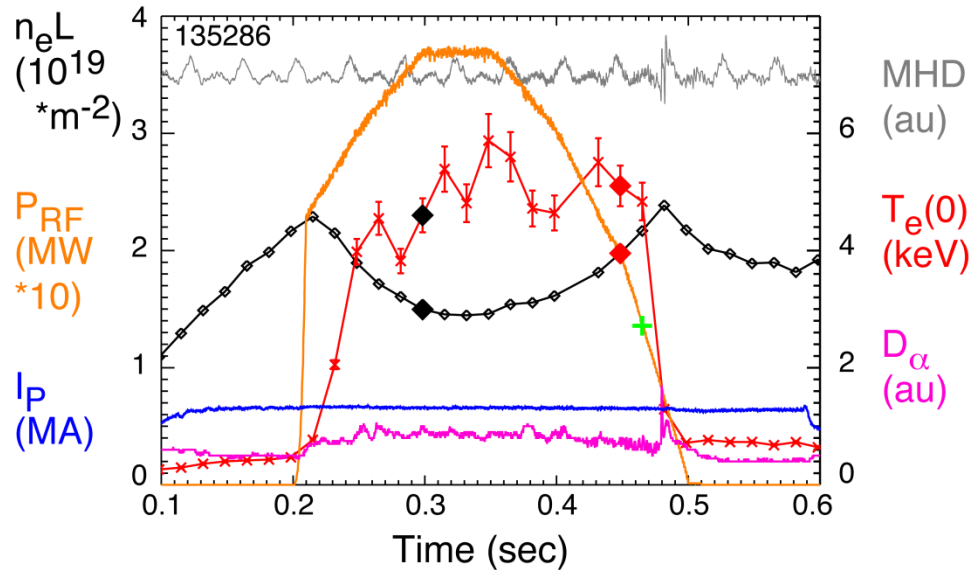
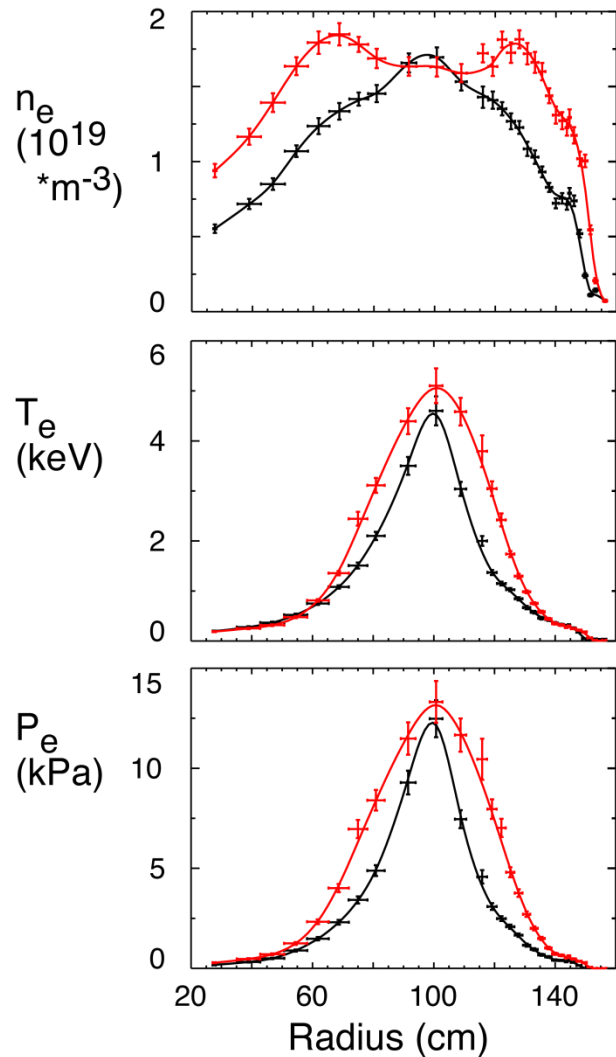
2010 operation widely separated over ~4 months
Almost all time spent on plasma conditioning
Operation < 3 MW, deteriorated with time

TRANSP-TORIC simulation with no RF coupling losses predicts ~180 kA Bootstrap CD + ~120 kA RFCD



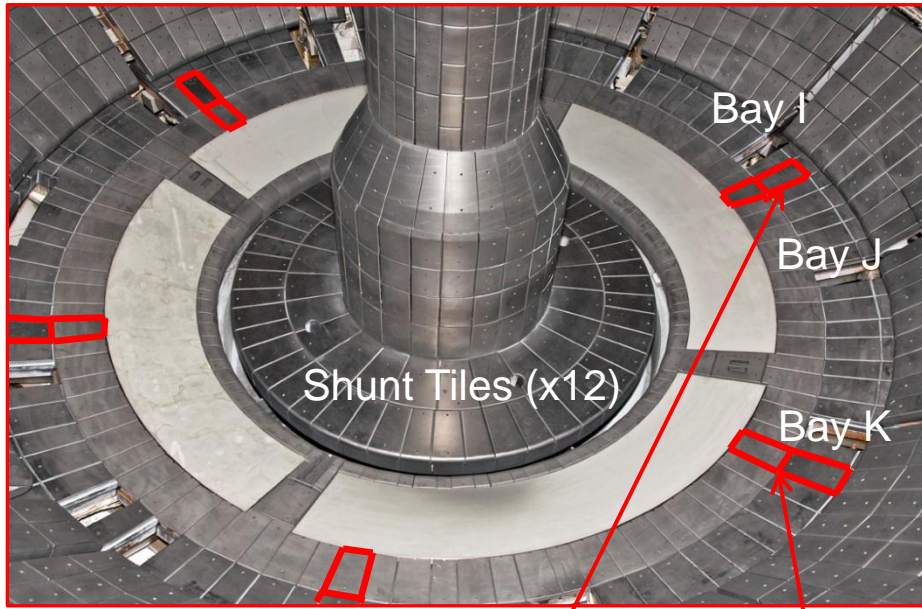
- RF coupling efficiency is typically ~ 60% for H-mode, giving $f_{NI} \sim 75\%$
- TRANSP-TORIC RF CD efficiency of ~ 85 kA/MW
- GENRAY-ADJ RF CD efficiency ~ 115 kA/MW

Slow fall of P_{RF} results in sustainment of high $T_e(0)$ and core electron heating even down to $P_{RF} < 1.4$ MW



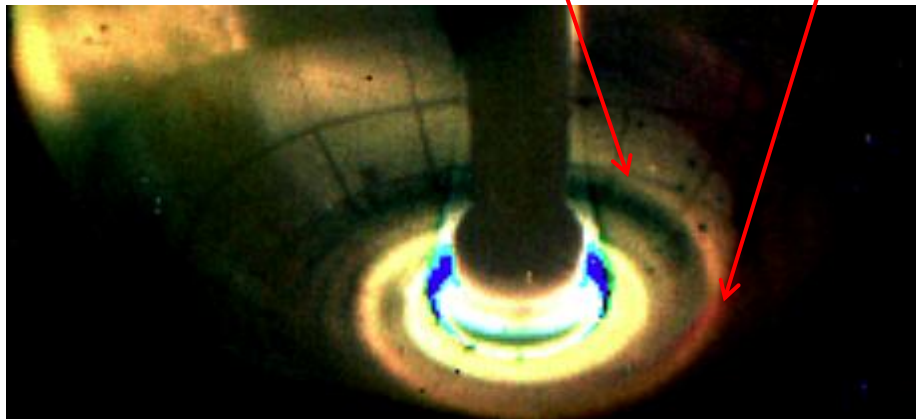
- Slow transition to H-mode from L-mode as power is ramped to 3.7MW
- During slow ramp down of P_{RF} , the core temperature is maintained and broadened in radius even down to 1.36 MW
- Large ELM at even lower power strongly reduces the stored electron energy and marks the transition back to the L-mode

Divertor tile currents are used to track presence of RF fields (sheath) and driven currents



Tile I3, I4

Tile K3, K4



- Tiles in row 3 and 4 of divertor plate are instrumented with Rogowski sensors
- Bay I and K tiles are in line with “hot” zone for RF edge deposition

Advanced Scenarios and Control Supplemental Slides

β_N Controller Implemented Using NB Modulations and rtEFIT β_N

- Controller implemented in the General Atomics plasma control system (PCS), implemented at NSTX.
- Measure β_N in realtime with rtEFIT.
- Use PID scheme to determine requested power:

$$e = \beta_{N, request} - LPF(\beta_{N, rEFIT}; \tau_{LPF})$$

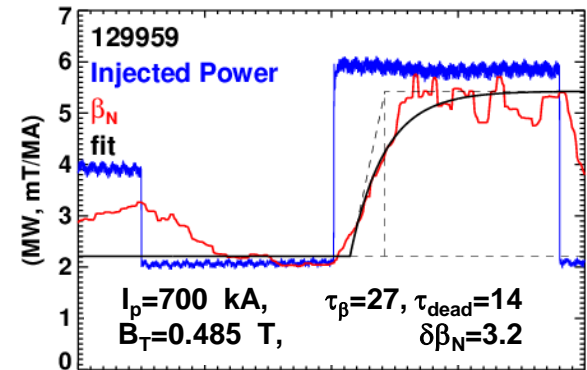
$$P_{inj} = P_{\beta_N} \bar{C}_{\beta_N} e + I_{\beta_N} \bar{C}_{\beta_N} \int edt + D_{\beta_N} \bar{C}_{\beta_N} \frac{de}{dt}$$

$$\bar{C}_{\beta_N} = \frac{I_P V B_T}{200 \mu_0 a \tau}$$

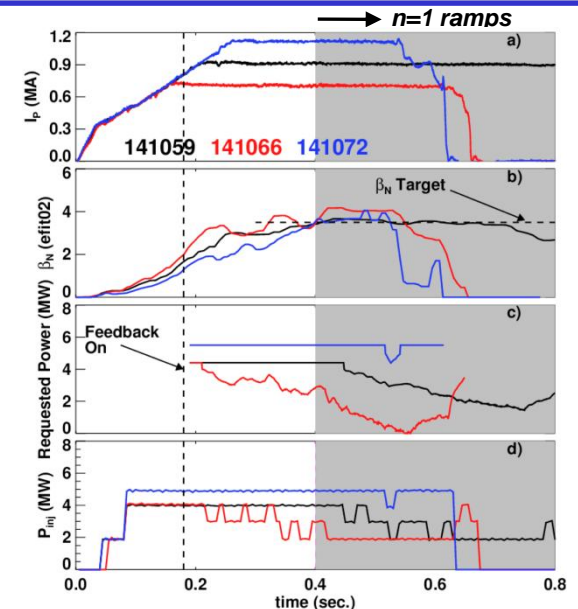
S. Gerhardt, FST, accepted 2011

- Use Ziegler-Nichols method to determine P & I.
 - Based on magnitude, delay, and time-scale of the β_N response to beam steps.
- Convert “analog” requested power to NB modulations.
 - Minimum modulation time of 15 msec.

Determination of Gains Using Ziegler-Nichols Method



Constant- β_N During I_p and B_T Scans



Improvements to the Shape Controller Will Allow Higher Performance Scenarios and Reduce Development Time.

- Key issue: individual controllers are “selfish”
 - Good control of individual quantities like outer gap or S.P. radius...
 - ...but bottom or inner gaps go to zero.

*Example high- κ shape and control segments
OH leakage flux drives the bottom gap to zero*

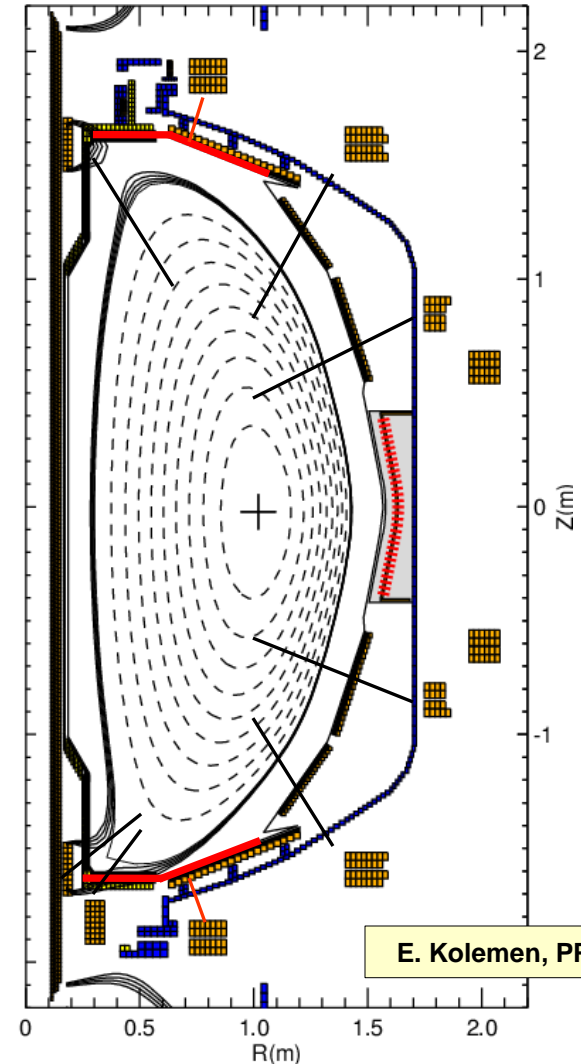
- ISOFLUX controller produces voltage requests via the “M-Matrix” of weights.

$$\begin{array}{c} \text{Coil} \\ \text{Voltages} \end{array} \begin{array}{c} \text{M-Matrix} \\ \text{Segment} \\ \text{Errors} \end{array}$$

$$\begin{bmatrix} V_1 \\ V_2 \\ \vdots \\ V_n \end{bmatrix} = \begin{bmatrix} M_{11} & & M_{1n} \\ & \ddots & \\ M_{n1} & & M_{nn} \end{bmatrix} \begin{bmatrix} (PID)_1 \\ (PID)_2 \\ \vdots \\ (PID)_n \end{bmatrix}$$

General Atomics

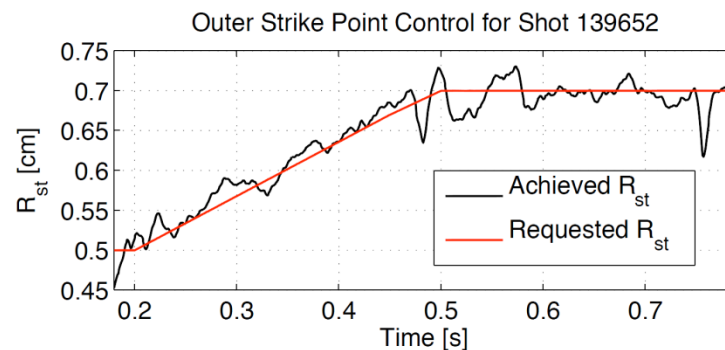
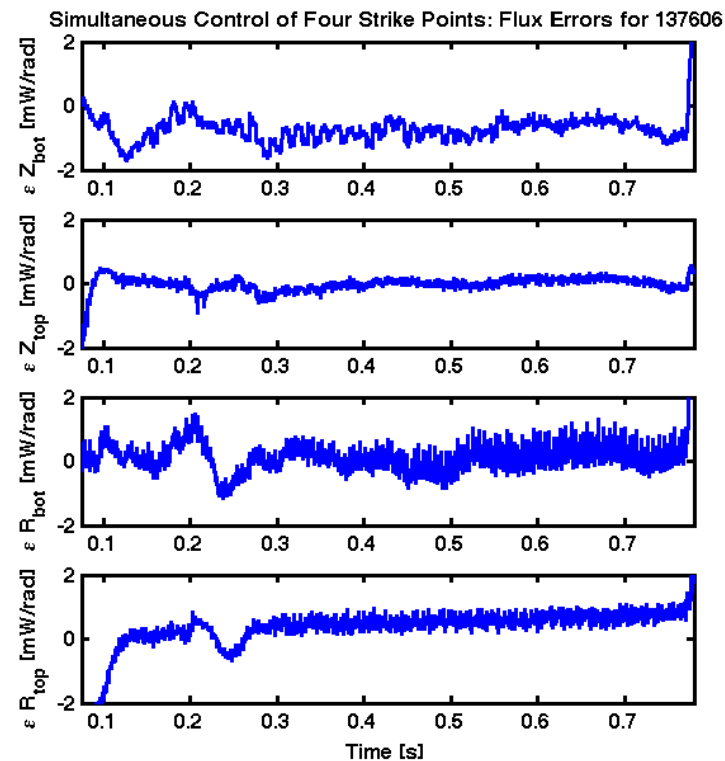
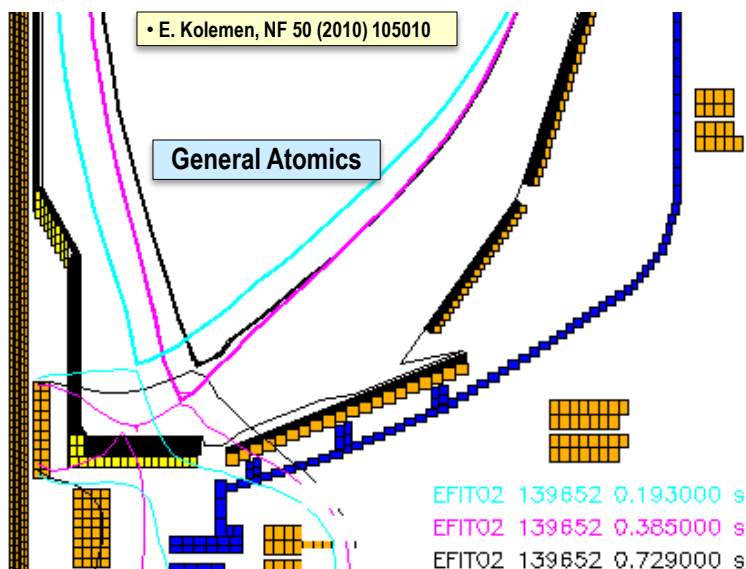
- M is essentially a diagonal matrix for present scenarios.
 - Implies that the controllers are ignorant of each other.
- More accurate boundary control can be achieved with more complex M-matrix.
 - Accounting for controller interactions.
 - Important at the number of coils increases.
 - Proper weighting of the most important parameters.
 - Can be scenario dependent.
- Desired physics and operations benefits:
 - Better regulation of inner and bottom gaps in high-performance plasmas.
 - More rapid development of complex scenarios.
- Highly desirable for NSTX-Upgrade, where manual programming of 16 coils, including interactions, will likely be impossible.



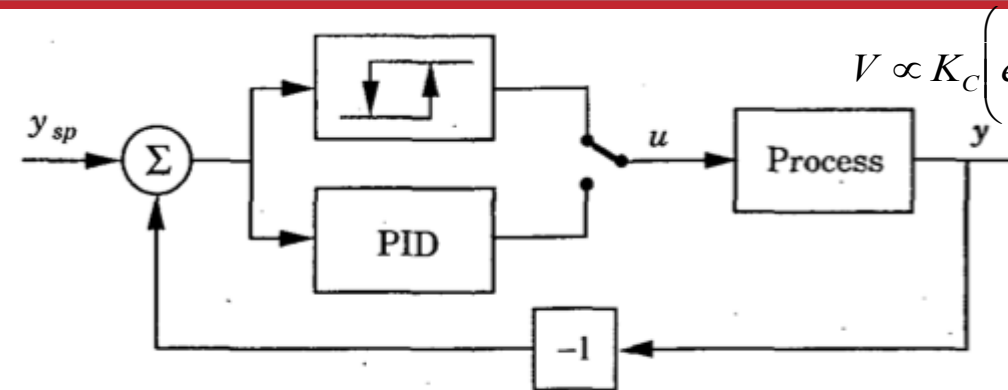
Control of 4 Strike Points (SP)

Developed To Support LLD Experiments

- FY-09 S.P. Control
 - Had uncontrolled dr_{sep} ramps when only lower S.P. under control.
- FY-10: Optimized 4 S.P. Controller
 - Eliminated dr_{sep} ramps.
 - Used for initial LLD experiments.

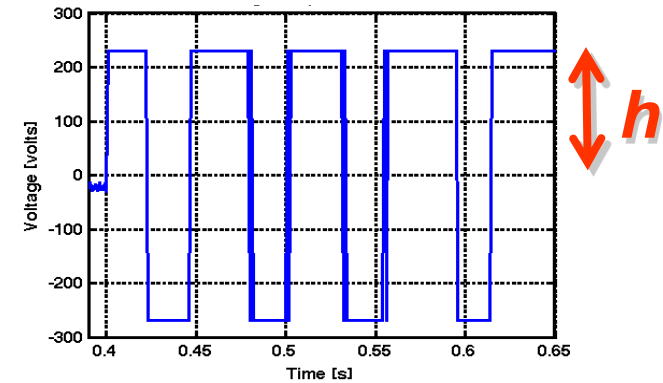


New Capability for Experimental System ID: Closed Loop Auto-tune with Relay Feedback



$$V \propto K_C \left(e + \frac{1}{\tau_I} \int e dt + \tau_D \frac{de}{dt} \right)$$

**Control Output
(PF-2L Coil Voltage)**

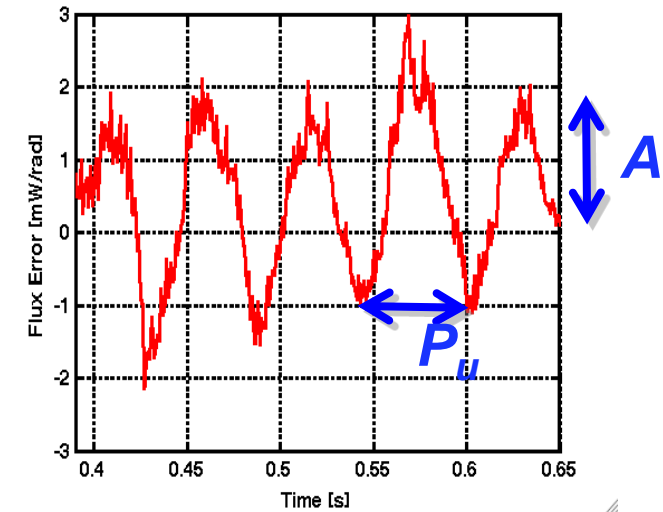


- The closed-loop plant response period (P_u) & amplitude (A) are used for PID controller tuning.

	K_c	τ_I	τ_D
P	$0.5K_{cu}$		
PI	$0.45K_{cu}$	$P_u/1.2$	
PID	$0.6K_{cu}$	$P_u/2$	$P_u/8$

$$K_{cu} = \frac{4h}{\pi A}$$

**Process Output
(Flux Error at Outer S.P.)**

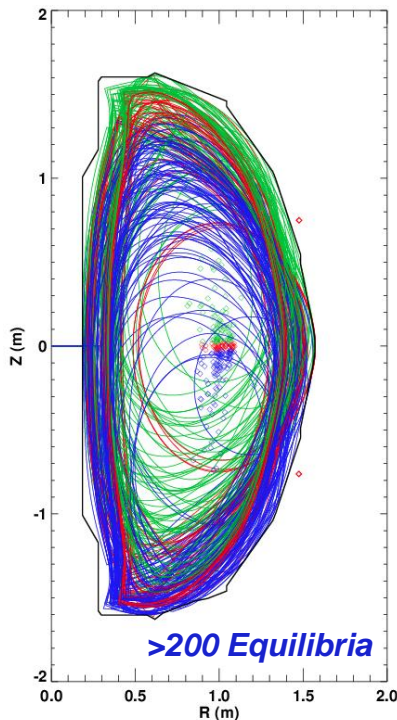


- Multiple advantages to closed loop tuning:
 - Single-shot system-ID
 - **Save experimental time.**
 - Enable system ID for actuators that can't be open loop
 - **e.g. vertical control.**

E. Kolemen, PPPL

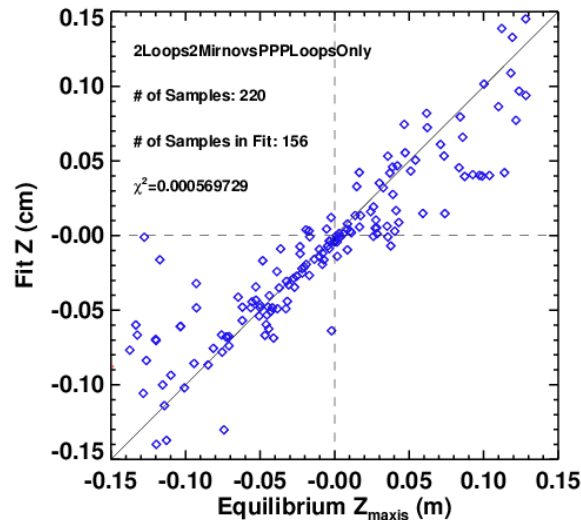
Developing a Better Realtime dZ/dt Estimator For Improved Vertical Control in 2011 & 12

- NSTX has historically used the voltage difference between two loops for derivative control on the vertical position.
 - Assume that $Z_p = \alpha(\psi_U - \psi_L)$, so that $\frac{dZ_p}{dt} = \alpha(V_U - V_L)$.
 - Proportional part of PD controller provided by ISOFLUX.
- Use of additional loops can significantly improve the fidelity of the position, and thus velocity, estimate.
- Bringing additional loop voltages into PCS for improved dZ/dt measurement

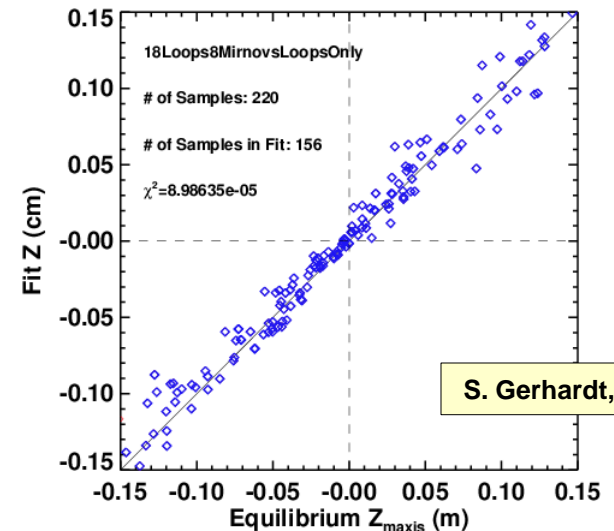


Fit Axis Location to Weighted Sum of Flux Loops: $Z_p = \sum_{j=1}^{N_{loops}} \alpha_j \psi_j$

Best fit of Z_p with 2 Loops



Best fit of Z_p with 18 Loops



Challenge of Snowflake: finding and controlling 2nd X-point

E. Kolemen, PPPL

- Locate snowflake centroid & 2nd X-point
- Locally expand of the Grad-Shafranov equation in toroidal coordinates:

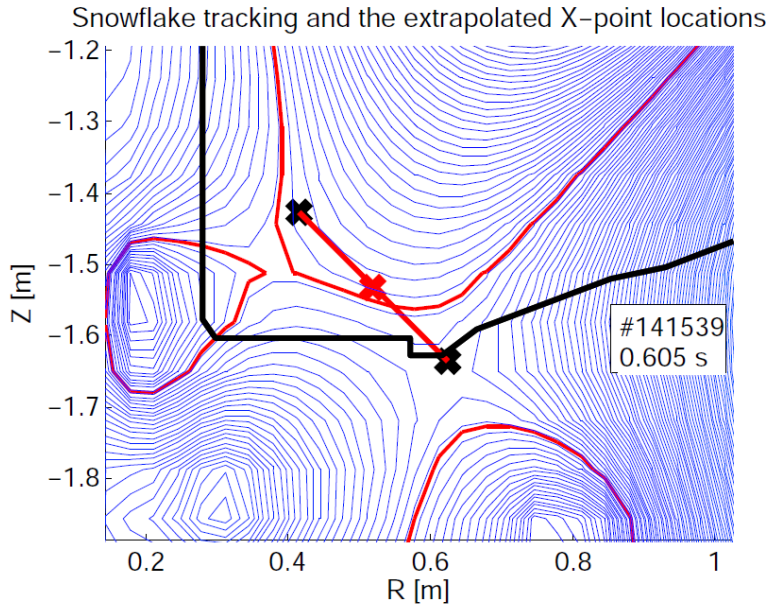
$$(R+x) \frac{\partial}{\partial x} \left(\frac{1}{R+x} \frac{\partial \Psi}{\partial x} \right) + \frac{\partial^2 \Psi}{\partial z^2} = 0$$

- Keep the 3rd order terms and find the magnetic nulls:

$$\begin{aligned} \Psi_{00} &= \Psi_f - \Psi(\rho_f \zeta_f) & \Psi_1 &= \Psi(\rho_1 \zeta_1) + \Psi_{00} \\ &= \Psi_f - [l_2 \zeta_f + q_3 \zeta_f^2 + c_4 \zeta_f^3 + l_1 \rho_f + 2q_2 \rho_f \zeta_f] & \Psi_2 &= \Psi(\rho_2 \zeta_2) + \Psi_{00} \\ & & & + (-3c_1 - q_3) \rho_f \zeta_f^2 + \frac{1}{2} (1_1 - 2q_3) \rho_f^2 + (-3c_4 + q_2) \rho_f^2 \zeta_f + c_1 \rho_f^3 \end{aligned}$$

- Find coefficients from sample points
- Very fast algorithm with good accuracy

Ref. M.A. Makowski & D. Ryutov, "X-Point Tracking Algorithm for the Snowflake Divertor" M.V. Umansky et al.. "Analysis of geometric variations in high-power tokamak divertors." LLNL-JRNL-410565.



Snowflake tracking for NSTX:

1. Red cross is the tracked snowflake centroid
2. Black crosses are the calculated X-point locations by snowflake tracking algorithm

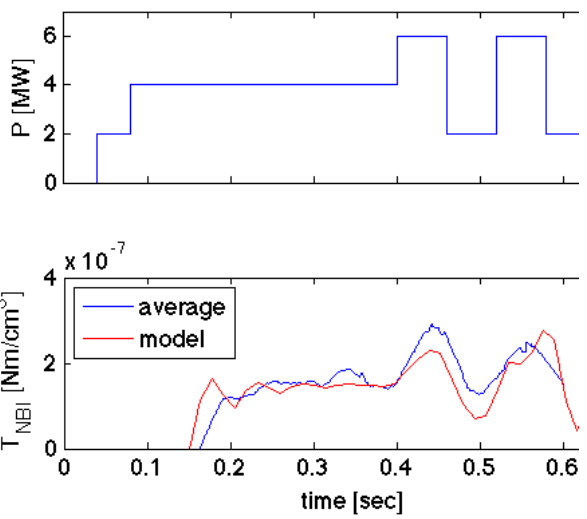
2011-2012 Run: Rotation Control

K. Taira, E. Kolemen, C.W. Rowley, and N.J. Kasdin, Princeton University.

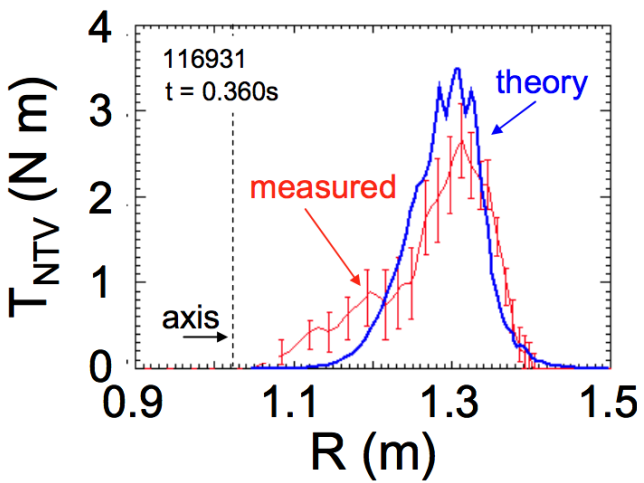
- Reduced order model for rotation control

$$\sum_i n_i m_i \langle R^2 \rangle \frac{\partial \omega}{\partial t} = \left(\frac{\partial V}{\partial \rho} \right)^{-1} \frac{\partial}{\partial \rho} \left[\frac{\partial V}{\partial \rho} \sum_i n_i m_i \chi_\phi \langle R^2 (\nabla \rho)^2 \rangle \frac{\partial \omega}{\partial \rho} \right] + \sum_j T_j + T_{\text{NBI}} + \mu \left(\frac{B_0}{B_{\text{eff}}} \right)^2 (\omega - \omega^*)$$

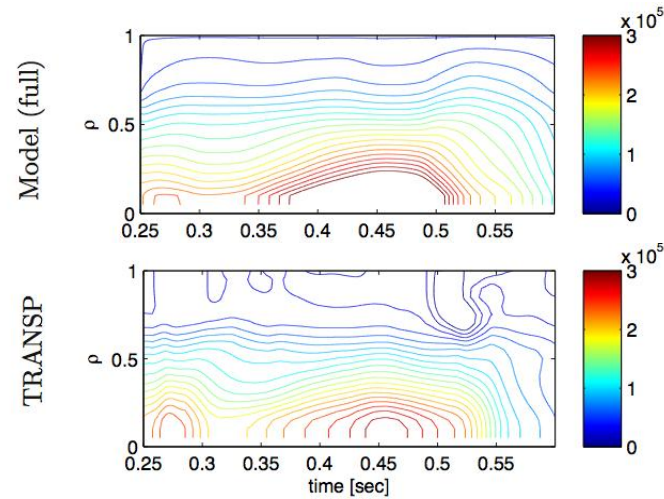
- Adequate models for torque inputs and time evolution



**NBI Torque profile prediction:
Model versus data**



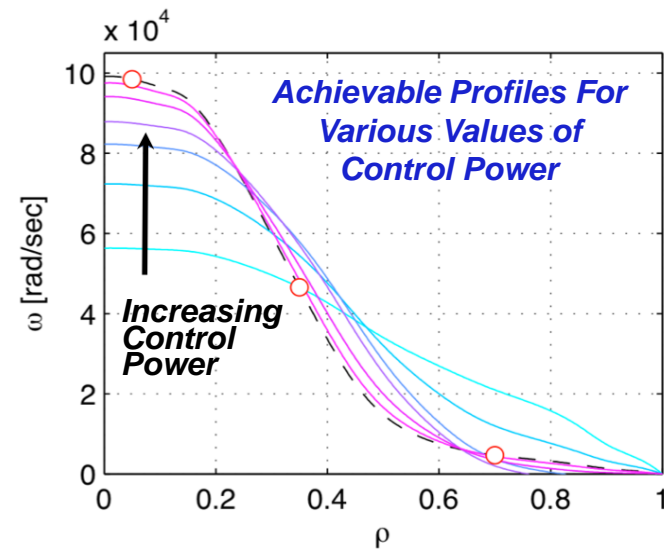
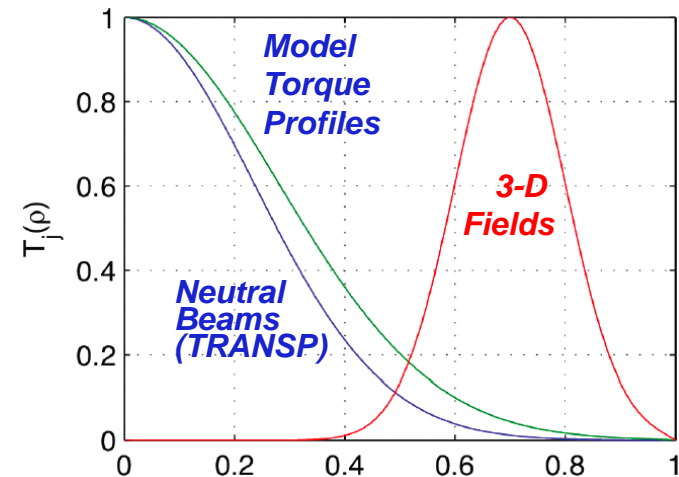
**NTV torque profile:
Calculations (Zhu et al.)
versus experimental data**



**Rotation time evolution:
Reduced model versus
TRANSP data**

Development of Real-Time NB Control Enables β_N and Rotation Control

- β_N control demonstrated in 2009, optimized in 2010.
- Long-term plan to control the rotation profile.
 - RWM & EF physics as a function of β and rotation.
 - Transport dynamics vs. rotation shear.
 - Pedestal stability vs. edge rotation.
 - **What is the optimal rotation profile for integrated plasma performance?**
- Use a state-space controller based on a momentum balance model.
 - Neutral beams provide torque.
 - 3-D fields provide braking.
 - Different toroidal mode numbers provide different magnetic braking profiles.
 - Use 2nd Switching Power Amplifier (SPA) for simultaneous n=1,2 &3 fields.
- Developing rt- V_ϕ diagnostic for FY-11.
 - Camera has been purchased.
 - Is being tested for real-time acquisition.
- PCS control algorithm implementation driven by the measurement.

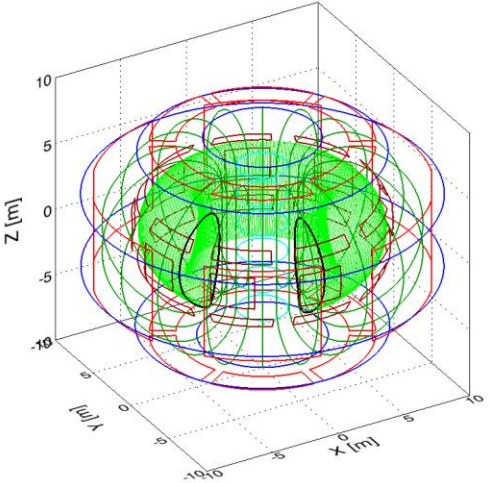


K. Taira, E. Kolemen, C.W. Rowley, and N.J. Kasdin, Princeton University.

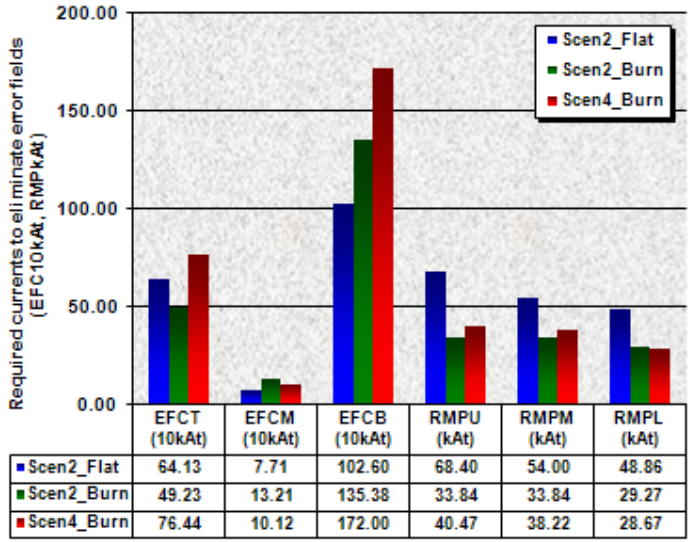
ITER Support Supplemental Slides

NSTX researchers led ITER Task Agreement on the study of error fields using Ideal Perturbed Equilibrium Code (IPEC)

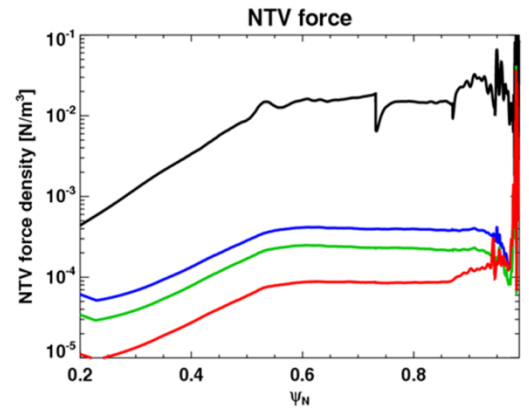
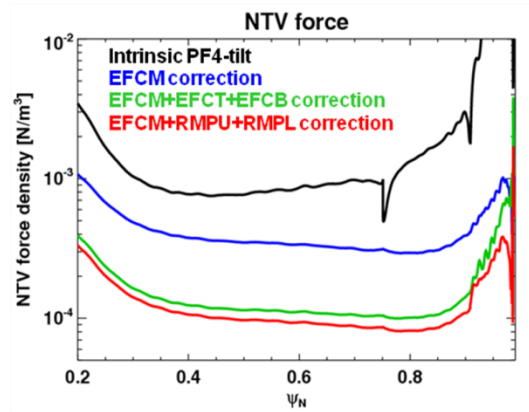
- Inclusion of plasma response (using IPEC) reduces effectiveness of top/bottom EFC
- Find RMP coils effective for EFC and NTV reduction



ITER coil geometry represented by each filament, for CS coils (Light Blue), PF coils (Blue), TF coils (Green), EFC coils (Red), RMP coils (Purple).



Required currents to eliminate worst n=1 error fields



NTV force density profiles for intrinsic PF4-tilt error and each correction, for Scen2_Burn (Top) and for Scen4_Burn. EFCM+RMPU+RMPL gives the best correction.

- J. Menard (PPPL-P.I.), J.-K. Park (PPPL-primary author), M.J. Schaffer (GA - contributing author)
- Final Report submitted October 2010



Measurements *Outside* TF Coil Could Identify Some Manufacturing and Assembly Defects

- Only field errors ($m, n \neq 0$) are present outside TF coil envelope
 - TF does not affect magnetization of distant ferromagnetic sources
- Ripple ($n = 18$) is dominant near coils *but*
- Higher n components fall off roughly as R^{-n} so
- Is there a region where $n = 1$ is detectable above intrinsic field?

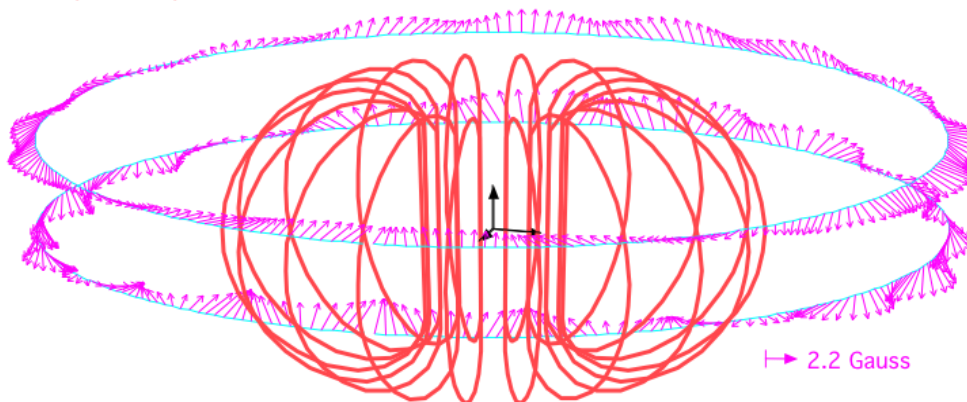
TF coil distortion:

$dR(n = 1) = 10\text{mm}$,

$dZ(n = 2) = 10\text{mm}$

Measurement circles:

$R = 18.0\text{m}$; $Z = 0.0, 4.0\text{m}$



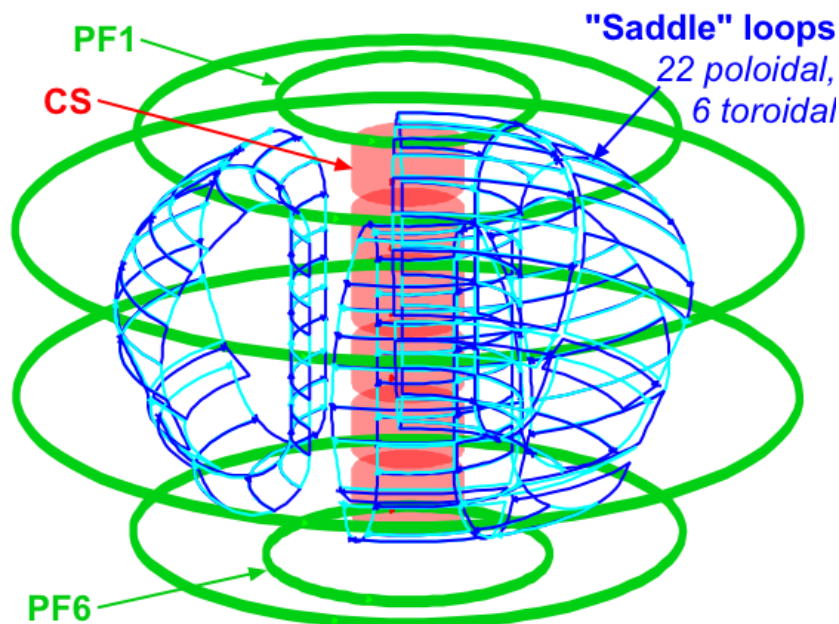
This is outside the cryostat in “open air” where measurements with Hall effect instruments could be made at well defined locations

- M. Bell (PPPL - P.I.), N. Pomphrey (PPPL), A. Boozer (Columbia University)
- Final Report submitted spring 2011

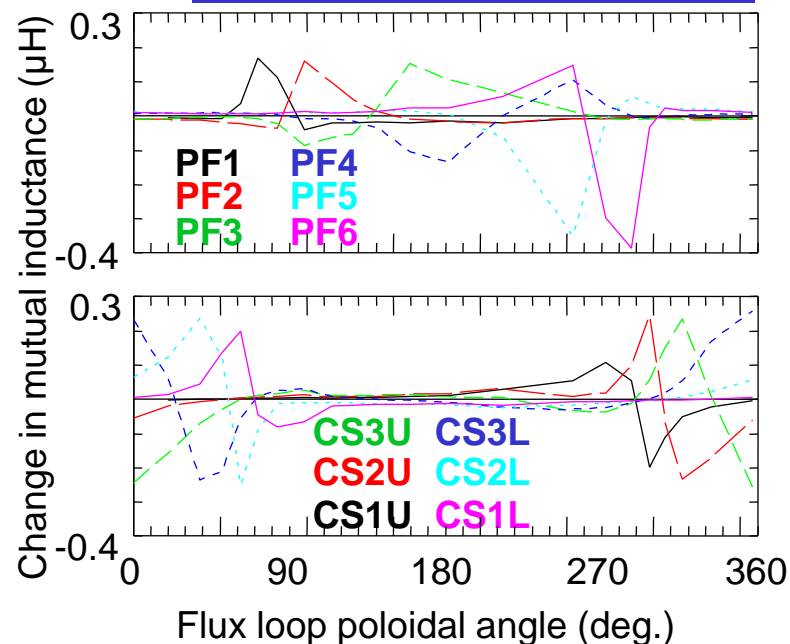
Columbia University

Planned Partial Flux Loops in ITER Can Be Used to Characterize Field Errors from PF Coils

- Partial Flux Loops (“saddle” loops) mounted on inside of VV inner wall, span all or part of a VV sector (40° toroidally)
- 22 loops span poloidal circumference in 6 of 9 VV sectors
- **Conductor positions are specified to be known to mm accuracy**



Change in mutual inductance for coil axis lateral shift 10mm

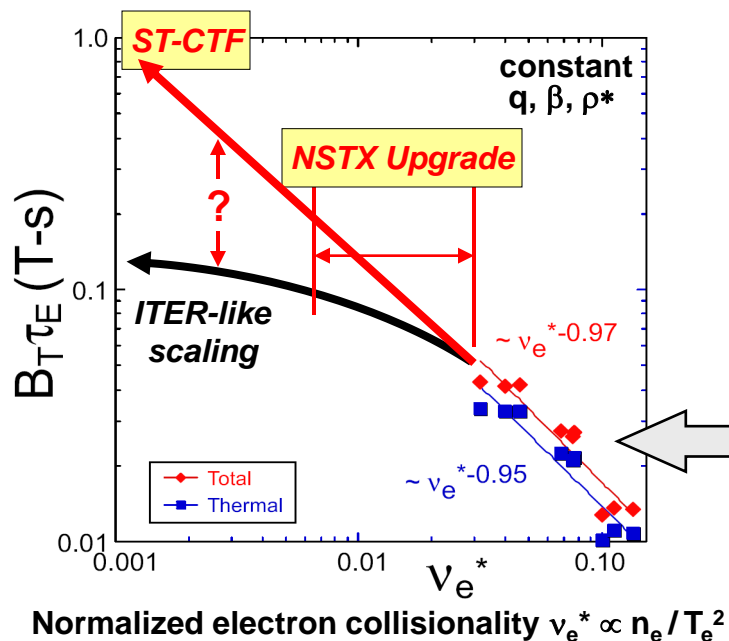


- M. Bell (PPPL - P.I.), N. Pomphrey (PPPL), A. Boozer (Columbia University)
- Final Report submitted spring 2011

Columbia University

NSTX Upgrade, ST-FNSF/Pilot Supplemental Slides

Access to reduced collisionality is needed to understand underlying causes of ST transport, scaling to next-steps



- Future ST's are projected to operate at 10-100x lower normalized collisionality ν^*
- Conventional tokamaks observe weak inverse dependence of confinement on ν^*

ITER $B_T \tau_E$ (e-static g-Bohm) $\propto \rho_*^{-3} \beta^0 \nu_*^{-0.14} q^{-1.7}$
Petty et al., PoP, Vol. 11 (2004)

NSTX observes much stronger scaling vs. ν^*

- Does favorable scaling extend to lower ν^* ?
- What modes dominate e-transport in ST ?
 - Electrostatic or electromagnetic?

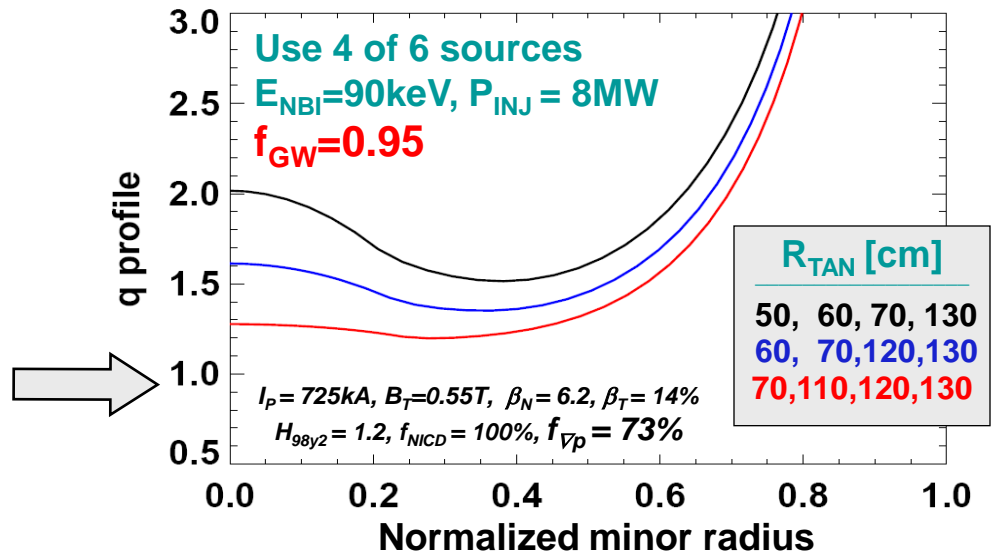
- ν^* also impacts RWM stability, rotation damping, range of other physics

- Higher toroidal field & plasma current enable access to higher temperature
- Higher temperature reduces collisionality, but increases equilibration time
- Upgrade: Double field and current + 3-5x increase in pulse duration to substantially narrow capability gap \rightarrow 3-6x decrease in collisionality

Increased auxiliary heating and current drive are needed to fully exploit increased field, current, and pulse duration

- Higher heating power to access high temperature and β at low collisionality
 - Need additional 4-10MW, depending on confinement scaling
- Increased external current drive to access and study 100% non-inductive
 - Need 0.25-0.5MA compatible with conditions of ramp-up and sustained plasmas
- Upgrade: double neutral beam power + more tangential injection
 - More tangential injection \rightarrow up to 2 times higher efficiency, current profile control
 - ITER-level high-heat-flux plasma boundary physics capabilities & challenges

- $q(r)$ profile very important for global stability, electron transport, Alfvénic instability behavior
 - Variation of mix of NBI tangency radii would enable core q control



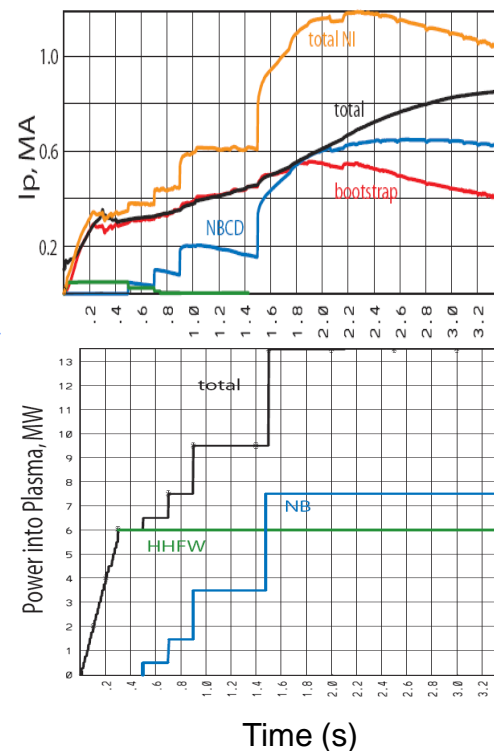
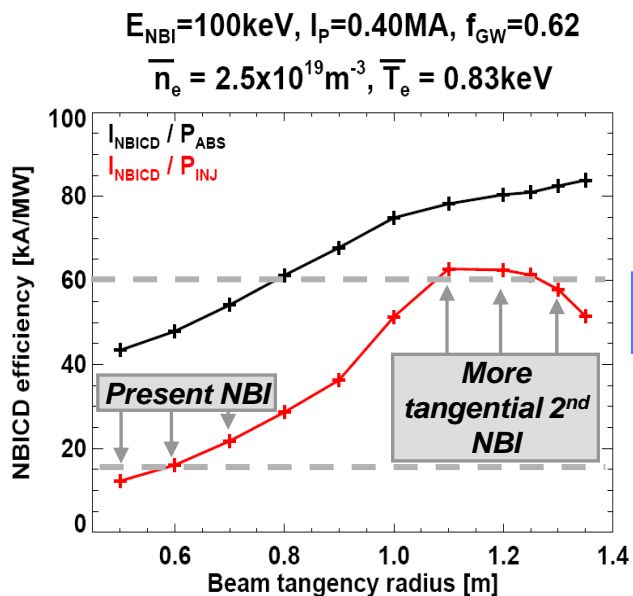
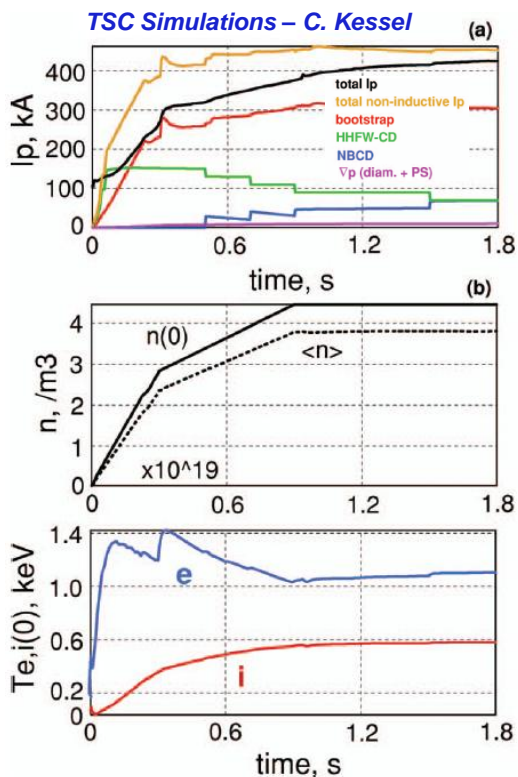
Non-inductive ramp-up to ~0.4MA possible with RF + new CS, ramp-up to ~1MA possible with new CS + more tangential 2nd NBI

Ramp to ~0.4MA with fast wave heating:

- High field $\geq 0.5T$ needed for efficient RF heating
- ~2s duration needed for ramp-up equilibration
- Higher field 0.5→1T projected to increase electron temperature and bootstrap current fraction

Extend ramp to 0.8-1MA with 2nd NBI:

- Benefits of more tangential injection:
 - Increased NBI absorption = 40→80% at low I_p
 - Current drive efficiency increases: x1.5-2
- New CS needed for ~3-5s for ramp-up equilibration
 - Higher field 0.5→1T also projected to increase electron temperature and NBI-CD efficiency



NSTX Upgrade reference operating scenarios highlight major research capabilities and needs of Upgrade

- Dual NBI capability ($P/\Delta t$): 15MW/1.5s, 10MW/5s, 5MW/10s
- TF flat-top capability: 1T for 6s, 0.75T for 10s, total OH flux = 2.1Wb
- Divertor peak heat flux limit = 10MW/m² for 5s ($T_{\text{carbon-tile}} \leq 1200^\circ\text{C}$)
- Plasma carbon $Z_{\text{eff}} \leq 2.5$ (goal)

$\beta_N \leq 5.5$, $\tau_E = \text{ITER-98y2 H-mode scaling}$, SOL width scaling $\propto I_p^{-1.6}$

Reference Scenario	B_T [T]	I_p [MA]	Δt_{flat} [s]	NICD [%]	$n_e / n_{\text{Greenwald}}$	P_{NBI} [MW]	P_{RF} [MW]	P_{TOT} [MW]	Unmitigated divertor peak heat flux [MW/m ²] ($f_{\text{exp}} = 20$)	Unmitigated divertor peak heat flux [MW/m ²] ($f_{\text{exp}} = 60$)	D pumping required (NBI fueling only) [10^{21} s^{-1}]
Long pulse	0.8	1	7	50-70	≤ 1	6	0	6	5	2	0.7
High non-inductive	1	0.8	5	80-100	≤ 1	8	0	8	5	2	1.0
High I_p	1	1.5	5	50-70	≤ 1	8	0	8	13	4	1.0
Max I_p	1	2	4-5	40-60	0.7-1	10	0	10	25	8	1.2
Max I_p & power	1	2	4-5	40-60	≤ 1	10	5	15	38	13	1.2

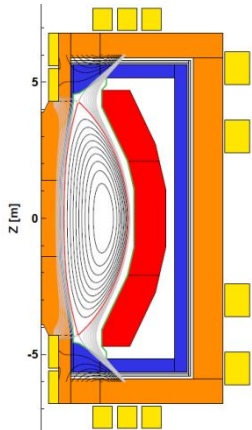
2MA operation may require $n_e / n_{\text{Greenwald}} = 0.7$ to aid achievement of sufficiently high T_e to reduce loop voltage to 0.25V for 5s flat-top

1.5-2MA operation for 5s will require heat-flux mitigation utilizing: U/L power sharing, detachment, and/or snowflake (possibly all three)

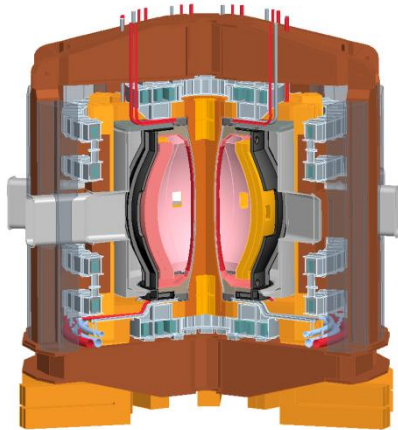
This is major goal of Upgrade research program

Developing design concepts for ST-based Fusion Nuclear Science Facility / Pilot Plant

Free-boundary equilibrium



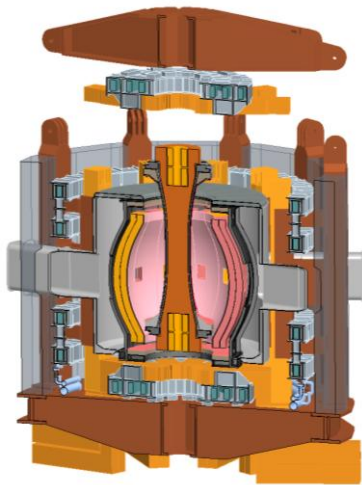
3D layout



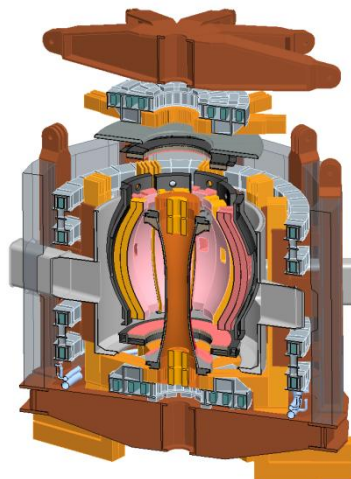
Some ST FNSF/Pilot design features:

- Minimize power losses to access $Q_{\text{eng}} \sim 1$
 - Flared TF rod to reduce power: 150-200MW
 - Outer PF coils superconducting
- Strong shaping for stability, bootstrap current
- PF coils in ends of TF rod to produce diverted high δ plasma, protect PF coils
- DN divertor for power sharing
 - May need snowflake, flowing Li, Super-X, radiation...
- 500keV NNBI for current drive (JT60-SA)
- Vacuum vessel independent of TF legs
- Low ripple $< 0.25\%$ at plasma boundary
- Conformal blankets to maximize TBR
- Entire blanket structure removable vertically
- Shielding for vessel, TF outer legs, PF coils outside center-stack \rightarrow lifetime components
- Center-stack shielded for 1-2 FPY

CS removal



Blanket removal



- **Have also begun meeting, sharing ideas with MAST/Culham CTF designers + other collaborators**